Genomic mosaicism in the opportunistic pathogen *Pseudomonas aeruginosa* and its contribution to virulence

Thesis submitted for the degree of Doctor of Philosophy

at the University of Leicester

by

Ewan Michael Harrison

Department of Infection, Immunity and Inflammation

University of Leicester

October 2009

UMI Number: U581997

UMI

Dissertation Publishing

ProQuest

Statement of Originality

This accompanying thesis submitted for the degree of PhD entitled "Genomic mosaicism in the opportunistic pathogen *Pseudomonas aeruginosa* and its contribution to the virulence" is based on work conducted by the author in the Department of Infection, Immunity and Inflammation at the University of Leicester during the period between October 2005 and September 2009.

All the work recorded in this thesis is original unless otherwise acknowledged in the text or by references.

None of the work has been submitted for another degree in this or any other University.

Signed:_____ Date:_____

Note

The following data were generated by others and is fully referenced in text as such. The data is included in this thesis for comparison and discussion with the data presented as part of this work:

All murine studies were carried out by Melissa Carter as part of her PhD studies (Carter, 2009) this work is presented in (Section and Figures numbers):

Section 5.17: Effect of deletion of PAPI-1 and PAPI-2 in murine models of pneumonia and bacteraemia. pg 159 - 63

Figure 5.22: (A) Survival graph for the acute murine pneumonia model monitored over 96 h; n = 10 for each strain.

Figure 5.23: Numbers of neutrophils (A), lymphocytes (B), macrophages (C) and monocytes (D) in lung tissue obtained 18 h post-infection in the murine acute pneumonia model; $n = 4$ for each strain.

Figure 5.24: (A) *P. aeruginosa* bacterial burdens in blood over a 24 h period following intravenous infection with 2 × 106 CFU; $n = 5$ for each strain.

The invasion assays were kindly carried out by Shelley Luck (Luck, S, personal communication) this work is presented in (Section and Figures numbers):

Section 5.16: Effect of loss of PAPI-1 and PAPI-2 on invasion of A549 cells: pg 158

Figure 5.21: Comparison of the invasive ability of A459 human lung carcinoma cells by *P. aeruginosa* PA14 and its isogenic mutants lacking PAPI-1 and/or PAPI-2.

Acknowledgements

Firstly I would like to thank my PhD supervisor Dr Kumar Rajakumar for his support, wisdom and encouragement all the way through my PhD and in particular for helping me to come away from my PhD studies even more interested in my field of study than when I began.

I would also like to thanks Dr Aras Kadioglu for his advice, encouragement and support throughout my studies.

I would like to thank all my colleagues and friends over the last four years in Lab 212 and around the department. But special thanks go to Barbara Rieck, Luisa Crosatti, Jon van Aartsen and James Lonnen who have been a constant support network, think tank, and great friends throughout my PhD.

Also I would like to thank Dr Hong-yu Ou for showing me the bioinformatics 'ropes' in the early days in lab and for supporting me throughout my time in Shanghai. I would also like to thank Dr Xinyi He for his wise advice in the lab and his help and support in Shanghai.

Thanks also go to my fellow 'Pseudomonas' researcher in Leicester, Melissa Carter for providing the murine data and useful discussions. Also thanks to Shelley Luck for carrying out the invasion assays. I would also like to thank all the technical and support staff in the Department of Infection, Immunity and Inflammation for all their help and advice throughout the course of my PhD.

Thanks to all my friends over the past four years for putting up with my rather random appearances and for showing interest (real or feigned!) in what I have been doing.

A huge thanks goes to Clara for all her love, support and patience. So very glad we shared our PhD journey together!

I would also like to thank my family for their support throughout my studies and for their encouragement and constant wisdom.

Finally I would like to acknowledge the financial support I received from the Medical research council and the University of Leicester for my PhD studentship.

Abstract

Pseudomonas aeruginosa is a ubiquitous Gram negative opportunistic pathogen which belongs to the γ subclass of proteobacteria. *P. aeruginosa* genomes consist of a highly conserved core component making up ~90% of the total genome and a highly variable accessory genome that makes up the remaining ~10% of the organism's DNA blueprint.

The extent and nature of tRNA-integrated genomic islands in the available sequenced *P. aeruginosa* genomes and clinical isolates were defined by both in silico comparative genomics methods and in vitro approaches. These investigations demonstrated that certain tRNA sites seemed to be favoured for integration and that most strains exhibited divergent tRNA site island-occupation profiles.

The contribution of three *P. aeruginosa* genomic islands PAPI-1, PAPI-2 and the $tRNA^{Pro21}$ island in strain PA14 to fitness and virulence were evaluated. By creating 'en bloc' deletant mutants that lacked islands and testing the resulting phenotype of the mutants alongside the wild-type parent, three islands (PAPI-1, PAPI-2 and $tRNA^{Pro21}$ island) were demonstrated to be important to full virulence of strain PA14.

The dynamics of site-specific integration of the PAPI-1 island into both of its cognate target attB sites were examined. A quantitative real-time PCR approach was used to measure the copy number of all 'states' of PAPI-1: chromosomally-integrated forms present at each of the two $tRNA^{Lys}$ sites, extra-chromosomal circular entities, and empty versions of the two *attB* sites. The pattern of occupation was clearly dynamic. Prior occupation of the $tRNA^{Lys10}$ site by an alternative genomic island in PAO1 and PA14 appeared to hinder integration of PAPI-1 into this occupied $tRNA^{Lys10}$ site through an as yet unknown mechanism. This hypothesis was supported by evidence that the deletion of the original occupying island allowed PAPI-1 to integrate at high frequency into this site. However, surprisingly this effect was found to be variable as several independently derived deletant mutants behaved distinctly. These studies also identified a potential link between the number of chromosomally-integrated copies of PAPI-1 and the stability of the island.

Several approaches, including the introduction of a third *attB* site within a 'neutral' genomic location combined with DNA signature copy number assays and pulsed field gel electrophoresis to identify large scale inversions, deletions or translocations involving *rrn* operons or tRNA genes were used to further investigate this mysterious 'dynamic-yet-stable genome'. The results demonstrated that *rrn* operon-mediated inversions are a constantly occurring in *P. aeruginosa* populations. Each strain does not have a single genomic orientation but rather a dominant orientation with other genomic variants also present within the population.

Abbreviations

Abbreviation	Explanation
bp	base pairs
DNA	deoxyribose nucleic acid
dNTP	dinucleotide triphosphate
DR	direct repeat
EDTA	ethylenediaminetetraacetic acid
GI	Genomic islands
ICEs	Integrative conjugative elements
IPTG	isopropyl-β-D-thiogalactopyranoside
IHF	Integration host factor
LA	Luria Bertani agar
LB	Luria Bertani broth
MIC	Minimum inhibitory concentration
MB	Megabase pairs
kb	kilobase pair(s)
kDa	kilodalton
OD600	optical density at 600 nm
ORF	open reading frame
PAI	Pathogenicity island
PCR	polymerase chain reaction
rDNA	ribosomal DNA
RT	reverse transcriptase
SDS	sodium dodecyl sulphate
sp.	species
TAE	Tris-acetate-EDTA
TE	Tris-EDTA
Tm	melting temperature
tRNA	transfer RNA
X-gal	5-bromo-4-chloro-3-indolyl-β-D-galactopyranoside

Table of Contents

7

List of Tables

List of Figures

1   Introduction

1.1   *P. aeruginosa* natural environments and epidemiology

Pseudomonas aeruginosa is a ubiquitous Gram negative opportunistic pathogen, a member of the genus *Pseudomonas*, which is part of the γ subclass of proteobacteria. It has been found in a wide range of environmental locations: soil, marshes, marine habitats, as well as producing biofilms in the presence of moisture on rocks and in soil (Stover *et al.*, 2000). *P. aeruginosa* has also been found growing in aircraft fuel tanks and other extreme environments. In the hospital setting *P. aeruginosa* has been isolated from nearly every environment (Driscoll *et al.*, 2007). The current view is that moist environments, and water fixtures and fittings (e.g. taps, sinks, showers etc) are the major reservoirs of *P. aeruginosa* in the hospital setting; however the full picture of the transmission of *P. aeruginosa* from the environment to humans is still not fully understood. But with reported carriage rates in hospitalized patients as high as 60% compared to 2-10% healthy persons, and reports of epidemic strain transmission in cystic fibrosis clinics (Salunkhe *et al.*, 2005), the role of humans in transmission of *P. aeruginosa* is probably not yet fully understood (Cholley *et al.*, 2008)

1.2   *Pseudomonas aeruginosa* Clinical infections

In the clinical setting *P. aeruginosa* can cause a wide range of infections in humans, though those at increased risk are the immunocompromised and immunodeficient. It is a major cause of hospital infections with ~10% of hospital acquired infections being caused by *P. aeruginosa* (El Solh *et al.*, 2008).

1.2.1 Respiratory infections

In the hospital environment *P. aeruginosa* is the second most common cause of hospital acquired respiratory infections (Driscoll et al., 2007). Patients undergoing mechanical ventilation are at risk of what is termed ventilator associated pneumonia (VAP). VAP infection with *P. aeruginosa* is associated with particularly high rates of mortality, (El Solh et al., 2008). Other respiratory infections caused by *P. aeruginosa* are in patients with some form of underlying condition, such as in patients with bronchiectasis, chronic obstructive pulmonary disease (COPD), and Cystic Fibrosis (CF) (Ryall *et al.*, 2008, Murphy *et al.*, 2008). In patients with human immunodeficiency virus (HIV), *P. aeruginosa* is one of the most commonly infecting bacteria, particularly causing high levels of bronchopneumonia. In patients with CF, *P. aeruginosa* infection is the leading cause of mortality, with some studies showing up to 80% of patients infected with *P. aeruginosa*. In CF patients *P. aeruginosa* infection is chronic, with hypermutable strains adapting over time to switch to a mucoid phenotype (Levy *et al.*, 2008), and multi-antibiotic resistance (Merlo *et al.*, 2007). Patients are often infected by multiple genotypic clones, with both mucoid and non-mucoid phenotypes (Driscoll et al., 2007). Patients also can have individually adapted clones, but increasingly are being 'superinfected' by one of the *P. aeruginosa* epidemic strains (Scott and Pitt, 2004). Chronic infection in CF patients is associated with decreased lung function and increased mortality rates (Treggiari *et al.*, 2007).

1.2.2 Bacteraemia

P. aeruginosa also causes bacteraemia; it is seventh among all pathogens for total number of cases, but ranks second in terms of case fatality with a mortality rate of 38% (van Delden, 2007). Patients at particularly high risk are those with serious underlying conditions (e.g cancer, diabetes, COPD and AIDS). Additional risk factors are: previous

single antibiotic therapy; and vascular or urinary catheters, or endotracheal intubation devices that damage the mucosal membranes and create an environment easily colonised by *P. aeruginosa*. Recent reports from the Health Protection Agency (HPA) have demonstrated that cases of *P. aeruginosa* bacteraemia are on the rise. Since 2004 there has been a 26% increase in the number of cases of *Pseudomonas* spp, with *P. aeruginosa* representing 93% of these cases (HPA, 2009).

1.2.3 UTIs

Urinary tract infections (UTIs) are also caused by *P. aeruginosa*, with *P. aeruginosa* accounting for 8.2 % of all UTI infections in a study in Europe (Bouza *et al.*, 2001). *P. aeruginosa* is particularly associated with complicated biofilm-associated UTIs (Mikuniya *et al.*, 2007). Complicated *P. aeruginosa* UTI infections can lead to fatal bacteraemia in the immunocompromised, and certain other high risk groups (Shigemura *et al.*, 2006).

1.2.4 Burns

P. aeruginosa also causes aggressive and hard to treat infections in burns victims. With up to 10% of patients going on to develop septicaemia which has mortality rates as high as 80% (Gang *et al.*, 1999). Additionally the increase in the number of multi-drug resistant (MDR) strains is making the successful treatment of *P. aeruginosa* burns infections harder to achieve (Douglas *et al.*, 2001) .

1.3 Community acquired infections

P. aeruginosa also causes a range of community acquired infections including infections of the eye, ear, and skin. *P. aeruginosa* is the leading cause of microbial keratitis (MK), either after trauma to the eye, or in persons who use extended-wear contact lenses (Willcox, 2007). The exact reasons for infection in contact lens wearers is

unknown, but it has been hypothesised, that use of contact lenses alters the correct function of tear-borne immune factors, and causes mechanical abrasion to the surface of the eye (Lyczak *et al.*, 2000). If left untreated, infection can have long term risks of vision damage or loss of vision. Other clinically important community acquired infections included otitis externa in immunocompromised patients and swimmers (Driscoll et al., 2007). *P. aeruginosa* also causes soft skin and tissues infections such as diabetic foot osteomyelitis and hot tub folliculitis (Driscoll et al., 2007).

1.4 Treatment of *P. aeruginosa* infections

Current treatment for *P. aeruginosa* infections is based on empirical use of antibiotics. However an increase has been seen in the number of strains with a multi drug resistant (MDR) phenotype to the standard used drugs, (e.g. piperacillin, ceftazidime, imipenem, ciprofloxacin and aminoglycosides). Accordingly, changes have been made to the historical treatment schedules of *P. aeruginosa* infection (van Delden, 2007). Particularly of importance is the initial treatment of infections. Inappropriate treatment e.g. single treatment with an antibiotic to which the bacterium is resistant, significantly affects patient outcome. In *P. aeruginosa* infections due to the increased incidence of MDR infections, initial combination therapy has proven greatly more effective (van Delden, 2007). Additionally, strains with MDR phenotypes, and the lack of new antibiotics has increased the use of older antibiotic such as colistin (Giamarellou and Kanellakopoulou, 2008) and polymyxin B (Zavascki *et al.*, 2007) which are associated with increased side effects. In CF patients a number of different treatment systems have been proposed and used for treatment of chronic lung infection. These include early and aggressive treatment of paediatric *P. aeruginosa* infections (Weiser and Kerem, 2007), use of aggressive combinational antibiotic therapy and the use of nebulised DNase and antibiotics such as tobramycin (Driscoll et al., 2007). Additionally

follow up diagnostic microbiology and antibiotic resistance testing form an important part of the treatment of CF infection.

1.4.1 Future prevention strategies

Vaccine development has reached phase III trials only twice for *P. aeruginosa*. A number of different antigens including pilus, flagella, whole cell live vaccine, O-antigen, and conjugated PS-Exotoxin A have been investigated (Doring and Pier, 2008). However, no vaccine has produced a high quality immune response, in the patient groups tested (Doring and Pier, 2008). This is further compounded by the fact that many of the antigens selected such as flagella undergo diversifying selection and variation in expression (Jyot *et al.*, 2007). This genetic and therefore phenotypic variation probably greatly affects the immunodominance of surface antigens present on *P. aeruginosa* strains which are targeted by these vaccines. Additionally, successful vaccine design is a greater challenge in *P. aeruginosa* than in many other pathogens, as most target patients have some form of immune deficiency. Another important consideration for target groups such as cystic fibrosis patients, are reports of vaccine trials in this group which have resulted in a deterioration in the patients' conditions (Doring and Pier, 2008). More recently the use of passive immunization using pre-formed antibodies against *P. aeruginosa* has gained ground, particularly in immunocompromised patients groups that would be unlikely to elicit a bactericidal antibody titre from vaccination (Doring and Pier, 2008). Clinical studies in this area are on ongoing. Additionally recently there has been a strong intrest in developing drugs that block quorum sensing molecules, with efforts focused on screening small peptide inhibitors and natural compounds such as garlic (Brown et al., 2009, Bjarnsholt et al., 2005b, Hentzer et al., 2003)

1.5 *P. aeruginosa* Virulence Factors and Pathogenesis

Combinational virulence is a hallmark of *P. aeruginosa* infection, with strains having a plethora of different virulence factors which cause the same disease pathology (Lee *et al.*, 2006b). In different strains and at different sites of infection, *P. aeruginosa* strains express a range of different virulence factors, and often as a result have very different pathogenic behaviour in the infectious process. This effect has been shown both *in vitro* experiments on clinical isolates, and in a range of invertebrate and mammalian *in vivo* infection models (Kukavica-Ibrulj *et al.*, 2008, Lee *et al.*, 2006b, Fonseca *et al.*, 2007, Wareham and Curtis, 2007). The result of the infection is directly related to the individual virulence profile of the infecting strain, and the immune response of the patient. Figure 1.1 is an overview of the major virulence factors of *P. aeruginosa*.
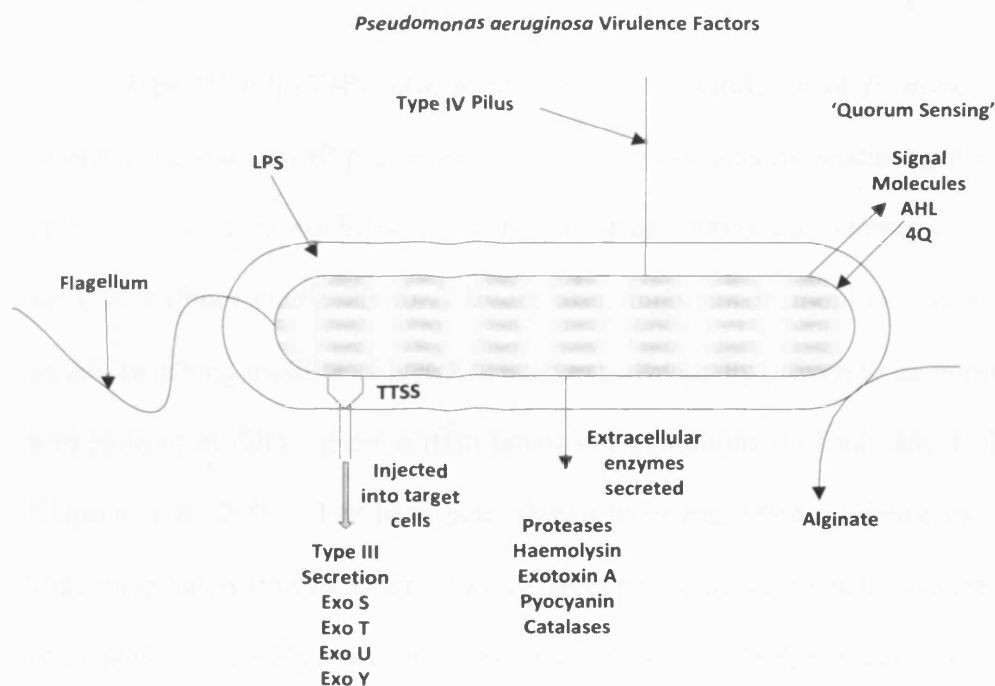
Diagram based on Figure 3 from: Sadikot, R. T., T. S. Blackwell, J. W. Christman & A. S. Prince, (2005) Pathogen-host interactions in Pseudomonas aeruginosa pneumonia. *Am J Respir Crit Care Med* 171: 1209-1223.

Figure 1.1: Virulence factors produced and secreted by *P. aeruginosa*

1.5.1 Motility and attachment related virulence factors

P. aeruginosa posses a wide range of virulence factors that are involved in attachment and motility. Most *P. aeruginosa* strains express polar flagella at some stage in the infectious process. Flagella are complex filamentous structures that have two major functions; facilitating movement in swimming motility (Rashid and Kornberg, 2000) and attachment to epithelial cells. Swimming motility is mediated by the flagella moving in a propeller like motion, and is essential for certain mechanisms in the development of biofilms (O'Toole and Kolter, 1998a). Flagella are also thought to be important for dissemination of the bacteria during the infectious process (Arora *et al.*, 2005). In addition, flagella have a pro-inflammatory role, by activating the NF-κB arm of the innate immune system by binding with Toll-like receptors TLR-5 and TLR-2, causing production of the pro-inflammatory IL-8 (Jyot et al., 2007).

Type IV pili (T4P) have a dual role in the virulence of *P. aeruginosa*. Many studies have shown T4P play a specific role in infections by mediating the attachment of *P. aeruginosa* to epithelial cells (Kipnis *et al.*, 2006) and binding to many abiotic surfaces (Giltner *et al.*, 2006). T4P are also important in motility, via a mechanism called 'twitching motility' which has been experimentally proven to be important in the formation of biofilms under certain laboratory conditions (O'Toole and Kolter, 1998a, Klausen et al., 2003). T4P have been shown to be important virulence factors *in vivo*, with nonpiliated mutant strains having reduced virulence in both murine models of acute pneumonia and corneal infection (Comolli *et al.*, 1999, Farinha *et al.*, 1994, Tang *et al.*, 1995, Zolfaghar *et al.*, 2003).

1.5.2 Cell surface and secreted virulence factors

1.5.2.1 *LPS*

The lipopolysaccaride (LPS) of *P. aeruginosa* is made up of three individual components; the lipid A portion that is anchored in the outer membrane, the core oligosaccharide, and the O-antigen which is made up of repeat saccharide units. The O-antigen portion of the *P. aeruginosa* LPS is responsible for conferring serogroup specificity of which there are 11 groups. This specificity was used for strain typing and epidemiology before advent of genomic methods (Kintz and Goldberg, 2008). *P. aeruginosa* produces two types of O-antigen; the B-band O-antigen and the A-band O-antigen. The B-band is a heteropolymer of repeating saccharide, and of the two antigens, it is longer and therefore is the immunodominant of the two (Kintz and Goldberg, 2008). The A-band antigen is homopolymer and made up of repeats of D-rhamnose. The role of the O-antigen in *P. aeruginosa* infections has been characterised; O-antigen has shown to be critical in burn, corneal, and pneumonia models of murine infection, particularly in dissemination from the site of infection (Kintz and Goldberg, 2008). Strains that lack the B-band antigen O-antigen side chains are serum sensitive (Kintz and Goldberg, 2008). The LPS also plays a role in the adherence to epithelial cells (Kintz and Goldberg, 2008) and has been demonstrated to bind to asialo-GM1 and CFTR. By the presence or absence of the B-band, O-antigen, strains are classified as 'smooth' (B-band +ve) or 'rough' (B-band –ve). The predominance of rough strains in CF is thought to be an adaptation to the lung environment, as LPS rough strains although not able to disseminate from the lung, are not attenuated in causing lung infections (Priebe *et al.*, 2004). The rough LPS phenotype is more like the lipooligosaccharide of *Haemophilus influenza* and *Neisseria meningitidis,* both of which are successful respiratory colonisers, this phenotype in *P. aeruginosa* has been

hypothesised as possible adaptation to the respiratory environment (Kintz and Goldberg, 2008).

1.5.2.2 *Alginate*

P. aeruginosa alginate is an excreted exopolysaccharide, made up of β-1,4-linked monomers of β-D-mannuronic acid and C5-epimer α-L-guluronic acid . The expression of alginate in *P. aeruginosa* is caused by mutations inactivating *mucA*, which encodes an anti-σ factor, this leads to the deregulation of an alternative σ factor (σ-22, AlgT or AlgU) which is required for expression of the alginate biosynthetic operon and the production of alignate (Mathee *et al.*, 1999). This switch in *P. aeruginosa* infection is known as mucoid conversion, and is associated with the change from planktonic to biofilm lifestyle. Mucoid strains are most frequently isolated from CF patients, suggesting the mucoid phenotype and therefore alginate production is an adaption that contributes to survival in the lung in chronic respiratory infection. In chronic lung infection alginate plays a number of roles that are advantageous to the bacteria: the alginate protects from antibody-dependent bactericidal mechanisms, additionally antibodies that form against alginate are non-opsonic (Jain and Ohman, 2004). Alginate also prevents correct leukocyte function, by preventing the oxidative burst, inhibiting opsonisation, and modulating the immune response by inducing pro-inflammatory cytokines and by suppressing lymphocyte transformation (Jain and Ohman, 2004). The physical coating of the bacteria by the alginate prevents antibiotics diffusing and reaching the bacteria cells and the thick viscosity of the alginate also prevents normal mucociliary function and clearance and the movement of phagocytes in the lung (Jain and Ohman, 2004, Kipnis et al., 2006).

1.5.2.3 *Type III secretion system and effectors*

The Type III secretion system (T3SS) in *P. aeruginosa* is a significant determinate of virulence. T3SS allows *P. aeruginosa* to damage host tissue, increase dissementation (Yahr and Wolfgang, 2006), allows intracellular growth (Angus *et al.*, 2008), and plays a major role in anti-phagocytosis. As in homologous systems in *Salmonella, Shigella,* and *Yersinia* species, the function of T3SS is to translocate / inject effector proteins into the cytoplasm of target eukaryotic target cells. In *P. aeruginosa* the TTSS, or injectisome, is of the Ysc type (Cornelis, 2006) closely related to that of *Yesinia spp*, and is made up of four parts. The four parts are the basal body, needle, translocator assembly platform PcrV, and translocation pore that is assembled on PcrV when the needle makes contact with the target cell membrane (Cornelis, 2006). The Translocation pore is formed in the target cell membrane allowing transfer into the cytsol of the effector protein (Cornelis, 2006). The T3SS of *P. aeruginosa* has four effector proteins (ExoS, ExoT, ExoU, and ExoY) that are variably present and expressed in different strains (Wareham and Curtis, 2007) (Table 1.1). It is hypothesised that strains like PA14 (Lee *et al.*, 2006b) that express ExoU, will lead a extracellular, cytotoxic and invasive lifestyle causing acute infections, while strains that express ExoS like PAO1 (Stover et al., 2000) are more suited to intracellular lifestyle and colonisation, and as a result more likely to cause chronic infections (Wareham and Curtis, 2007). The *P. aeruginosa* T3TS has also been shown to be essential in infecting eukaryotic hosts such as *Acanthamoeba castellanii,* and *Galleria mellonella* (Abd *et al.*, 2008, Matz *et al.*, 2008, Miyata *et al.*, 2003). Reinforcing the view that virulence factors present in the *P. aeruginosa* population and individual strains have evolved due to *P. aeruginosa* being a multihost pathogen (Lee *et al.*, 2006b). Finally, mutants strains that are unable to express any effector proteins (Kipnis et al., 2006) but with functional

T3SS apparatus are still cytotoxic, possibly due to the pore forming activity of the T3SS needle (Stepinska and Trafny, 2008). However this demonstrates that there are still unknown roles of the T3SS still to be elucidated.

Table 1.1: Type three secretion effectors

Effector	Target(s) and mechanisms of action	Role	Abundance	Reference s
ExoS	- Small Rho GTPases - Causes structural damage to the target cell cytoskeleton. - Binds to host proteins	- Inhibition of phagocytosis. - Causes cytotoxicity.	~72% of strains	(Deng et al., 2007, Stepinska and Trafny, 2008)
ExoU	-Targets both neutral lipids and phospholipids in the plasma membrane causing cell lysis	- Inhibition of phagocytosis and invasion. - Prevents pyroptotic cell death in macrophages.	~28 % (higher proportion in bloodstream isolates)	(Rabin and Hauser, 2005b, Plotkowski et al., 2008a, Stirling et al., 2006, Angus et al., 2008, Diaz et al., 2008)
ExoY	-Host factor dependent cyclase. -Clevates intracellular cAMP concentration	-Increases tissue permeability. -Inhibition of bacterial uptake by host cells.	~89% of isolates	(Kipnis et al., 2006, Feltman et al., 2001, Hauser, 2009)
ExoT	- GAP activity towards Rac, Rho and CDC42 -Inhibition of cytokinesis - Disrupts the actin cytoskeleton.	- Anti-internalisation factor, and causes cell rounding . - Brings about apoptotic-like cell death -Blocks phagocytosis and disrupts epithelial barriers	~92–100% of isolates	(Engel and Balachandran, 2009, Hauser, 2009, Shafikhani and Engel, 2006)

1.6 Other P. aeruginosa virulence factors

In addition to the virulence factors already described, Table 1.2 shows the wide range of other *P. aeruginosa* secreted virulence factors that play varying roles in the numerous types of infection caused by *P. aeruginosa*. The large range of virulence factors is part of *P. aeruginosa* 'combinational virulence' that uses different combinations of virulence factors dependent on the type of infection and allowing it to cause infection in a wide range of hosts and tissues (Lee *et al.*, 2006b, Rahme *et al.*, 1995).

Table 1.2: *P. aeruginosa* virulence factors.

Virulence factor	Target / mode of action	Role	References
Exotoxin A	Exotoxin A is an ADP-ribosyl transferase which inhibits elongation factor -2 (EF-2) causing an inhibition of protein synthesis which results in cell death.	Impairs the host response.	(Vasil et al., 1986, Rumbaugh et al., 1999, Schultz et al., 2001, Wolf and Elsasser-Beile, 2009)
Pyocyanin	Affects a mammalian cell by inhibiting cell respiration, ciliary function, epidermal growth, and inactivates catalase causing oxidative stress damage	Induces IL-8 expression, influx and apoptosis in neutrophils, and affects the general host response. Tissue damage.	(Lau et al., 2004b, Lau et al., 2004a, Allen et al., 2005, Bianchi et al., 2008)
Pyoverdine	Primary siderophore (iron uptake).	Regulates a number of other virulence factors including exotoxin A	
Phospholipase C	Targets phospholipids found on eukaryotic cell membranes.	It has been demonstrated to be cytotoxic and specifically alters signalling processes in eukaryotic cells, including the suppression of respiratory burst in neutrophils. Inhibit surfactant function.	(Woods et al., 1997, Terada et al., 1999, Barker et al., 2004, Kipnis et al., 2006)
Elastase	Destroys the tight junctions, degrade collagen, fibrin, and elastin. Cleaves immunoglobulin, serum complement factors, surfactant proteins A and D. Along with alkaline protease acts synergistically to inactivate interferon-γ and tumor necrosis factor alpha (TNF-α)	Makes the epithetical barrier more permeable. Pro-inflammatory action by increasing IL-8 production. Modulates immune response. Overall impairment of host response.	(Rust et al., 1996, Mun et al., 2009)
Protease IV	Serine endoprotease degrades surfactant proteins A and B. Breaks down immunoglobulin, complement components, elastin, fibrinogen, and plasminogen.	Prevent surfactant proteins A (SP-A) and B (SP-D) mediated bacterial aggregation and uptake by macrophages. Breaks down immunologically and structurally important proteins.	(Caballero et al., 2004, Malloy et al., 2005, Smith et al., 2006, Willcox, 2007, Engel et al., 1998)

1.7 Quorum sensing

Cell to cell communication via Quorum sensing (QS) has been shown to play an important role in the regulation of bacterial behaviour. It was first discovered in *Vibrio fischeri,* when it was observed that the bioluminescence produced by this bacterium was produced above certain numbers of bacteria in the population (Nealson et al., 1970). In simple terms quorum sensing works by members of a bacterial population secreting signal molecules into the environment. Once the molecules have reached a threshold concentration (and therefore a certain number of bacteria present within the population) the bacteria detect this and respond by up and down regulating genes co-ordinately as a population. In terms of virulence this synchronised group behaviour is thought to allow pathogens to only express certain virulence factors at a point when the population is large enough to sustain the infection. A large number of *P. aeruginosa* virulence factors and bacterial behaviours are regulated by QS. It has been shown by microarray that >5% of the *P. aeruginosa* genome is part of the QS regulon (Wagner et al., 2003). The quorum system in *P. aeruginosa* is based on two separate signal systems; Acyl homoserine lactone (AHL) signal molecules and 4-quinolones (4Qs). *P. aeruginosa* has two AHL systems; *las* and *rhl*, each of which has its own LuxRI homologue; LasRI (Latifi et al., 1995) and RhlRI (Ochsner and Reiser, 1995) respectively. The LasI system signal molecule 3-oxo-C12-HSL together with the transcriptional regulator LasR controls the production of LasA protease, alkaline protease, elastases, and exoxtoxin A virulence factors (Popat *et al.*, 2008). The Rhl signalling molecule C4-HSL activates RhlR and together they control production of rhamnolipid, LasA protease, hydrogen cyanide, pyocyanin, and siderophore virulence factors (Popat et al., 2008, Pearson et al., 1997, Pessi and Haas, 2000, Winson et al., 1995). The *las* and *rhl* systems have a hierarchical structure, with the *las* system having control over the *rhl* system, although

more recent work has demonstrated that the *rhl* system can be independently activated

(Winson et al., 1995) possibly through the PQS system (Diggle *et al.*, 2006). The 4Q

system is also important for virulence in *P. aeruginosa*, one of these compounds termed

'the pseudomonas quninolone signal' (PQS) is another important regulator of virulence

genes in *P. aeruginosa* (Popat et al., 2008). The PQS system is regulated by both the *las*

and the *rhl* systems through regulation of expression PqsR which regulates to the

production of PQS (Wade et al., 2005, Diggle et al., 2003). The expression of PqsR is

positively regulated by the *las* quorum-sensing system and negatively by the *rhl*

quorum-sensing system (Wade et al., 2005). The PQS system regulates the production

of elastase, rhamnolipid, and pyocyanin (Diggle et al., 2006, Pearson et al., 2000,

Pearson et al., 1997). The importance of QS in murine, rat, *C. elegans* and *Arabdopsis*

models of *P. aeruginosa* infection has been demonstrated (Rumbaugh et al., 2000,

Winstanley and Fothergill, 2009, Imamura et al., 2005). QS has been shown to play a

role in biofilms, although with some contradictory and conflicting reports regarding if

QS is required for the formation of normally structured biofilms (Davies et al., 1998,

Heydorn et al., 2002, Bjarnsholt and Givskov, 2007) However *in vitro* it has been

shown that lacking QS produces less structured biofilms that are more susceptible to

clearance with antibiotics (Diggle *et al.*, 2007a). A number of studies have shown a role

for QS in antibiotic resistance and tolerance of detergents, including resistance to many

clinically important antibiotics for the treatment of *P. aeruginosa* infections (Bjarnsholt

et al., 2005a, Hentzer et al., 2003, Shih and Huang, 2002). QS compounds also seem to

have a immunomodulatory role. For example, 3-oxo-C12-HSL regulates IL-1α, IL-2,

IL-6, IL-8, and IL-12 levels (Smith et al., 2001, Boontham et al., 2008), activates T-cell

production of TNF-α (Chhabra et al., 2003), and reduces the life span of macrophages

and PMNs via apoptosis (Tateda et al., 2003). The effect of QS on population ecology is

a fascinating area, with mutants lacking functional QS systems being found as part of QS +ve populations. The current thinking is that these bacteria are exploiting the fitness of the QS population as a whole, while themselves not expending the higher costs that are associated with producing QS signals and expression of QS regulated genes. This behaviour has been termed 'social cheating' (Diggle *et al.*, 2007b). Finally there is still controversy regarding the role of QS on pathogenicity with some studies suggesting that QS is lost as part of a chronic infection, and that in some cases QS may actually be detrimental to bacterial fitness (Winstanley and Fothergill, 2009).

1.8 *Pseudomonas aeruginosa* as a multihost pathogen

P. aeruginosa has been shown to be pathogenic to a wide range of different fungi, plant, insects, and animal species (Hendrickson *et al.*, 2001, Tan *et al.*, 1999, Rahme *et al.*, 1997, Rahme *et al.*, 1995). Many of the virulence factors shown to play a role in humans and other mammals have been demonstrated to be important to infection in a wide range of other hosts. Plants and organisms that *P. aeruginosa* has found to be pathogenic against include; *Caenorhabditis elegans, Galleria mellonella, Drosophila melanogaster, Arabidopsis thaliana, Acanthamoeba* spp., Yeast, and Romaine lettuce (*Lactuca sativa* L. var. *Longifolia)* (Mahajan-Miklos et al., 2000, Rahme et al., 2000, Jander et al., 2000). This finding is not extraordinary given the wide range of environments that *P. aeruginosa* is isolated from, and the overlap in the presence of some of the hosts. For example *Acanthamoeba* spp. and *P. aeruginosa* are found ubiquitously throughout aqueous environments (Matz et al., 2008). It has been demonstrated that *Acanthamoeba* spp. can be pathogenic towards *P. aeruginosa*. Therefore it is not surprising that *P. aeruginosa* has also evolved mechanisms to be pathogenic towards *Acanthamoeba* spp, to prevent *P. aeruginosa* being grazed upon (Matz et al., 2008, Abd et al., 2008). These findings suggest that the virulence factors

that are essential for full virulence in humans have evolved to protect and support *P. aeruginosa* strains in interactions with other organisms in natural environments. However this ability of *P. aeruginosa* to infect a wide range of hosts, linked with the availability of full genome sequences, is proving to be a most useful combination in understanding the pathogenicity of *P. aeruginosa*, and therefore in the long term discovery of therapeutics. Use of non-mammalian models allows for the high throughput identification of virulence factors, without the need to encounter the ethical and financial costs associated with mammalian models of infection. Furthermore, the simplicity and reproducibility of the non mammalian assays allows for virulence testing being a routine laboratory practice.

1.9 Bacterial Genomes

1.9.1 Overview

Since the publication of the first bacterial genome sequence of *Haemophilus influenzae* in 1995 by J. Craig Venter's group (Fleischmann *et al.*, 1995) hundreds of bacterial genomes have been sequenced to date. This exponential flow of new sequence data has profoundly changed the way biological scientists view bacterial diversity, and spawned whole new fields of research such as comparative genomics. The production of the vast amount of new sequence data has led to the rapid expansion of bioinformatics, which is needed more and more as new sequence data is generated and in need of analysis. With the advent of pyrosequencing and the other rapid sequencing technologies that are decreasing the cost and time required to sequence a whole bacterial genome, we are rapidly approaching a time when whole genome sequencing will become a routine laboratory procedure.

1.9.2 Core genome and accessory genome

The sequencing of bacterial genomes has led to a wider understanding of the structure, conservation and dynamics of bacterial genomes. The genes encoded on bacterial genomes can be divided into two separate groups; the highly conserved 'core' genome, and highly variable and often mobile 'accessory' genome. The core genome is defined as the essential genes for the basic biology and phenotype of the particular bacterial species (Tettelin *et al.*, 2008). All members of a bacterial species will share the majority of these genes, with a very high level of conservation. The accessory genome conversely, is highly divergent even within the same bacterial species. As more bacterial genomes are sequenced it has now been realised that most individual bacterial strains have unique accessory genomes, which in some species can account for a large variation in genome size and content. This has given rise to the idea of a 'pan' or 'supra' -genome which encompasses all the genes encoded on both the core and accessory genomes in all the strains within a species (Tettelin *et al.*, 2005). However the lifestyle of the bacterium in question, profoundly affects the size of the pan genome. Bacterial species can be grouped according to their lifestyles and genomic content and diversity (Table 1.3) (Ochman and Davalos, 2006), with different selective pressures altering bacterial genomes in different ways. In general, free living bacteria have larger genome sizes, due to the selection for genes encoding the ability to survive in a wide range of environments, and thus having an 'open' pan genome (Pallen and Wren, 2007). Whereas bacteria that are environmentally isolated or limited to a finite niche do not have the access to other bacteria and phages for horizontal DNA transfer and may also be under selective pressure to reduce their genome size, and have a 'closed' pan genome.

Table 1.3: Effects of Bacterial Lifestyle on Genome content and structure[1]

Lifestyle	Free living	Recent or facultative pathogen	Obligate symbiont or pathogen.
Genome size	5-10Mb	2-5Mb	0.5-1.5Mb
Pseudogenes	Few	Many	Rare
Horizontal gene transfer	Frequent	Frequent to rare	Rare to none
Selfish genetic elements	Few	Common	Rare
Genomic organisation	Stable or unstable	Unstable	Stable
Population size	Large	Small	Small
Example Species	*Myxococcus xanthus (9Mb)*	*Yersinia pestis (4Mb)*	*Mycoplasma pneumonia (816Kb)*

The size of the accessory genome in bacterial species is strongly correlated with the need to allow for niche adaptation. The accessory genome is made up of various horizontally acquired elements. Horizontally acquired elements include prophages, transposons, integrons, plasmids, integrative conjugative elements, and genomic islands. In many bacterial species the largest variation within the genome is in genomic islands.

1.9.3 Genomic islands

The term genomic island originates from 'Pathogenicity islands' (PAI) (Hacker *et al.*, 1990) which are defined as large regions of DNA encoding virulence factors that were found to be deleted from uropathogenic *E.coli*, and were found not to be present in closely related strains. In its broadest sense, a genomic island is a region of a bacterial genome that has been acquired from a lateral source, irrespective of the method of transfer; this can be from bacteria of the same or divergent species. It is a region of the genome that has a different origin or has been more recently acquire than the rest of the 'core' genome. In this work, this is the definition that will be used.

---

[1] Table reproduced and modified from OCHMAN, H. & DAVALOS, L. M. (2006) The Nature and Dynamics of Bacterial Genomes. *Science,* 311, 1730-1733.

The term genomic island has become to mean many different things. This is because genomic islands originate from many different types of mobile elements and are often made up of different combinations of mobile elements inserted into the genome. It seems the analogous structure of genomic islands; including core functional components and mechanistic features that are associated with genomic islands, have formed through convergent evolution into what now is referred to and described above as a 'genomic island'(Juhas et al., 2009, Juhas et al., 2007b, Vernikos and Parkhill, 2008). Other publications have named these broader genomic regions as regions of genome plasticity (RGP) (Mathee *et al.*, 2008).
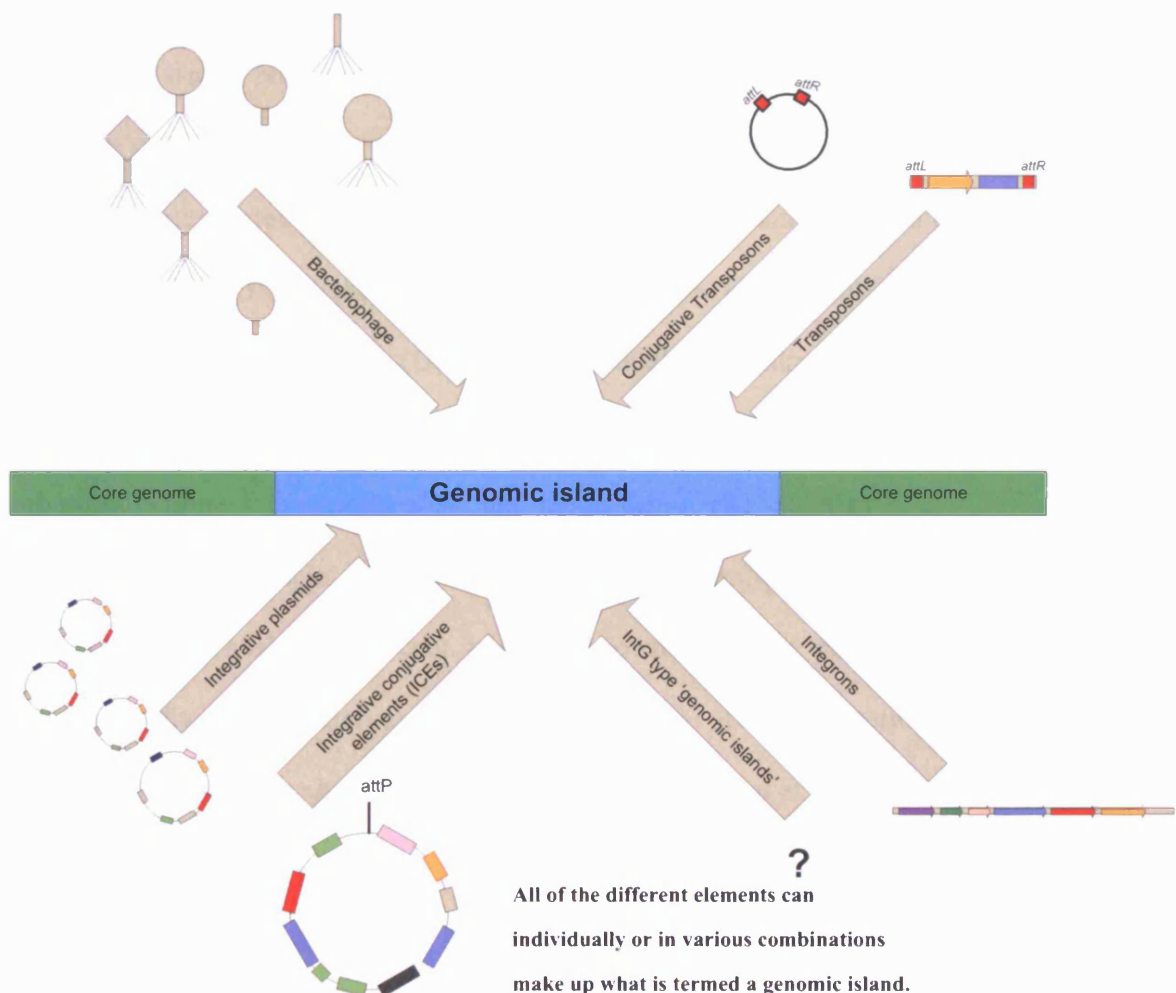
Figure 1.2: Elements that can make up genomic islands.

1.9.3.1 *Structure of archetypical genomic islands*

The structure of an archetypical genomic island is shown in Figure 1.2, in general they are 10 – 300Kb (<10 Kb is known as a genomic islet) in size. The insertion of genomic islands is often by site-specific recombination. In ~75% of all known islands the 3'-end of a tRNA gene is used as the *attB* site to insert into the genome (Vernikos and Parkhill, 2008). The integration mediated by site- specific recombination is further supported by the fact they often encode motility genes (e.g integrases / transposases) and are flanked by direct repeats (DR) 16-20bp long, that act as the recognition sites for site specific integration (Pavlovic *et al.*, 2004). Genomic islands usually show divergence in nucleotide content (e.g. G/C content (Figure 1.3)) to that of the core genome of the bacteria, as would be expect with the transfer of DNA from one species to another. However this is not always true; especially in islands that may have transferred from closely related species with similar nucleotide bias. The islands are also often found to contain multiple IS elements, which can mediate recombination within islands producing significant diversity (Doublet et al., 2008b), and take part in island instability and excision (Gal-Mor and Finlay, 2006). Islands are further sub-divided into numerous sub types (Figure 1.3) dependent on the 'cargo genes' (Klockgether *et al.*, 2007a) that they carry. For example genomic islands that carry antibiotic resistance genes are termed 'resistance islands'. Recent work has shown that many genomic islands can be experimentally demonstrated to be mobile and capable of transfer between members of the same and divergent species (Chen and Novick, 2009, Qiu et al., 2006, Gaillard et al., 2008), with varying frequency of transfer. How they do this depends on their evolutionary origins, as some genomic islands like the *Staphylococcus aureus* pathogenicity islands (SaPIs) are transferred packaged as phage (Novick *et al.*, 2001).

GC Content (%)

Divergent G/C content from Core Genome

DR of 3' tRNA
(attL)

DR of 3' tRNA
(attR)

Core Genome

tRNA

Integrase

IS

IS

Core Genome

Cargo genes on Genomic islands- define island sub-type:
Pathogenicity island = Virulence factors
Metabolic islands = Genes for metabolic pathway
Fitness islands= Fitness genes
Symbiosis islands = Symbiosis genes
Resistance Islands= Antibiotic resistance genes

Figure 1.3: Diagram showing archetypical features of a genomic island.

Other elements like the *clc* element in *Pseudomonas* sp. strain B13 are thought to transfer conjugatively, mediated through type IV pili (Sentchilo *et al.*, 2009)   Genomic islands are often unstably integrated into the genome and delete at varying frequencies dependent on the specific islands and bacterial species but most are within the region of 10^{-5} to 10^{-4} (Klockgether *et al.*, 2007b).

1.9.3.2 *Pathogenicity islands*

Genomic islands have attracted much attention in recent years as many key determinates of bacterial pathogenicity have been found to be encoded by pathogenicity islands (Gal-Mor and Finlay, 2006). In many bacterial species (Table 1.4) pathogenicity islands are the key determinates of that species pathogenicity, and without the island, strains would be avirulent. A classic example is the High pathogenicity island (HPI) required for iron uptake in *Yersinia spp* (Schubert *et al.*, 2004). Furthermore, the acquisition of a pathogenicity island in an avirulent strain has been experimentally demonstrated to instantly transform the stain into a pathogen, in what is often referred to

as a 'quantum leap' in evolution (McDaniel and Kaper, 1997, Groisman and Ochman, 1996). Recent studies have shown how transcriptional regulators (Coburn *et al.*, 2008, Abe *et al.*, 2008) and small RNAs (sRNAs) (Pichon and Felden, 2005) encoded on islands regulate the expression of genes on the core genome, demonstrating that the genes encoded on genomic islands can modulate global gene expression. However, not all genes encoded on genomic islands are thought to be expressed. This is due to expression difficulties associated with bacterial promoters in non-host species (Wilson and Nickerson, 2006). Also island DNA expression is regulated via transcriptional repression due to the histone-like nucleoid structuring (H-NS) protein binding to foreign DNA in its role as the so called 'genome-guardian' (Dorman, 2007, Navarre *et al.*, 2007, Lucchini *et al.*, 2006). Up regulation has also been reported by nucleoid-associated proteins such as integration host factor (IHF) (Fass and Groisman).

1.9.4 Genomic islands: origins and evolution

'How genomic islands form and evolve is still an area of active research with no clear models of how islands form. However, in many islands the hallmarks of bacteriophage, transposons, integrons and plasmid genes are still present suggesting that the considerable diversity of genomic islands is driven by the convergent evolution of a wide range of elements into what we now call genomic islands. A widely accepted hypothesis is that plasmids and bacteriophage that are capable of integrating into the genome lose their ability to replicate independently of bacterial chromosome replication via mutation or insertion in motility genes of mobile elements, and therefore become 'locked in'(Kulasekara et al., 2006). However, other findings offer alternatives: the normally non-mobile HPI in *E.coli* ECOR31 was found to be mobile due to acquiring a separate mobility module, suggesting island mobility process may be both lost and gained (Boyd et al., 2009).

Table 1.4: Pathogenicity islands in different bacterial species pathogenic to humans

Species	Island	attB	Size	Key genes	Role	Reference
E.coli	PAI-1	tRNA^{selC}	76 kb	alpha-hemolysin-encoding gene cluster, adhesins, fimbriae	Attachment and full pathogenicity in uropathogenic *E.coli* strains	(Brzuszkiewicz *et al.*, 2006)
E.coli	LEE PAI	tRNA^{selC}	35kb	Type III secretion system (T3SS), secreted translocator proteins, ahesins.	Attachment to host intestinal epithelium and efface brush border microvilli in Enteropathogenic *E. coli* (EPEC) strain	(Gal-Mor and Finlay, 2006)
Yersinia spp.	HPI	*tRNA^{asn}*	~40kb	Sidephore yersiniabactin	Acquisition of iron from host, confers a highly pathogenic phenotype	(Schubert et al., 2004)
Salmonella spp.	SPI-1	flhA-mutS	40kb	T3SS system and an iron uptake system	Invasion of non-phagocytic cells by *Salmonella* and the inflammation of the intestinal epithelium and associated diarrhoeal symptoms	(Hensel, 2004)
Enterococcus faecalis	*E. faecalis* PAI	non-coding region	150 kb	Esp and cytolysin	Colonization of the bladder and biofilm production capability	(Shankar *et al.*, 2002)
Staphylococcus aureus	SaPI1	*tyrB* (but has secondary attB sites)	~15 kb	*tst* a potent superantigen and *sek* a second super antigen	Non-specifically activate T lymphocytes (15 -50% of Total T-cells) causing high fever, rash, vomiting, diarrhoea, renal and hepatic dysfunction, and desquamation. They are also directly cytoxic;.	(Novick, 2003, Novick *et al.*, 2001)

Many genomic islands like the integrative conjugative element (ICE) PAPI-1 in PA (He et al., 2004) exist in an extrachromosomal circular plasmid-like form, and are mobile via conjugation, but do not possess an origin of replication. These elements share high levels of homology with related entities that have been demonstrated to possess an origin of replication and exist in plasmid form in multiple copies like the related pKLC102 (Klockgether et al., 2007b, Wurdemann and Tummler, 2007). Other work has shown the presence of related non-mobile islands locked into the genome, in forms that seem to have undergone significant reductive deletions until only genes that provide a high level of fitness are left (Kulasekara et al., 2006, Pavlovic et al., 2004).

Recently the case has been made that the original group of genomic islands from which the archetypical definition of a genomic islands is derived are an unique lineage (Boyd et al., 2009) It is argued that these genomic islands in E.coli, Salmonella and Shigella etc should be classified as a separate group called 'genomic islands' that are an evolutionary separate lineage. This study compared integrase genes, and defined a group with integrases all related to InG1, distinct from phage integrase. Genomic islands in this group were found not to have any phage, conjugation systems, or self mobility genes encoded on them (Boyd et al., 2009). The authors suggest compellingly that they are a separate lineage distinct from ICEs, conjugative transposons, phage, integrons etc, and should be named as such. This is a fascinating finding that opens up many questions regarding the evolutionary history and dynamics of this group of genomic islands. But it can be argued that the term genomic island is now widely used as a much broader term, and cannot just be applied to a single group. It is probably better that these islands be classified as InG1 type genomic islands to avoid more unnecessary complexity.

However, most of the work on genomic island evolution is theoretical, based on sequence and/ or phylogenetic analysis. There as yet there is no definitive experimental data to show the exact mechanisms of island evolution, particularly as loss and gain of mobility is likely to be a dynamic process. Genomic island-like structures encoding fitness determinates could also evolve to become mobile or replicative by acquisition of respective genes on transposons etc. The ability for these entities then to be able to autonomously replicate would remove the link between their survival and the survival of the host genome. This would make evolutionary sense in a selfish DNA model (Orgel and Crick, 1980). In summary, genomic islands form from combinations of many different elements and seem to undergo reductive evolution gradually losing genes that are not selected for in the inhabited niche, as well as gaining *de novo* DNA via transposons, insertion sequences (IS), integrons, composite and tandem island integrations. It seems that no one model of genomic island evolution will fit, due to the vast diversity of genomic islands themselves and their origins.

1.9.5 attB sites

The attachment site (*attB*) for the majority of genomic islands is located at the 3'-end of a tRNA or tmRNA gene (Ou *et al.*, 2006c). Functional *attB* sites are generally around ~50bp in size but regions as small as 15bp have been described to be functional (Williams, 2002, Wilde *et al.*, 2008). The *attB* sites for integrases such as tyrosine family recombinases XerC and XerD, are made up of a core region of 6–8 bp where the 5' strands are exchanged, which is flanked by two core sites (CSs) of 9–13 bp (often inverted) (Wilde et al., 2008, Williams, 2002). This model of *attB* sites although not being truly generic, is a good basic structure for most *attB* sites used by genomic islands. Evolutionary reasoning for the selection of tRNA sites as the *attB* site for integration, is that tRNA are highly conserved at both inter and intra species level,

allowing for transfer across species. tRNA show an average six fold lower rate of sequence divergence compared to protein coding genes (Williams, 2002). The small size of tRNAs may also have selected them, as only a small region of DNA is required to be in the *attP* region to restore the target gene in which the *attB* is present (Williams, 2002). However the selection of certain tRNA loci for integration is still an area of active research with tRNA copy number relative to codon usage, local and tRNA expression levels, and both global and local DNA secondary structure being hypothesised to play a role in the selection of integration sites (Germon *et al.*, 2007).

1.9.6 Mechanisms of island transfer

Genomic islands can be transferred from host strain to host strain by a number of different methods but essentially there are three major mechanisms of island transfer: conjugation, transduction and natural transformation.

1.9.6.1   *Conjugation*

Conjugation is thought to play an important role in the transfer of genomic islands. In many genomic islands the genes for Type IV pilus or other related structures have been found. In particular one group of pilus know as the 'GI type' which is distinct from the other described, is found on genomic islands in a wide range of bacterial species (Juhas *et al.*, 2008, Juhas et al., 2007a). The deletion of one such GI type pilus cluster on the ICE*Hin1056* genomic island of *H. influenzae* caused a dramatic reduction in conjugation efficiency (Juhas et al., 2007a), demonstrating the role of these pili in conjugation and transfer of genomic islands. The mechanism of the conjugation of plasmids / ICEs / genomic islands is thought to take place as follows: firstly the two cells make contact and the pilus and / or other adhesins known as coupling proteins hold the donor and the recipient cell together (Juhas et al., 2008, Matxalen *et al.*, 2002). This then activates the relaxase which is a DNA endonuclease which binds to the origin of

transfer (*oriT*) and then makes a single strand break at the *oriT* sequence (Snyder and

Champness, 2007, Matxalen et al., 2002). Then with the action of a DNA helicase to

unlink the double helix, the relaxase and one of the single strands of DNA is transferred

either through a pore in two conjugating cells or directly through the pilus structure

itself (Snyder and Champness, 2007, Matxalen et al., 2002). A DNA primase enzyme

which was injected with the DNA from the host cell, then primes the replication via

rolling cycle-like replication of the complementary strand. The remaining single strand

copy of the island in the host cells is then replicated using the nicked 3' end as a primer,

thereby ensuring that both cells have a copy (Snyder and Champness, 2007, Matxalen et

al., 2002). Some of the fine detail in this model of conjugation is yet to be exactly

characterised. However, recently some very eloquent studies using visualisation

techniques to watch the conjugation process and horizontal gene transfer in 'real-time'

are starting to reveal much greater detail of this dynamic process (Babic *et al.*, 2008). If

genomic islands either encode their own functional systems or hitch a ride with other

plasmids and conjugative elements remains to be seen.

1.9.6.2 *Transformation*

Natural transformation occurs as the uptake of naked DNA from the environment, this

has been reported occurring in a number of different bacterial strains. The uptake of

DNA through bacteria being naturally competent; that is in a specific physiological state

caused by expression of genes involved in the DNA uptake mechanisms (Juhas et al.,

2009). Transformation has been especially studied in a number of gram positive

pathogens such as *Neisseria gonorrhoeae* and *Streptococcus pneumoniae.* Some

bacteria such as *N. gonorrhoeae* and *H. influenzae* have uptake mechanisms that

specifically favour DNA containing a defined 10 bp sequence allowing for species

specific uptake (Juhas et al., 2009). The gonococcal genetic island (GGI) which encodes

a Type four secretion system (T4SS) that secretes genomic DNA (itself including) is one example of island transfer by transformation (Holly and Joseph, 2006).

1.9.6.3   *Transduction*

Transduction is the process in which DNA is transferred from one bacterium to another by being incorporated within a bacteriophage, either specifically (specialised transduction) or non- specifically, that is packaged by accident by general transduction. The specialised transduction transfer of genomic islands has been reported and especially well studied in the case of the SaPaI island family which carry the superantigens of *Staphylococcus aureus* (Novick *et al.*, 2001). The SaPaI pathogenicity islands excise from the genome and are packaged into a phage, the phage then transfers to a new host and injects the DNA which then integrates back into the genome (Novick, 2003). Most interestingly in a recent publication this was shown to occur across bacterial species from *S. aureus* into *Listeria monocytogenes* (Chen and Novick, 2009).

1.10 *Pseudomonas aeruginosa* genome diversity, dynamics, and evolution

1.10.1 *P. aeruginosa* genome sequencing and diversity

At the time of writing there are a total of twelve *P. aeruginosa* genomes being, or fully, sequenced. The first *P. aeruginosa* genome was the genome of the wound isolate and laboratory strain PAO1 published in 2000, (Stover et al., 2000). Since then six more genomes have been completely sequenced. The published genomes range from 6.2 Mbp of the CF derived Manchester epidemic strain C3719 to the 6.9 Mbp again CF derived 2192. Additional studies have shown, using pulse field gel electrophoresis (PFGE) that *P. aeruginosa* genome size can vary from 5.2 to 7 Mbp (Head and Yu, 2004, Cornelis, 2008). Studies investigating the genome plasticity of *P. aeruginosa* strains globally showed they differ from each other on average by ~11% (Shen *et al.*, 2006). The most

detailed analysis so far of five fully sequenced *P. aeruginosa* genomes (PAO1, PA14, PACS2, PA2192, and C3719) revealed that within the five genomes there were 5,021 genes shared with a >70% sequence identity, that the authors defined as the *P. aeruginosa* core genome (Mathee et al., 2008). Furthermore they demonstrated that within these 5,021 genes >90% show 98% sequence identity, demonstrating the high level of conservation of the 'core genome' of *P. aeruginosa*. The *P. aeruginosa* genome demonstrates a leading strand bias towards coding (~55%) and essential (~66%) genes, although at somewhat lower levels than *E. coli* and *Bacillus subtilis* genomes (Mathee et al., 2008). Phylogenetic analysis (Figure 1.4) of the six of the *P. aeruginosa* genomes reveals the levels of divergence between strains, with the two strains isolated from Cystic fibrosis patients the UK (C3719 and LES) showing the highest level of similarity. With the hypervirulent multihost strain PA14 (Lee *et al.*, 2006a) being the most diverse from the rest, suggesting that the evolutionary pressures that moulded the PA14 genome may be significantly diverse from that of the other genomes, resulting in the hypervirulent phenotype.
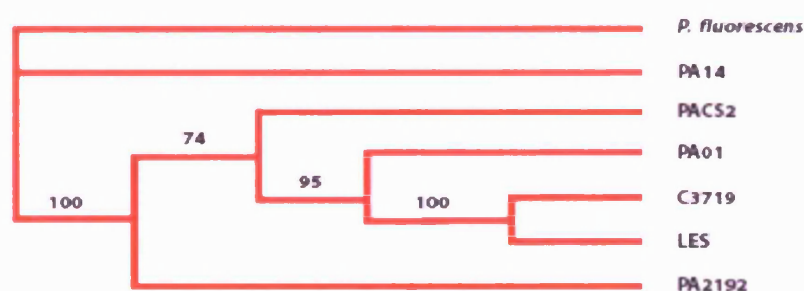
Figure 1.4 :Phylogenetic analysis of genomes of various *P. aeruginosa* strains. [2]
Another finding from the analysis of the five genomes was that three of the five genomes investigated had ribosomal RNA (*rrn*) operon mediated inversions (Figure

---

[2] Image taken from: MATHEE, K., NARASIMHAN, G., VALDES, C., QIU, X., MATEWISH, J. M., KOEHRSEN, M., ROKAS, A., YANDAVA, C. N., ENGELS, R., ZENG, E., OLAVARIETTA, R., DOUD, M., SMITH, R. S., MONTGOMERY, P., WHITE, J. R., GODFREY, P. A., KODIRA, C., BIRREN, B., GALAGAN, J. E. & LORY, S. (2008) Dynamics of Pseudomonas aeruginosa genome evolution. *Proc Natl Acad Sci U S A*, 105, 3100-5.

1.5). This has been previously reported in strain PAO1 with the sequenced strain having undergone a large scale inversion between the *rrnA* and *rrnB* as compared to PA14 and other versions of the PAO1 strain held in different laboratories (Lee *et al.*, 2006b). Large scale inversions of this nature and those mediated by IS6100 have been reported in other work investigating the variability of *P. aeruginosa* genomes (Kresse *et al.*, 2003, Romling *et al.*, 1997). Large scale inversions have been reported in a range of bacterial species (Mullany, 2005, Kothapalli *et al.*, 2005), at varying levels of frequency. The exact selection pressures and fitness costs of genomic inversions are as yet not fully understood. However it is most likely that variation of gene expression, replichore balance, antigenic variation, and general fitness all play roles in the selection of genomic inversions (Mullany, 2005). Particularly in *P. aeruginosa* where the high frequency of inversions in strains isolated from CF patients demonstrates that genomic inversions are part of the tool box of bacterial genome evolution (Kresse et al., 2003) and are therefore worthy of further study.

1.10.2 Accessory and mobile genomes

An average 11 % variation between strains has been described between the full sequenced *P. aeruginosa* genomes and strains compared in other studies (Spencer *et al.*, 2003, Mathee et al., 2008). This variation is mainly caused by the presence or absence of genomic islands. Additionally a large number of phage and prophage have been reported in *P. aeruginosa* (Winstanley *et al.*, 2009, Rice *et al.*, 2008, Finnan *et al.*, 2004) The large overall genome size of *P. aeruginosa* combined with the large variation is probably selected upon by the varied number of habitats *P. aeruginosa* is found in, thus giving *P. aeruginosa* strains the greatest metabolic and environmental adaptability.
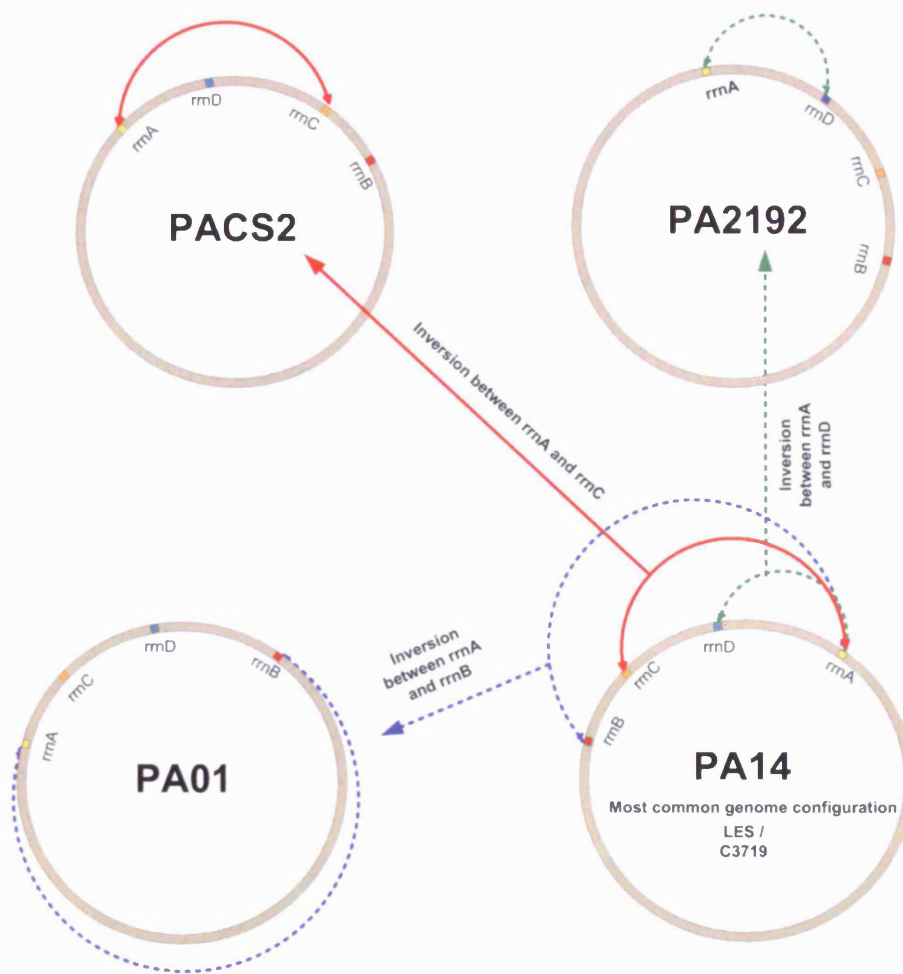
Figure 1.5: Showing *rrn* operon mediated genome inversions in sequenced *P.aeruginosa* genomes

1.10.3 *P. aeruginosa* genomic and pathogenicity islands

1.10.4 pKLC102-Family

Over the past decade the number of described *P. aeruginosa* genomic islands has rapidly increased with a number of distinct lineages being described. The first PA island to be described was in 2000 by Kiewitz and co workers (Kiewitz *et al.*, 2000). They described two large plasmids pKLC102 (102 Kb) and pKLK106 (106 Kb) that

integrate into the $tRNA^{Lys}$ genes. The pLKC102-like genomic islands (Wurdemann and Tummler, 2007), have been described in a number strains (Table 1.5). They range in size from 81Kb in C3719 to 108 Kb PAPI-1 in strain PA14, and have been described in six of the eight *P. aeruginosa* genomes, (Lee *et al.*, 2006b, Stover *et al.*, 2000, Wurdemann and Tummler, 2007, Mathee *et al.*, 2008).

Table 1.5: pKLC102 family of islands

Strain	Island name	Size	Integration $tRNA^{Lys}$	Excision / circular form	Reference
PA14	PAPI-1	108kb	PA0976.1 PA4541.1	Yes / Yes	(He et al., 2004)
C3719	C3719-RGP41[3]	85kb	PA4541.1	Yes / Yes	(Mathee et al., 2008)
PACS2	PACS2-RGP41	106kb	PA4541.1	Yes / Yes	(Mathee et al., 2008)
PA2192	PA2192-RGP41	85kb	PA4541.1	Yes / No	(Mathee et al., 2008)
PA7	PA7 – RGP41	85kb	PA4541.1	No / No	(Wurdemann and Tummler, 2007)
Clone C	pKLC102	104kb	PA4541.1	Yes/ Yes	(Klockgether *et al.*, 2004)
Clone K	pKLK106	106kb	PA0976.1 PA4541.1	Yes/Yes	(Kiewitz et al., 2000)

1.10.5 Genetics of pKLC102 -family

Within the pKLC102-family there exists a core set of genes that are highly conserved within islands, including the tyrosine family integrase (*xerC*) and the chromosome partitioning protein (*soj*) which has been shown to be essential for maintenance of the circular form of PAPI-1 (Qiu et al., 2006) In most of the islands so far investigated these two genes have been found to be located at either end of the island, with the integrase gene next to the tRNA at the proximal end and *soj* at the distal end of the

---

[3] Referred to as C3719-PAI in this work.

island. Other conserved genes include a novel type IV pilus biosynthesis cluster, that has been demonstrated to be conserved in mobile genetic islands in a variety of bacterial species (Juhas et al., 2007a). Each of the individual islands also carries its own 'cargo' genes. Of particular interest is the array of virulence factors that are found on the PAPI-1 island, which are not found on any of the other islands from sequenced genomes (Wurdemann and Tummler, 2007).

1.10.6 Population and Epidemiology of pKLC102/ PAGI-2 Family

A recent study investigated the presence of pKLC102 and PAGI-2 islands in a panel of 71 geographically and habitat diverse strains. pKLC102 / PAGI-2 related islands were identified in 50 and 31 strains respectively. This study also demonstrated a wide variety of subtypes of islands based on island specific genetics. Another recent study of the population of *P. aeruginosa* (Wiehlmann et al., 2007) showed that many of the genes located on the pKLC102 family of islands are under-represented in strains originating from cystic fibrosis (CF) patients suggesting that some kind of purifying selection works against the presence of pKLC102-like islands in the CF lung. The study also demonstrated that exact copies of islands are only found on a clonal level and that only certain subsets of *P. aeruginosa* strains carry pKLC102 like islands. Genomic islands that are found integrated in tRNA and share a syntenic set of homologous genes with the pKLC102-family have been identified in thirty different bacterial species including: *Haemophilus influenzae, Burkholderia pseudomallei, Salmonella enteric* subsp. *enterica* serovar Typhi CT18, *Neisseria gonorrhoeae*, and *Legionella pneumophila* (Klockgether et al., 2006).

1.10.7 Excision and circularisation of pKLC102/PAPI-1 family

Many of the pKLC102-family of islands has been demonstrated to undergo excision and form a circular 'plasmid like' form (Table 1.5) (Kiewitz et al., 2000, Klockgether et al.,

2004, Klockgether *et al.*, 2007b, Mathee *et al.*, 2008) (Table 4) The site mediated excision in pKLC102 has been detected at levels as high as 1×10^{-1} and the copy number during growth was estimated at 1 to 30 copies per cell for pKLC102 (Kiewitz *et al.*, 2000, Klockgether *et al.*, 2004, Klockgether *et al.*, 2007b). The excision from the genome is thought to be part of the process that allows transfer from one strain to another.

1.10.8 Integration sites

The islands in this family are conserved in their integration site, and are all associated with tRNA sites. In particular $tRNA^{Lys}$ sites, except for PAGI-2 and PAGI-3 which integrate into $tRNA^{Gly}$ sites (Klockgether *et al.*, 2007b). There are two $tRNA^{Lys}$ sites within in the all the *P. aeruginosa* genomes sequenced so far. For this work the tRNAcc output number (Ou *et al.*, 2006b) will be used to describe the tRNA loci, so the PAO1 locus PA0976.1 will be $tRNA^{Lys10}$, and PA4541.1 will be $tRNA^{Lys47}$. Many of the pKLC102/islands can insert into both of the $tRNA^{Lys}$ sites, such as PAPI-1 and pKLK106. Whereas pKLC102 can only insert into the $tRNA^{Lys47}$, as it is postulated that due to PAGI-4 being 'locked in' to $tRNA^{Lys10}$, this somehow blocks the integration of pKLC102 by an unknown mechanism (Klockgether et al., 2004). Also in a subset of Clone C strains, pKLC102 had a composite transposon TNCP23 inserted, causing the pKLC102 island to be 'locked in' to its chromosomal location (Klockgether et al., 2004).

1.10.9 PAPI-1

Strain PA14 carries two pathogenicity islands: PAPI-1 is a 108 kb island integrated within a lysine $tRNA^{Lys47}$ gene (PA4541.1), and PAPI-2, a much smaller 11 kb island inserted into a tRNA^{Lys10} gene (PA0976.1). Both islands share a limited but recognizable degree of synteny. PAPI-1 codes for factors that have been implicated in pathogenesis

58

in murine, plant and nematode models of infection (Lee *et al.*, 2006b, He *et al.*, 2004). Likely virulence factors include; a type IVB pili, *cupD1- D5* fimbrial biogenesis gene cluster, and PvrR/S, a two-component response regulator involved in biofilm synthesis antibiotic resistance, and fimbrial expression. However, the large majority of PAPI-1 predicted proteins have no assigned function and many of these are encoded by homologues on related islands in other *P. aeruginosa* strains (He et al., 2004).

1.10.10 PAPI-2 and ExoU-family of islands

PAPI-2 is a stably integrated island belonging to the ExoU island family (He et al., 2004, Kulasekara et al., 2006). PAPI-2 encodes the cytotoxin ExoU, a potent phospholipase, and its cognate chaperone SpcU. One other gene on PAPI-2 has been implicated in virulence, a mutant of gene PA14_5160 which is predicted to code for membrane lipoprotein has been shown to be significantly attenuated in an Arabidopsis model of infection (He et al., 2004). Other members of the ExoU family of islands include the 81 kb ExoU A island, the 29.8 kb ExoU B island, and the 3.8 kb ExoU C islet (Kulasekara et al., 2006). These islands are also related to the 8.9 kb $tRNA^{Lys}$ associated island in PAO1 and all seem to have common ancestral relationships to the wider pKLC102-family (Kulasekara et al., 2006).

1.10.11 *Pseudomonas aeruginosa* genomic islands (PAGI)

Over the past eight years a number of papers have been published describing a number of *P. aeruginosa* genomic islands. These islands have all been given names: *Pseudomonas aeruginosa* genomic islands (PAGI) and in total there are eleven PAGI islands (PAGI-1 to PAGI-11) which are shown in Table 1.6. As can be seen they vary greatly in content and in size - ranging from 2.03 to 104.9 kb. Some of the islands such as PAGI-2, PAGI-4, and PAGI-5 are part of the wider pKLC102 / PAGI-2 family of genomic islands. PAGI-2, 3, 4, 5, 6, and 8 are found inserted in tRNA genes, with the

others being inserted in non-tRNA loci. The PAGI-2 island has also been demonstrated to be present in ~50% of strains tested, and can also be found in a diverse range of other species including; *Cupriavidus metallidurans* and *Cupriavidua campiniensis*. Also multiple copy numbers of PAGI-2 containing two, three or four copies, have been reported (Klockgether *et al.*, 2006). Of particular interest is the recently described PAGI-5; found inserted in *tRNA*^{Lys10} in strain PSE9, this strain was found to be the most virulent of a panel of thirty-five isolates from ventilator associated pneumonia. The PAGI-5 island has been experimentally demonstrated as a pathogenicity island, with two novel regions (NR), NR-I and NR-II that confer this phenotype. NR-II was also demonstrated to be found only in the most virulent of isolates in the thirty-five isolates, suggesting it is associated with a high virulence phenotype.

1.10.12   Glycosylation islands

P. aeruginosa flagellins can be split in to two groups; a and b type flagellins based on molecular weights and reactivity with specific sera (Verma et al., 2006) . Two genomic islands that insert downstream of the *flgL* gene have been identified (Verma et al., 2006, Arora *et al.*, 2004, Schirm *et al.*, 2004). The a-type *P. aeruginosa* strain PAK has a 16 kb Genomic island containing 14 ORFs, while the b-type like in PAO1 is an 8 kb island with 4 ORFs. Both islands have been experimentally demonstrated to be responsible for glycosylation of the flagellin. Glycosylation in *P. aeruginosa* has shown to be important in both murine models of infection, and in triggering an inflammatory response, suggesting another important virulence determinate in *P. aeruginosa* is horizontally acquired (Verma et al., 2006).

Table 1.6: Pseudomonas aeruginosa genomic islands (PAGI) 1 to 11

Island	Inserted site	Size (kb)	Key genes / feature	Strain	Ref.
PAGI-1		48.8 kb	Transposases, dehydrogenases, parquet-inducible proteins, acetate permase,	X24509	(Liang *et al.*, 2001)
PAGI-2	*tRNA*^{Gly}	104.9 kb	Phage integrase, Cytochrome biogensis proteins, Haeme exporter, PilL (Type IV pili), *radC* DNA repair protein, Mercuric transport proteins, DNA topisomerase III, Transposases, Sensor kinase, and large number of hypothetical proteins.	Clone C	(Larbig *et al.*, 2002)
PAGI-3	*tRNA*^{Gly}	103.3 kb	Phage integrase, IS, transposases, PilL (Type IV pili), *radC* DNA repair protein, DNA topisomerase III, *soj*, *bphR* LysR regulatory protein, *adh* alcohol dehydrogenase, and large number of hypothetical proteins.	SG	(Larbig et al., 2002)
PAGI-4	*tRNA*^{Lys}	23.4 kb	*xerC*, transposase, *tnpS* Cointegrate resolution protein S, plasmid, Conserved hypothetical's with homology to pKLC102.	Clone C	(Klockgether et al., 2004)
PAGI-5	*tRNA*^{Lys}	99.2 kb	Pathogenicity island, highly homogoug to PAPI-1 79 of 121 ORFs share homology to PAPI-1. *xerC*, *soj*, Type IVB pilus, Novel regions NR-I and NR-II both experimentally implicated in virulence.	PSE9	(Battle *et al.*, 2008)
PAGI-6	*tRNA*^{Thr}	44.3 kb	A number of φCTX phage proteins, Phage integrase	PSE9	(Battle *et al.*, 2009)
PAGI-7		22.4 kb	RtrR transcriptional regulator, *ptx*ABCDE operon found in *Pseudomonas stutzeri* (phosphorous acquisition), recombinases, a type III restriction enzyme, a putative transposase, group II intron.	PSE9	(Battle et al., 2009)
PAGI-8	*tRNA*^{Phe}	16.1 kb	type IV secretion system proteins, binding transcriptional regulator, ATPase, transposons related genes, site-specific recombinase and phage integrase.	PSE9	(Battle et al., 2009)
PAGI-9		7.1 kb	similar to *Rhs* elements	PSE9	(Battle et al., 2009)
PAGI-10 (Islet)		2.1 kb	similar to *Rhs* elements	PSE9	(Battle et al., 2009)
PAGI-11 (Islet)		2.03 kb	Replaces a 5.8 kb region of PAO1 (PA1935-1938)	PSE9	(Battle et al., 2009)

1.11 Aims

1. Investigate the genetic diversity mediated by tRNA loci in *P. aeruginosa*.

2. Create mutants of known pathogenicity islands PAPI-1 and PAPI-2 in strain PA14.

3. Create a mutant of the $tRNA^{Pro21}$ island in strain PA14

4. Test the phenotype of the mutants in various *in vitro* and *in vivo* assays.

5. Investigate the site specific recombination and stability of PAPI-1 in various strain backgrounds and isogenic mutants to identify the factors that affect it.

2   Materials and methods

2.1   Organisms, plasmids and growth conditions

Bacterial strains were routinely grown at 37°C on Luria Bertani (LA) plates unless otherwise stated. Routine growth in liquid culture was carried out in 5ml Luria Bertani broth (LB) at 37°C and 200 rpm shaking.

2.2   Strains and plasmids

P. aeruginosa wild type and mutant strains along with *E.coli* strains used and plasmids are listed in Appendix J.

2.3   Genomic and plasmid DNA extraction

2.3.1   Genomic DNA extraction

A single colony was inoculated into 5 ml of LB with antibiotics if required and incubated at 37°C overnight shaking at 200 rpm. Genomic DNA was extracted from 400 μl of overnight culture ~2 x 10^6 CFU using the Qiagen Blood and tissue kit (Qiagen, UK) following manufacturer's instructions, with the modification that the DNA was eluted using 2x 75μl of sterile nanopure H_2O instead of the provided elution buffer.

2.3.2   Plasmid DNA extraction

Plasmid DNA was extracted using either modified alkaline lysis or using the QIAprep spin Miniprep kit (Qiagen, UK). The modified alkaline lysis method was based on that described by Birnboim and Doly (Birnboim and Doly, 1979). A single colony was inoculated into 5 ml of LB with appropriate antibiotics and was grown for ~16 hours. 3 ml of the culture was pelleted by centrifugation, and resuspended in 200 μl of 50 mM glucose, 25 mM Tris-HCL (Sigma, UK), 10 mM EDTA (Sigma, UK), 0.8 mg of lysozyme (Sigma, UK) and incubated at room temperature for 10 min. 400 μl of

freshly prepared 0.2 M NaOH, 1% (w/v) SDS (Fisher, UK) was added, the solution

mixed by gentle inversion and incubated on ice for 5 min. Next 300 µl of 7.5 M

ammonium acetate (Sigma, UK) solution was added, and the solution mixed by

repeated gentle inversion and incubated on ice for 10 min. The mixture was then

centrifuged at 14,600 rpm for 10 min, and 800 µl of the supernatant removed to a fresh

tube. The plasmid DNA was precipitated by adding 480 µl of 2-propanol (Fisher, UK),

incubated at room temperature for 10 min then centrifuged at 14600 rpm for 30 min.

The supernatant was removed and the pellet was then washed twice with 700 µl of 70%

(v/v) ethanol, dried down by vacuum centrifugation and resuspended in 50 µl H_2O for

high copy number plasmids and 20 µl for low copy number plasmids. 2 µl of 10 mg/ml

RNAse (Sigma, UK) was then added and incubated overnight at 4°C. The plasmid DNA

was then finally stored at –20°C.

Plasmid extraction was carried out using using the QIAprep spin Miniprep kit (Qiagen,

UK), A single colony was inoculated into 5 ml of LB with appropriate antibiotics and

was grown for ~16hours. Plasmid DNA extracted following manufacturer's

instructions, with the exception that the DNA was eluted in 50µl of nH_2O instead of the

provide elution buffer.

2.4   DNA quantification

DNA was quantified using a NanoDrop 8000 (Thermofisher, UK), or approximately

quantified by comparison to a known DNA standards (Generuler and λ-*Hind*III ladders

(Fermentas, UK)) run along samples in agarose gel electrophoresis.

2.5   Restriction enzymes and restriction digests

Restriction enzymes were purchased from New England biolabs (UK), Roche (UK),

Promega (UK), or Fermentas (UK). Digests were carried out following manufacturer

instructions, using appropriate buffers at 1x and when required 1x BSA. Following

incubation for the appropriate time and temperature, restriction digests were heat inactivated according to manufactures instructions. Digests were cleaned up by vacuum drying the digest followed by two cycles of washing with ~500μl 70% (v/v) ethanol and centrifugation at 14600 rpm for 10mins, final vacuum drying and elution in nH$_2$O. In some cases restriction digests were cleaned up using commercially available DNA clean up kits purchased from either Yorkshire Biosciences (UK) or Omega Bio-tek (VWR, UK) following manufactures instructions and elution in 20 – 50μl of nH$_2$O.

2.6   Dephosphorylation

Restriction-digested vector DNA in water was mixed with Shrimp Alkaline Phosphatase (SAP) (Promega, UK) at concentration of 1 unit per μg of vector DNA and incubated at 37°C for 15 minutes in 1X SAP reaction buffer in a final volume of 30μl. The SAP was then inactivated by heating to 65°C for 15 minutes. After quantification the resulting dephosphorylated vector was stored at -20°C and used downstream in ligation reactions as required.

2.7   A-Tailing of PCR products

In order to clone PCR fragments into the pGEM-T-Easy vector system using PCR fragments generated using KOD Polymerase, which generates blunted ended PCR fragments were required to be A-tailed. 200 – 500 ng of the PCR fragment was mixed in a 10 μl reaction with 1 x Go Taq PCR buffer (Promega, UK), 0.2 mM dATP, 2 units GoTaq Polymerase (Promega, UK). The reaction was heated to 72°C for 30 - 40 mins.

2.8   Ligations

Ligations were carried using T4 DNA ligase and reaction buffers purchased from Promega (UK). In general the reaction size was 10 – 20μl with insert to vector ratio of at least 3:1. Two different reaction buffers were used dependent on the incubation time and temperature; 2x Rapid Ligation buffer for rapid ligation (~1 hour) at room temperature (~22-25°C) or 10x buffer for overnight (~16 hours) ligations at 4°C.

Ligations were heat inactivated by heating at 70°C for 10 minutes. If the ligation was to be used downstream in electroporation the ligation was cleaned up by vacuum drying the digest followed by two cycles of washing with ~500µl 70% (v/v) ethanol and centrifugation at 14600 rpm for 10 mins, final vacuum drying and elution in 5-10µl nH$_2$O. In some cases restriction digests were cleaned up using commercially available DNA clean up kits purchased from either Yorkshire Biosciences (UK) or Omega bio-tek (VWR, UK) following manufactures instructions and elution in 5-10µl nH$_2$O.

2.9   PCR primer synthesis and DNA sequencing

PCR oligonucleotide primers were synthesised by VHBio, UK or MWG Biotech, Germany. DNA sequencing was carried out by MWG Biotech, Germany.

2.10   Polymerase chain reaction

2.10.1 Standard PCR conditions and reaction set up

For standard diagnostic PCR or for sequencing the thermostable polymerase used was Go Taq (Promega, UK). Deoxynucleotide triphosphates (dNTPs) were purchased from Bioline, UK. The standard reaction set up (that was scaled up and down) is shown in Table 2.1. The cycle conditions used for standard PCR are shown in Table 2.2.

Table 2.1: Standard PCR reaction set up

Reagent	Volume (µl)
5X Buffer	4
dNTPs (10mM)	0.2
Primer forward (10pmol)	1.0
Primer reverse (10pmol)	1.0
Go Taq enzyme (0.625u)	0.125
nH$_2$0	12.675
Template DNA	1
Total	**20**

Table 2.2: Standard PCR cycling conditions

No.	Temperature	Time
1	95^0C	2 mins
2	95^0C	30 seconds
3	Lowest Tm of primers -1^0C	30 seconds
4	72^0C	1 min / kb
5	Cycle to 2 X 35	
6	72^0C	10 mins
7	15^0C	∞

When problems were encountered with specificity in PCR reaction or two primers had large variation in Tm, a touch down PCR protocol was used to increase specificity. The touchdown protocol is the same as that of the standard PCR, except that for the first ten cycles the starting annealing temperature used is 10°C higher than the lowest Tm $-$ 1°C of the primers used, and is reduced by 1°C per cycle for the first ten cycles. After the first ten cycles the annealing temperature is at the lowest primer Tm $-$ 1°C and this is used for the reminder of the cycles.

2.11 Colony PCR

A large single colony was picked from a freshly grown plate, using a sterile toothpick or pipette tip, the bacterial material on the end of the toothpick / pipette tip was then transferred to 30 µl of sterile nH_2O in a sterile eppendorf. The eppendorf was then heated to 100°C for 10 mins in a heat block or water bath. The eppendorf was then centrifuged at 14,600rpm for 2 mins. Then 2 µl of the supernatant was used as template in a standard PCR reaction.

2.12 Specific PCR product re-amplification: Band-stab PCR.

In the case that a PCR produced only a weak amplicon, or multiple bands, and one was of specific interest the bands were re-amplified using the band stab method. The method was carried out by careful repeatedly stabbing the specific band of interest in the agarose gel (stained with ethidium bromide and viewed under UV light) repeatedly with

a P200 micropipette tip. The agarose gel taken up inside the tip was then washed out by repeated aspiration and purging of the pipette in 30 µl nH_2O in a sterile eppendorf, this was then heated at 65°C for 10 mins to melt the agarose, 1 µl of the solution was then used as template in a further round of PCR.

2.13   Splicing overlap extension (SOE) PCR

To join multiple fragments together for construction of suicide vectors and related constructs a splicing overlap extension PCR protocol was used to join the fragments together. The protocol is based on that described by Choi and Schweizer (Choi and Schweizer, 2005). In outline, multiple independent fragments are first amplified by PCR, these fragments include at the 5' end overlapping homologies to those on the other fragments that are to be joined together. The 5' homologies are included in the fragments as the 5'end of the primers used to amplify the fragments. In the SOE PCR the PCR fragments to be joined together are mixed in an equimolar ratio in a single reaction (Table 2.3) and undergo a primary thermocycle (Table 2.4) without primers. In the initial three cycles the overlapping homologies anneal to each other, forming a single 'fusion' fragment. PCR primers that bind to the 5' and 3' ends of the 'fusion' fragment are then added to the reaction after the fourth cycle to amplify the newly formed fragment. In this work the primers used to amplify the fusion product, contained *attB1* and *attB2* allowing for rapid site directed recombination using the Gateway site directed recombination system. To ensure the fidelity of the reaction the *high-fidelity* KOD Hotstart DNA polymerase (Merck, UK) was used for all amplifications.

Table 2.3: SOE PCR reaction set up

Reagent	Volume (µl)
10X	5
dNTPs	5
MgSO$_4$	3
P1 (Gw-attB1) (Not added at start, see thermocycle)	1.5
P2 (Gw-attB2) (Not added at start, see thermocycle)	1.5
KOD enzyme	1
nH$_2$0	up to 50µl
UF 50ng (dependent on Conc / ul)	X*
DF 50ng (dependent on Conc / ul)	X*
Gm-FRT 50ng (dependent on Conc / ul)	X*
Total	50µl

Table 2.4: SOE Thermocycle conditions

No.	Temperature	Time
1	95^{0}C	2 mins
2	95^{0}C	15 seconds
3	55^{0}C	30 seconds
4	68^{0}C	1m 30 seconds
5	Cycle to 2 X 3	
6	95^{0}C	15 seconds
7	55^{0}C	30s
8	68^{0}C	45s
9	Add primers	
10	70^{0}C	45s
11	95^{0}C	15 seconds
12	56^{0}C	30secs
13	68^{0}C	1min /kb
14	Cycle to 11 x 25 cycles	
15	68^{0}C	10mins

2.14 Quantitative PCR (qPCR)

A minimum of two biological replicates were generated for each strain by growing two single colonies for 12 hours in 5ml LB broth at 37°C and 200 rpm shaking. Genomic DNA was extracted using a Qiagen DNeasy kit, eluted in Nano pure H$_2$O and quantified using a Nanodrop spectrophotometer. The DNA was then standardised to ~5 ng / µl in nanopure H$_2$O. Standard curves were generated by serially diluting PCR generated amplicons containing the target region. Standard curves were made freshly for every run, and the copy number calculated based on the size of the DNA fragment and the initial concentration of DNA. qPCR was carried out using a Rotor-gene 6000 (Corbett

Life Sciences, UK) and SensiMixPlus SYBR (Bioline, UK) mastermix according to manufacturers recommendations. The qPCR were carried out by comparison of the triplicate repeat values for each sample against the standard curve using the Rotorgene 6000 series software 1.7 (Corbett Life sciences, UK). Values were only accepted if the Repeat Ct standard deviation was <0.5. All copy number values were normalised to 1 x 10^6 genomes relatively to the genome copy number of the single copy $gyrB$ gene for each repeat.

2.15   Agarose gel electrophoresis

Agarose gel electrophoresis was carried out using 0.4 – 2.0 % molecular biology grade agarose (Bioline, UK) in TAE buffer. DNA was visualised by inclusion of 10 µg/ml ethidium bromide (Sigma, UK) in the agarose and viewed under ultraviolet light. DNA size and approximate quantification markers used were λ-$Hind$III and Generuler DNA ladders (Fermentas, UK). Samples were loaded in 1x loading dye.

2.16   Pulse Field Gel Electrophoresis

Pulse field gel electrophoresis was carried out using the ARPAC (MacKenzie et al., 2005)   Pseudomonas   aeruginosa   PFGE   protocol (http://www.hpa.org.uk/web/HPAwebFile/HPAweb_C/1194947324361)   as   a   basic guide, but modification were required, possibly due to variations in reagents and laboratory conditions.

2.16.1 Plug preparation

The method used was as follows; all strains to be tested were grown overnight in duplicate in 5 ml at 37°C with 200 rpm the next day the cells were pellet by centrifugation (3,000 rpm for 5 mins) and resuspended in 4 ml of SE buffer. 2% Low melting point (LMP) agarose (Geneflow, UK) was made up in SE buffer, agarose melted, and placed in waterbath set a 56°C to equilibrate. 350µl of the bacterial

suspension was mixed with an equal volume of 2% LMP and mixed by pipetting and transferred to the plug mould. Blocks placed in the fridge (4°C) to set. Then transferred to a sterile 5 ml universal tube and 3 ml of Gram-positive lysis buffer + 0.5 mg/ml lysozyme (Sigma, UK) added and incubated overnight (~16 hours) at 37°C. The next day the Gram-positive lysis buffer was removed and 3 ml Gram-negative lysis buffer + 500 µg/ml proteinase K (Roche, UK) added and incubated overnight at (~16 hours) 56°C with gentle shaking at 50 rpm. The next day the Gram-negative lysis buffer was removed and the plugs washed once in sterile 4 ml of TE buffer (pH 7.5) the tube was gently inverted to wash the plug. The TE buffer was then removed and the plug transferred to a fresh 20 ml Universal tube and washed five times with 10 ml of sterile TE buffer (pH 7.5) with incubations of one hour at 4°C between washes. The plugs were then stored at 4°C in TE buffer (pH 7.5) until required.

2.16.2 Restriction digests

Before digests plugs were cut to produce a plug with the approximate dimensions of 4 mm wide by 8 mm long. The plugs were then transferred to a sterile 1.5 ml eppendorf, and equilibrated in 200µl of the relevant 1 x restriction buffer and BSA (if required), for 2 hour at 4°C. The buffer was then removed and 100 µl total volume of the 1 x restriction buffer and BSA (if required) and approximately 10 units of restriction enzyme (*Pac*I, *Spe*I, or I-*ceu*I (NEB, UK)) were added, and placed directly in the fridge (4°C) overnight to allow the enzyme to penetrate the agarose, then the next day the plug digest was removed from the fridge and incubated at for 4 hours at 37°C.

2.16.3 Pulse field gel conditions

After the plugs had been digested they were loaded directly on the combs of the gel mould, along with *S. cerevisiae* markers (Biorad, UK) at each end, then melted agarose gel was then poured using Certified megabase agarose (Biorad, UK) at 1 to 1.5% in

TBE buffer. After the gel had set (~30 mins) the comb was removed and the wells

sealed with the agarose at the same percentage. The gel was then run in 0.5% TBE on a

CHEF-DR II System (Biorad, UK). The conditions varied dependent on the size of the

bands to be resolved. After the run had finished the gel was stained in ethidium bromide

solution (10 µg/ml in TBE) for 1 hour with gentle shaking, then de-stained in distilled

H_2O for 1 hour with gentle shaking. The gel was then visualised and photographed

under UV light.

2.17 Gateway Cloning

2.17.1 BP Clonase reaction

To transfer the SOE PCR products to the relevant suicide vectors using the Gateway

system, the first stage was to carry out a BP clonase reaction to transfer the fragment to

the Gateway Entry vector pDONR-221. Reactions were carried out according to the

manufactures protocol. The reaction set up included: 1.0µl pDONR221 (150ng /µl)

(supplied by Invitrogen, UK), 1.0 µl BP Clonase II enzyme mix (Invitrogen, UK), 1-7

µl of SOE Product (in TE buffer, pH 8.0) (equimolar to the pDONR221) made up to a

final volume of 10 µl with TE buffer, pH 8.0. The reaction was then mixed gently by

vortexing and incubated overnight at 25°C, the next day the reaction was stopped by the

addition of 1µl of proteinase K and incubation at 37°C for 10 mins. The 5µl of the

reaction was then used to transform into chemical competent *E. coli* and the remainder

stored at -20°C

2.17.2 LR Clonase reaction

To transfer the SOE PCR products from the Gateway Entry vector pDONR221 to the

gateway compatible destination vector using the Gateway way site specific

recombination system. Reactions were carried out according to the manufactures

protocol. The reaction mixture included: 1-5µl pDONR221 (~150 ng, equimolar to the pEX18ApGW) in TE buffer, pH 8.0, 1.0 µl LR Clonase II enzyme mix (Invitrogen, UK), 1µl of pEX18ApGW (150 ng) in TE buffer, pH 8.0. The reaction is made up to a final volume of 10 µl with TE buffer, pH 8.0. The reaction was then mixed gently by vortexing and incubated overnight at 25°C, the next day the reaction was stopped by the addition of 1µl of proteinase K and incubation at 37°C for 10mins. The 5µl of the reaction was then used to transform into chemical competent *E. coli* and the remainder stored at -20°C

2.18 *E .coli* chemical competent cells and heat shock transformations

2.18.1 Preparation of cells

Heat shock competent cells were made by using the following method. A single colony of *E.coli* DH5α, DH10β or Oneshot T1-R (Invitrogen) was inoculated into 5 ml of LB broth and incubated over night at 37°C and 200 rpm. The next day the 500 µl of the overnight culture was used to inoculate 1 L of LB medium. The cells were then grown at 37°C with shaking at 200 rpm until they reached an OD 600 nm of 0.3 to 0.4 (1 cm path length cuvette). The cells were then centrifuged at 3,000 x g for 10 minutes at 4°C. The supernatant was then removed and the bacterial cell pellets were then gently resuspended in 50 ml of ice cold 100 mM MgCl₂, taking 3 to 5 minutes for this procedure using a pipette and electronic pipette aid. The cells were then centrifuged again at 3,000 x g for 10 minutes at 4°C. The supernatant was then discarded and the cells gently resuspended the in 50 ml of ice cold 100 mM CaCl₂ (Sigma, UK) using a pipette and electronic pipette aid. The cells were then incubated for 10 min on ice. The cells were then centrifuged at 3,000 x g for 10 minutes at 4°C, the supernatant removed

and the cells resuspended in 4 ml of ice cold, sterile 100 mM CaCl₂ (Sigma, UK) in 15% glycerol (w/v) (Fisher, UK). The cells were then frozen at -80°C in 50 µL aliquots.

2.18.2 Heat shock transformation

To transform plasmid DNA or ligation into chemical competent cells as described above the following method was used. A 50µl aliquot of Chemical Competent *E.coli* (DH5α, etc) was taken from the from -80°C freezer and placed straight on ice and allowed to defrost for ~5 mins. The ligation or plasmid was then added (1-10 µl), the cells and DNA / ligation was then incubated on ice for 30mins. The cells were then placed in a heat block / water bath at 42°C for 45 seconds, and then immediately returned to ice for 2 mins. After the incubation on ice 0.2 – 1 ml of room temperature LB or SOC broth was added and the cells incubated at 37°C with 200 rpm for 1 hour. The cells were then plated on the appropriate selective / differential media and grown overnight at 37°C.

2.19 *P. aeruginosa* electrocompent cells and electroporation

To introduce suicide vectors, transposons, and replicative plasmids *P. aeruginosa* strains were made electrocompent and electroporated, using the method described by Choi *et al* (Choi et al., 2005). The cells were always prepared fresh on the day, prior to the electroporation. The method used was as follows, a single colony was inoculated into a 6 ml LB culture (for small volumes) or a large volume (~250 ml) when preparing large quantities. After overnight growth, 6 ml of culture was distributed evenly (1.5 ml) into four sterile microcentrifuge tubes and centrifuged at 16,000g at room temperature for 2 min. The supernatant was removed and the cell pellet fully resuspended in 1 ml of 300 mM sucrose (room temperature) by pipetting. The cells are centrifuged again at 16,000g at room temperature for 2 min, and the supernatant removed and the cells

resuspended again in 1 ml of 300 mM sucrose (room temperature). Finally the cells were centrifuged again at 16,000g and the supernatant removed the four cells pellets were resuspended in a combined volume 100 µl of 300 mM sucrose (room temperature).To carry out the electroporation, 100 µl of electrocompetent cells to a 2-mm gap-width electroporation cuvette (Geneflow, UK) and the relevant DNA added and mixed gently by tapping the cuvette. The cells were electroporated in a Genepulser II system (Biorad, UK) with following settings 25 mF, 200 O, 2.5 kV. Immediately after the application of the pulse 1 ml of sterile LB medium was added to the cuvette and the contents transferred to 10 ml bijoux. The cells were incubated for 1 to 2 hours at 37°C and 200rpm to allow recovery and then plated onto the relevant selective medium and grown until colonies appeared at 37°C.

2.20 Conjugations

To enable transfer of suicide vectors and plasmids as part of the Tn7 system, conjugation was carried out to enable the transfer of plasmids from *E.coli* host strains to recipient *P. aeruginosa* strains. The method used was as follows, a single colony of the recipient and donor stain was used to inoculate 5 ml LB cultures (supplemented with antibiotics as required) that are grown overnight at 37°C with 200 rpm shaking. After overnight growth 200 µl of each of the donor (*E. coli* carrying plasmid) and recipient (*P. aeruginosa* strain) cultures were transferred to an eppendorf tube pre-warmed at 37°C and containing 0.6 ml of LB broth. This was then centrifuged for 2 min at room temperature and low speed (7,000g). (Reduced speeds yield softer cell pellets, which are easier to suspend and therefore minimize damage to cell surface pili required for conjugation). The supernatant is discarded, and the cells resuspended (gently) in 1 ml of warm (37°C) LB broth and centrifuged again. The supernatant was then removed again and cells resuspended in 1 ml of warm (37°C) LB broth, and centrifuged as before.

Finally the supernatant was discarded and the cell pellet gently resuspended in 30 μl of warm (37°C) LB broth. The whole 30 μl cell suspension was pipetted onto a piece of sterile 13-mm cellulose acetate filter membrane placed on no selective LB agar (the filter is added to the plate to pre-warm and absorbed nutrients at 37°C for at least 30 min to maximize conjugation efficiencies by avoiding a temperature 'shock') and incubated at 37°C for at least 5 h (mostly done overnight). The conjugation is carried out on a solid support as it has been reported that this helps to facilitate oriT-mediated conjugation by immobilizing cells in close proximity to one another (Choi and Schweizer, 2006b). The filter is used to facilitate the recovery of cells, and nonselective medium is required to avoid killing nontransformed recipient cells. After the required incubation time (5 h to overnight) using alcohol- and flame sterilized tweezers the filter is picked up and placed into a sterile eppendorf tube containing 300 ul of 0.9% NaCl (saline). The bacterial cells were dislodged and resuspended by vortexing for 1 min. 100 μl and serial dilutions were then plated onto Vogel-Bonner minimal media (VBMM) agar plates with the appropriate antibiotics plates and incubate at 37^0C until exconjugants appeared (usually 24 hours as *P. aeruginosa* grows slowly on VBMM). Using the citrate based VBMM medium counterselects against *E. coli* donor cells, which cannot use citrate as their sole carbon and energy source. The antibiotics select against non exconjugant *P. aeruginosa*, and recipient and donor only controls were also always run. In the case of the Tn7 transposon system the conjugations were tri-paternal, or four-parental dependent on the plasmids and *E .coli* host strains used, as the plasmid expressing the transposase is required to be conjugated along with the plasmid containing the Tn7 transposon.

2.21 Conjugations for island transfer

Both the donor PA14-Isprob (KR848) and the recipient were grown overnight in 5 ml LB broth with 30 µg/ml Gentamicin or 50 µg/ml Tetracycline for PA14-Isprob and recipient respectively to an OD of ~2 at 600 nm. 50µl of the donor strain (PA14-Isprob) was inoculated in to a 5 ml universal containing 1 ml of LB broth pre-warmed to 37°C, and incubated at 37°C for 2 hours. Then 50 µl of the recipient strain (PAO1-TetR) was added to the universal and was incubated for 48 hours at 37°C without shaking. After 48 hours 1 ml of LB broth was added and the mixture and then vigorously vortexed to break up the bacterial clumps. The transconjugants were then selected for by plating onto LA + 75µg/ml Tetracycline and 75µg/ml Gentamicin and serially diluted and plated onto LA + 75 µg/ml Tetracycline to calculate the total number of recipients and incubated overnight at 37°C.

2.22 Island probing

Single colonies of test strains were grown in duplicate overnight at 37°C and 200 rpm shaking with selection of Gentamicin 30 µg/ml or Carbenicillin 200 µg/ml. After 17 hours growth, 1 ml of the culture was centrifuged at 14,000 g for 2 minutes. The supernatant was then removed and the cell pellet gently resuspended in 1 ml of room temperature LB broth, and the process repeated. After the second wash and centrifugation the cells were gently resuspended in 1 ml of room temperature LB. 50 µl was then used to inoculate 5 ml of room temperature LB broth, before incubation 100 µl was removed and serially diluted and plated on LA , LA + Gentamicin 30µg /ml or Carbenicillin 200µg/ml, and LA + 5% (w/v) sucrose in triplicate to calculate CFU/ml. The strains were then incubated for 8 hours at 37°C with shaking at 200 rpm. After the 8 hours growth 100 µl was removed and serially diluted from 10^{-6} to neat and plated on LA , LA + Gentamicin 30µg /ml or Carbenicillin 200µg/ml, and LA + 5% (w/v) sucrose

in triplicate to calculate CFU/ml. Plates were incubated at 37°C overnight. Experiments were repeated at least once to give data for four independent biological repeats.

2.23 Growth Curves

Strains were grown for 16 hours at 37°C at 200 rpm in 5 ml LB broths, and inoculated 1/100 into LB broth, M63 with glucose (0.2%), $MgSO_4$ (1 mM),and casamino acids (CAA, 0.5%), or M9 with glucose (0.2%), $MgSO_4$ (1 mM), and $CaCl_3$ (1mM) and 200µl inoculated into a Honeywell plate and the OD measured using a Bioscreen apparatus (Life Sciences) at 37°C with continuous shaking for 24 or 48 hours. The initial inoculate were confirmed with serial dilutions and plating for CFU on LA plates.

2.24 Biofilm assays

The assay used to study biofilms formation is a modification of the method described by O'Toole, and Kolter (Malloy et al., 2005, Smith et al., 2006) A single colony inoculated for each test strain in 5ml of LB medium (37°C at 200rpm). After 12 hrs of growth the overnight culture diluted into 1/100 in 1ml (10µl culture into 990µl M63) of M63 with glucose (0.2%), MgSO4 (1 mM),and casamino acids (CAA, 0.5%). After mixing by vortexing, 100µl is taken to calculate colony forming units (CFU) per ml by serially diluting and plating from 10^{-1} to 10^{-6} onto a LA plate and incubating over night. Eights wells are then inoculated with 100µl of the 1/100 dilution for each of the three biological repeats of each strain into either a NUNC 96 well polystyrene plates (NUNC, Roskilde, Denmark) or a PVC Falcon plate (VWR, UK). The plates are then incubated for 8 hours at 37°C with no shaking. After the elapsed time the media was discarded into a waste container containing 1% Microsol solution. The plates were then immersed in distilled water by inserting from one side and allowing all the wells to fill with water. The water was discharged into the waste container and the plate shaken thoroughly. The plate was then tapped on an absorbent surface to remove excess water. 125µl of 0.1%

(v/v) Crystal violet (CV) (Sigma, UK) was added to each of the test, M63 control and 0.1% CV wells and incubated for 10 mins at room temperature. The CV was then discarded into the waste container, and the plates washed twice in the two different wash containers, discarding the waste water into the waste container. Finally the plates were tapped firmly face down on an absorbent surface and left to air dry. Once the plates were dry 200 µl of 95% Ethanol was added to all wells and incubated at room temperature for 15 mins. The plates were then read at 595nm.

2.25 Twitching motility assay

The twitching motility assay was essentially carried out as described by Rashid and Kornberg (Rashid and Kornberg, 2000) with modifications. Overnight cultures of the test strain were grown in 5 ml LB broth, the next day a freshly made 1.5% agar LA plate was stabbed through the agar until making contact with the bottom of the petri dish with a sterile toothpick inoculated with the test strain grown in the LB broth. The plates were then incubated for 24 hours at 37°C. The final stage was to gently remove the agar, and dry the petri dish base at 65°C to remove any moisture and kill the bacteria. The plate was then stained to visualise the 'twitch' area with 0.1% (v/v) crystal violet solution (Sigma, UK) for 10 mins at room temperature (~22°C) after which the excess strain was removed and the plate allowed to air dry. The diameter of the twitch area was then measured, and representative petri dishes photographed with a Nikon D40 camera (Jessops, UK).

2.26 Swimming motility assay

Overnight cultures of the test strain were grown in 5ml LB broth until stationary phase, the next day the centre of a freshly made 0.3% LA agar plate was inoculated with 5µl of the culture, and incubated for 20 hours at 30°C. After 20 hours the diameter of the swimming area was measured.

2.27   Cell culture

A549 lung carcinoma cells were maintained in RPMI-1640 + glutamine (Sigma, UK), and 10% Foetal calf serum and the addition of Penicillin / Streptomycin (Pen / Strep) solution (Sigma, UK). Cells were grown at 37°C with 5% CO_2, cells were split regularly to prevent the cells reaching >80% confluency.

2.28   Cytoxicity assay.

The cytotoxicity assay was carried out using A549 lung carcinoma cells, and the cell viability assayed using CytoTox-ONE Homogeneous Membrane Integrity Assay (Promega, UK) which measures the release of lactate dehydrogenase (LDH) from cells with a damaged membrane. Firstly, 24 well NUNC cell culture plates (VWR, UK) were seeded with 1 x 10^5 /ml A549 cells and incubated overnight at 37°C with 5% CO_2. Single colonies of the bacteria to be tested were inoculated into 3 ml LB broth and incubated overnight with at 37°C with 200 rpm shaking. The bacteria were then serially diluted in PBS and plated onto LA plates to ascertain CFU/ml of the inoculums. The next day the A549 cells were washed in warm (37°C) PBS to remove the Pen-Strep media, then 0.5 ml of warm (37°C) RPMI 1640 was added to each well. The overnight cultures of P .aeruginosa were diluted 1 in 2 in PBS and 10 µl of each strain to be tested added to three wells. A further three wells had 10µl of 9% (weight/volume) solution of Triton X-100 in water (Lysis solution) (Promega, UK) added which act as a time zero positive maximum LDH release control in the cytotoxicity assay. The bacteria were then spun on to the cells by centrifugation at 250 rpm for 4 mins, and the cells and bacteria were then incubated for 2 hours at 37°C with 5% CO_2. After the two hours incubation, the plates were removed to room temperature and 100 µl of supernatant removed from each well and added to a 96 well NUNC plate (VWR, UK). Then 100 µl of the CytoTox-ONE reagent (Promega, UK) was added, to each well and the plate gently shaken. Additionally three wells with cells and no bacteria added had 10µl of

Lysis solution added to calculate maximum LDH release control. The two types of negative controls; just cells with media and media alone also had reagent added. After 20 minutes incubation at room temperature, 50 μl of stop solution was added to each test well and the plate gently shaken. The fluorescence with an excitation wavelength of 560nm and an emission wavelength of 590nm was then measured using a Varioskan mulitplate reader (Thermo-Fisher Scientific, UK).

2.29   Assay for Pyocyanin production

5 ml LB cultures were inoculated with 1/100 of a stationary phase LB culture, and incubated for 20 hours at 37°C with shaking at 200 rpm. 1 ml of the overnight culture was mixed with 2 ml of chloroform and mixed for five minutes by inversion, and centrifuged for 5 mins at 2,000 rpm. The chloroform phase (light blue) was added to 1 ml of 0.1M HCL and mixed by inversion (turns pink). The optical density of the pink layer was then measured at 520 nm.

2.30   *Galleria mellonella* assay

The *Galleria mellonella* larvae were purchased in bulk from Livefood UK, UK. Test strains were grown overnight in 5 ml LB broth at 37°c and 200 rpm shaking. The next day a fresh 5 ml LB broth was inoculated 1/ 100 with the overnight culture and grown for four hours at 37°C and 200 rpm. After four hours growth the strains were briefly centrifuged at 2,000 rpm to pellet the cells. The supernatant was removed and the cells resuspended to an OD of ~0.2 in sterile 10mM MgSO₄. The strains were then serially diluted in 10mM MgSO₄ to obtain the relevant CFU/ml for inoculation.   The *G. mellonella* were inoculated with 10μl of the suspension in-between two of the rear thoracic segments using a 0.3 ml 32 gauge Terumo insulin syringe (VWR, UK). Before inoculation the inoculation site was swabbed with 70% ethanol to remove surface commensals. The larvae were inoculated in groups of five and incubated in sterile petri

dishes at 37°C. Larvae were scored dead when they did not respond to mechanical stimulation of the head. Negative controls inoculated with 10mM $MgSO_4$ were used as controls. Test strains were serially diluted and plated on LA plates to ascertain CFU/ml of innocula.

2.31 Bioinformatics

2.32 Genome sequences

Full or partial *Pseudomonas aeruginosa* genome sequences were downloaded from the NCBI Genome database (http://www.ncbi.nlm.nih.gov/) , the Broad institute (http://www.broadinstitute.org/), the Sanger centre (http://www.sanger.ac.uk/), or Pseudomonas genome database (Winsor et al., 2009).

2.33 tRNAcc

tRNAcc software (Ou *et al.*, 2006b, Ou *et al.*, 2007) was run as a locally installed version following default settings.

2.34 Primer design

For design of conserved primers based on multiple sequence alignments Primaclade software was used (Gadberry et al., 2005). For other primers the online Primer3 program (Rozen S, 2000), or locally installed versions of Primer select (DNAstar Inc, USA), or Vector NTI (Invitrogen, UK) .

2.35 Multiple sequence alignments

Multiple sequence alignments were carried out using a locally installed version of Clustal X2 (Larkin *et al.*, 2007)

2.36 Plasmids maps and *in silico* construction of mutant genomes.

Plasmid maps and the construction of the various genomes of the *P. aeruginosa* whole island mutants with different integrations of PAPI-1 were all constructed using the Vector NTI (Invitrogen, UK)

2.37   *In silico* PFGE

In silico PFGE was carried out using the Vector NTI (Invitrogen, UK) software.

2.38   Statistics

Statistical analysis was done using Graph pad prism 5, (GraphPad Software Inc.)

3 Results

4 Genomic diversity and *P. aeruginosa* genomic islands

4.1 Chapter overview

This chapter describes the identification of tRNA 'hotspots' for the acquisition of genomic islands. It then describes the diversity of occupation of these islands and relates this into overall genome diversity in *P. aeruginosa*.

4.2 Overview and principles

A range of diverse genomic islands (GIs) have been identified in *P. aeruginosa*, in so called 'regions of genome plasticity' (RGPs) (Mathee *et al.*, 2008). The majority of characterised islands have been found within two RGPs that map to insertion sites within the tRNA genes *tRNA^Gly* and *tRNA^Lys* (Mathee *et al.*, 2008, Klockgether *et al.*, 2007b, Larbig *et al.*, 2002). As tRNA loci seem to be the major site of integration for the majority of GIs (Juhas *et al.*, 2009) in many bacterial species, this work was carried out to investigate if other tRNA sites are used for the insertion of GIs in *P. aeruginosa*. An expanding array of bioinformatics software; using approaches such as hidden markov models, machine learning and composition bias are available to aid putative GI identification (Langille *et al.*, 2008, Pundhir *et al.*, 2008, Waack et al., 2006, Yoon et al., 2005, Vernikos and Parkhill, 2008). In this work a piece of previously described software was used that allows both *in silico* and *in vitro* discovery of GIs and subsequent analysis of genomic diversity. The program is called tRNAcc for tRNA gene content and context analysis and was first described for the identification of novel GIs in *E.coli* and *Shigella* spp (Ou *et al.*, 2006b, Ou *et al.*, 2006a). In essence the program works by identifying regions of conserved DNA across multiple genomes that are

associated with tRNA sites. It firstly identifies all the tRNA loci across the genomes being analysed, using a defined set of tRNA genes from the reference genome. Then the program extracts sequences corresponding to the 4 kb upstream and 200 kb downstream segments with reference to the tRNA loci being analysed, with subsequent alignment of these regions using the Mauve alignment software (Darling *et al.*, 2004), to identify regions of conservation / homology within the upstream and downstream tRNA locus flanks. Any sequence that falls between the regions of conservation is assumed to be 'novel' or strain specific DNA. The data for each locus is then exported in a tabular format and as fasta file DNA sequences for further analysis to identify putative GIs. After analysis, the putative GIs can then be investigated further both *in silico* and *in vitro* for further characterisation. This approach can then be used to analyse multiple sequenced genomes and identify 'hot spots' that are frequently occupied by GIs. This approach is particularly useful in identifying sites and islands that may have been unnoticed in previous analysis (Ou *et al.*, 2006b). However the most useful aspect of the tRNAcc software package to the 'wet' laboratory scientist is the rapid identification of the conserved up and downstream flanking regions corresponding to each of the tRNA sites investigated. These regions can then be extracted automatically from multiple genomes and aligned to identify the highly conserved segments that would be suitable for primer design. tRNAcc requires a minimum of two genomes (reference and test genome) but yields better GI predictions when multiple closely related genomes are compared. The alignments of conserved flanking sequences can then be used to design primers that are very likely to anneal correctly to the conserved flanking on either side of the tRNA locus in question in most, if not all, strains of the same species.

A
Genomic island occupied tRNA site

GI inserted - region to long to be amplified
- no PCR amplicon produced

Upstream primer

Upstream conserved flank   Genomic island (GI)   Downstream conserved flank

tRNA

Downstream primer

B
Empty tRNA site

No GI present - region amplified
by - PCR amplicon produced

Upstream primer

Upstream conserved flank   Downstream conserved flank

tRNA

Downstream primer

C

A B C D E F G H I J K L M -ve

Example gel for tRNA_arg38 using primers tRNA_arg38 U / D.

The arrow shows one of the positive 1108 bp 'empty site' (A, B, C, G, J, and K) while the rest of the strains are negative (D, E,F, H, I, L, and M) , suggesting the site is being occupied by a genomic island

1 kb

Figure 4.1: Principle of tRIP (tRNA site interrogation for pathogenicity islands, prophages and other GIs) - PCR.
A. Diagram of occupied tRNA site **B.** Diagram of unoccupied 'empty' tRNA site. **C.** Example agarose gel showing results tRIP-PCR analysis of the tRNAArg38 site, showing positive and negative tRIP –PCR results with *P. aeruginosa* strains 15, 16, 17, 18, 19 , 20, 21, 22, 23, 24, 25, 26 and 27, respectively (China Isolates see Table 5).

This approach was named tRNA site interrogation for pathogenicity islands, prophages and other GIs (tRIP) PCR (Ou *et al.*, 2006b) and was first optimised and used successfully for GI identification in *Shigella* spp (Lonnen, 2006), and then later in *E. coli* (Bin Thani, 2007). The tRIP technique makes use of primers located in the conserved upstream and downstream flanks; if a GI is present and integrated within the site, the distance between the two primers is too great and no PCR amplicon is produced. However if the site is unoccupied (referred to as 'empty' henceforth) the flanks are close enough to produce an amplicon (< 5 kb), and therefore can be detected using standard PCR. An outline of this principle is shown in graphical form in Figure

4.1. If tRIP PCR fails to yield a detectable amplicon (negative tRIP PCR) the interrogated site is considered to be putatively 'occupied' by a GI. Further work can be carried out to elucidate if this site is truly occupied by a GI, or if a deletion, inversion, rearrangement or sequence polymorphism of one or both of the tRNA flanking regions has occurred in this strain (Ou *et al.*, 2006a).

4.3   tRNAcc for *Pseudomonas aeruginosa*

At the beginning of this project (Oct, 2005) there were two publicly available *P. aeruginosa* genome sequences; the fully annotated wound isolate PAO1 (Stover *et al.*, 2000) and the unfinished sequence of PA14 (Lee *et al.*, 2006b) originally isolated from a burn related infection. These two strains were previously used as input into the tRNAcc program to identify putative tRNA hotspots in *P. aeruginosa* genomes as part of the testing of the tRNAcc (Ou *et al.*, 2006b). However the PA14 genome scaffold was significantly realigned (~December 2005) and the initial GI predictions, although still correct, contained inappropriate coordinates; hence, the program was run again. tRNAcc was run as a locally installed program with PAO1 as the reference genome; the location of the sixty three tRNA genes, and the single *tmRNA* gene were identified. The tRNA genes were numbered from 1 to 63 dependent on their genome location starting from coordinate 1 on the genome, and the *tmRNA* was numbered 64 (Appendix D). The nomenclature used for each tRNA gene was as follows: $tRNA^{Arg1}$ (the first tRNA gene in the genome coding for an arginine-specific tRNA molecule) or $tRNA^{Lys47}$ (the forty seventh tRNA on the genome) depending of the location relative to genome coordinate 1. To avoid confusion, for the rest of this work all tRNA genes will be identified using PAO1 tRNA designations (Appendix D). 2 kb segments corresponding to the conserved tRNA upstream and downstream flanking sequences identified by tRNAcc were extracted and analysed using the web based version of the Primaclade primer design

software (http://dousta.umsl.edu/cgi-bin/primaclade.cgi) (Gadberry *et al.*, 2005). tRIP-PCR primers were then designed to interrogate the following tRNA loci: $tRNA^{Arg1}$, $tRNA^{Gly5}$, $tRNA^{Lys10}$, $tRNA^{Pro21}$, $tRNA^{Gly23}$, $tRNA^{Arg38}$, $tRNA^{Lys47}$, *tmRNA,* and $tRNA^{Ser11}$. Additional primers were designed for the $tRNA^{Ser11}$ site despite the fact that this site was not identified as a hotspot in the initial tRNAcc analysis that had used only two input genomes. However, as a GI was reported to be inserted at this tRNA locus (Scott and Pitt, 2004) in the Manchester epidemic strain C3719, so this site was picked as well. The primers designed are shown in the Table 4.1.

4.4 Six genome tRNAcc comparison to two genome tRNAcc.

By September 2006, there were six PA genomes with preliminary genome sequence data available online. These additional genomes were PACS2 (Mathee et al., 2008), C3719 (Mathee et al., 2008), 2192 (Mathee et al., 2008), and LES (Winstanley *et al.*, 2009). These genomes, along with the original PAO1 and PA14, were analysed as before using tRNAcc, the data was then compared to the original tRNA-associated GI predictions to identify how well the tRNAcc program had functioned. The data were also examined further to gain insights into how the different sequenced genomes varied in terms of GI content and nature within the full repertoire of tRNA genes.

The first tRNAcc analysis based on only two genomes (PAO1 and PA14) identified seven tRNA loci ($tRNA^{Arg1}$, $tRNA^{Gly5}$, $tRNA^{Lys10}$, $tRNA^{Pro21}$, $tRNA^{Gly23}$, $tRNA^{Arg38}$, $tRNA^{Lys47}$) and the *tmRNA* gene as sites that harboured genomic islands (Appendix C: Fig. 1 and Table 1.). In this analysis, PAO1 was found to have two GIs and PA14 seven inserted within the eight hotspots identified. When six genomes were analysed, tRNAcc identified a total of sixteen tRNA loci 'hotspots' (Appendix C: Fig. 2 and Table 2).

Table 4.1: tRIP-PCR primers for *P. aeruginosa* designed based on tRNAcc analysis of PAO1 and PA14

tRNA gene	Size of empty site (bp)[1]	Primer	5' to 3' sequence	Primer	5' to 3' sequence
A^{Arg1}	1066	tRNA-Arg1_U	CGAAATCACGAACGTACGC	tRNA-Arg1_D	AGTCTGATTGTCCAAACGTTCAC
tRNA^{Gly5}	2883 / 2897	tRNA-Gly5_U	ACTGACGCTCACGTTGTGAC	tRNA-Gly5_D	GTCGGTAGAACCTGTAATCATCG
tRNA^{Lys10}	1219	tRNA-Lys10_U	AAGGTATACCGGTGACTTACGTG	tRNA-Lys10_D	ACTGAAAACGAGAAAGAATGCG
tRNA^{Ser11}	618	tRNA-Ser11_U	GTTCTTCGTACAAGCTGGTATCAT	tRNA-Ser11_D	TACTTCGAGATATTGAAACAGGCG
tRNA^{Pro21}	unknown	tRNA-Pro21_U	AGGCTGTTTGATGTGTATCACG	tRNA-Pro21_D	AGAAGTGGCGTTGAAGGAGATTG
tRNA^{Gly23}	3115	tRNA-Gly23_U	AATGGCGATTAGGAGGGC	tRNA-Gly23_D	CGCGAAACCCTTTATACTGC
tRNA^{Arg38}	1108	tRNA-Arg38_U	GACCACCATGTCTTCGAGAATC	tRNA-Arg38_D	CTGTACGTATGCGTTAGGTTCG
tRNA^{Lys47}	411	tRNA-Lys47_U	ATCGGGGTATAGCGCAGTC	tRNA-Lys47_D	GCCACTACAACCTGTGAATCG
tmRNA	1637	tmRNA_U	GGCCATCCTTTTACTGGTTCTC	tmRNA_D	TACCCTGGTAGTGAGTGTCTAGCTC

[1] The size of the empty site tRIP-PCR product was predicted using a locally installed copy of e_PCR (Schuler, 1997) and the genomes PAO1, PA14, C3719, PACS2, PA7, LES, and 2192 as alternative templates. If more than one product size was obtained, both sizes are given.

The large increase in the number of sites identified as occupied (an increase of nine tRNA loci) was the result of considerable strain-to-strain diversity within the panel of six *P. aeruginosa* strains examined. For example, when the larger data set was used, PAO1 and PA14 had six and nine GI identified compared to two and seven, respectively, for the two genome tRNAcc run. The program now identified $tRNA^{Lys10}$ (an important site of GI insertion (Kulasekara *et al.*, 2006)) as a site of insertion in PAO1 and PA14 which had been missed in the two genome tRNAcc. This is probably because the two islands inserted in $tRNA^{Lys10}$ in PAO1 and PA14 shared considerable homology impairing the ability of the programme to successfully identify the conserved upstream and downstream flanking regions and the interspersed island. A similar finding occurred at $tRNA^{Arg\ 1}$, in the original tRNAcc study the program found a 22.7 kb GI in PA14 and none in PAO1 (Appendix C, Fig. 1). In the six genome analysis, tRNAcc found a 34.8 kb island in PA14 and a 10.4 kb island in PAO1 (Appendix C, Fig 2.), this suggested that both PAO1 and PA14 may have islands at $tRNA^{Arg1}$ with shared homology. Only by increasing the number of genomes analysed were the correct $tRNA^{Lys10}$ and $tRNA^{Arg1}$ conserved flanking regions defined accurately. This finding meant that the primers for $tRNA^{Arg1}$ needed to be redesigned as the original primers would only detect GI with significant homology to the PAO1 tRNA^{Arg1}-associated island. Five of the sixteen sites identified as occupied were found to be occupied in only one genome each ($tRNA^{Ser11}$, $tRNA^{Leu14,}$ $tRNA^{Ser20}$, $tRNA^{Leu39}$, and $tRNA^{Phe60}$) (Table 4.2), while other sites such as $tRNA^{Pro21}$ and the *tmRNA* gene were occupied in all six strains. This suggested that certain sites are more commonly targeted by mobile genetic elements, or are more suitable for integration than others. .

The number of tRNA associated GI ranged from six in PAO1 and C3719 and seven in LES, to nine in PA14 and 2192 to finally, eleven in PACS2. Table 4.2 shows the total

size of the tRNA associated islands in the six strains in comparison to genome size. The most fascinating finding from this is the variation between individual strains. The accessory genome of PA makes up about ~11% of the genome (Mathee et al., 2008) Strain PAO1 has 51.96 kb of tRNA associated GI DNA which makes up only 0.8% of the total genome. This is in stark comparison with strain 2192 which has 555.05 kb which makes up a huge 8.1% of the total genome size. The finding in strain 2192 that 8.1 % of the genome is made up of tRNA associated islands highlights the important role that tRNA associated genomic islands and prophages play in making up a large component of the accessory genome of some PA strains (Mathee et al., 2008, Shen *et al.*, 2006). Furthermore, both strains PAO1 and 2192 are pathogenic; PAO1 was isolated from wound isolate and 2192 from a CF lung infection. Their large variation in tRNA associated GI content obviously does not affect their ability to cause disease. However it is not known what role the horizontally acquired elements play in strain specific virulence. In the paper describing the PA14 genome, the authors compared the PA14 genomic structure to that of PAO1 and looked for an association between strain specific genes and virulence in *C. elegans* across a panel of strains. No correlation was found between PA14-specific or PAO1-specific genes and virulence, from which the authors concluded *P. aeruginosa* virulence is combinational, and due to a cooperation between genes present in the core and accessory genome and not specific genes or islands (Lee *et al.*, 2006b). However, this was only studied in one model of infection, and a number of known virulence genes in mammals are not involved in virulence in *C. elegans* (Wareham et al., 2005).

Table 4.2: Table showing tRNAcc predicted tRNA associated GIs in strains PAO1, PA14, 2192, C3719, LES, and PACS2.

Strain	PAO1	PA14	2192	C3719	LES	PACS2
GI sizes (kb)	10.48	34.81	10.49	10.49	10.48	4.32
	12.64	35.11	10.6	13.26	113.11	7.58
	9.3	10.9	43.9	16.33	50.19	91.99
	11.77	3.79	63.89	6.94	44.95	46.19
	2.07	17.89	63.36	81.73	6.94	6.95
	5.7	6.95	224.52	4.26	10.35	8.74
		7.84	85.73		5.83	4.39
		108.57	6.93			107.07
		11.47	45.65			10.05
						9.13
						13.21
Total GI DNA kb	51.96	237.33	555.05	133.01	241.85	309.62
Total GI DNA bp	51960	237330	555050	133010	241850	309620
Genome size Bp	6,264,404	6,537,648	6,826,253	6,146,998	6,601,757	6,492,423
% of Genome	0.83	3.63	8.13	2.16	3.66	4.77

4.5 Comparison of the tRNAcc program with experimental approaches.

Two studies using the PAO1 GeneChip® *Pseudomonas aeruginosa* Genome Array (Affymetrix, USA) have been published that investigated genomic diversity in clinical and environmental isolates. The first of the papers tested eighteen strains; this identified eight tRNA genes (*tRNA^{Arg1}*, *tRNA^{Gly5}*, *tRNA^{Lys10}*, *tRNA^{Ser20}*, *tRNA^{Pro21}*, *tRNA^{Gly23}*, *tRNA^{Thr46}*, *tRNA^{Asn55}*) and *tmRNA* as 'hotspots' (Wolfgang *et al.*, 2003). The second study investigated twenty strains, and identified insertion 'hotspots' within five tRNA genes (*tRNA^{Arg1}*, *tRNA^{Gly5}*, *tRNA^{Lys10}*, *tRNA^{Pro21}*, *tRNA^{Gly23}*) and *tmRNA*, all of which were identified in the previously described study by Wolfgang *et al* (Ernst *et al.*, 2003). Both these studies used an experimental *in vitro* approach, but identified less tRNA 'hotspots' with a larger sample size than the tRNAcc analysis with six genomes. This is probably due to the fact that the PAO1 is probably not a 'typical' PA genome. Also a

large number of GIs share 'core' and 'cargo' regions, so regions of plasticity will be missed due to the conserved regions being present at a certain locus (Wurdemann and Tummler, 2007). Therefore the array will not show any variation at that locus. However the array approach did identify two tRNA loci that were missed by the tRNAcc; $tRNA^{Thr46}$ and $tRNA^{Asn55}$. Again this can probably be put down to strain to strain diversity; meaning that 'hot spots' can only be identified in strains that have integrations at those sites, a probability that is affected by sample size and bias. The sixteen tRNA hotspots were identified by tRNAcc using what could be argued is a biased data set (four of the six genomes were isolated from CF patients) compared to the eight identified by an *in vitro* approach investigating 38 strains. Although this bias may be a pitfall, the much larger number of 'hotspots' identified using a smaller panel of strains compared to the genome array approach is a testament to the power of *in silico* tools like tRNAcc for comparative genomics.

4.6 tRIP analysis of China and UK derived *P. aeruginosa* strains

To investigate the occupancy and diversity of the eight tRNA loci and the *tmRNA* gene, two separate panels of strains (Table 4.3) were screened. The first panel of twelve strains were isolated in the UK and are from patients with keratitis, CF, and blood stream (BSI) infections. Strains PAO1 and PA14 were used as controls. The second set of strains were isolated from patients with blood stream infections in Huashan University Hospital, Shangahi, Peoples Republic of China. The strains were tested using the previously described tRIP PCR primers (data not shown). The results of the PCRs for the UK isolates are shown in Table 4.5, and for the China isolates in Table 4.6.

Table 4.3: : Strains and Clinical source of strains tested by tRIP PCR.
Alternative strain names shown in brackets. Bloodstream infection (BSI), cystic fibrosis (CF). Strains highlighted in grey from Huashan University Hospital, Shanghai, PRC. All others excluding K124 (PAO1) and KR125 (PA14) isolated in the UK

Strain Number	Source	Strain Number	Source	Strain Number	Source
KR115	BSI	KR159	BSI	27	BSI
KR124	Wound (PAO1)	15	BSI	28	BSI
KR125	Burns (PA14)	16	BSI	29	BSI
KR126	CF (MID92)	17	BSI	30	BSI
KR127	CF (Clone C)	18	BSI	31	BSI
KR131	Keratitis	19	BSI	32	BSI
KR132	Keratitis	20	BSI	33	BSI
KR133	Keratitis	21	BSI	34	BSI
KR134	Keratitis	22	BSI	35	BSI
KR154	BSI	23	BSI	36	BSI
KR155	BSI	24	BSI	37	BSI
KR156	BSI	25	BSI	38	BSI
KR158	BSI	26	BSI	39	BSI

The result of the tRIP PCR screening across thirty seven strains in the two groups revealed a number of interesting findings. Firstly, like in the six sequenced genomes, the $tRNA^{Pro21}$ site was found to be occupied in all thirty seven strains examined (Table 4.4). In larger scale studies, this site was always found to be occupied and contained both a number of conserved and diverse genomic islands (Rieck, B. personal communication). This suggested that this site was important for the integration of horizontally acquired DNA in *P. aeruginosa*. However, at the time of writing no work has yet been carried out to characterise the role that horizontally acquired DNA integrated in this site plays. The lack of an 'empty site' tRIP-PCR profile (positive empty-site amplicon) suggested that this site was invariably occupied, and hinted that the islands integrated at this locus may no longer retain mobility, hence their persistence within the species. If so, the latter feature would suggest likely ancient integration events as many recently acquired GI have been shown to retain the capacity for

spontaneous site-specific excision and integration. Further work is currently underway to investigate the GIs mapping to this site.

In contrast to $tRNA^{Pro21}$, the results for the $tRNA^{Lys47}$ site suggested that this site was empty in all the strains investigated (Table 4.4). However, this was known not to be the case, as in strain PA14 there was the mobile island, PAPI-1, inserted into this locus. This suggested that the tRIP-PCR assay as originally performed could not be relied upon to detect of the presence of islands that are still highly mobile or unstable. This is due to the fact that within the population of cells derived from a single strain that harbours a highly mobile / unstable island there will always be a proportion of cells with an empty site, as well as cells bearing an occupied site. Depending on the relative abundance of these two populations and the degree to which the tRIP PCR assay has been optimised for sensitivity, amplification will be likely to produce a PCR amplicon. For example two of the strains that tested tRIP negative for this site (KR127 and KR158), were both found later to have an island integrating in this site (see section 4.8). Like $tRNA^{Lys47}$, the $tRNA^{Ser11}$ site was found to be unoccupied in all genomes tested, despite a previous description of a GI associated with this site in strain C3719 (Scott and Pitt, 2004). This suggested that GI integration into this site was rare compared to other sites examined. However without further confirmation like described for $tRNA^{Lys47}$ this cannot be confirmed as definite.

The second most frequently occupied site was $tRNA^{Gly23}$ which was found to be occupied in 89% of isolates (96% China, 75% UK), again highlighting this as a hotspot for foreign DNA integration (Table 4.4). Unsurprisingly the $tRNA^{Lys10}$ site was found to be occupied in 71.5% of strains (76% China, 67% UK). This site has been described to be occupied by PAPI-2 in PA14, ExoU islands A, B and C in various PA strains, and by a remnant PAPI-2-like island in PAO1 (Kulasekara et al., 2006).

The *tmRNA* gene was found to be occupied in 65% of strains (64% China, 65% UK) demonstrating this as an important hotspot for the integration of GI in PA. This would be expected as this site has been identified as an important site of integration of GIs in a number of bacterial species (Williams, 2002).

Almost equally occupied were *tRNA*^{Gly5} and *tRNA*^{Arg38} with occupation levels of 54% (64% China, 30% UK) and 51% (56% China, 42% UK), respectively (Table 4.4). It is worth noting that both sites appeared to be occupied more often in the China strains than in the UK strains. However a much large sample sizes would be required to investigate if there is a statistically significant geographical difference in site occupancy. As described before, the data corresponding to the final site *tRNA*^{Arg1} is only measuring the presence of a region 10 kb downstream of the tRNA end of the PAO1 tRNA^{arg1}-associated GI and is not measuring the occupancy of the tRNA site. However, 27% (16% China, 50% UK) of strains were negative by tRIP PCR, with the remaining 73% producing a positive band suggesting this region was present in 73% of strains tested. This implies that this region of the PAO1 island detected by the PCR (also present in sequenced strains 2192, LES and C3719) is highly prevalent in the PA population. As described before in regard to the *in silico* tRNAcc results, the reason why some tRNA sites are found to be occupied at much higher frequencies than others is still unknown, but once a more comprehensive picture of site occupancy has been obtained further studies can be initiated to investigate this phenomenon.

Table 4.4: tRIP-PCR predicted occupation frequencies for the 8 tRNA genes and the 1 tmRNA site in the 12 UK and 25 China isolates.

tRNA site	China (n = 25)	UK (n = 12)	Combined (n= 37)
Arg1	4	6	10
%	16	50	27
Gly5	16	4	20
%	64	33	54
Lys10	19	8	27
%	76	67	73
Ser11	0	0	0
%	0	0	0
Pro21	25	12	37
%	100	100	100
Gly23	24	9	33
%	96	75	89
Arg38	14	5	19
%	56	42	51
Lys47	0	0	0
%	0	0	0
tmRNA	16	8	24
%	64	67	65

4.7   tRNA site occupancy genotyping (tRIP genotype)

To investigate the prevalence of the various 'tRIP genotypes', a genotype designation based on the tRIP-PCR-predicted occupancy of the tRNA sites was given to each strain (Table 4.7). For each occupied site the tRNA gene number was given; for an occupied *tmRNA* gene the label tmRNA was given. So for a strain with the $tRNA^{Lys10}$, $tRNA^{Pro21}$, $tRNA^{Arg38}$ and *tmRNA* sites occupied the genotype would be: 10, 21, 38, tmRNA. All recognized tRIP genotypes were then given an arbitrary genotype number. The genotype details, assigned genotype numbers, numbers of sites predicted to be occupied, frequency of genotype, and the source countries of the strains are all shown in Table 4.7.

Table 4.5: tRIP PCR results for 12 clinical isolates isolated from the UK and PAO1 and PA14.
Eight tRNA sites and tmRNA screened. tRIP genotype (Sites deemed occupied by tRIP), number of sites occupied, and assigned genotype number. The two fully sequenced control strains are shown in red. + = Positive PCR - = Negative PCR.

No.	Strain	Arg1	Gly5	Lys10	Ser11	Pro21	Gly23	Arg38	Lys47	tmRNA	PA tRIP Genotype	No.	Genotype
1	PAO1	+	-	-	+	-	+	+	+	+	5, 10, 21	3	3
2	PA14	-	-	-	+	-	-	-	+	-	1, 5, 10, 21, 23, 38, tmRNA	7	19
3	KR115	+	+	-	+	-	-	-	+	-	10, 21, 23, 38, tmRNA	5	14
4	KR126	-	-	+	+	-	-	-	+	+	1, 5, 21, 23, 38,	5	15
5	KR127	-	-	-	+	-	-	-	+	-	1, 5, 10, 21,23 , 38, tmRNA	6	19
6	KR131	+	-	-	+	-	+	-	+	-	5, 10, 21, 38, tmRNA	5	16
7	KR132	-	+	-	+	-	-	+	+	+	1, 10, 21, 38	4	7
8	KR133	-	+	-	+	-	-	+	+	-	1, 10, 21, 38, tmRNA	5	24
9	KR134	+	+	-	+	-	-	-	+	-	10, 21, 23, tmRNA	4	8
10	KR154	+	+	+	+	-	-	+	+	-	21, 23, tmRNA	3	5
11	KR155	-	-	-	+	-	-	+	+	-	1, 5, 10, 21, 23, tmRNA	6	20
12	KR156	+	+	+	+	-	-	-	+	-	21, 23, tmRNA	3	5
13	KR158	-	+	+	+	-	-	+	+	+	1, 21, 23	3	4
14	KR159	+	+	-	+	-	+	+	+	+	10, 21	2	1

Table 4.6: tRIP PCR results for 25 bloodstream isolates isolated from the Huanshan University Hospital, Shanghai, PRC.
Eight tRNA sites and tmRNA screened. tRIP genotype (Sites deemed occupied by tRIP), number of sites occupied, and assigned genotype number. .
+ = Positive PCR - = Negative PCR.

No.	Strain	Arg1	Gly5	Lys10	Ser11	Pro21	Gly23	Arg38	Lys47	tmRNA	PA tRIP Genotype	No.	Genotype
15	58	+	-	-	+	-	-	+	+	-	5, 10, 21, 23, tmRNA	5	17
16	68	+	-	-	+	-	-	+	+	-	5, 10, 21, 23, tmRNA	5	17
17	79	+	-	-	+	-	-	+	+	+	5, 10, 21, 23	4	9
18	81	+	+	-	+	-	-	-	+	-	10, 21, 23, 38, tmRNA	5	14
19	82	+	-	+	+	-	+	-	+	-	5, 21, 38, tmRNA	4	11
20	83	-	+	-	+	-	-	-	+	-	1, 10, 21, 23, 38, tmRNA	6	21
21	85	+	+	+	+	-	-	+	+	+	21, 23	2	2
22	86	-	+	-	+	-	-	-	+	-	1, 10, 21, 23, 38, tmRNA	6	21
23	87	+	-	+	+	-	-	-	+	+	5, 21, 23, 38	4	10
24	88	+	+	-	+	-	-	+	+	+	10, 21, 23,	3	6
25	91	+	-	+	+	-	-	+	+	-	5, 21, 23, tmRNA	4	11
26	92	-	-	-	+	-	-	-	+	+	1, 5, 10, 21, 23, 38	6	22
27	95	+	+	-	+	-	-	-	+	-	10, 21, 23, 38, tmRNA	5	14
28	98	-	+	-	+	-	-	-	+	-	1, 10, 21, 23, 38, tmRNA	6	21
29	99a	+	-	-	+	-	-	+	+	-	5, 10, 21, 23, tmRNA	5	17
30	99b	+	-	-	+	-	-	-	+	-	5, 10, 21, 23, 38, tmRNA	6	23
31	104	+	-	-	+	-	-	+	+	-	5, 10, 21, 23, tmRNA	5	17
32	106	+	-	-	+	-	-	+	+	-	5, 10, 21, 23, tmRNA	5	17
33	107	+	-	-	+	-	-	+	+	+	5, 10, 21, 23	4	12
34	108	+	-	+	+	-	-	+	+	-	5, 21, 23, tmRNA	4	11
35	109	+	-	-	+	-	-	-	+	+	5, 10, 21, 23, 38	5	18
36	112	+	-	-	+	-	-	-	+	-	5, 10, 21, 23, 38, tmRNA	6	23
37	114	+	+	-	+	-	-	-	+	-	10, 21, 23, 38, tmRNA	5	14
38	115	+	+	-	+	-	-	-	+	+	10, 21, 23, 38	4	13
39	118	+	-	+	+	-	-	-	+	+	5, 21, 23, 38	4	10

In the thirty nine strains examined, including PAO1 and PA14, there were twenty three different tRIP genotypes which suggested that based on the nine tRNA/tmRNA loci analysed alone there is a significant level of diversity. Another sixteen genotypes have only one member, meaning that a minimum of 42% of the tested strains had a unique accessory genome complement when compared to one another. tRIP genotypes 17, 14, and 21 made up 31% of strains tested. All three of these abundant profiles were indicative of five or six sites being occupied, suggesting that strains with more occupied sites and therefore more horizontally acquired DNA are possibly selected for in natural populations of PA. All strains that possessed the three most common genotypes were isolated from BSIs, raising the question whether certain strains with a particular complement of GIs are better suited to invasive diseases such as BSI. Strain PA14 which was one of the two strains in the tRIP genotype 19 (Table 4.7) had been previously reported to the be the most prevalent worldwide clone in a population study (Wiehlmann et al., 2007). The other member of genotype no. 19 was strain KR127 ((Table 4.7)) which was a Clone C strain which was a previously defined as a distinct genotype from PA14 (Wiehlmann et al., 2007). Interestingly, in this strain panel PAO1 was one of the fourteen strains that had a unique tRIP genotype. This finding suggests that even though PAO1 is used as the standard laboratory strain it is probably actually a 'rare' clone in terms of its accessory genome content. Although easily genetically manipulated for experimentation, the results gained from this strain are probably not representative of a widespread or major clonal group of P. aeruginosa. This highlights the need for the selection of representative strains for future genome projects and experimental work.

Table 4.7: tRIP genotyping.
Genotype numbers, tRIP genotype, number of sites occupied, frequency of genotype, and source of strain country were the genotype was isolated.

Genotype No.	PA tRIP Genotype	No. sites occupied [1]	No. of isolates[2]	Source countries[3]
17	5, 10, 21, 23, tmRNA	5	5	China × 5
14	10, 21, 23, 38, tmRNA	5	4	UK x1 , China × 3
21	1, 10, 21, 23, 38, tmRNA	6	3	China × 3
19	1, 5, 10, 21, 23, 38, tmRNA	6	2	UK x1, USA x1
5	21, 23, tmRNA	3	2	UK x1 , UK x1
10	5, 21, 23, 38	4	2	China x2
11	5, 21, 23, tmRNA	4	2	China x2
23	5, 10, 21, 23, 38, tmRNA	5	2	China x2
1	10, 21	2	1	UK x1
2	21, 23	2	1	China x1
3	5, 10, 21	3	1	Aus x1
4	1, 21, 23	3	1	UK x1
6	10, 21, 23,	3	1	China x1
8	10, 21, 23, tmRNA	4	1	UK x1
9	5, 10, 21, 23	4	1	China x1
12	5, 10, 21, 23	4	1	China x1
13	10, 21, 23, 38	4	1	China x1
15	1, 5, 21, 23, 38,	5	1	UK x1
16	5, 10, 21, 38, tmRNA	5	1	UK x1
18	5, 10, 21, 23, 38	5	1	China x1
20	1, 5, 10, 21, 23, tmRNA	6	1	UK x1
7	1, 10, 21, 38	4	1	UK x 1
22	1, 5, 10, 21, 23, 38	6	1	China x1
24	1, 10, 21, 38, tmRNA	5	1	UK x1

Note: [1] Number of the eight tRNA genes and tmRNA gene (Total nine) occupied. [2] Number of isolates screened in panel of thirty seven with this tRIP genotype. [3] Number of strains and source country isolated.

4.8 Design of conserved primer for $tRNA^{Lys}$ associated islands

Although all tRIP-PCR assays targeting $tRNA^{Lys47}$ had yielded an amplicon consistent with an empty site, the $tRNA^{Lys47}$ site was found to be frequently occupied when this site was examined using island-specific primers in conjunction with $tRNA^{Lys47}$ flanking primers. In the case of PA14, C3719, and Clone C strains it was known that pKLC102-like islands integrated into both $tRNA^{Lys10}$ and $tRNA^{Lys47}$. A conserved primer was designed that could detect the presence of pKLC102-like islands integrated into either of the $tRNA^{Lys}$ sites. This primer was designed by aligning all the ends proximal to the 3' end of the tRNA for all known pKLC102 like islands using ClustalX, which was then used as an input for Primerclade to design a PCR primer located in a conserved region facing out of the GI towards the tRNA. The primer (pKLC102-LikeIntR -5'-CTGGAAGCTGGTGCAGCGCG-3') was then combined with either of the upstream tRIP primers for the $tRNA^{Lys10}$ and $tRNA^{Lys47}$. These primer pairs were used against a panel of twenty four diverse clinical isolates obtained from various sites of infection and strains PA14, 2192, and C3719 as controls (not included in calculations of occupancy) (Table 4.8). The region that the primer pKLC102-LikeIntR binds is highly conserved amongst pKLC102 family islands (data not shown), providing for a high likelihood of detection of pKLC102-like islands at these sites were these to be present. However, it should be noted that the results of this assay do not confirm that a whole pKLC102-like island is present but rather that its conserved extremity is. Also, importantly the assay would fail to detect the presence of non-pKLC102-like islands at these sites,

The results were most revealing: 74.1 % of the strains (not including control strains) carried a pKLC102-like island in one or both of the two $tRNA^{Lys}$ genes. This finding fits with that reported by Klockgether *et al* who tested 71 strains from diverse habitats and

geographical locations using a pKLC102-based macroarray to detect the presence of the PAPI-1-like pKLC102 island (Klockgether *et al.*, 2007b). They found that 70% (51 of 71) of strains carried a pKLC102-like island.

Table 4.8: Epidemiology and tRNA^{Lys} of PAPI-1-like islands in clinical isolates.
Showing: Lab number, clinical source, presence of islands in tRNA^{Lys47} and tRNA^{Lys10}. Strains in red are fully sequenced control strains.

Number	Lab Number	Clinical Source	Island in tRNA^{Lys47}	Island in tRNA^{Lys10}	Both sites	Island
1	KR115	BSI	Yes	No		Yes
2	KR125 (PA14)	low pyocanin production	Yes	Yes	Yes	Yes
3	KR126 (MID9245)	Midland epidemic strain	No	No		No
4	KR127 (Clone C)	CF	Yes	Yes	Yes	Yes
5	KR131 (K1)	Keratitis	No	No		No
6	KR133 (K6)	Keratitis	No	Yes		Yes
7	KR134 (K30)	Keratitis isolate	No	No		No
8	KR154	BSI	No	Yes		Yes
9	KR155	BSI	No	Yes		Yes
10	KR156	BSI	No	Yes		Yes
11	KR158	BSI	Yes	No		Yes
12	KR159	BSI	No	Yes		Yes
13	KR223	Sputum - Brochiectasis	No	No		No
14	KR225	Sputum (ITU)	Yes	No		Yes
15	KR226	Endo.Trac. Aspirate (ITU)	Yes	No		Yes
16	KR227	Ear Swab Discharging Ear	Yes	Yes	Yes	Yes
17	KR228	Sputum (ITU)	No	No		No
18	KR229	Sputum - Brochiectasis	Yes	No		Yes
19	KR230	Sputum - Brochiectasis	Yes	No		Yes
20	KR231	Sputum (ITU-Renal patient)	No	No		No
21	KR232	Wound Swab	Yes	Yes	Yes	Yes
22	KR233	Wound Swab	Yes	No		Yes
23	KR234	Otitis Media	Yes	Yes	Yes	Yes
24	KR235	Wound Swab	Yes	Yes	Yes	Yes
25	KR365	UTI	No	No		No
26	KR732 (2192)	CF	Yes	No		Yes
27	KR479 (C3719)	CF (Manchester epi. Strain)	Yes	No		Yes
		Total no.	15	11	6	20
		% test strains	55.55555556	40.7	22.2	74.1
		Strains in Red denotes control strains				

This finding links in with this study and suggests that PAPI-1 / pKLC102 family islands are found in the majority of *P. aeruginosa* strains. The ubiquitous presence of this family of islands suggests that their presence is advantageous within PA strains and that there are selective pressures to maintain the PAPI-1 / pKLC102 islands throughout diverse PA populations and habitats despite the high level of tRIP-PCR demonstrable spontaneous excision of this island. In 55.5% of strains PAPI-1-like islands were integrated in *tRNA^{Lys47}*, compared to 40.7% of strains with equivalent islands in

$tRNA^{Lys10}$, indicating that $tRNA^{Lys47}$ may be slightly favoured as the site of integration of this family of islands. 22.2% of strains had a PAPI-1-like island inserted in both sites, however without further work it was not possible to ascertain if this represented two independent islands in the one cell or one island integrating into either of the two lysine tRNA gene sites in different cells within the population.

4.9 Sequencing of pKLC102 islands

To investigate which islands were integrated into the two $tRNA^{Lys}$ sites of each strain, a number of amplicons were sequenced from the $tRNA^{Lys}$ specific primers. Four strains had both $tRNA^{Lys}$ sites occupied. The regions downstream of the $tRNA^{Lys}$ (the island DNA) were extracted from the sequences and blasted against the NCBI nucleotide database.

Table 4.9: Sequencing results of amplicons derived using the pKLC102-specific primer and either $tRNA^{Lys10}$ or the tRNA^{Lys47} upstream flank primers.
Blastn hits shown correspond to the best hit versus the island-specific segment of sequence data only. Table shows strain number, sequence quality (clipped / un-clipped), primer used (tRNA-Lys47U is upstream of $tRNA^{Lys47}$ and tRNA-Lys10_U is upstream of $tRNA^{Lys10}$). Strains highlighted in colour represent strains with both sites occupied.

Strain	Clipped / Un	Primer	Blastn Island hit	% Hit
KR127	Clipped	tRNA-Lys47_U	pKLC102	100%
KR158	Clipped	tRNA-Lys47_U	PAGI-4	94%
KR225	Clipped	tRNA-Lys47_U	PAGI-4	99%
KR226	Clipped	tRNA-Lys47_U	ExoU B	92%
KR227	Clipped	tRNA-Lys47_U	PAPI-1	99%
KR232	Clipped	tRNA-Lys47_U	PAPI-2	96%
KR235	Un Clipped	tRNA-Lys47_U	PAPI-1	93% (Short seq)
KR127	Clipped	tRNA-Lys10_U	PAGI-4	98%
KR133	Clipped	tRNA-Lys10_U	n/a seq too short	
KR155	Un Clipped	tRNA-Lys10_U	n/a seq too short	
KR156	Clipped	tRNA-Lys10_U	PAPI-2	92%
KR159	Clipped	tRNA-Lys10_U	PAGI-4	99%
KR227	Clipped	tRNA-Lys10_U	PAPI-2	100%
KR232	Clipped	tRNA-Lys10_U	PAPI-2	97%
KR235	Clipped	tRNA-Lys10_U	PAGI-4	96%

The top blastn hits were taken as the closest related island, the results are shown in Table 4.9. In all cases pKLC102-like islands were found to be integrated at these sites based on the high level of DNA similarity. However without further experimentation and sequencing of the whole islands it cannot be ascertained if the identified structures represent intact islands or smaller remnant segments. Of the four strains investigated with both sites occupied (KR 127, 227, 232 and 235) only one (KR232) was found to a have the same pKLC102-like island integrated at both sites (based on sequence comparison), demonstrating that in this small sample the majority of strains with two occupied $tRNA^{Lys}$ have two distinct islands integrated at these sites.

4.10 Discussion

This investigation has further cemented the ability of the tRNAcc algorithm to identify integration 'hotspots'. The newly performed tRNAcc analysis linked with previous studies has increased the number tRNA and *tmRNA* genes identified as hotspots for the integration of GIs to eighteen of a total sixty four *P. aeruginosa* PAO1-set tRNA genes and tmRNA. These sites are found to be variably occupied between strains with a predilection to certain sites ($tRNA^{Pro21}$, $tRNA^{Gly23}$, *tmRNA*). At most other sites, however, significant diversity exists and a large number of strains have a unique occupancy of tRNA sites, demonstrating the previously established diversity within the PA strain population. In some strains up to 8% of the genome is made up of DNA integrated in tRNA loci, emphasising the importance in mediating diversity in *P. aeruginosa*.

Further why some of the tRNA sites are found more occupied than others is interesting. In a study investigating the occupancy of tRNA sites in *E.coli*, which also found that certain sites are favoured (Germon *et al.*, 2007). The authors found that tRNA that code

for frequent codons or those that are highly transcribed were occupied less, possibly as integration within these sites would affect tRNA expression and could be deleterious to the host cell. Germon *et al* also found that *polycistronic* tRNA were targeted less often, something that was not found to be the case in *P. aeruginosa*: $tRNA^{Gly23}$ and $tRNA^{Lys47}$, which are occupied in six and five out of the six analysed genomes respectively and are the most distal tRNA genes in two distinct three-tRNA polycistronic configurations (Apendix C, Table 2). Germon *et al* also highlighted that the most highly occupied sites had altered local DNA structure (DNA curvature). They found a decrease of DNA curvature inside the tRNA loci and a sharp increase at the end of the loci. If this affects *P. aeruginosa* genomes in the same way remains to be elucidated.

A study investigating the population structure of *P. aeruginosa* (Wiehlmann et al., 2007) investigated two hundred and forty, geographically diverse strains isolated from a range of environmental and clinical sources. This was done using a custom microarray (referred to henceforth as the '58 genotype microarray') containing fifty eight different regions from the core and accessory genome. This study found that there are two large non-overlapping clusters, one containing seven of the 16 most common clones. Outside these two clonal groups were another forty-five individual clones with very few related strains identified.

This study investigated the association between a number of single nucleotide polymorphisms (SNPs) on the core genome and the presence of specific regions from ten genomic islets and six genomic islands (Wiehlmann et al., 2007). They found that some regions of the core genome are found associated with a defined subset of others, suggesting that some combinations are advantageous, whereas others are selected against in the population. On the other hand, other regions on the core genome appeared to be free to recombine. The study concluded that elements on the core genome

(selected SNPs) and certain regions on the accessory genome are non-randomly associated. This suggests in evolutionary terms that certain combinations of core genome SNPs linked with certain factors encoded on the accessory genome are advantageous. The authors concluded that the *P. aeruginosa* genome is made up clone specific regions in both the core and accessory genomes, with some regions in the core genome that have unrestricted gene flow (Wiehlmann et al., 2007). However, this study did not measure the variation at all hotspots identified by tRNAcc and the two previously discussed microarray studies. Therefore a larger scale study investigating diversity at all tRNA sites highlighted in this work, and at valine-glycine repeats (vgr) also identified as insertion hotspots in one of the PAO1 microarray studies (Ernst et al., 2003) should be carried to try to give a better measure of the variation within the accessory genome. As the work in this study has demonstrated, there may be considerable diversity at the tRNA sites which was not investigated as part of the 58 genotype microarray population study. Therefore it is possible that the 58 genotype microarray study actually underestimated the level of diversity. Meaning the proposed model for the population structure (Figure 4.2 A) which is based on a two level core and accessory genome although accurate based on the data examined, may be potentially missing an added level of diversity reminiscent of that identified in this study.

From the data in the 58 genotype microarray study combined with the data presented here it is likely that the *P. aeruginosa* genome structure has three different levels of conservation (Figure 4.2 B). Firstly 90% of *P. aeruginosa* genome is made from the highly conserved core genome, with clonal fitness polymorphisms at various loci under selective pressure (Figure 4.2 C). The second level is made up of a number of semi-conserved, clonally specific genomic islands (e.g *exoU* family islands (Kulasekara

et al., 2006)) with some internal variable regions) (Figure 4.2 C). This second level could be defined as the 'outer core' genome; made up of more ancient acquisitions of horizontally acquired DNA, most of which are stably integrated at a number of loci (Figure 4.2 C). With some of these 'outer core' regions gradually moving towards becoming part of a clone specific genome. These would be the regions that were found to be linked to certain core genome SNPs in the Wiehlman *et al* population study (Wiehlmann et al., 2007). Over longer time scales, these regions in the 'outer core' will undergo selection and in certain clones become essential to certain lifestyles / niches, a process which has been described in the pathoadaptation of *E. coli* strains (Brzuszkiewicz *et al.*, 2006). The third and final level which is excluded in the previously described population model can be defined as the true 'accessory' genome or 'mobilome'. This is made up of a diverse range of strain specific integrations of phages, GIs and other mobile elements, many of which are integrated within tRNA genes. Some of these elements will be found more commonly in larger numbers of strains due to their promiscuity or strong selective advantages in certain niches. Other elements may be rare and only found in a small number of strains such as the Manchester (MA) island inserted in *tRNA^{Ser11}* in the Manchester epidemic strains C3719 (Lewis *et al.*, 2005). These rare islands may reflect very recent *de novo* emergence of new islands that have yet to disseminate within the *P. aeruginosa* species, or alternatively islands that offer a selective advantage in very narrow niches
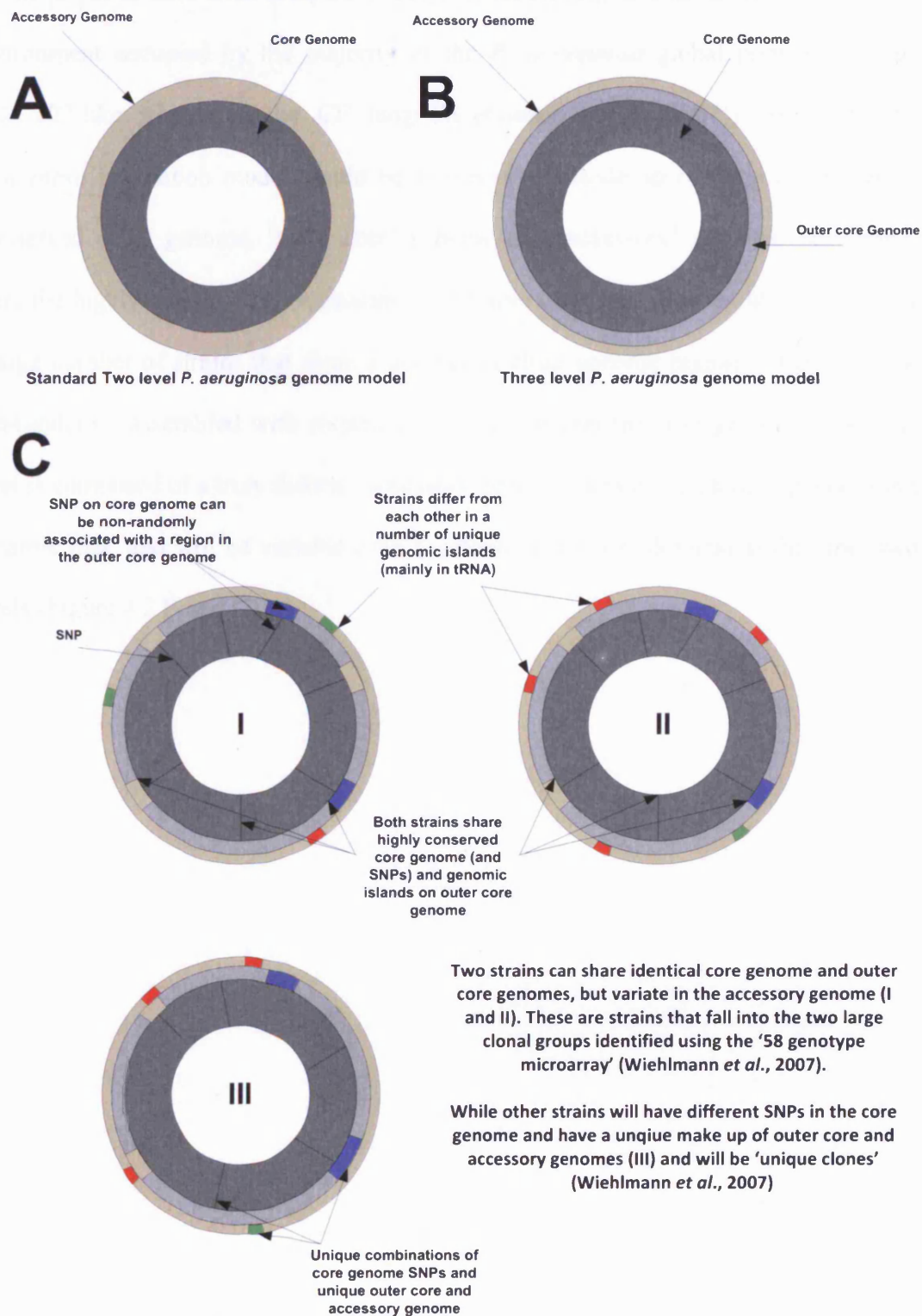
Figure 4.2: Models of *P. aeruginosa* genome structure.
A. Standard two level model **B.** Revised three level model. **C.** Types of strain to strain variation

that have yet to have been sampled widely, whilst serving as a handicap in the wider environment occupied by the majority of the *P. aeruginosa* global population (e.g. pKLC102-like islands in the CF lung (Wiehlmann et al., 2007)). Thus, the *P. aeruginosa* population model would be refined to be made up of three components: 'conserved core' genome, 'outer core' genome and 'accessory' genome. All strains share the highly conserved core genome. The 'outer core' genome should be present in a large number of strains that share a number of clone specific regions which may be non-randomly assembled with respect to the elements on the core genome. The final level is composed of a truly diverse 'accessory genome' which is undergoing a constant dynamic flux, and will be variable even in strains which are identical at the other two levels (Figure 4.2 B and C).

5 Evaluation of the contribution of genomic islands to the virulence and fitness of *Pseudomonas aeruginosa*

5.1 Chapter overview

This chapter investigated the contribution of genomic islands to the biological fitness and virulence of *P. aeruginosa* strain PA14. This was investigated by developing and using techniques to create large (>10kb) genomic island deletion mutants of three genomic islands in PA14. The islands deleted were the previously described PAPI-1 and PAPI-2 (He et al., 2004) and a novel genomic island integrated in a proline-tRNA site named $tRNA^{Pro21}$ island. The deletion mutants of the islands were then evaluated compared to wildtype PA14 in a range of *in vitro* (growth curves, motility and biofilm) assay and in *in vivo* infection models to identify any role played by any of the three genomic islands in these processes.

5.2 Deletion of PAPI-2: optimization of a deletion method for precise surgical excision of large chromosomal regions in *P. aeruginosa.*

5.2.1 Overview

The PAPI-2 island is a member of the Exo-U family of island; it carries the potent type three secreted cytotoxin *exoU* and its chaperone *spcU*. The PAPI-2 island also encodes a number of other genes with unknown function. Most studies examining the role of ExoU have concentrated on the effect of the acquisition and loss of the *exoU* alone (Allewelt et al., 2000, McMorran et al., 2003, Schulert et al., 2003, Shaver and Hauser, 2004). The *exoU* gene is always found on genomic islands (Kulasekara *et al.*, 2006), and the genes located with these different genomic islands could conceivably have undergone selection as single units. Therefore use of a 'whole island' deletion approach should facilitate identification of the fitness and/or niche-associated benefits

that may have selected for the acquisition and maintenance of the whole island. This approach as opposed to a single-gene knock-out strategy should help elucidate possible synergistic effects between one or more genes on the island, the functions of many of which still remain unknown.

5.3 Deletion of PAPI-2

The aim was to delete the 10,642bp region between the PA14 genome coordinates 4580544 to 4591006 thus deleting the whole PAPI-2 island (Figure 5.1).

5.4 Construction of suicide vector for deletion of PAPI-2 island.

Oligonucleotide PCR primers (Table 5.1) were designed for a splicing overlap extension (SOE) -PCR based on sequences designed by Choi and Schweizer (Choi and Schweizer, 2005). The primer 3'-end was designed to amplify the overlapping homologies flanking the target for deletion; either up or downstream of the area to be deleted. Figure 5.3 gives a graphical representation of the principal of SOE-PCR. The 5'-end of these primers were designed to either have an overlapping homologies to a gentamicin-FRT cassette amplified from pPS856 (Hoang et al., 1998), or include a Gateway *attB* recombination site (Choi and Schweizer, 2005) (Table 2.1).
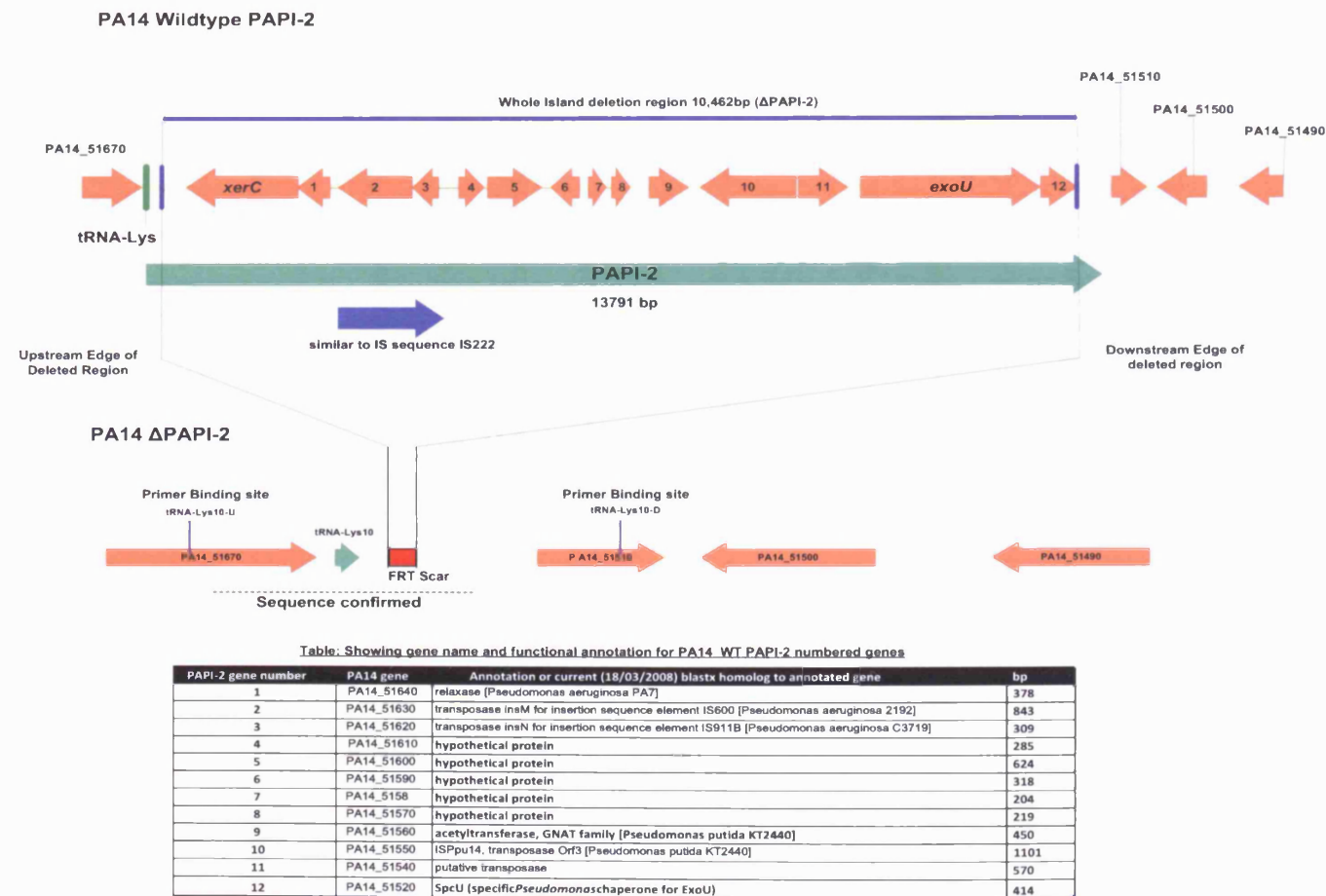
Figure 5.1: Showing the genetic map of the wildtype PA14 PAPI-2 island region.
Showing the targeted region for deletion by allelic exchange in strain PA14ΔPAPI-2 (KR573). Map also shows position of upstream and downstream tRIP-PCR primers used to sequence the deletion site. The table below gives PAPI-2 genes; PA14 gene name, current (04/2009) highest NCBI blastx hit, and size in bp for the numbered PAPI-2 gene.

113

5.5   Construction of suicide vector for deletion of PAPI-2 island.

Oligonucleotide PCR primers (Table 5.1) were designed for a splicing overlap extension (SOE) -PCR based on sequences designed by Choi and Schweizer (Choi and Schweizer, 2005). The primer 3'-end was designed to amplify the overlapping homologies flanking the target for deletion; either up or downstream of the area to be deleted. The 5'-end of these primers were designed to either have an overlapping homologies to a gentamicin-FRT cassette amplified from pPS856 (Hoang et al., 1998), or include a Gateway *attB* recombination site (Choi and Schweizer, 2005) (Table 5.1).

5.5.1   Amplification of up and downstream homologous regions

To delete the PAPI-2 island, upstream and downstream homologous regions were amplified by PCR from *P. aeruginosa* strain PA14 (KR125) genomic DNA as template with KOD-Hotstart polymerase (Merck, UK), using primers PAPI2UFFW-Gm + PAPI2UFRS-GWR. The downstream homologous region was amplified using primers PAPI2DFFW-GWL + PAPIDFRS-Gm respectively (Table 5.1). The FRT site flanked Gentamicin cassette (Gm-FRT) from plasmid pPS856 was amplified from purified plasmid DNA using primers Gm-F / R (Choi and Schweizer, 2005). A PCR product with the correct size was confirmed with visualisation by gel electrophoresis (Figure 5.2 A). The fragments were then extracted and cleaned up from the agarose gel, and quantified by gel electrophoresis.

Table 5.1: PCR primers used for construction of PAPI-2 deletions

Primer Name	Primer sequence (Red = homology for SOE)	Target / Function / Reference
PAPI2UFFW-Gm	AGGAACTTCAAGATCCCCAATTCGACG TCAATGCGGGCCTAATGTTCG	Upstream of PAPI-2 overlap to Gm-FRT cassette
PAPI2UFRS-GWR	TACAAGAAAGCTGGGTGCTGCCCCCTG CGCTGTCACT	Upstream of PAPI-2 –overlap to GWR
PAPI2DFFW-GWL	TACAAAAAAGCAGGCTGCAGACCGTCC AGGCAATGTT	Downstream of PAPI-2 –overlap to GWL
PAPIDFRS-Gm	TCAGAGCGCTTTTGAAGCTAATTCGGC AAGGGGAAGGAGCGATACTG	Downstream of PAPI-2 – overlap to Gm-FRT cassette
Gm-F	CGAATTAGCTTCAAAAGCGCTCTGA	Amplification of Gm-FRT cassette from pPS856 (Choi and Schweizer, 2005)
Gm-R	CGAATTGGGGATCTTGAAGTTCCT	Amplification of Gm-FRT cassette from pPS856 (Choi and Schweizer, 2005)
GW-attb1	GGGGACAAGTTTGTACAAAAAAGCAG GCT	Gateway *attB* primers (Choi and Schweizer, 2005)
Gw-attb2	GGGGACCACTTTGTACAAGAAAGCTGG GT	Gateway *attB* primers (Choi and Schweizer, 2005)

5.5.2 Splicing overlap extension (SOE) PCR

To create the fragments for homologous recombination 50 ng of each of the upstream (UF-PAPI-2) and downstream flank (DF-PAPI-2) and the Gm-FRT cassette were amplified using a SOE-PCR protocol (see Materials and Methods), using primers GW-attB1 / 2. The PCR products were visualised by gel electrophoresis (Figure 5.2 B) and the bands of the correct size excised from the gel, and cleaned up. The resulting products were eluted in TE buffer (pH 8.0) and visualised by gel electrophoresis to ensure a specific and correct size product had been extracted (Figure 5.2 C).

Gel A. PCR fragments for Splicing overlap extension (SOE) PCR

Gel B. Splicing overlap extension (SOE) PCR

Key
A= 1053bp Gm-FRT cassette

B=1476bp-UFtRNA-Lys10-PA14

C=1009bpDF-PAPI-2-PA14

Key
A= 3597bp ΔPAPI-2 SOE fragment
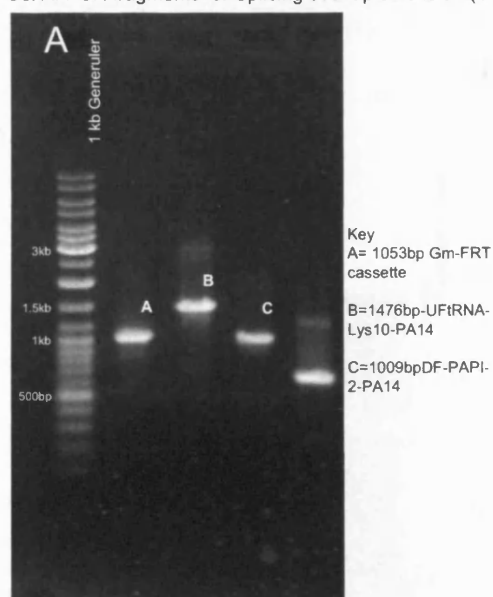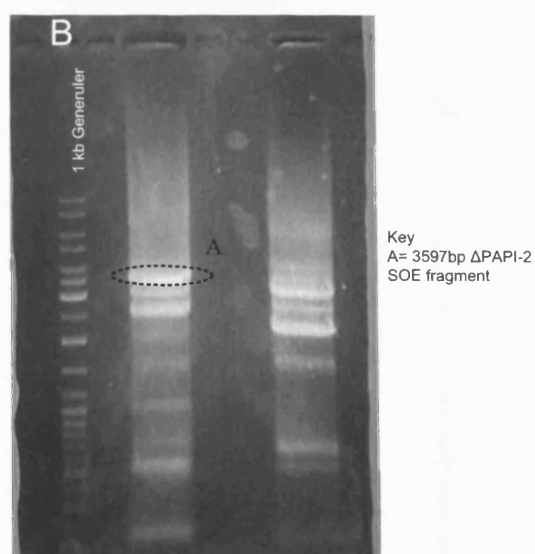
Gel C. Sizing of Splicing overlap extension (SOE) PCR fragment

Key
A= 3597bp ΔPAPI-2 SOE fragment
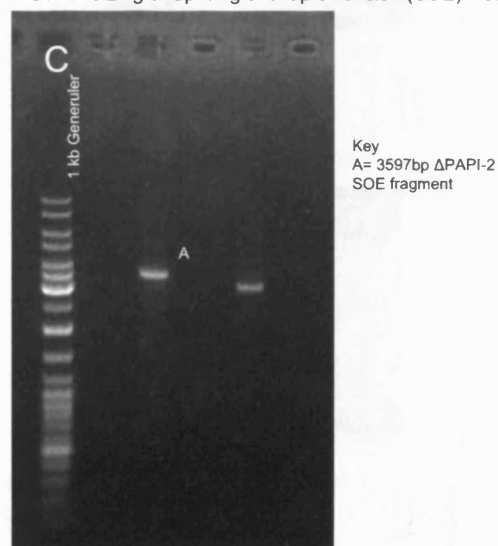
Figure 5.2:Construction of ΔPAPI-2.
Showing three agarose gel electrophoresis: **(A)** Shows the component fragments of the Splicing overlap extension (SOE) PCR. **(B)** Shows the SOE PCR reactions run out on the gel; the eclipses highlighting the specific fragment cut out of the gel. **(C)** Shows the size of the cleaned up specific SOE product used in the Gateway BP clonase reaction.
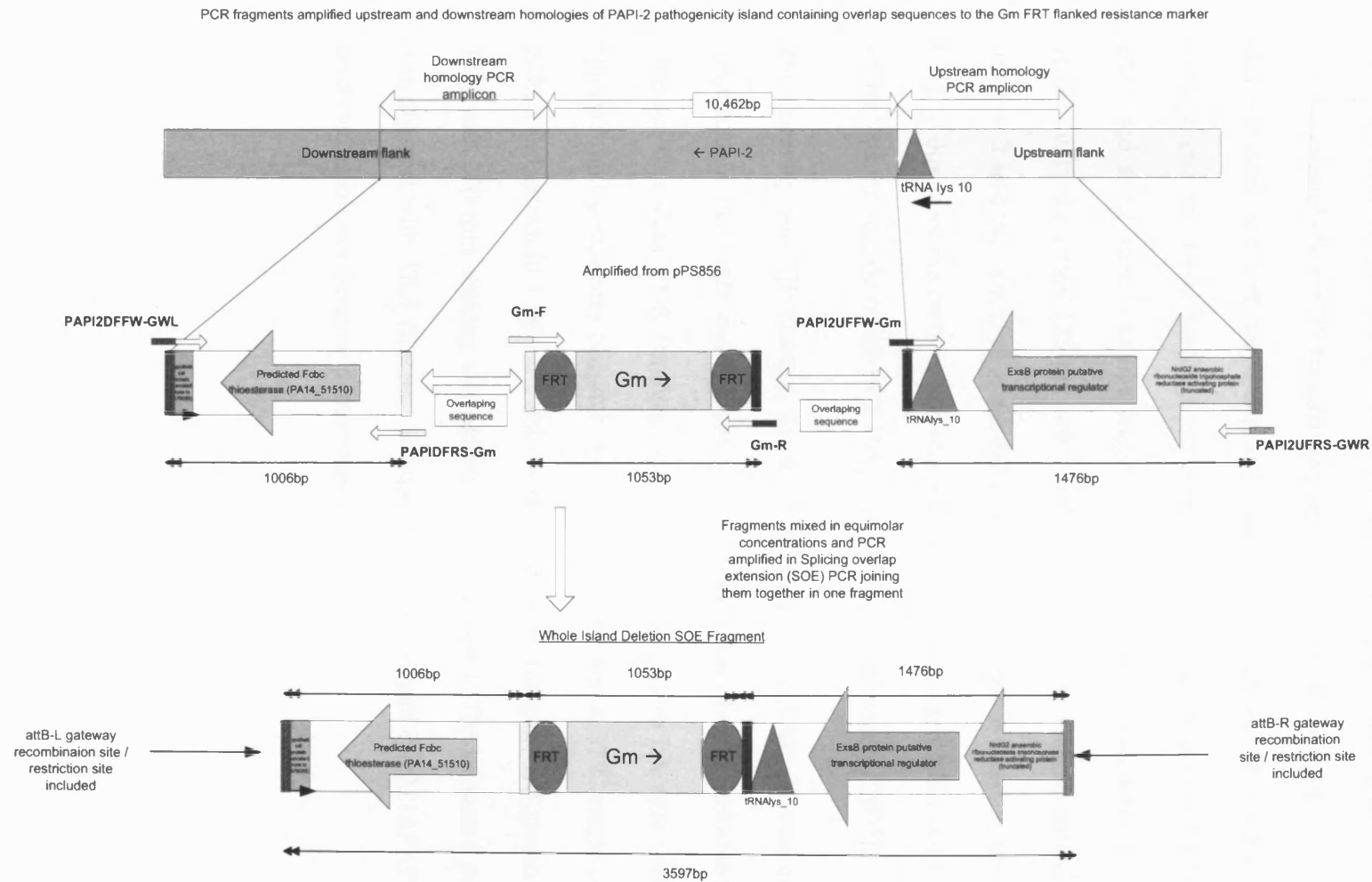
Figure 5.3: Showing the basic principle of the splicing overlap extension (SOE) PCR using the construction of the ΔPAPI-2 fragment as an example.

5.5.3 Gateway BP Clonase reaction

The Gateway site specific recombination system from Invitrogen (Invitrogen, UK) was used to construct the suicide vector. Briefly, this system makes use of site specific recombination between 25 bp *attB* sites incorporated at the ends of the DNA fragment and is recombined with the 200bp *attP* sites in the 'entry vector' mediated by the BP Clonase enzyme. Once the fragment is in the Entry vector it is now flanked by 100bp attL1 and attL2 sites it can be transferred to any other vector termed a 'destination vector' with the target 125 bp *att*R1 and *att*R2 sites. The recombination between the *att*L1 + 2 and the *att*R1+ 2 is mediated by the LR Clonase enzyme mix (Invitrogen, UK). In this work the entry vector was pDONR221 (Invitrogen, UK) and the destination vector was the suicide vector pEX18ApGW (Choi and Schweizer, 2005).

The Gateway way BP reaction for the SOE fragment (ΔPAPI-2) was carried out as described in materials and methods. The reaction was then transformed into *E.coli* Oneshot Omnimax T1-R (Invitrogen, UK), and plated on to LA agar with kanamycin 50μg/ml, and gentamicin 10μg/ml. After overnight growth at 37°C single colonies were picked and grown in 5 ml LB broths with Gentamicin 10μg/ml and grown overnight at 37°C and 200 rpm shaking and plasmid DNA extracted. The extracted plasmid DNA was digested with *Xba*I (Roche, UK) and the construct pDONR221ΔPAPI-2 gave the predicted restriction banding pattern shown in Figure 5.4.
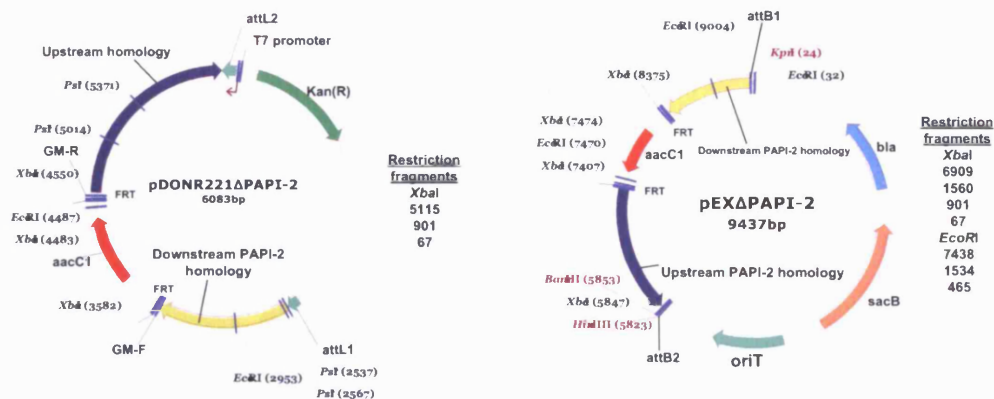
Figure 5.4: Showing the plasmid maps, restriction sites, and predicted restriction fragments for plasmids pDON221ΔPAPI-2 and pEXΔPAPI-2.

5.5.4 Gateway LR Clonase reaction

The Gateway LR reactions were carried out as described in Materials and methods. The reactions were then transformed into *E.coli* Oneshot Omnimax T1-R (Invitrogen, UK) and plated on to LA agar + 100µg/ml Ampicillin and 10µg/ml Gentamicin and then incubated overnight at 37^0C. 20 single colonies of each construct were then picked and patched onto LA + Ampicillin (Amp) 100µg/ml, LA+ Gentamicin (Gm) 10µg/ml, and LA + Kanamycin (Km) 50µg/ml. Patch plating was used to detect which of the clones had lost the entry vector. As any clones that were Km^R still harboured the entry vector in the strain along with the correct pEX18ApGW clones or as cointegrate of both plasmids had formed during the LR recombination (Choi and Schweizer, 2005). For pEXΔPAPI-2 colonies picked: 16% were Km^R Amp^R Gm^R and therefore harboured both pDONR221ΔPAPI-2 and pEXΔPAPI-2. One colony of each pEXΔPAPI-2 and that was Km^s Amp^R Gm^R was grown overnight in 5ml LB + 10µg/ml Gentamicin at 37^0C and 200 rpm shaking. Plasmid DNA was extracted and digested with *Xba*I and *EcoR*I to check the correct fragment were present in the vectors. All clones gave the correct predicted restriction pattern (Figure 5.5) as predicted (Figure 5.4). The suicide vector

for deletion of the whole island was named pEXΔPAPI-2 and for the 2.9kb proximal end deletion pEXΔ2.9kbPAPI-2.

1. pEXΔPAPI-2 un cut
2. pEXΔPAPI-2 *Xba*I
3. pEXΔPAPI-2 *Eco*RI
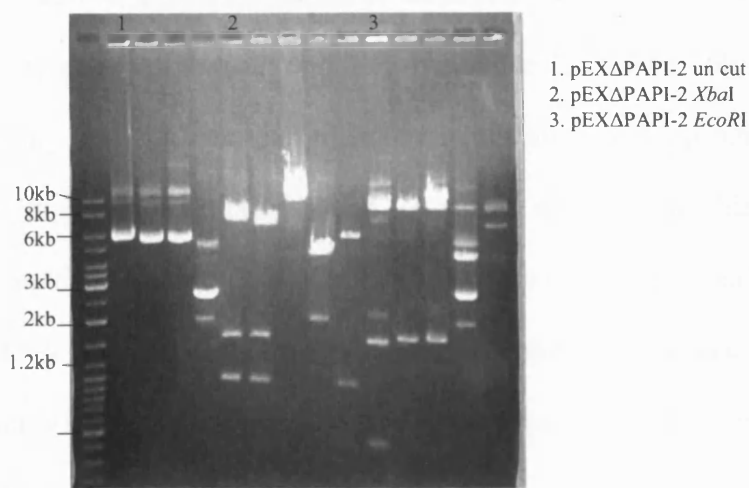
Figure 5.5: Restriction analysis of PAPI-2 deletion suicide vectors.
pEXΔPAPI-2 and pEXΔ2.9kbPAPI-2, undigested and digested with *Xba*I and *Eco*RI.

5.5.5 Conjugation of pEXΔPAPI-2 into PA14 and PAO1

The method of delivery of the suicide vectors into *P. aeruginosa* was conjugation. The technique used was based on that first described by Simon *et al* (Simon *et al.*, 1983) and that described for the transfer of Tn7 based vectors into *P. aeruginosa* reported by Choi and Schweizer (Choi and Schweizer, 2006b) the techniques were also optimised later to function when using multidrug resistant strains of *P. aeruginosa*. The basic technique was as follows; the vectors pEXΔPAPI-2 to be conjugatively transferred was transformed into the *E.coli* mobilizer strain SM10λ-pir (Simon et al., 1983) to create strains KR553. The *P. aeruginosa* PA14 strain (recipient) and *E.coli* SM10λ-pir (donor) were conjugated as described in Materials and Methods. After the conjugation process 2 × 200 μl aliquots of the conjugations were spread on to 2 x VBMM plates (Vogel and Bonner, 1956) supplemented with gentamicin 30 μg/ml. Plates were then incubated for 24 hours at 37°C

5.5.6 Results of conjugation

As can be seen in Table 5.2, the conjugations were all successful, with no real pattern as to the two different volumes of cultures being more or less successful. Both the donor only and the recipient only negative controls showed only very low colony numbers. Forty colonies were picked from conjugation 1 and 2 patch plated onto VBMM plates with 30µg/ml gentamicin and LA plates with carbenicillin 200µg/ml to differentiate single crossovers (Gm^R, Cb^R) from double crossovers (Gm^R, Cb^S). Also from both the donor and recipient control plates small colonies were picked and streaked for isolation on VBMM plates with 30µg/ml Gentamicin. All plates were incubated overnight at $37^\circ C$.

Table 5.2: Conjugations carried out with difference ratios of donor to recipient and the results of growth after 24 hours at $37^\circ C$.

Conjugation no.	Donor strain	Volume of culture.	Recipient strain	Volume of culture	Result
1	*E.coli* SM10-λ pEXΔPAPI-2	200	PA14	200	>1000 (normal sized colonies)
2	*E.coli* SM10-λ pEXΔPAPI-2	200	PAO1	200	~500 (normal sized colonies)
3	*E.coli* SM10-λ pEXΔPAPI-2	200	PA14	400	>1000 (normal sized colonies)
4	*E.coli* SM10-λ pEXΔPAPI-2	200	PAO1	400	A few colonies (normal sized colonies)
5	*E.coli* SM10-λ pEXΔPAPI-2	200	**Donor control**	0	Pin prick sized colonies
6	**Recipient control**	0	PA14	400	Very small pin prick colonies

5.5.7 Results of patching and PCR screening of transconjugants

Table 5.3: Shows result of patching of transconjugants onto VBMM + Gm30µg/ml and LA+Cb200µg/ml.

Conjugation	Strain (p= putative)	Number of colonies	Single crossovers $Gm^R Cb^R$	Double crossovers $Gm^R Cb^S$
1	PA14pΔPAPI-2	33	25 (76%)	8 (24%)
2	PAO1pΔLys10 island	40	40 (100%)	0 (0%)

Table 5.3 shows the results of the conjugations, and shows various ratios of single to double crossover dependent on the strain and the vector used. This variation has been reported previously with some constructs and strains yielding frequent double cross-over events whilst others rarely produce double-cross-over outcomes (Choi and Schweizer, 2005). All the small colonies from the negative controls (Conjugations 5 and 6) that were streaked onto VBMM with 30µg/ml Gentamicin did not grow, showing the colonies present were not truly resistant to gentamicin. Putative clones resulting from both single and double crossover events corresponding to PA14pΔPAPI-2 and PAO1pΔPAPI-2 were picked and streaked for isolation on VBMM with 30µg/ml gentamicin. After overnight growth at 37°C colonies were picked and prepared for colony PCR. Colonies were screened by PCR using primers Gm-F / R, Bla-F / R, tRNA-Lys10 U / D, ExoU-F / R and VIC-1 / 2 (*P. aeruginosa* specific primers). The PCR primers pairs were to detect; the presence absence of; the Gentamicin resistance cassette (presence / absence of SOE fragment), the β-lactamase resistance cassette (presence / absence of pEX18ApGW backbone), occupancy of the $tRNA^{Lys10}$ locus (tRIP PCR), *exoU* gene (presence / absence of PAPI-2 island) and finally a positive control (*P. aeruginosa* specific primers) respectively. The results of the PCRs are shown in Table 5.4

Table 5.4: PCR screening of transconjugants (P = predicted, O = observed)

Strain (SC = Single crossover, DC = Double crossover)	tRNA-Lys10U+D		Gm		ExoU		Bla		Results (SC / DC)
Predicted = P Observed = O	P	O	P	O	P	O	P	O	
1. PA14ΔPAPI-2 SC 1	+	+	+	+	+	+	+	+	All correct -SC – stored on glycerol - KR565
2. PA14ΔPAPI-2 SC 2	+	+	+	+	+	-	+	-	DC
3. PAO1ΔLys10 SC 1	+	+	+	+	n/a	n/a	+	+	All correct - SC
4. PAO1ΔLys10 SC 2	+	+	+	+	n/a	n/a	+	-	SC
5. PA14ΔPAPI-2 DC 1	+	-	+	-	-	-	-	-	DC
6. PA14ΔPAPI-2 DC 2	+	-	+	+	-	-	-	-	DC
7. PA14ΔPAPI-2 DC 3	+	+	+	+	-	-	-	-	All correct - DC – ΔPAPI-2 stored KR701

As can be seen from Table 5.4; PCR testing confirmed the phenotypes of both single and double crossovers. The single crossover strain for PA14ΔPAPI-2 (strain 1 in Table 5.4) was stored at -20°C / -80°C in 30% glycerol BHI given the strain numbers KR565. The single crossover for PAO1ΔLys10 (genotype PAO1ΔLys10:pEXΔPAPI-2:Gm^R:Cb^R) was then taken onto sucrose counter-selection for resolution of merodiploidy. The double crossover strain for PA14ΔPAPI-2:Gm^R was stored at -20°C / -80°C in 30% glycerol BHI given the strain number KR701.

5.5.8   Sucrose counter-selection of PA01ΔLys10-pEXΔPAPI-2-Gm^R, Cb^R

Single colonies of strain PAO1ΔLys10-pEXΔPAPI-2-Gm^R, Cb^R were streaked heavily onto VBMM plates + 5% w/v sucrose and 30µg/ml Gentamicin. The plates were incubated overnight at 37°C. Forty single colonies were picked and patched onto LA + 30µg/ml Gentamicin and 5% sucrose and LA + Carbencillin 200µg/ml and incubated overnight at 37°C.   20 colonies (50%) were Gm^R and Cb^S thus indicating the β-lactamase resistance borne on the pEX18ApGW backbone had been lost in a double

crossover event. Colonies were then PCR tested using colony PCR to confirm the correct genotype using PCR primers to detect the 'empty' $tRNA^{Lys10}$ site (should only be positive when the island has been deleted), the presence of the Gentamicin cassette, and the β-lactamase cassette (which detects the presence of the pEX18ApGW backbone integrated in the genome in a single crossover).

Primer set 1- tRNA-Lys10U + D
1. PAO1ΔLys10Island
2. PAO1WT – ve control
3. -ve control (no template)
Primer set 2- Bla-F + R
4. PAO1PAO1ΔLys10Island
5. +ve control (pEX18Ap)
6. PA14 WT -ve control
7. -ve control (no template)
Primers set 3 -Gm-F + R
8. PAO1ΔLys10Island
9. +ve control (pPS856)
10. PA14 WT -ve control
11. -ve control (no template)
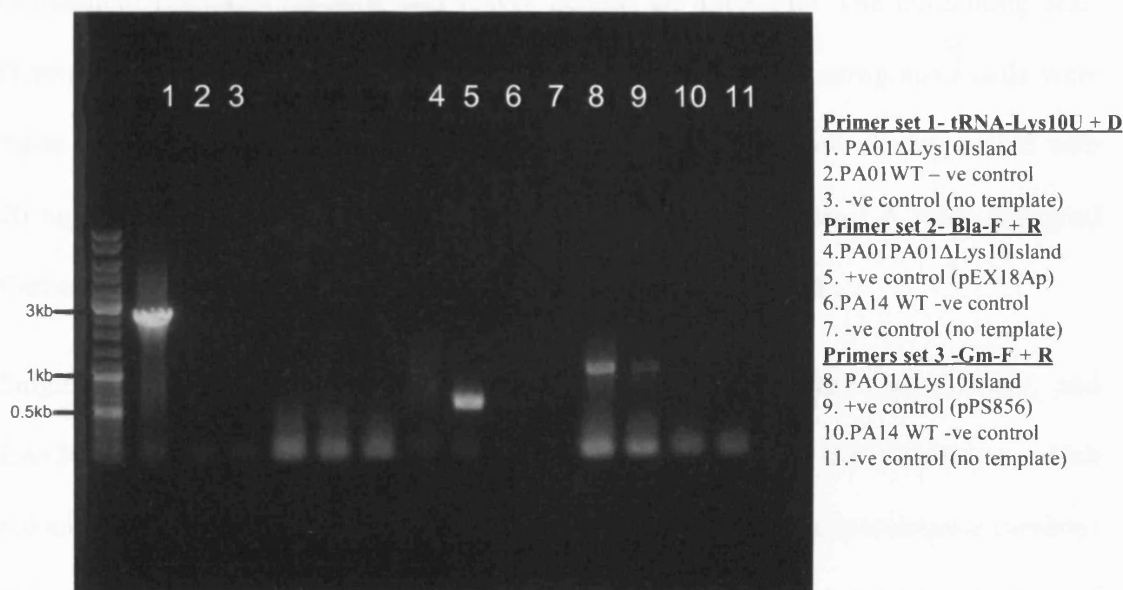
Figure 5.6: Agarose gel electrophoresis showing the results of the PCR assays for confirmation of the double crossover event strain PAO1ΔLys10 Island.
The PCRs shown in Figure 5.6, confirmed that the double crossover event had occurred and the pEX18ApGW backbone (Primer set 2), the PAO1 $tRNA^{Lys10}$ island had been deleted (Primer set 1) and that the strain still carried the Gentamicin resistance cassette (Primer set 3). The strain was then stored on -20°C / -80°C in 30% glycerol BHI given the strain number KR601.

5.5.9 Deletion of Gentamicin cassette in strain PAO1ΔLys10Island:Gm^R and PA14ΔPAPI-2:Gm^r

To delete the resistance cassettes from both PAO1ΔLys10Island:Gm^R (KR601) and PA14ΔPAPI-2:Gm^R (KR701); the method originally described by Hoang and co-

workers was used (Hoang et al., 1998). The Flp recombinase expressing plasmids pFLP2 plasmid was delivered into *P. aeruginosa* cells by electroporation. The Gentamicin cassette used to create the deletions in both strains is flanked 48 bp Flp recombinase target sites. When the FLP recombinase is expressed in the cell it mediates a recombination event between to the two FRT sites causing a 967 bp region of the Gentamicin resistance cassette and leaves behind an 85bp FRT site containing scar. Overnight cultures of KR601 and KR701 were grown. The *P. aeruginosa* cells were made electrocompetent as described in materials and methods and electroporated with 20 ng of pFLP2. The strains were plated out from 10^{-4} to 10^{0} on LA with 200µg/ml Carbenicillin and grown overnight at 37°C until colonies appeared.

Single colonies were picked and patched onto LA+ 200µg/ml Carbenicillin, and LA+30µg/ml Gentamicin. Colonies that were Gm^S and Cb^R (to determine which colonies had undergone FLP recombination and lost the Gentamicin resistance cassette) were then streaked onto LA+ 5% Sucrose plates. This was negative selection for loss of the pFLP2 plasmid which encodes the counter-selectable marker *sacB*. Colonies were picked and patched onto LA+ 5% Sucrose, LA+ 200µg/ml Carbenicillin, and LA+30µg/ml Gentamicin plates and grown overnight at 37°C. Gm^S Cb^S strains were streaked for isolation on LA plates from the LA + 5% sucrose plate. Colonies from the LA plates were screened by colony PCR for the presence of the Gentamicin resistance cassette (Gm-F / R), the pFLP2 plasmid (Bla-F/ R), and the deletion of the 967 bp region (using the tRIP primers tRNA-Lys10U + D). After the PCR confirmation of the deletion of the Gentamicin cassette (data not shown), the two strains PA14ΔPAPI-2 and PA01ΔLys10 were stored at -20°C / -80°C in 30% glycerol BHI and given the strain numbers KR573 and KR716 respectively.

5.6 Deletion of the large pathogenicity island PAPI-1 from strains PA14 and PA14ΔPAPI-2 using a negative selection based approach.

5.6.1 Overview

PAPI-1 is a 108 kb island that is a member of the pKLC102-family of genomic islands (Klockgether *et al.*, 2007b, He *et al.*, 2004). PAPI-1 like other members of this family inserts into either of the two $tRNA^{Lys}$ genes (Qiu *et al.*, 2006). The PAPI-1 island encodes for a number of known and putative virulence factors, including a type IVB pilius biosynthesis cluster, pyocin S5, *cupD* fimbrial biogenesis system, as well as PvrR/S, a two component response regulator involved in biofilm synthesis, fimbrial expression and antibiotic resistance (He et al., 2004, Mikkelsen *et al.*, 2009). Twenty genes borne on PAPI-1 have been previously implicated in virulence using defined PA14 single gene knockouts and the Arabidopsis leaf infiltration, murine burnt skin, and *C. elegans* slow killing infection models (He *et al.*, 2004, Lee *et al.*, 2006b, Miyata *et al.*, 2003). Most interestingly the PAPI-1 island carries *rcsC* and *rcsB* which are part of the Rcs phospho-relay signal transduction system that has been associated with regulation of capsule, polysaccharide, flagella, and biofilms formation in *Enterobacteriaceae* (Majdalani and Gottesman, 2005, Huang et al., 2006, Hinchliffe et al., 2008). However, PAPI-1 and other *P. aeruginosa* strains lack *rcs*D the phosphate transfer protein, a key competent of the phospho-relay pathway, responsible for the transfer of the phosphoryl group from RcsC to RscB. However in both *E. coli* and *Yesinia pestis,* a fully functional RcsD does not seem to be essential for RcsB functionality (Tobe *et al.*, 2005, Hinchliffe et al., 2008). This adds to the recent findings of Nicastro & Baldini (Nicastro and Baldini, 2007) who have shown that a mutant lacking *rcsC* and *rcsB* showed variation in O-antigen polysaccharide chain length, while the *rcsB* single mutant exhibited reduced virulence in *Dictyostelium dsicoideum*, mice

and *Arabidopsis* (He et al., 2004, Boechat and Baldini, 2007) models. The *rcsC* single mutant was also attenuated as determined using the murine and *Arabdopsis* models (He et al., 2004). These data seem to demonstrate that the Rcs phosphor-relay system is functional in *P. aeruginosa*. However, its exact mechanisms of function and the genes under its regulatory control have yet to be identified. The function of one part of the RcsBC system has been demonstrated by a recently published study by Mikkelsen and co-workers in which it was demonstrated that the PAPI-1-encoded RcsBC and PvrRS systems antagonistically regulated the expression of the PAPI-1-borne fimbrial *cupD* operon, impacting on the ability of the bacteria to attach and form biofilms (Mikkelsen et al., 2009). However, *cupD* regulation was not directly demonstrable under laboratory growth conditions suggesting specific, as yet undefined, stimuli were required to engage the two component systems.

The PAPI-1 Island is known to be mobile and capable of self transmission between *P. aeruginosa* strains (Qiu *et al.*, 2006). We were interested to see the effect that the loss of the whole PAPI-1 island would have on virulence of strain PA14. Previous work had demonstrated that various individual PAPI-1 genes had roles in virulence based on data obtained using models derived from plants, animals, and nematodes (He et al., 2004).

5.6.2 Overview of deletion method

The PAPI-1 island like many members of the $tRNA^{Lys}$ associated island shares a number of key genes that can be postulated to be essential for its excision, integration, transmission and maintenance. One such gene that has been experimentally validated to play a role is *soj*, which encodes the Soj protein which is a member of the ParA family of chromosome partitioning proteins which along with ParB are responsible for the segregation of low-copy plasmids during cell division (Qiu et al., 2006). Recent work showed that a deletion of the PAPI-1 *soj* gene caused the PAPI-1 island to be lost from

the population (Qiu et al., 2006).. The *soj* gene was therefore targeted for a insertional inactivation with a vector containing the *sacB* gene which encodes *Bacillus subtilis* levansucrase (Ortiz-Martin *et al.*, 2006). When the *sacB* gene is expressed in strains grown on sucrose it is lethal to the bacteria, allowing for selection of strains lacking PAPI-1. This combined with the increased instability of the PAPI-1 island due to the inactivation of *soj* allowed for selection for the loss of the PAPI-1 island. This work then aimed at focused on designing a system that would be generic to allow for deletion of any *soj* carrying island that is still mobile (capable of site-specific recombination) from its host strain. As the *soj* gene is found to be conserved in a large number of pKLC102-family *P. aeruginosa* genomic islands and in diverse bacterial species (Mohd-Zain et al., 2004, Wurdemann and Tummler, 2007)

5.6.3 Design of conserved primers for amplification of *soj* fragment for single crossover integration of pEX18Ap.

Initially a multiple sequence alignment was carried out using the nucleotide sequences of the *soj* gene from strains PA14, KR115, KR158 and from pKLC102. The multiple sequence alignment was carried out in ClustalX and the output uploaded into the web based Primaclade software (Gadberry et al., 2005) primers were designed to be conserved in the all the five sequences. This was to try to aim to allow for generic primers that would amplify from any *soj* gene. Primers Soj-F and Soj-R were designed.

5.6.4 Amplification and cloning of the *soj* fragment into pEX18Ap

Primers Soj-F and Soj-R were used to amplify a 495bp region from the genomic DNA of strain PA14 (KR125), Clone C (KR127), KR115, and KR158 using KOD-Hotstart polymerase (Merck, UK). The PCR products were sized by gel electrophoresis and the correct sized bands excised from the gel and cleaned up. The PCR products were cloned using the TOPO TA cloning system following manufacturer instructions into pCR®4-

TOPO® (Invitrogen, UK) this was then transformed into *E.coli* DH5α and plated onto

LA+ 40μg/ml Kanamycin and 40 μg/ml X-gal. The plates were grown overnight at

37°C. The next day, white colonies were picked and grown in 5 ml LB broth with

40μg/ml Kanamycin at 37°C and 200 rpm shaking. Plasmid DNA was then extracted

and digested with *EcoR*I (Roche) and run on an agarose gel to confirm the presence of

an insert. The correct inserts for the different strains (KR115, KR125, KR127, and

KR158) were then excised from the gel and cleaned up. The inserts were then mixed

with *EcoR*I digested pEX18Ap and ligated with T4 DNA ligase (Roche). The ligation

was then transformed into *E. coli* DH5α and plated onto LA + 100μg/ml Ampicillin and

40 μg/ml X-gal. After incubation overnight at 37°C white colonies were picked and

grown overnight at 37°C with 200 rpm shaking in 5 ml of LB supplemented with

100μg/ml Ampicillin. Plasmid DNA was extracted and digested with *EcoR*I and *Hin*dIII

(Roche) to confirm the presence of the 518bp *soj* containing insert (data not shown).

The *E.coli* DH5α strains containing the respective plasmids pEX115SOJ, pEX15SOJ,

pEX127SOJ, pEX158SOJ were then stored at -20°C / -80°C in 30% glycerol BHI with

the strains numbers KR537, KR538, KR539, KR540 respectively.

5.6.5 Transfer of pEX125SOJ into PA14 by conjugation

The plasmid pEX125SOJ was then transformed into *E. coli* SM10 λ-pir to create strain

KR556. Strain PA14 (KR125) and KR556 were then plate mated as described in

materials and methods. Two different incubation periods for the plate mating were

evaluated; 5 hours and 12 hours (overnight), both yielded colonies, with the overnight

incubation yielding ~500 and the 5 hours ~200, demonstrating the improved efficiency

of the overnight plate mating. Four single colonies were picked and streaked for

isolation onto VBMM + 500μg/ml and grown overnight at 37°C. Colonies were picked

and subjected to colony PCR to detect the presence of the integration via single

crossover of the pEX125SOJ into the PA14 genome. Figure 5.7 A shows the location of the PCR primers and Figure 5.7 B shows the PCR results confirming the integration of pEX125SOJ into the PAPI-1 island. The positive PCR 2A shown in Figure .7 B confirmed the integration of pEX125SOJ. As the primer SOJ-R2 is located upstream of the *soj* gene and amplification can only occur if the pEX125SOJ vector is inserted in the genome in the orientation shown aligning the Bla-R primer. The result of PCR 1A further confirmed the integration and orientation of pEX125SOJ at the other end of the island with primers Bla-F and Soj-F amplifying a product (Figure 5.7 B). The result of PCR 3A in Figure 5.7B was amplified using Bla-F / R confirming the presence of the *bla* gene on pEX125SOJ. Finally, as can be seen in Figure 5.7 A, the insertion of pEX125SOJ should remove the first 10bp of the *soj* gene and thereby inactivating it. The strain PA14:pEX125SOJ was then stored at -20°C / -80°C in 30% glycerol BHI with the strain number KR567.
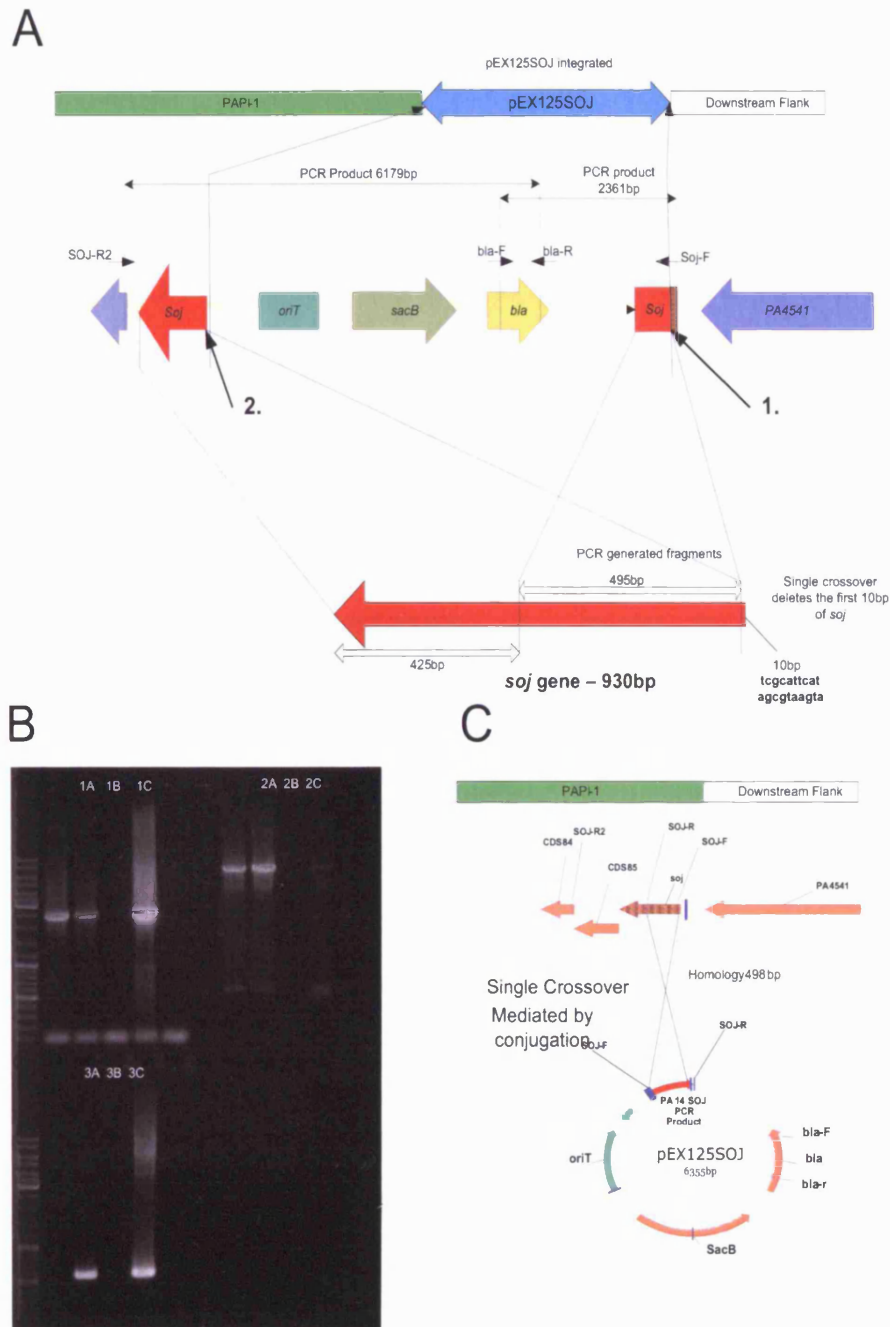
Figure 5.7: Construction of PA14 with the *soj* gene interrupted.
A. Showing the local DNA structure of a single crossover insertion of pEX125SOJ, showing the location of PCR primers used to confirmed the integration. Note: 1. Denotes the 505bp downstream Soj remnant. 2. Denotes the 920bp upstream Soj remnant. **B.** Gel electrophoresis of PCR products confirming presence of integration: 1A, 1B, and 1C are PA14ΔPAPI-1, PA14 WT, and positive control respectively, amplified using primers soj-F and bla-F. 2A, 2B, and 2C are PA14ΔPAPI-1, PA14 WT, positive control amplified using primers SOJ-R2 and bla-R. 3A, 3B, and 3C are PA14ΔPAPI-1, PA14 WT, positive control using primers bla-F and bla-R. **C.** Showing structure of the wildtype distal end of PAPI-1 and map of pEX125SOJ.

131

5.6.6   Deletion of the PAPI-1 island by sucrose counter-selection

Strain KR567 (PA14ΔSOJ-pEX125SOJ) was serially grown in 5 ml LB broths for five overnight incubations at 37^0C and 200 rpm and then plated onto LA+5% sucrose, LA, and LA with Carbenicillin in a serial dilutions from 10^{-1} to 10^{-9}. Table 5.5 shows the results of the plating, demonstrating the effect of the five serial cultures and plating onto LA (Total CFU/ml), LA + 5 % Sucrose (CFU/ml that had lost *sacB* and therefore PAPI-1), and LA + 200 µg/ml Carbencillin (CFU/ml still carrying the pEX125SOJ).

Table 5.5: CFU/ml for Strain KR567 on LA, LA + 5% sucrose, and LA + Cb200µg/ml after five serial overnight cultures.

Media	CFU/ml
LA	5.3×10^9
LA + 5% Sucrose (presence of *sacB*)	2.3×10^7
LA + Cb200 (presence of Amp^r)	6.1×10^9

The virtually identical CFU/ml on LA and LA + Cb200 µg/ml (presence of pEX125SOJ integrated in PAPI-1) suggested that over the five serial overnight dilutions in LA (with no selection for the presence of PAPI-1) that PAPI-1 had not been lost. This result was not expected as the single crossover into *soj* was predicted to cause a loss of the PAPI-1 island from the strain as has been reported before (Although the authors of the study do not stipulate the time / number of generations for this loss) (Qiu et al., 2006). However, it is possible that the fact that the insertion of the pEX125SOJ into the *soj* gene has not inactivated it. As can be seen in

Figure 5.7 A, the whole *soj* is present minus the ten base pairs deleted from the beginning of *soj* (marked with arrow as no. 2, Figure 5.7 A). It is possible that the 505 bp remnant (marked with arrow as no. 1, Figure 5.7 A) in the original location, still codes for a functional protein. The full length Soj protein is 310 aa long, while the predicted truncated version created by the deletion is 173 aa long. As can be seen in

Figure 5.8; most of the conserved domains within the Soj protein, are present in the truncated version, suggesting that the truncated version may still be functional. PCR testing for the presence of the circular form of the tagged PAPI-1 were ambiguous, but suggested, a very low copy number of the circular copies may exist (data not shown).
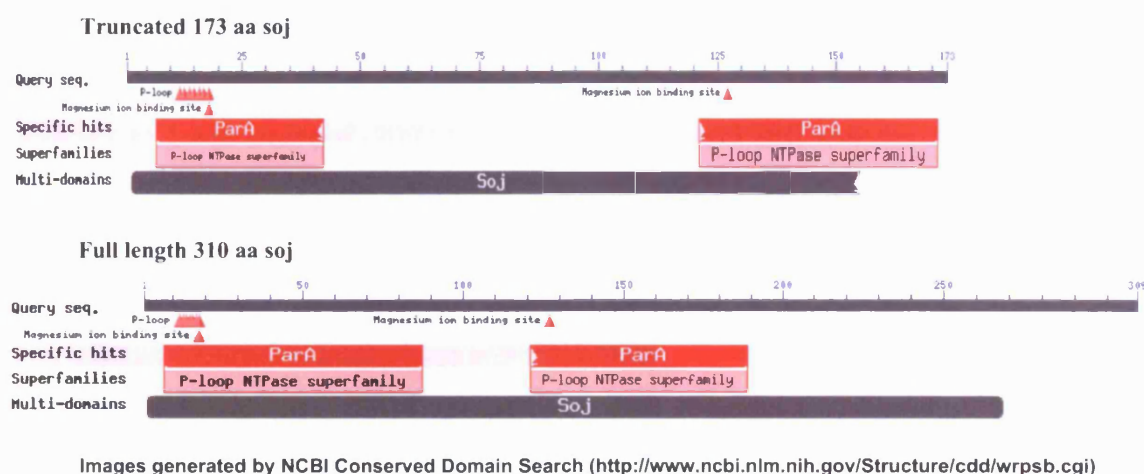
Figure 5.8: Showing conserved domains present in WT Soj (310aa) and the truncated Soj (173aa) created by insertion of the single crossover of pEX125SOJ.

However, 148 of the colonies that grew on LA + 5% sucrose were then patched onto LA + 5% and LA + 200µg/ml carbencillin, and incubated overnight at 37^0C. All 148 were Cb^s and grew well on LA+ 5% indicating that they had lost carbencillin resistance and therefore pEX125SOJ. To test that the whole PAPI-1 island had been lost and not just pEX125SOJ, colonies from LA+ 5% Sucrose were streaked onto LA plates to isolate single colonies. Twenty single colonies were picked at random and screened by PCR to identify the empty *attB* site at *tRNA*^{Lys47} using primers tRNA-Lys47 U / D. The PAPI-1 island integrates into the *attB* site at the 3' *tRNA*^{Lys47}, if the island has been deleted then PCR should be positive and if the island is still present the PCR should be negative. As can be seen in Figure 5.9, 19 of 20 PCRs were strongly positive like that of the PAO1

133

which has an unoccupied *attB*. Compared to the faint band in the PA14 WT suggesting

that all 19/20 colonies had lost the PAPI-1 island. One of the colonies was then picked

for further analysis to show the PAPI-1 island had been deleted. PCRs were carried out

using five sets of PAPI-1 specific primers; PP-1-1 to PP-1-5. Figure 5.9 shows the result

of the PCRs, in which the colony tested was negative for all five PAPI-1 targets

confirming the PAPI-1 island had been deleted from this strain. The strain now called

PA14ΔPAPI-1 was stored at -20°C / -80°C in 30% glycerol BHI with the strain number

KR572.
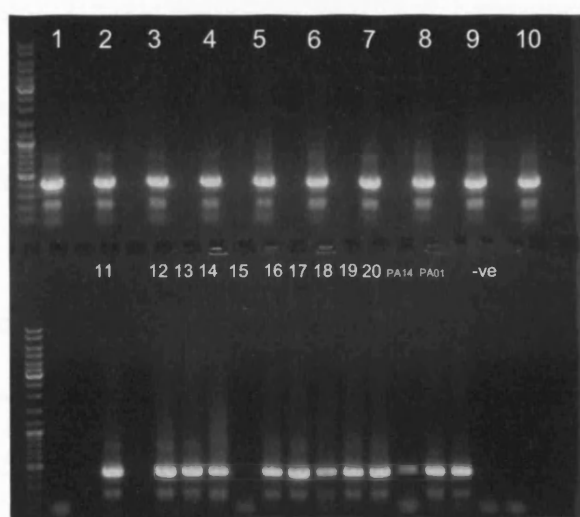
Figure 5.9: Gel electrophoresis of PCRs to confirm the 'empty' tRNA-Lys47 attB sites in putative PAPI-1 deletions.
Lanes 1-20 test colonies, PA14 WT, PAO1 (positive control with empty *tRNA^{Lys74}*attB), and –ve control. Generuler marker. Predicted band size 411 bp.
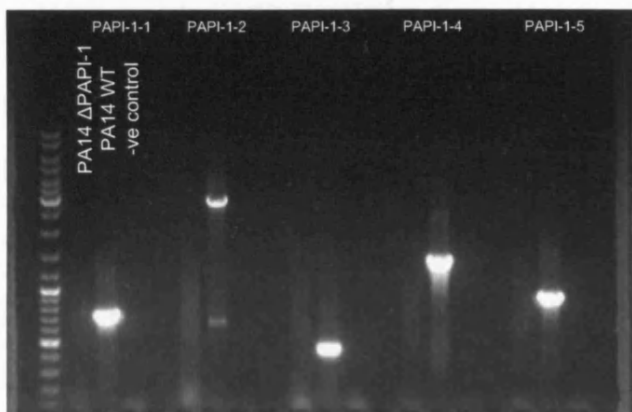
Figure 5.10: Gel electrophoresis PCRS for 5 PAPI-1 specific regions to confirm deletion of PAPI-1 from strain PA14. Generuler marker. Predicted band size from left to right: 721, 2749, 432, 1376 and 925 bp respectively.

5.6.7 Construction of a double pathogenicity island mutant strain PA14Δ1Δ2.

To create a double mutant strain to investigate the effect the loss of both islands PAPI-1 and PAPI-2 would have on the PA14, a double mutant strain was constructed. The strain PA14 ΔPAPI-2 (KR573) was used a start point to create the double mutant. The double mutant was constructed by deleting the PAPI-1 Island as following the same method described previously in this work for the deletion of PAPI-1 to create the strain PA14ΔPAPI-1. The double mutant strain was called as PA14 ΔPAPI-1ΔPAPI-2 (PA14Δ1Δ2) was stored at -20°C / -80°C in 30% glycerol BHI with the strain number KR608.

5.7 Deletion of $tRNA^{Pro21}$ island in strains PA14 and PA14Δ1Δ2

5.8 Overview of the $tRNA^{Pro21}$ island

All strains sequenced thus far or tested using tRIP to assay occupation of the $tRNA^{Pro21}$ site have been found to exhibit likely occupied $tRNA^{Pro21}$ sites. The $tRNA^{Pro21}$ island in PA14 has the classic profile of a genomic island with a lower G/C content of 56% compared to the PA14 genome average of 66% (

Figure 5.11). The island is 17.6 kb in length and has twelve putative genes. It has classic genomic island related genes including three transposases related to IS elements (PA14_28860, PA14_28870 and PA14_28760), another IS related gene (PA14_28750) and a DNA helicase gene (PA14_28810). Of particular interest are PA14_28780 and PA14_28790 which encode homologs of the *Shigella flexneri MvpT / MvpA* genes which encode a toxin and antitoxin, respectively, that function cognately as a plasmid stability system (Sayeed *et al.*, 2000). Interestingly deletion of the homologous plasmid-borne *vagC / vagD* genes in *Salmonella* Dublin resulted in reduced virulence (Pullinger and Lax, 1992). Another gene (PA14_28800) was found to encode a Fic protein originally designated on the basis of the filamentation induced by cAMP phenomenon observed in *E. coli* mutants. Fic proteins harbour the conserved Fic / DOC domains and have been hypothesized on rather limited data to be involved in cell division (Komano *et al.*, 1991) and recently have been implicated in virulence (Roy and Mukherjee, 2009). The death on curing (DOC) domain was first described in an *E.coli* plasmid-borne prophage encoded addiction protein that was shown to be essential to prevent bacterial cell death that was demonstrated to occur following loss of the cognate gene (Lehnherr *et al.*, 1993). Three other genes associated with putative functional annotations were PA14_28810 and PA14_28840 that encoded candidate DNA helicases and PA14_28830 which encoded a likely biotin carboxylase.
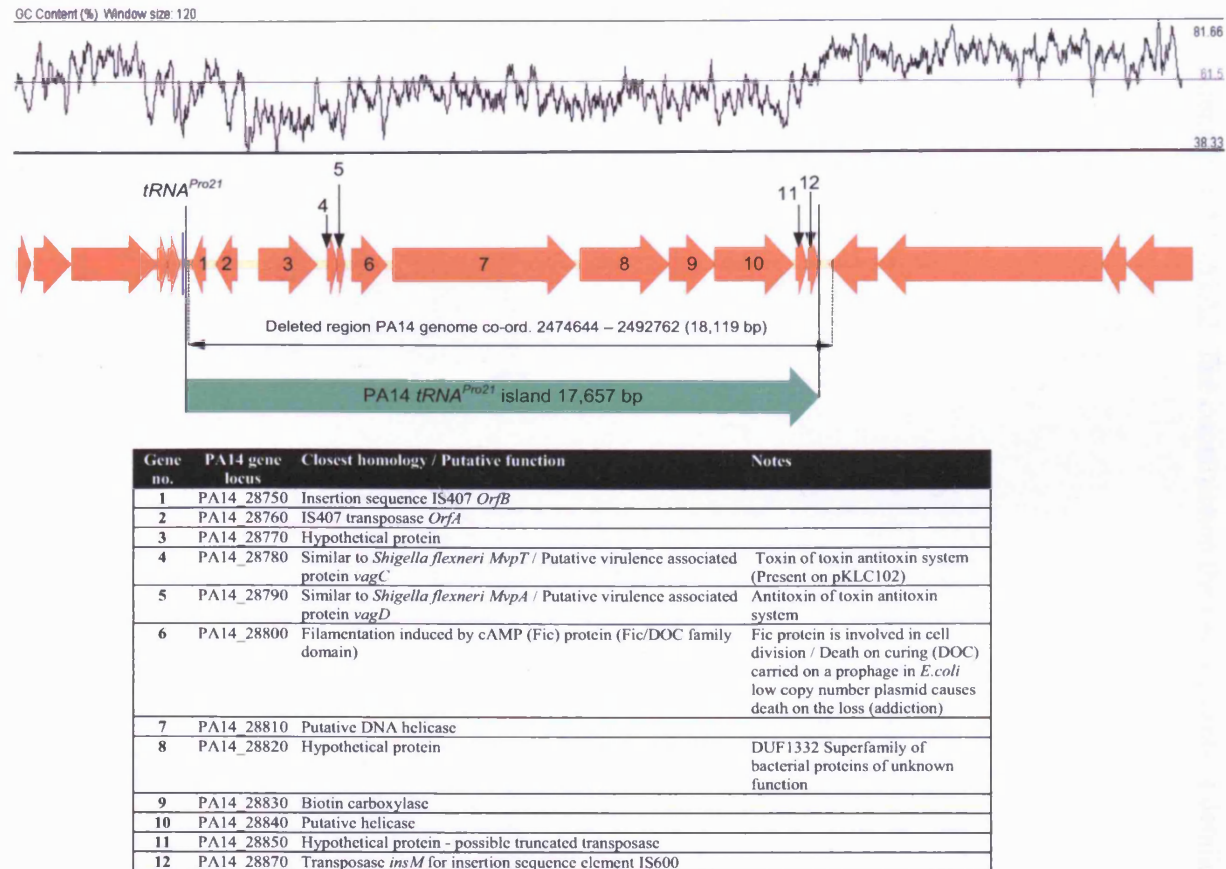
Figure 5.11: *tRNA^Pro21* island in PA14.
Figure local structure, location of genes, G/C content, and region deleted. Table shows gene numbers corresponding to those labelled on tRNAPro21 island, PA14 gene locus, Closest homology / Putative function, and further notes where applicable.

Gene no.	PA14 gene locus	Closest homology / Putative function	Notes
1	PA14_28750	Insertion sequence IS407 *OrfB*	
2	PA14_28760	IS407 transposase *OrfA*	
3	PA14_28770	Hypothetical protein	
4	PA14_28780	Similar to *Shigella flexneri MvpT* / Putative virulence associated protein *vagC*	Toxin of toxin antitoxin system (Present on pKLC102)
5	PA14_28790	Similar to *Shigella flexneri MvpA* / Putative virulence associated protein *vagD*	Antitoxin of toxin antitoxin system
6	PA14_28800	Filamentation induced by cAMP (Fic) protein (Fic/DOC family domain)	Fic protein is involved in cell division / Death on curing (DOC) carried on a prophage in *E.coli* low copy number plasmid causes death on the loss (addiction)
7	PA14_28810	Putative DNA helicase	
8	PA14_28820	Hypothetical protein	DUF1332 Superfamily of bacterial proteins of unknown function
9	PA14_28830	Biotin carboxylase	
10	PA14_28840	Putative helicase	
11	PA14_28850	Hypothetical protein - possible truncated transposase	
12	PA14_28870	Transposase *insM* for insertion sequence element IS600	

137

5.9 Mutant construction

A PA14ΔPro21 mutant was constructed to investigate the effect of deletion of a non-tRNA^{Lys} genomic island on site-specific integration of PAPI-1 (see Chapter 3 for further details). A second $tRNA^{Pro21}$ deletion mutant was constructed at the same time in the previously constructed PA14Δ1Δ2 background to create a triple-island deletion mutant PA14Δ1Δ2ΔPro21 to investigate if deletion of the $tRNA^{Pro21}$ island would further attenuate PA14Δ1Δ2. The construction the two mutants is detailed in Appendix G.

5.10 Evaluation of the role of PAPI-1, PAPI-2 and $tRNA^{Pro21}$ islands to the fitness and virulence of PA14.

5.10.1 Growth curves

The effect of the deletions of the PAPI-1 and PAPI-2 island on the relative fitness of the strain PA14 to grow in three different media were tested; LB broth representative of a 'rich' medium (Figure 5.12), M63 with glucose (0.2 %), $MgSO_4$ (1 mM) and casamino acids (0. 5%) (Figure 5.13) (the media used to evaluate the biofilm production of strains), and M9 with glucose (0.2 %), $MgSO_4$ (1 mM) and $CaCl_3$ (1 mM) representative of a minimal media (Figure 5.14). All strains were grown in triplicate from single colonies picked from LA plates and grown overnight in 5ml LB broths at 37°C at 200rpm. After overnight growth three separate 1/100 dilution of the overnights cultures were made in the growth media to be tested. A minimum of six repeats of two hundred μl of each strain was placed in a Honeywell plate and the OD measured using a Bioscreen apparatus (Life Sciences) at 37°C with continuous shaking for 24 or 48 h. The CFU of the initial inoculums were checked by serial dilutions and plating for CFU.

5.10.2 PAPI-1 and PAPI-2 mutants display no growth defects in rich media

As can be seen in Figure 5.12 the deletion of the PAPI-1 and PAPI-2 islands had no effect on the growth rate of the strains compared to PA14 WT in LB. This is probably to be expected as growth in a media rich in nutrients and energy sources are unlikely to identify any growth defects other than a major growth defect in the strains. However interestingly it seems that strain PAO1 has a different growth profile to that of PA14 background strains, PAO1 reaches the final OD (the highest OD reached) at 10 h, five hours before PA14 background strains. PAO1 rapidly goes from short stationary phase at 10h (~1 h) into a gradual death phase almost an hour later at 11 h. This compared to

the PA14 background strains that reached the final OD much more gradually ~ 14h and later at 15 h and then entered a long stationary phase ~5 h before gradually entering death phase at 20 h.
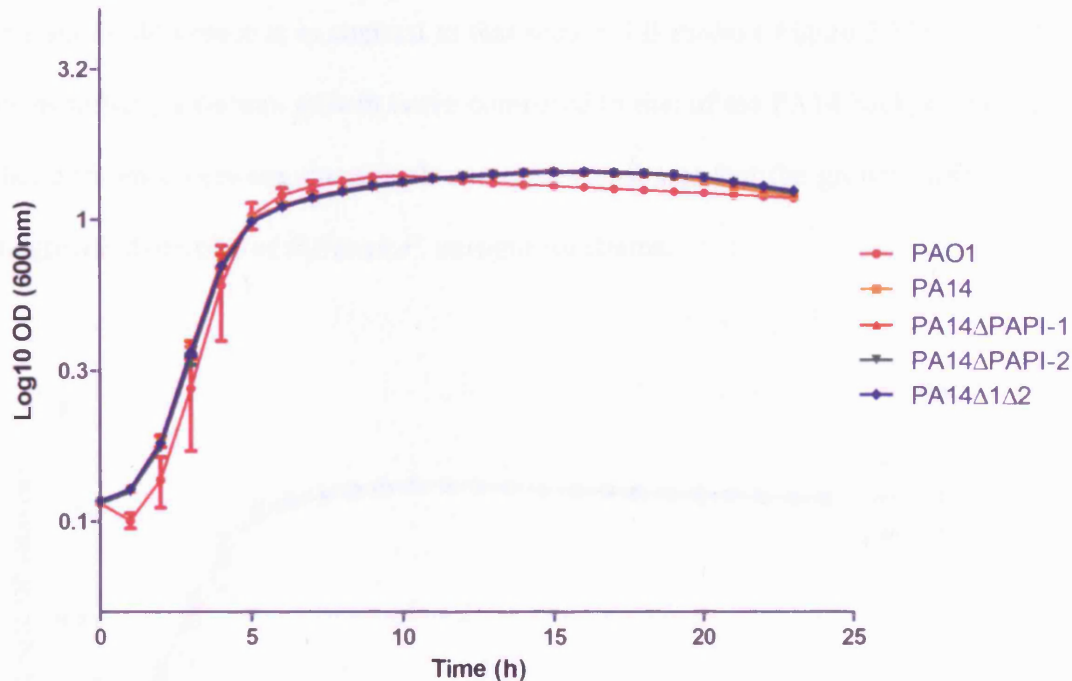
Figure 5.12: Showing relative growth curves of PAO1, PA14, PA14ΔPAPI-1, PA14ΔPAPI-2, and PA14Δ1Δ2 in LB broth at 37oC with continuous shaking.
Points and bars represent mean and standard deviation respectively of three biological repeats.

5.10.3 PAPI-1 and PAPI-2 mutants display no growth defects in media used for biofilm assays

To evaluate if there was any changes in growth dynamics in the media used in the biofilms assays PAO1, PA14, and the three PA14 isogenic mutants' were grown in the same media as used in the biofilms assays (M63 with glucose (0.2 %), $MgSO_4$ (1 mM) and casamino acids (0. 5%)). Therefore if any difference in biofilm production was detected this could be associated with a loss of ability to produce biofilms, and not due

140

to a growth defect. Once again as in the LB growth curves no difference was seen between PA14 and the three pathogenicity island mutants (PA14ΔPAPI-2, PA14ΔPAPI-2, and PA14Δ1Δ2) (Figure 5.13). Furthermore, PAO1 also seemed to have a similar growth profile, although it does seem to reach a slightly higher OD than PA14. This subtle difference is in contrast to that seen in LB media (Figure 5.12) were PAO1 seems to have a distinct growth curve compared to that of the PA14 background stains. This difference between the growth curves demonstrates that the growth media affects the growth dynamics of different *P. aeruginosa* strains.
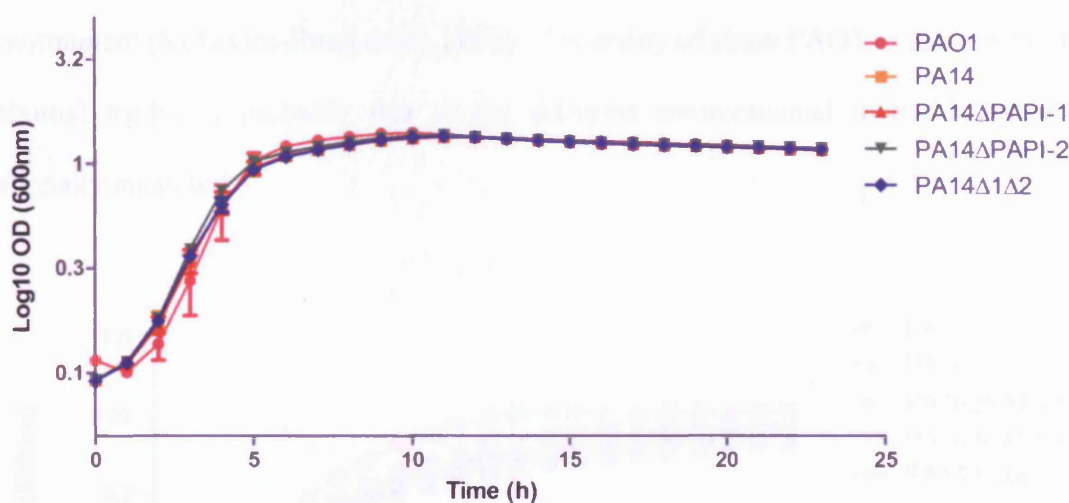
Figure 5.13: Showing relative growth curves of PAO1, PA14, PA14ΔPAPI-1, PA14ΔPAPI-2, and PA14Δ1Δ2 in M63 with glucose (0.2 %), MgSO₄ (1 mM) and casamino acids (0. 5%) at 37oC with continuous shaking.
Points and bars represent mean and standard deviation respectively of three biological repeats.

5.10.4 PAPI-1 and PAPI-2 mutants display no auxotrophism in minimal media

To investigate if the deletion of the two islands PAPI-1 and PAPI-2 caused any change in growth dynamics in the PAPI-1 and PAPI-2 mutants due to auxotrophism or an increased / decreased relative fitness in a less nutrient rich media. PAO1, PA14 and the three mutants (PA14ΔPAPI-2, PA14ΔPAPI-2, and PA14Δ1Δ2) were grown in M9 media. Figure 5.14 shows the growth curves. The results again showed there was no

141

reproducible difference between PA14 and the three mutants (PA14ΔPAPI-2, PA14ΔPAPI-2, and PA14Δ1Δ2), as was seen before in LB and M63 media. This finding suggested that under these growth conditions the three mutants were not attenuated or auxotrophic. However, strain PAO1 is able to grow at a much faster rate than the PA14 background strains, reaching stationary phase at 12 h compared to PA14 background strains not reaching it during the course of the experiment. This increased growth rate suggests that PAO1 has a fitness determinate that allows for faster growth in the M9 media. The *in vivo* growth in rat lungs of PAO1 and PA14 was compared in a recent study which concluded that they have similar growth dynamics in this environment (Kukavica-Ibrulj *et al.*, 2008). The ability of strain PAO1 to grow better in minimal media is probably due to the different environmental niche that PAO1 originally inhabited.
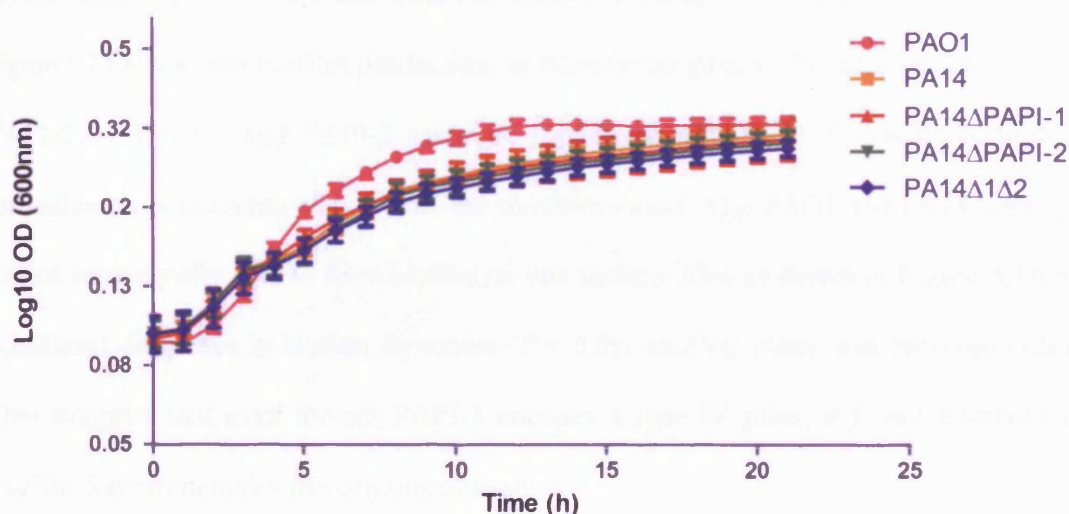
Figure 5.14: Showing relative growth rates of PAO1, PA14, PA14ΔPAPI-1, PA14ΔPAPI-2, and PA14Δ1Δ2 in M9 with glucose (0.2 %), MgSO₄ (1 mM) and CaCl₃ (1 mM) at 37oC with continuous shaking.
Points and bars represent mean and standard deviation respectively of three biological repeats.

5.10.5 Effect of the loss of PAPI-1 and PAPI-2 on biofilm production

The PAPI-1 island encodes *pvrR* and a type IVB pilus cluster, both of which have been implicated in biofilms (Drenkard and Ausubel, 2002, O'Toole and Kolter, 1998a). Biofilms formation is a thought to be significant virulence factor and an important part of both the *P. aeruginosa* environmental and pathogenic lifestyles. Investigations were carried out to see the effect on the loss of the either PAPI-1 or PAPI-2 contributed to a change in biofilm production. The biofilms assays were carried using the microtiter plate method described by O'Toole and Kolter (O'Toole and Kolter, 1998a, O'Toole and Kolter, 1998b). Two different types of plate, made from polystyrene and polyvinylchloride (PVC) were used. This was due to the fact that some mutants defective in biofilm formation on one surface have been found to be able to form biofilms like the wildtype strain on other surface (O'Toole and Kolter, 1998b).

5.10.6 Deletion of PAPI-1 and PAPI-2 causes no change in biofilm formation

Figure 5.15 shows the biofilm production on polystyrene plates. The deletion of PAPI-1, PAPI-2, or PAPI-1 and PAPI-2 made no significant difference ($P < 0.05$) to biofilm formation on polystyrene plates under the conditions used. Also PAO1 and PA14 wildtype strains were equally able to form biofilm on this surface. Also as shown in Figure 5.16 no significant difference in biofilm formation ($P < 0.05$) on PVC plates was observed either. This suggests that even though PAPI-1 encodes a type IV pilus, it is not involved in biofilm formation under the conditions used.
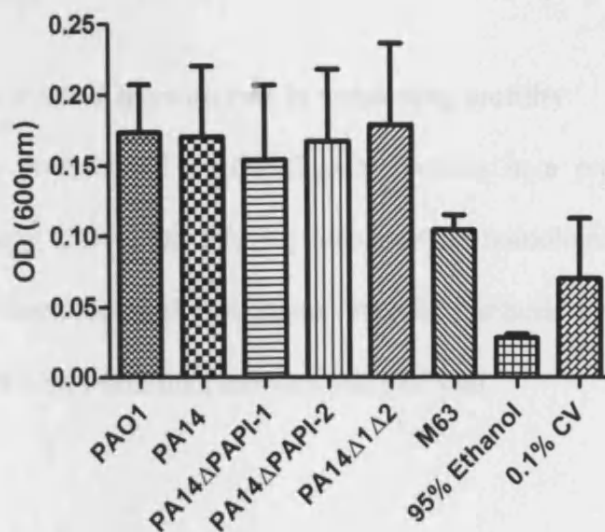
Figure 5.15: Biofilm formation on polystyrene
PAO1, PA14, PA14ΔPAPI-1, PA14ΔPAPI-2, PA14Δ1Δ2, Media only control (M63), 95% ethanol only control, and crystal violet (CV) solution only control on polystyrene (Nunc, Denmark) 96 well plates after 8 hours static growth at 37°C. Biofilm formation is expressed as absorbance (OD) at 600 nm. Bars represent mean and standard deviation of 8 independent biological repeats.
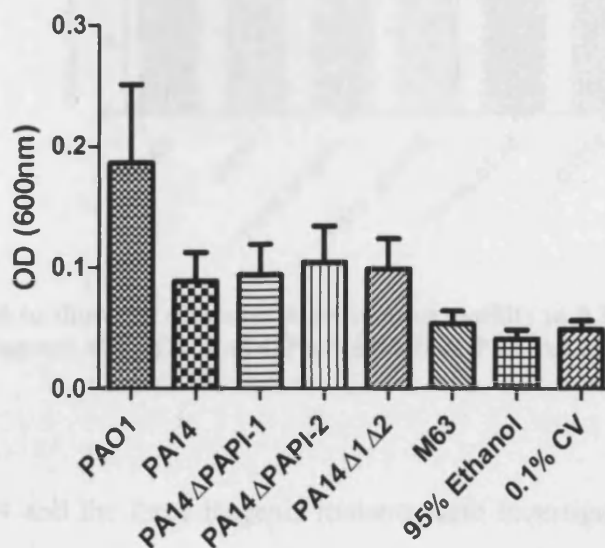
Figure 5.16: Biofilm formation on PVC
PAO1, PA14, PA14ΔPAPI-1, PA14ΔPAPI-2, PA14Δ1Δ2, Media only control (M63), 95% ethanol only control, and crystal violet (CV) solution only control on PVC (Falcon, UK) 96 well plates. Biofilm formation expressed as Absorbance at 600 nm. Bars represent mean and standard deviation of 8 independent biological repeats.

144

5.11 Motility assays

5.11.1 PAPI-1 and PAPI-2 have no role in swimming motility

Swimming motility is mediated by the flagella moving in a propeller like motion (Rashid and Kornberg, 2000). The PAPI-1 island carries homologues to *rcsB/C* which in Salmonella have been reported to regulated flagella synthesis therefore the effect of the deletion of PAPI-1 on swimming motility was assessed.
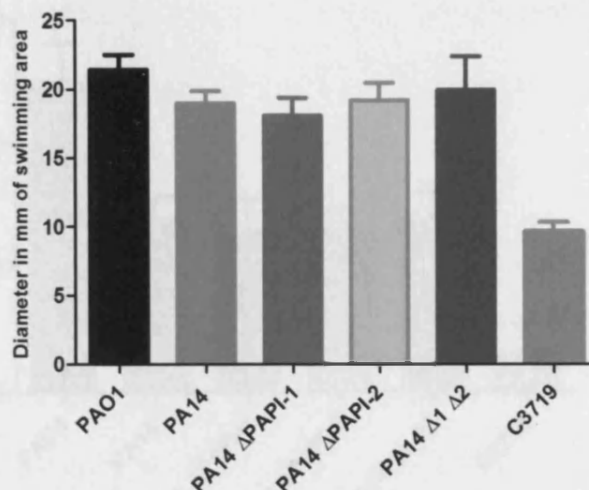
Figure 5.17: A graph to show the diameter of swimming motility in 0.3% agar LA after 20 h incubation at 30 degrees of PAO1, PA14, PA14ΔPAPI-1, PA14ΔPAPI-2, PA14Δ1Δ2, and C3719

The ability of PA14 and the three isogenic mutants were investigated in a swimming mobility assay, along with PAO1 and C3719. As can be seen in Figure 5.17 the deletion of PAPI-1 or PAPI-2 did not significantly affect the swimming motility of any of the mutant strains ($P < 0.05$). Also strain C3719 which was previously reported to be non-motile can actually swim but just at a reduced level (Lewis *et al.*, 2005, Jones *et al.*, 2001) (Figure 5.17). This suggests that is the strain is not completely unable to swim but

perhaps is significantly impaired or only a small number of cells are capable of swimming.

5.11.2 PAPI-1 and PAPI-2 have no role in twitching motility

Twitching motility is a type of bacterial motility which is independent of the flagella. It occurs by the attachment and retracement of type IV pilus on moist surfaces. As the PAPI-1 island encodes a type IVB pilus, it was investigated to see if this had any effect on twitching motility.
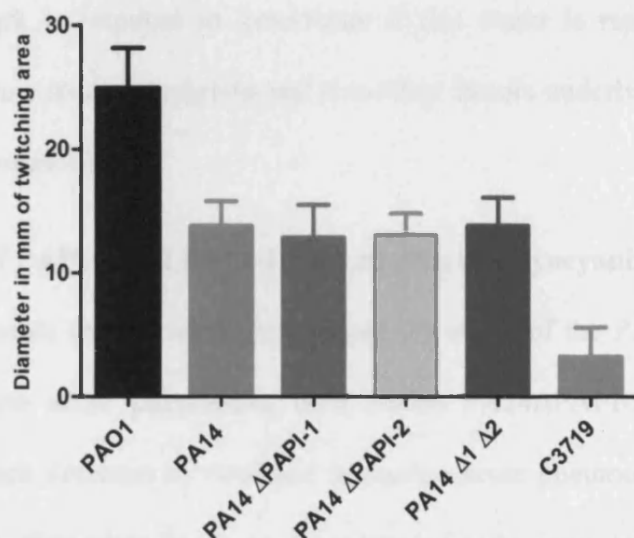
Figure 5.18: A Graph to show the diameter of twitching motility at the agar / plate interface in 1.5% agar LA after 24 h incubation at 37 degrees of PAO1, PA14, PA14ΔPAPI-1, PA14ΔPAPI-2, PA14Δ1Δ2, and C3719.

As can be seen in Figure 5.18 the deletion of the PAPI-1 and PAPI-2 islands had no effect on twitching motility. Interestingly strain PAO1 again showed a significant ($P <$ 0.05) increase in twitching than PA14. This finding was seemly corroborated by electron microscopy of PAO1 and PA14 (data not shown) in which pili were detectable in much greater abundance on the surface of PAO1 compared to PA14 when grown on the same media. This would suggest that PAO1 expresses more pili which has been

146

previously shown to correlate to increase in twitching motility (Asikyan et al., 2008). A previous study using the same conditions did not report the same finding (Kukavica-Ibrulj et al., 2008), suggesting that there is significant variation between the same laboratory strains. Like in the swimming motility, C3719 (Manchester epidemic strain) only twitched a very small amount compared to PAO1 and PA14. This strain was previously reported as non-motile (Lewis et al., 2005, Jones et al., 2001). However some twitching motility was detected, again suggesting the strain is either impaired in twitching or only a small number of cells are capable of this type of motility (Figure 5.18). Further work is required to investigate if this strain is representative of the Manchester epidemic strain population and if so what factors underlie the reduction but not complete loss of motility.

5.11.3 Deletion of PAPI-1 and PAPI-2 have no effect on pyocyanin production

In murine experiments carried out to investigate the effect of the PAPI-1 and PAPI-2 deletions in murine acute pneumonia, both strains PA14ΔPAPI-2 and PA14Δ1Δ2 showed a significant decrease in virulence in murine acute pneumonia (Carter, 2009) (see Section 5.13). Pyocyanin has been demonstrated to be important for virulence in mice and mediates significant tissue damage (Lau *et al.*, 2004a, Lau *et al.*, 2004c), and functions to suppress the host immune response (Bianchi *et al.*, 2008, Allen *et al.*, 2005). As a reduction lung tissue damage was also observed in the PA14ΔPAPI-2 and PA14Δ1Δ2 (Carter, 2009) the measurement of the production of pyocyanin was undertaken , as it was postulated that the reduction in tissue damage and virulence could be due to pyocyanin production.
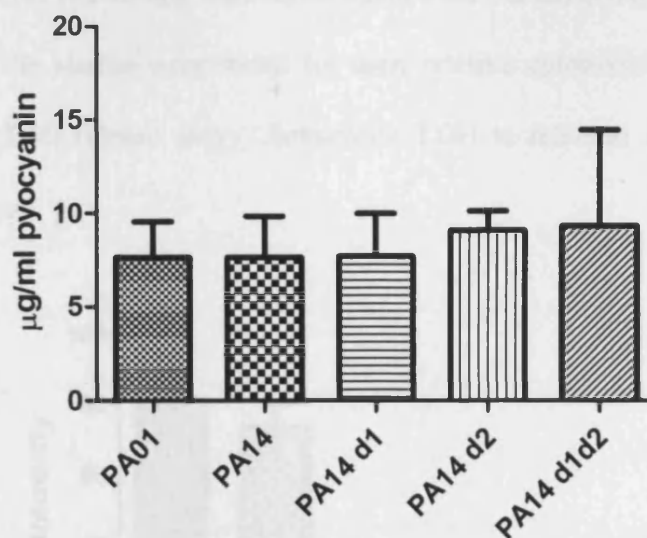
Figure 5.19: Pyocyanin (µg/ml) production in LB broth by strains PAO1, PA14, PA14ΔPAPI-1, PA14ΔPAPI-2, and PA14Δ1Δ2. d = Δ
Bars represent means and standard deviations of three independent experiments.

As can be seen in Figure 5.19 the production of pyocyanin was not altered in any of the mutants compared to PA14. This finding suggests that that the loss of PAPI-1 and PAPI-2 does not affect pyocyanin production under the conditions used in the assay. pyocyanin production is regulated by quorum sensing (Dubern and Diggle, 2008), as a result the lack of any difference in pyocyanin production under the conditions tested suggested that the deletion of PAPI-1 and PAPI-2 did not affect quorum sensing under the conditions used in this assay.

5.11.4 Effect of the loss of PAPI-1 an PAPI-2 on cytotoxicity

The PA14 and the three isogenic mutants were tested to see the effect of the deletion of the two islands would have an effect on the cytotoxicity of strain PA14, as in *Yersinia enterocolitica*, *ysaE* promoter expression is regulated by *rcsB* (Walker and Miller, 2009). The expression of YsaE is required for expression of many T3SS apparatus genes, and is related to ExsA (27% a.a. identity) the core regulator of T3SS in *P. aeruginosa*. Therefore we were interested to see if the loss of PAPI-1 affected the

148

cytotoxicity of PA14. The strains were tested against the human alveolar basal epithelial cells line A459. The strains were tested for their relative cytotoxicity using a lactate dehydrogenase (LDH) release assay. Eukaryotic LDH is released from cells with a damaged membrane.
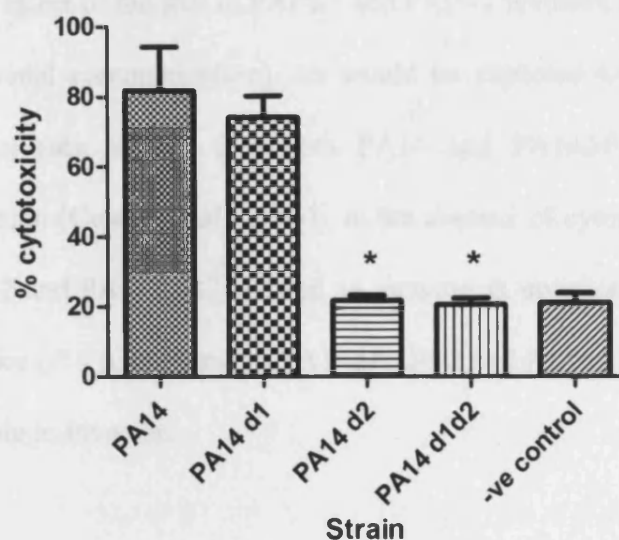
Figure 5.20: Comparison of the cytotoxicity of *P. aeruginosa* strain PA14 and its isogenic mutants lacking PAPI-1 and/or PAPI-2 against A459 human lung carcinoma cells.
Percentage cytotoxicity calculated relative to a maximum LDH release control cytotoxicity. Bars represent the means and standard deviation values. Asterisk symbols denote a significant difference when compared with PA14 ($P < 0.05$).

The results showed as expected that both PA14ΔPAPI-2 and PA14Δ1Δ2 showed significant reduction ($P < 0.05$) in cytotoxicity compared to PA14 and PA14ΔPAPI-1. In fact the two mutants showed the same level of cytotoxicity as the no bacteria control. This suggests the complete loss of cytotoxicity of PA14ΔPAPI-2 and PA14Δ1Δ2 which is consistent with previous reports of loss of the potent cytotoxin ExoU encoded on PAPI-2 (Miyata *et al.*, 2003). The lack of any significant difference between ($P < 0.05$) PA14 and PA14ΔPAPI-1 strongly suggests that PAPI-1 plays no role in the cytotoxicity of PA14, at least under these conditions. This is probably to be expected as the *rscB/C*

system seems to require an as yet unknown environmental stimulus so it is likely that any difference in type three secretion may not be detected under these conditions (Mikkelsen et al., 2009).

5.12 Effect of loss of PAPI-1 and PAPI-2 on invasion of A549 cells[4]

To investigate the effect of the loss of PAPI-1 and PAPI-2 invasion assays were carried out (Luck, S, personal communication). As would be expected to be seen cytotoxic strains (*exoU* +ve) (see section 2.7) both PA14 and PA14ΔPAPI-1 showed no differences in invasion (Cowell *et al.*, 2003). In the absence of cytotoxicity (*exoU* –ve) both PA14ΔPAPI-2 and PA14Δ1Δ2 showed an increase in invasion. But there was no significant difference ($P < 0.05$) between PA14ΔPAPI-2 and PA14Δ1Δ2 suggesting that PAPI-1 plays no role in invasion.
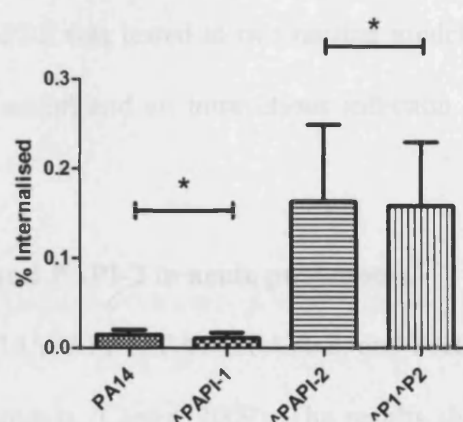
Figure 5.21: Comparison of the invasive ability of A459 human lung carcinoma cells by *P. aeruginosa* PA14 and its isogenic mutants lacking PAPI-1 and/or PAPI-2.
The percentages of internalized bacteria protected from amikacin-killing recovered after lysis of remaining intact A459 cells relative to the original inoculums are shown. Bars represent the means and standard deviation values. The asterisk symbols denotes no significant difference between the two pairs of strains compared.

---

[4]The data presented here in Section 5.16 was not carried out as part of this work, but is presented for discussion of the results in relation to the deletion of PAPI-1 and PAPI-2. Please see statement of originality.

5.13 Effect of deletion of PAPI-1 and PAPI-2 in murine models of pneumonia and bacteraemia.[5]

5.13.1 Overview

Previously studies using single-gene transposon and gene knock out mutants and the murine burnt skin model, *Arabidopsis* leaf inflation model, and *C .elegans* model have implicated twenty-two genes on PAPI-1 and PAPI-2 as coding for potential virulence factors (He *et al.*, 2004, Lee *et al.*, 2006b). Additionally a substantial body of work has been previously undertaken to investigate the role ExoU in a wide range of models (Hauser, 2009). As many life threatening infections caused by *P. aeruginosa* involve pneumonia and/or bacteraemia, murine infection experiments were carried out as part of Melissa Carters' PhD research to specifically model these infections (Carter, 2009), please see statement of originality for further details. This section reviews the data generated, for further discussion of data generated in this work. The effect of loss of the entire PAPI-1 and/or PAPI-2 was tested in two murine models, an intranasal infection-based acute pneumonia model and an intravenous infection based bacteraemia model (Carter, 2009).

5.13.2 Role of PAPI-1 and PAPI-2 in acute pneumonia[6]

Strain PAO1, PA14, PA14ΔPAPI-1, PA14ΔPAPI-2, and PA14Δ1Δ2, were all tested in a murine model of pneumonia (Carter, 2009). The results showed that the deletion of PAPI-1 had little effect on the mortality of mice with PA14 and PA14ΔPAPI-1 mice all been required to be culled at the same time (18 hours) (Figure 5.22 A) They also had

---

[5] The data presented here in Section 5.17 was not carried out as part of this work, but is presented for discussion of the results in relation to the deletion of PAPI-1 and PAPI-2. Please see statement of originality

[6] The data presented here in Section 5.17.2 was not carried out as part of this work, but is presented for discussion of the results in relation to the deletion of PAPI-1 and PAPI-2. Please see statement of originality

similar bacterial loads in the nasopharynx, lung and blood (data not shown). Comparatively mice infected with the PAPI-2 mutant PA14ΔPAPI-2 displayed an increase in survival time from 18 to 24 hours and a 1 to 2 log reductions in bacterial loads in the nasopharynx, lung and blood. This result is consistent with that reported previously regarding the impact of *exoU* on virulence and showed that a PA14 strain lacking PAPI-2 is as virulent as PAO1 (Shaver and Hauser, 2004). If other genes on PAPI-2 such as *PA14_5160*; a predicted membrane lipoprotein, that has previously been demonstrated to play a role in virulence in an Arabidopsis model remains to be seen (He et al., 2004). Work is ongoing to investigate this.
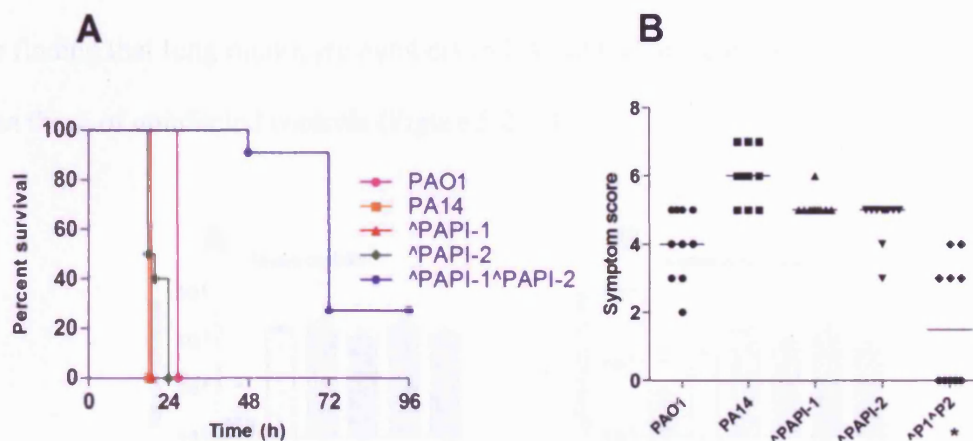
Figure 5.22: (A) Survival graph for the acute murine pneumonia model monitored over 96 h; n = 10 for each strain.
Data were generated over two independent experiments for each strain. Horizontal lines represent the percentage of mice surviving post-infection for each strain. (B) Acute murine pneumonia symptom scores at 18 h post-infection; n = 10 for each strain. Each dot represents a single mouse. All data were generated over two independent experiments for each strain. The asterisk denotes significant difference when compared with wild-type PA14 (P < 0.05). The bar represents the median symptom score. (Carter, 2009)

Most fascinatingly however, was the finding that despite the loss of PAPI-1 alone not causing attenuation, the double mutant PA14Δ1Δ2 was even further attenuated compared to the PA14ΔPAPI-2 mutant. 25% of mice survived until the end point of the experiment (96 hours) with 90% of mice surviving until 48 hours (Figure 5.22 A). This

was further reflected in the reduction of CFU of nasopharynx, lung and blood specimens compared to even PA14ΔPAPI-2 (data not shown) and significant reduction in symptom scores (P < 0.05) (Figure 5.22 B). This finding demonstrates that PAPI-1 does play a role in virulence in murine acute pneumonia; but its role was masked by the presence of PAPI-2. The drastic reduction in virulence suggests that PAPI-1 and PAPI-2 work synergistically together to produce the high virulence of strain PA14. Also of particular interest was the finding that the lungs from mice infected with PA14Δ1Δ2 showed a significant reduction (P < 0.05) in the numbers of macrophages and monocytes as compared to lungs from the PA14 infected mice (Figure 5.23 C and D). Furthermore, none of the other mutant strains caused this. Particularly interesting was the finding that lung monocyte numbers in PA14Δ1Δ2-infected mice were ~1 log lower than those of uninfected controls (Figure 5.23 D).
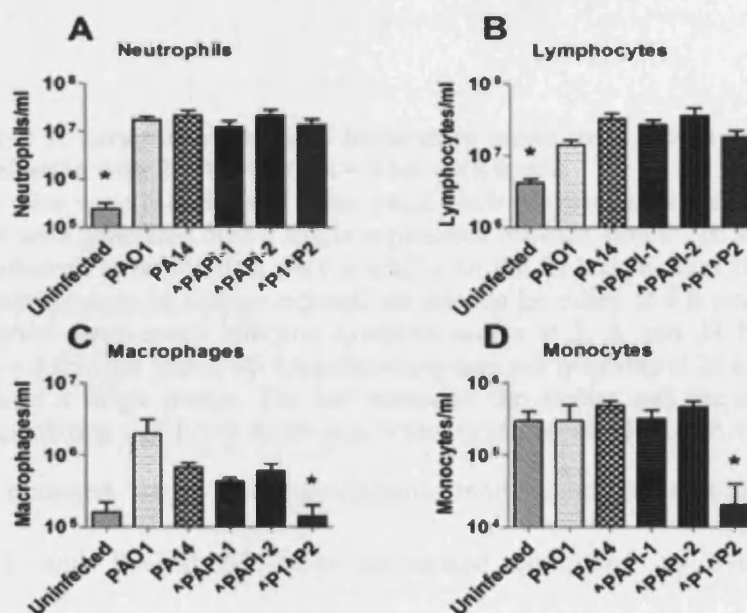
Figure 5.23: Numbers of neutrophils (A), lymphocytes (B), macrophages (C) and monocytes (D) in lung tissue obtained 18 h post-infection in the murine acute pneumonia model; *n* = 4 for each strain.
The measurements refer to number of target cells per ml of lung homogenate. The asterisk symbols denote significant differences when compared with wild-type PA14 (P < 0.05) The standard error of the mean is shown.(Carter, 2009)

153

5.13.3 Effect of the deletion of PAPI-1 and PAPI-2 in a murine bacteraemia model [7].

Due to the finding that both PA14ΔPAPI-2 and PA14Δ1Δ2 were found in significantly lower numbers in the blood stream compared to PA14 following intranasal infection in the acute murine pneumonia model (Harrison et al., 2009, Carter, 2009) the strains were tested to see if this was due to an increase in serum sensitivity or inability reduced ability to seed from the lungs into the blood. An intravenous infection-based murine bacteraemia model was used to attempt to differentiate between these two scenarios.
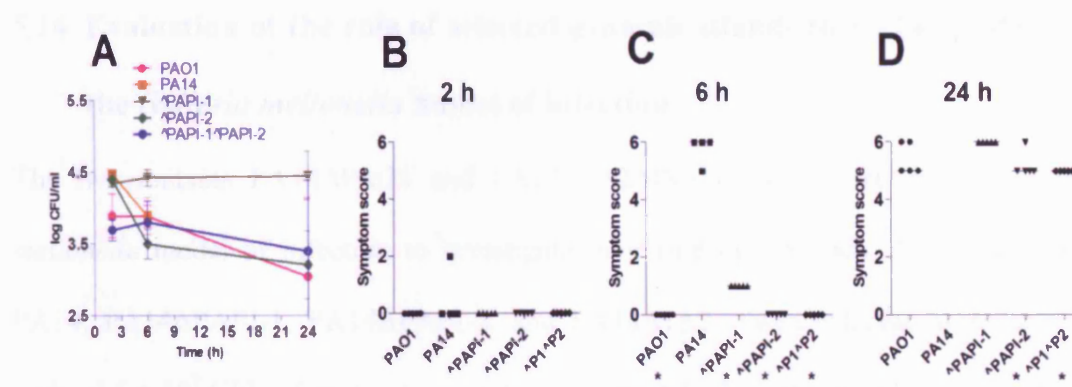
Figure 5.24: (A) *P. aeruginosa* **bacterial burdens in blood over a 24 h period following intravenous infection with 2 × 10^{6} CFU;** *n* **= 5 for each strain.**
The same five mice were used for each time point. Each dot represents the mean CFU/ml of blood. All data were generated over a single experiment for each strain. The standard error of the mean is indicated. Note: No data were available for the 24 h time point for mice infected with PA14 as severe signs of disease required the mice to be culled at 6 h post-infection. (B), (C), and (D) show intravenous infection symptom scores at 2, 6, and 24 h post-infection, respectively; n = 5 for each strain. No symptom score data was available at 24 h for PA14. Each symbol represents a single mouse. The bar represents the median and the asterisk symbols denote strains exhibiting significant differences when compared with PA14 (P < 0.05).

The results obtained using the bacteraemia model showed that PA14ΔPAPI-1, PA14ΔPAPI-2 and PA14Δ1Δ2 were attenuated compared to PA14; this was demonstrated by a significant reduction (*P* < 0.05) in symptom scores at the 6 hour time point (Figure 5.24 C). All PA14-infected mice exhibited the maximum symptom score

---

[7] The data presented here in Section 5.17.3 was not carried out as part of this work, but is presented for discussion of the results in relation to the deletion of PAPI-1 and PAPI-2. Please see statement of originality

by 6 hours post-infection and therefore were required to be culled. The remaining test mice survived until the 24 hour time point (Figure 5.24 D). PA14ΔPAPI-2 and PA14Δ1Δ2 also showed a reduced symptom score, compared to PA14ΔPAPI-1 suggesting that PA14ΔPAPI-1 was slightly more virulent in the bloodstream than PA14ΔPAPI-2 and PA14Δ1Δ2. Also as can be seen in Figure 5.24 A; PA14ΔPAPI-1 seemed to survive in the bloodstream better than the other strains, suggesting that the loss of PAPI-1 somehow improved survival of the bacterium in the bloodstream.

5.14 Evaluation of the role of selected genomic islands to PA14 virulence in the *Galleria mellonella* model of infection.

The two mutants PA14ΔPro21 and PA14Δ1Δ2ΔPro21 were tested in the *Galleria mellonella* model of infection to investigate their role in virulence. Also tested were PA14, PA14ΔPAPI-1, PA14ΔPAPI-2, and PA14Δ1Δ2. Twenty larvae were infected with ~3.5 x 10^2 CFU of each strains and incubated at 37°C as described in materials and method. As can be seen all twenty larvae infected with either PA14 or PA14ΔPAPI-1 were dead by 14 hours (the next morning). However, for larvae infected with PA14ΔPAPI-2 or PA14Δ1Δ2 the median survival times were 16 and 15.5 hours, respectively, suggesting that both mutants were equally attenuated relative to PA14 in this model of infection. This suggested that the extra deletion of PAPI-1 in PA14Δ1Δ2 did not make this strain any more attenuated than the single PA14ΔPAPI-2 mutant. This would lead to the conclusion that PAPI-2 was much more critical than PAPI-1 with regards to virulence in *G. mellonella*. Previous reports had shown that the loss of *exoU* increased the LD$_{50}$ of a mutant relative to its parent in a *G. mellonella* model by ~one log (Miyata *et al.*, 2003). As in the acute pneumonia model, further work would be required to see if any other genes on PAPI-2 played a role in this attenuation.
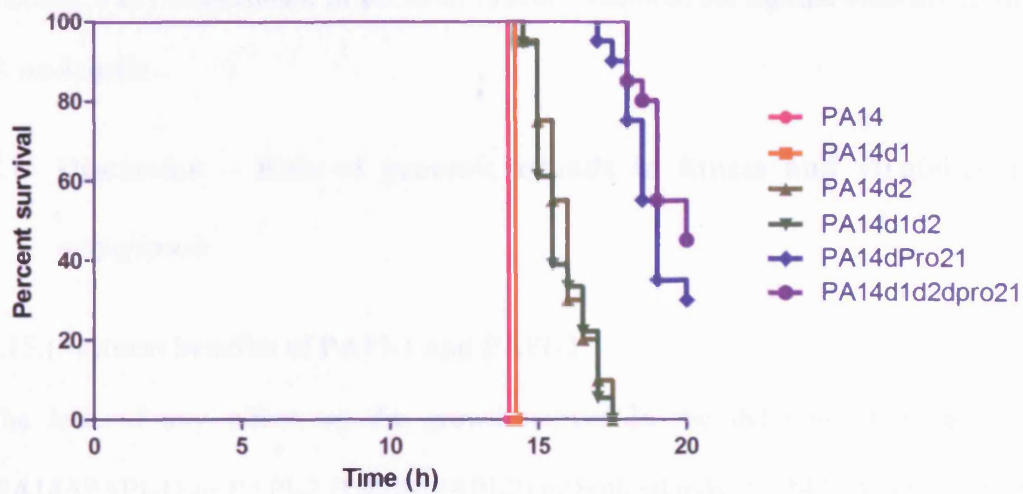
Figure 5.25: Survival curve of *Galleria melleonella* larvae inoculated with 3.5 x 10^2 CFU of strains PA14, PA14ΔPAPI-1, PA14ΔPAPI-2, PA14Δ1Δ2, PA14ΔPro21, PA14Δ1Δ2ΔPro21. n = 20. d = Δ.

The most interesting result from this experiment was the significant increase in survival of larvae infected with PA14ΔPro21 and PA14Δ1Δ2ΔPro21 with median survival times of 19 and 20 hours respectively. Six and nine larvae survived, respectively, for PA14ΔPro21 and PA14Δ1Δ2ΔPro21 to the end point (20 hours) of the experiment. This was a significant increase in survival compared to the PA14ΔPAPI-2 and PA14Δ1Δ2 *P<0.0001* (Log-rank (Mantel-Cox) test). Although not significant, the increased median survival of 20 hours for PA14Δ1Δ2ΔPro21 compared to 19 h for PA14ΔPro21 was also associated with the greater number of larvae surviving to the end point (nine compared to six). These data suggested that the triple mutant (PA14Δ1Δ2ΔPro21) may have been even more attenuated and the single PA14ΔPro21 in this model of infection. The results obtained with the two *tRNA*^{Pro21} mutants were of particular interest from a pathogenesis point of view as these suggested that the PA14 *tRNA*^{Pro21} island encoded either a significant virulence factor that is even more potent than ExoU or that the island

encoded a key determinant of bacterial function required for normal viability/growth in

G. mellonella .

5.15 Discussion – Role of genomic islands in fitness and virulence in *P. aeruginosa*

5.15.1 Fitness benefits of PAPI-1 and PAPI-2

The lack of any effect on the growth curves in the deletion of either PAPI-1 (PA14ΔPAPI-1) or PAPI-2 (PA14ΔPAPI-2) or both islands (PA14Δ1Δ2) is probably to be expected. A recent study investigating the effect of the acquisition of the *Pseudomonas* sp. strain B13 103Kb *clc* genomic island on strain PAO1 showed no significant effects on the growth of strain PAO1, carrying a similar sized genomic island to PAPI-1, in a range of growth media (Gaillard *et al.*, 2008). The authors speculate that no major changes are seen in fitness, because this would prevent the transmission of such island so freely, because if the genomic island place a to great fitness cost on the host bacterium, in conditions when they are not selected for then they would undergo purifying selection and be rapidly lost from populations. This would seem to make sense if large genomic islands are viewed as endosymbionts. Further studies investigating large scale deletions in genomic islands in *Brucella melitensis* showed no growth defects in rich media (Rajashekara *et al.*, 2008) in a number of islands. Another study in *Corynebacterium glutamicum* genomic deletions of 11 strain-specific islands (SSIs) totalling 250Kb (7.5% of total genome size) were created, again no effect was seen on the growth rate of any of the mutant strains (Suzuki *et al.*, 2005). Indeed when creating a so called 'minimal genome' of *E. coli* K-12 deletions of 15% of the total genome were also found to have little effect on growth (Posfai *et al.*, 2006). It would seem that in bacterial genomes the flexibility to rapidly lose or gain large regions

of DNA is a conserved trait amongst many bacterial species. Equally, the ability of bacterial cells to 'buffer' any detrimental effects of the acquisition of horizontally acquired DNA would allow bacteria to gain or loss large regions of DNA with little or no fitness cost. This in effect would allow for the 'testing' the fitness benefits of horizontal acquired regions

5.15.2 PAPI-1 and PAPI-2 in motility and biofilm

The lack of any significant difference in biofilm production or in twitching and swimming motility was mirrored by that of He et al who also did not find any difference in the twenty three PAPI-1 and PAPI-2 single gene mutants investigated in their study (He et al., 2004). This work confirms that PAPI-1 or PAPI-2 do not directly affect ability of PA14 to form biofilm under the conditions used. However, recent work by Mikkelson and co workers (Mikkelsen *et al.*, 2009) demonstrated that the PAPI-1 CupD fimbrial genes are antagonistically regulated by the *rcs/pvr* two-component systems encoded on PAPI-1, and that CupD fimbriae are involved in biofilm formation. However, this phenotype could not be demonstrated under similar biofilm growth conditions as used in this work, without overexpression of *rcsB* (which positively regulates the assembly of CupD fimbriae). Suggesting that the *cupD* expression mediated biofilm phenotype is regulated by the *rcs/pvr* two-component systems, under as yet unknown conditions. This raises the questions regarding if the conditions used in the *in vitro* assays in this work were suitable to detect any differences. It is conceivable that like the regulation of *cupD*; factors on PAPI-1 (the type IVB pilus) or regulated by PAPI-1 on the core genome (flagella) that are involved in biofilm and motility are regulated by *rcs/pvr* two-component systems. As a result no difference would be detected; further work is needed to identify the conditions that stimulate the *rcs/pvr* two-component systems and repeat the experiments here.

5.15.3 The role of PA14 genomic islands in virulence

In the *Galleria melleonella* model as expected the deletion of PAPI-2 caused a significant reduction in the virulence of PA14 due to the loss of *exoU* as has been previously reported (Miyata et al., 2003). However, further work is required to determine if are additional virulence factors encoded on PAPI-2 that play a role in *G. melleonella*. No difference in virulence was seen between the single PA14ΔPAPI-2 and the double mutant PA14Δ1Δ2 suggesting that PAPI-1 does not pay any role in virulence in *Galleria melleonella*. This finding suggests that the role of PAPI-1 is not crucial for infections in all species. Suggesting that is role is host specific and may regulate or control specific virulence factors that are not important for virulence in this model.

The finding that the deletion of the $tRNA^{Pro21}$ island attenuates PA14 more than the loss of the two previously defined pathogenicity islands is startling. This finding suggests that $tRNA^{Pro21}$ island either encoded a significant virulence factor or its deletion seriously affects the fitness of PA14. The $tRNA^{Pro21}$ island is stably integrated into the PA14 genome and large homologous regions are found in other *P. aeruginosa* genomes (strains PA7 and PAC181). Therefore the $tRNA^{Pro21}$ island could be described as part of an 'outer core genome' of certain strains.

Encoded on the $tRNA^{Pro21}$ island there a two likely candidates for the cause of attenuation seen in the *G. mellonella* model. The first is the loss of either of the *vagC* / *vagD* homologs PA14_28780 and PA14_28790 the loss of which was previously reported to reduce virulence in *S. dublin* (Pullinger and Lax, 1992). The second likely candidate is the PA14_28880 which has a conserved Fic domain (HPFxxGNGR) this domain has recently been identified as being involved in bacterial pathogenesis (Worby et al., 2009). In *Histophilus somni*, *Vibrio parahaemolyticus* and *Legionella pneumophila* Fic domains proteins have been demonstrated to be involved in virulence

(Worby et al., 2009, Roy and Mukherjee, 2009). The role of Fic domain proteins seems to be as bacterial toxins, that use their 'AMPylation' activity to posttranslationally modify Rho GTPases and interfere with eukaryotic cytoskeletal dynamics (Roy and Mukherjee, 2009). Further work is required to identify if this is case in PA14 and *P. aeruginosa* in general as there are other proteins with a conserved Fic domain (HPFxxGNGR) in the several sequenced *P. aeruginosa* genomes (LESB58, PA7 and 2192). PA14 itself encodes a second Fic domain protein located within yet another likely foreign DNA island.

In the murine studies of particular interest was the finding regarding the reduced macrophage and monocytes numbers. This finding could be attributed to apoptosis of monocytes and/or macrophages as part of a successful modulation of the immune response to PA14Δ1Δ2 infection. This kind of immune modulation as a part of the host defence mechanism has been previously hypothesised to occur during *P. aeruginosa* lung infection (Zhang *et al.*, 2008). This finding also fits with data derived from studies looking at *P. aeruginosa* infections in both human patients and a rabbit sepsis model (Giamarellos-Bourboulis *et al.*, 2006, Antonopoulou *et al.*, 2007). Both studies showed that early apoptosis of blood monocytes was correlated with positive resolution of infection. This was hypothesised to be due to a reduced inflammatory response and a consequent dampening of the sepsis cascade. This has been previously reported to be true in the case of pneumococcal pneumonia and the likelihood of its progression to bacteraemia (Marriott *et al.*, 2006). It is possible that the significant attenuation of PA14Δ1Δ2 enables the host to mount a protective immune response and resultantly changes recruitment of monocytes and macrophages in lung. However, an alternative hypothesis would be that the double mutant PA14Δ1Δ2 was unable to modulate the immune response in its favour. Previous studies have shown that *P. aeruginosa,* like

Salmonella (Knodler and Brett Finlay, 2001), was capable of preventing Kupffer cell (Ashare *et al.*, 2007) and epithelial cell (Zhang *et al.*, 2004) apoptosis by secretion of as yet unknown anti-apoptotic factors.

Also of interest was the apparent increased ability of PA14ΔPAPI-1 to survive in the blood relative to the wild type PA14, the two other PA14 mutants and PAO1 following intravenous inoculation in the bacteraemia model (Figure 5.24). One possible clue to explaining this was provided by recent work by Nicastro and Balidini (Nicastro and Baldini, 2007) that demonstrated that a double PA14 *rscC/rscB* mutant exhibited an altered lipopolysaccharide O-antigen profile, as has been previously reported in *Salmonella* (Kintz and Goldberg, 2008). The length and structure of O-antigen chains are a key factor in serum resistance, type III secretion and humoral immunogenicity (Rocchetta et al., 1999, Augustin et al., 2007). Therefore the deletion of the PAPI-1 island and the *rscC/rscB* genes encoded on it may have altered the O-antigen profile of the mutant potentially in turn contributing to increased serum resistance.

5.15.4 Genomic island synergy

Synergistic relationships between pathogenicity islands have been described before in *E. coli* a synergistic relationship between two pathogenicity islands PAI-I and II has been reported (Brzuszkiewicz et al., 2006). Synergistic relationships between islands has also been described between *Salmonella* pathogenicity islands 1 (SPI-1) and 4 (SPI-4), which encode factors that work synergistically to breach epithelial barriers (Roman *et al.*, 2008), suggesting this is common route in the evolution of bacterial virulence. However, the finding in this work was the first description of such a phenomenon in *P. aeruginosa*. This finding of likely synergy also highlights the need for further work investigate the exact function of PAPI-1 and related islands such as PAGI-5 (which has also been implicated in virulence) in murine acute pneumonia (Battle et al., 2008). The

161

lack of any synergistic relationship between PAPI-1 and PAPI-2 in the *Galleria melleonella* model suggests that this synergistic relationship may be host and infection site specific. Further work is required to elucidate the mechanism of synergy between the two islands in murine pneumonia. Overview of the role of genomic islands in *P. aeruginosa* virulence

This work has clearly demonstrated that the use of a 'whole island' deletion strategy is a valid approach for the screening of large horizontally acquired regions of DNA. The whole island deletion approach has been used successfully before in other bacterial species including Salmonella (Haneda *et al.*, 2009), *Brucella melitensis* (Rajashekara et al., 2008), and in *E.coli* (Brzuszkiewicz *et al.*, 2006). This is the first time that such an approach has been used in *P. aeruginosa*. If generic vectors for each tRNA site are used, this makes for a high throughput and cost effective approach to screen for horizontally acquired virulence factors.

6 *Pseudomonas aeruginosa* genome dynamics and 'island hopping': site specific recombination and stability of the PAPI-1 pathogenicity island.

6.1 Chapter overview

The deletion of the PAPI-2 island (described in Chapter 5) in strain PA14 was found to effect the integration of PAPI-1 by causing it to move from integrating in one $tRNA^{Lys}$ gene to another distinct but sequence identical $tRNA^{Lys}$ in a different genomic location (from $tRNA^{Lys47}$ to $tRNA^{Lys10}$). This chapter aimed to investigate the factors underpinning the effect seen that the deletion of the PAPI-2 and other genomic islands has on the site specific recombination of the PAPI-1 island. This was particularly focused on why the deletion of PAPI-2 caused the site specific integration of PAPI-1 to be changed from one $tRNA^{Lys}$ gene to another.

This was investigated by creating a range of mutants in single genes and genomic islands in strain PA14 and then quantifying the site specific recombination of PAPI-1 in the various PA14 isogenic backgrounds. Further this chapter investigated how the PAPI-1 island behaved in distinct genomic backgrounds by transfer of the PAPI-1 island and quantification of the site specific recombination of PAPI-1.

6.1.1 Introduction

Islands in the pKLC102/PAGI-2 family exhibit a preference for tRNA-associated *attB* integration sites. Particularly favoured are $tRNA^{Lys}$ sites, except for the island PAGI-2 and PAGI-3 which integrate into $tRNA^{Gly}$ sites (Klockgether *et al.*, 2007b). There are two $tRNA^{Lys}$ sites within all *P. aeruginosa* genomes sequenced thus far. As described in Chapter 3, the tRNAcc tRNA identifier for the PAO1 genome (Ou *et al.*, 2006b) was

used throughout to describe syntenic tRNA loci in other *P. aeruginosa* genomes, so the

$tRNA^{Lys}$ at PAO1 locus PA0976.1 was referred to as $tRNA^{Lys10}$, and PA4541.1 as

$tRNA^{Lys47}$. Many of the islands in the pKLC102 family can insert into both of the

$tRNA^{Lys}$ sites, such as PAPI-1 and pKLK106; whereas pKLC102 is reported to be only

able to insert into $tRNA^{Lys47}$. It has been postulated that due to another island PAGI-4

being locked in to $tRNA^{Lys10}$, this blocks the integration of pKLC102 by an unknown

mechanism (Klockgether *et al.*, 2004). Additionally in a subset of Clone C strains,

pKLC102 is found with a composite transposon TNCP23 inserted, causing the

pKLC102 island to be locked in to its chromosomal location (Klockgether et al., 2004).
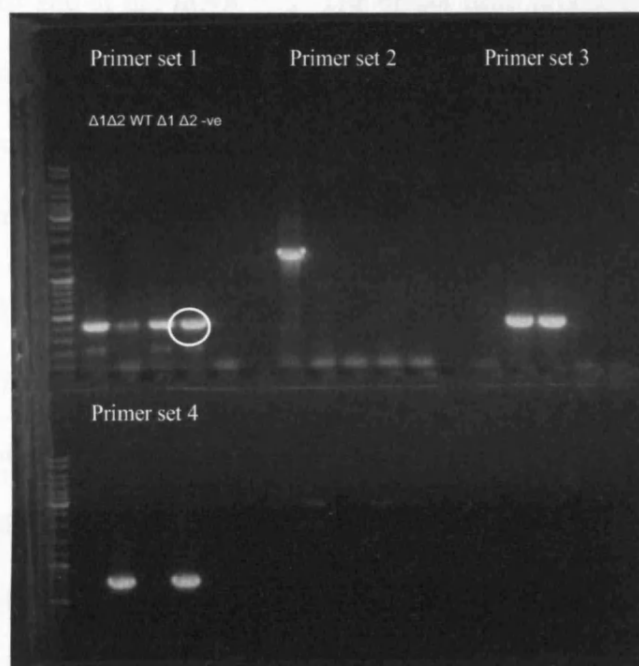
Figure 6.1: Agarose gel electrophoresis of PCR amplifications.
Primer set 1; tRIP-PCR of tRNA-Lys47 (411 bp), Primer set 2; tRIP-PCR of tRNALys10 (1.5 kb), Primer set 3; Exo-u (presence of *exoU* PAPI-2) (428 bp), Primer set 4; PAPI-1-1 (presence of PAPI-1) (721 bp) all primers set with template PA14 Δ1Δ2, PA14 WT, PA14ΔPAPI-1, PA14ΔPAPI-2, and negative control respectively. The PCR band of interest for PA14ΔPAPI-2 is marked with white circle. Generuler marker.

6.1.2 Deletion of PAPI-2 changed the occupation of $tRNA^{Lys47}$

During the confirmation of the deletion of the PAPI-1 and PAPI-2 islands from PA14 or its derivatives an unexpected result was obtained following the amplification using the tRIP-PCR primers (tRNA_Lys47U / D) for the $tRNA^{Lys47}$ site. As can be seen in Figure 6.1 strains PA14ΔPAPI-1, PA14ΔPAPI-2 and PA14Δ1Δ2 all produced a bright PCR amplicon compared to that of PA14. PA14 only produced a relatively faint band due to the PAPI-1 island been inserted at this site and therefore the number of copies of the empty site was low. For strain PA14ΔPAPI-1 and PA14Δ1Δ2 the bright band was expected as the PAPI-1 island had been deleted from these strains producing an 'empty' attB site at the $tRNA^{Lys47}$. The bright band produced for PA14ΔPAPI-2, however was puzzling, as the PAPI-1 island was still present in this strain and therefore should still occupy the $tRNA^{Lys47}$. Further work was carried out to investigate why this had occurred.

6.1.3 Occupancy of $tRNA^{Lys47}$ is changed throughout PA14ΔPAPI-2 population.

To confirm that the occupancy of the $tRNA^{Lys47}$ had changed in the entire PA14ΔPAPI-2 population compared to PA14. PCR amplifications were repeated using 20 independent colonies. Both PA14 and PA14ΔPAPI-2 were grown overnight on LA plates and 20 individual colonies were picked for each strain and tested using colony PCR using the $tRNA^{Lys47}$tRIP primers. The results from the 20 colonies show (Figure 6.2) that the increased amplification of the $tRNA^{Lys47}$ 'empty site' is present throughout the PA14ΔPAPI-2 population, and not in PA14. As the results were obtained using a colony PCR (see Materials and Methods) which produces a un-quantified template input and thus is not comparable from one strain to another. The next step was to repeat the same experiment using 50 ng of Genomic DNA as used before in studies of similar phenomena (Klockgether et al., 2007b)
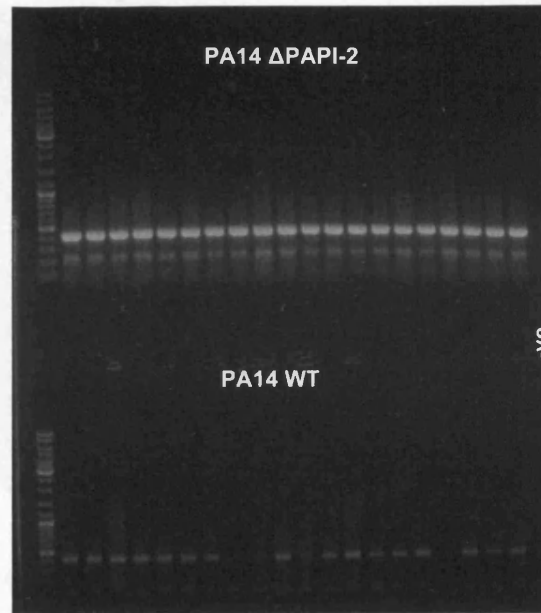
Figure 6.2: Agarose gel electrophoresis of colony PCR amplification.
Using tRIP *tRNA^{Lys47}* primers (411 bp product), 20 individual colonies of each PA14 WT and PA14ΔPAPI-2 served as template. Generuler marker.

6.1.4 Confirmation of tRIP-PCR *tRNA^{Lys47}* result with quantified genomic DNA

Genomic DNA was extracted in triplicate for strain PA14, PA14 ΔPAPI-2 after 16 hours growth (late stationary phase) It had previously been demonstrated that PA14 and PA14ΔPAPI-2 grow at the same rate in LB (see section 4.13), and produce ~2 x 10^9 CFU/ml (daa not shown) after 16 hours growth. The tRIP-PCR was carried out again using the primers *tRNA^{Lys47}* tRIP primers with 50 ng genomic DNA template. The results show again that the PA14ΔPAPI-2 had an increased amplification of the empty site at *tRNA^{Lys47}* compared to PA14 (Figure 6.3). Qualitatively the band intensity for PA14 (Figure 6.3) is similar to that seen in similar work (Klockgether *et al.*, 2007b) amplifying the same region (the empty *tRNA^{Lys47}* region) but with a different primer set. Demonstrating the wild-type PA14 strain used in this study had a comparable occupancy of the *tRNA^{Lys47}* site in PA14 WT as seen in other laboratories (Klockgether *et al.*, 2007b).
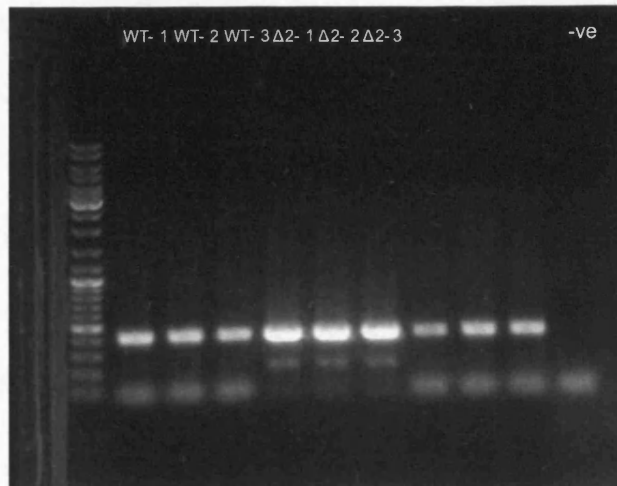
Figure 6.3: Agarose gel electrophoresis of tRIP-PCR using tRNA_LysU / D.
Using 50ng of G DNA for each strain (in triplicate). The strains investigate are PA14 WT (WT), PA14 ΔPAPI-2 (Δ2) respectively. Generuler marker. Expected product 411 bp.

This result using quantified DNA suggested that the $tRNA^{Lys47}$ was less occupied in the PA14ΔPAPI-2 strain than in the PA14. This suggested that the deletion of the PAPI-2 somehow effected the integration of PAPI-1 in the $tRNA^{Lys47}$ site.

6.1.5 PAPI-1 is still present in PA14ΔPAPI-2

The result generated by the previous experiment raised the question if the PAPI-1 island was absent from the $tRNA^{Lys47}$ was it still present in PA14ΔPAPI-2 at all. This was tested using a PCR for a target located on PAPI-1 using primers PP-1-5 F / R. The result of this PCR (data not shown) revealed that indeed the PA14ΔPAPI2 strain like PA14 was positive for PAPI-1. Demonstrating that the PAPI-1 island had not been lost from PA14ΔPAPI-2.

6.1.6 PAPI-1 integration in tRNA^{Lys47} is reduced in PA14ΔPAPI-2.

Once it was established that the PAPI-1 island was still present in PA14ΔPAPI-2 strain, the next question raised was is the PAPI-1 island present at both the $tRNA^{Lys10}$, $tRNA^{Lys47}$ and in the extrachromosomal circular form. Previous investigations (Qiu et al.,

2006) had shown that the PAPI-1 island can form both a circular intermediate form like pKLC102 and pKLK106 (Kiewitz et al., 2000, Klockgether et al., 2004) and can integrate into *attB* sites in both *tRNA^{Lys}* genes. To detect if the deletion of PAPI-2 had effected the integration of the PAPI-1 island into the *tRNA^{Lys47}*, PCRs were carried out using a primer located on the PAPI-1 island at the end proximal to the tRNA (PAPI-1(Qiu)-R (Qiu et al., 2006)) and another primer upstream of the tRNA gene (tRNALys47U-F) . The result of the PCR in Figure 6.4 show bright amplicons for the PA14 and very faint bands for PA14ΔPAPI-2. This result suggested that in PA14ΔPAPI-2 the integration of PAPI-1 into *tRNA^{Lys47}* was reduced compared to PA14.
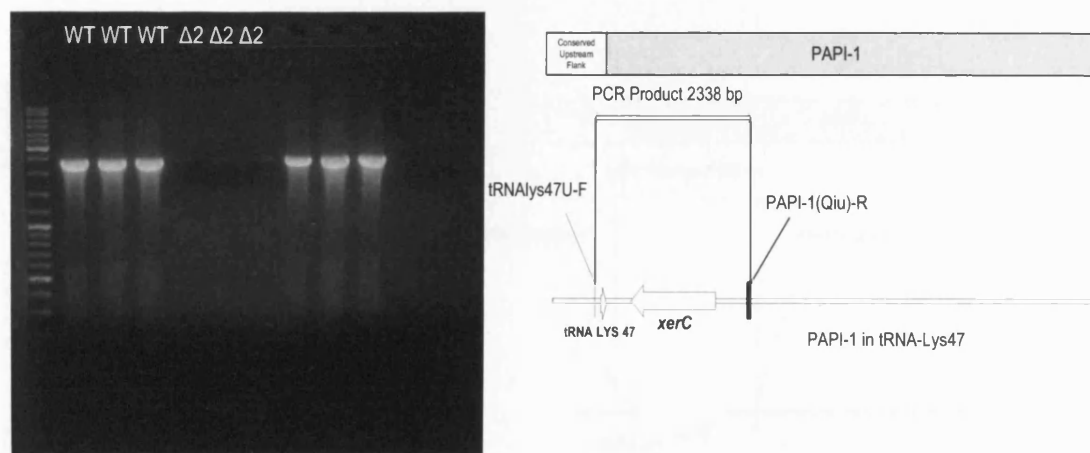
Figure 6.4: Agarose gel electrophoresis PCR amplification to detect the presence of PAPI-1 integrated at *tRNA^{Lys47}*.
Using primers tRNA-Lys47-U and PAPI-1(Qiu)-F locus. Primer binding locations are shown in accompanying diagram. The strains investigated are PA14 WT, and PA14 ΔPAPI-2 in triplicate respectively. Generuler marker

6.1.7 PAPI-1 integrated in tRNA^{Lys10} in PA14ΔPAPI-2 increased

As in PA14ΔPAPI-2 strain the presence of PAPI-1 integrating into *tRNA^{Lys47}* seemed to be greatly reduced and the only difference between PA14 and PA14ΔPAPI-2 was the deletion of the PAPI-2 island located at *tRNA^{Lys10}*. Therefore it seemed logical that,

deleting the PAPI-2 island at $tRNA^{Lys10}$ had somehow made the PAPI-1 island move to integrating into the $tRNA^{Lys10}$ gene. PCRs were carried out using one primer upstream of the $tRNA^{Lys\ 10}$; PA0976(Qiu)-F and the same primer as used before at proximal end of PAPI-1: PAPI-1(QIU)-R. The result is shown in Figure 6.5. PA14 generated a faint band suggesting that PAPI-1 is only present in $tRNA^{Lys10}$ in a small percentage of the population. While PA14ΔPAPI-2 produced a strong band confirming the hypothesis that PAPI-1 had switched from integrating in the majority of cells into the $tRNA^{Lys47}$ gene to targeting the $tRNA^{Lys10}$ site instead. However as the PCR assay used was a standard PCR, this would need to be further confirmed using a more quantitative method.
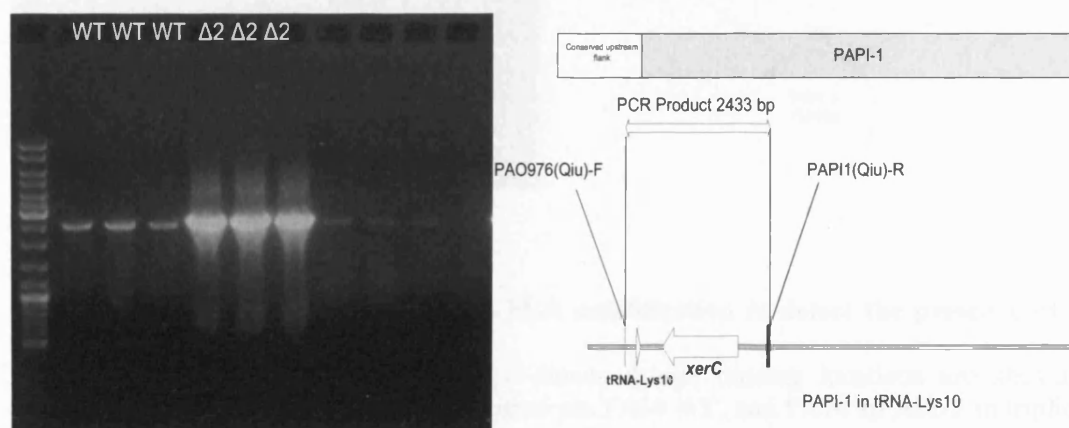
Figure 6.5: Agarose gel electrophoresis PCR amplification to detect the presence of PAPI-1 integrated at tRNA-Lys10.
Using primers tRNA-Lys47-U and PAPI-1(Qiu)-F locus. Primer binding locations are shown in accompanying diagram. The strains investigate are PA14 WT, and PA14 ΔPAPI-2 in triplicate respectively. Generuler marker

6.1.8 Confirmation of circular form of PAPI-1

As the location of the integration of PAPI-1 in the genome had changed, and as the circular form of PAPI-1and related islands is thought to play an important role in the integration and transfer dynamics of these islands. The possibility that PAPI-1 was still forming a circular intermediate was investigated by PCR. Two previously designed

primers were used at the opposite ends of the island; Int(Qiu)-F at the end proximal to the $tRNA^{Lys}$ and Soj(Qiu)-R at the distal end (Qiu et al., 2006). If PAPI-1 formed a circle the two primers would be correctly directed in a convergent fashion and a PCR amplicon would be produced. As can be seen in Figure 6.6, PA14ΔPAPI-2 produced a PCR amplicon with the same intensity to that of PA14. Confirming that in PA14ΔPAPI-2 a circular form of the island was still formed.
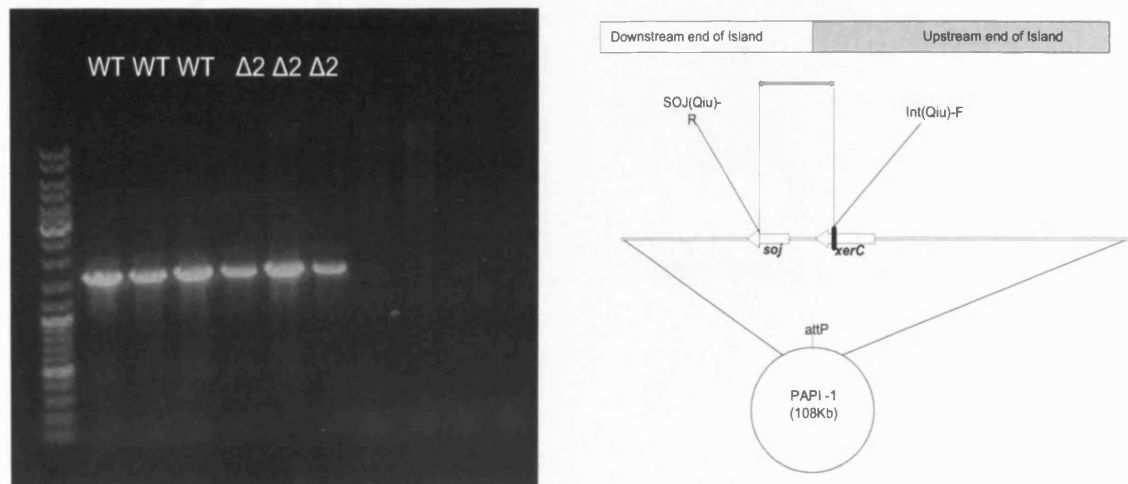
Figure 6.6: Agarose gel electrophoresis PCR amplification to detect the presence of the circular form of PAPI-1.
Using primers SOJ(Qiu)-R and Int(Qiu)-F locus. Primer binding locations are shown in accompanying diagram. The strains investigate are PA14 WT, and PA14 ΔPAPI-2 in triplicate respectively.

6.1.9 Overview of initial identification of 'island hopping' phenomena

The initial results using the PCR assays showed that in strain PA14ΔPAPI-2 the integration of PAPI-1 had moved from integrating in $tRNA^{Lys47}$ to $tRNA^{Lys10}$ (Figure 6.7). The integration of PAPI-1 in the $tRNA^{Lys10}$ as well as $tRNA^{Lys47}$ in a PA14 background had been reported (Qiu et al., 2006), but the authors did not report the that PAPI-1 island seemed to prefer to integrate into the $tRNA^{Lys47}$ site. Further studies were therefore required to investigate why the PAPI-1 island had switched its preferential integration

170

site from $tRNA^{Lys47}$ to $tRNA^{Lys10}$ ('island hopping' (Figure 6.7)) and to try to identify how deletion of PAPI-2 island caused the change in this "genotype-phenotype" switch.
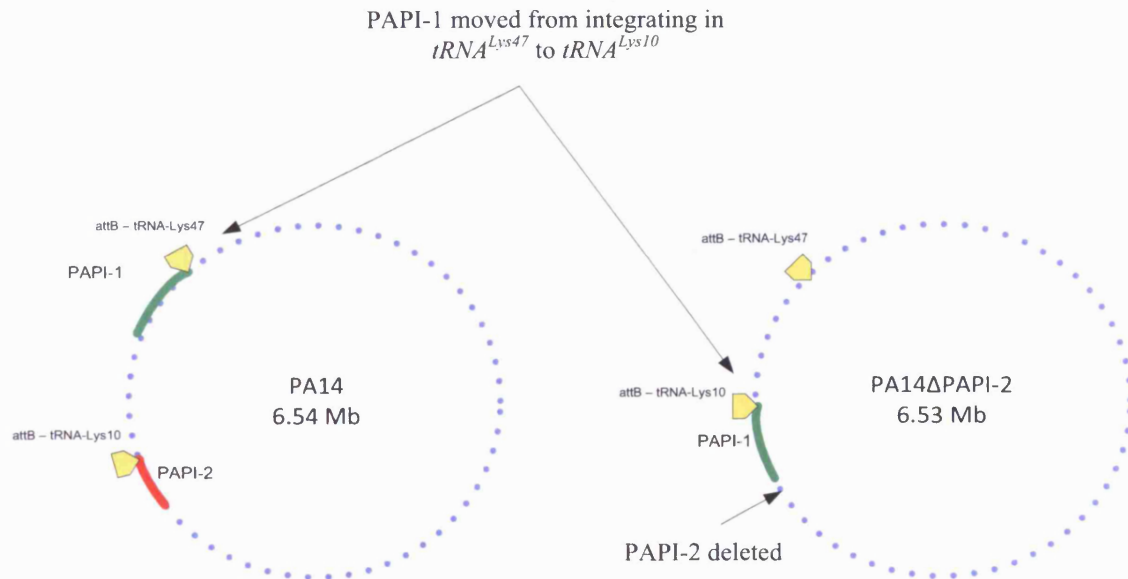
Figure 6.7: Overview of preliminary results of 'island hopping'. The deletion of PAPI-2 causing PAPI-1 to move integration site.

6.2 Investigations into 'island hopping'

After the initial results for the island hopping had been tested. A number of hypotheses were generated to what could be causing the island hopping phenomena. The initial hypotheses were:

1. The deletion of PAPI-2 had introduced a mutation in or around the tRNA *attB* site.
2. A gene or genes on PAPI-2 plays an unknown role in recombination of PAPI-1.
3. A change in local DNA structure was caused by the deletion of PAPI-2.
4. A genome inversion had occurred.
5. Introduction of an FRT site somehow effected recombination.

The following experiments were carried out to investigate which, if any, of the hypothesis were correct.

6.3   Sequencing and comparison of $tRNA^{Lys10}$ site and flanking sequences

Previous reports investigating site specific recombination of genomic islands in *E.coli* reported that small changes in the *attB* target site and surrounding DNA can cause major changes in recombination rates (Wilde *et al.*, 2008, Sentchilo et al., 2009). So the area around the $tRNA^{Lys10}$ site was amplified from PA14 using the tRIP PCR primers tRNA-Lys10-U / D. The PCR amplicons were then fully sequenced and compared to the wildtype PA14 and other $tRNA^{Lys}$ *attB* sites, to see if the *attB* and flanking sequences had been altered by the deletion process. The results of the sequencing showed no polymorphisms in any of the sequence proximal to the $tRNA^{Lys}$. The region around the multiple *attB* sites at $tRNA^{Lys10}$ and $tRNA^{Lys47}$ is shown is shown in Figure 6.8. The multiple alignments show the upstream region of the $tRNA^{Lys}$ gene is conserved, presumably due to a common promoter sequence (data not shown). Downstream of the $tRNA^{Lys}$ however is not conserved across all sites. The alignment did identify seven conserved bases (TATTNNANANG) starting at the distal end of the $tRNA^{Lys}$ gene that are conserved across all the empty *attB* sites at $tRNA^{Lys10}$ and $tRNA^{Lys47}$ sites. This suggests that these conserved bases maybe part of the tRNA *attB* site and therefore play a role in the recombination of the genomic islands into these loci. Interestingly of the five known non-mobile islands integrated into this locus (marked in a black hatched box in Figure 6.8), all have single-nucleotide polymorphisms (SNPs) in one of the seven conserved bases suggesting that SNPs in this region may play a role in the stability of the integration of the island

.
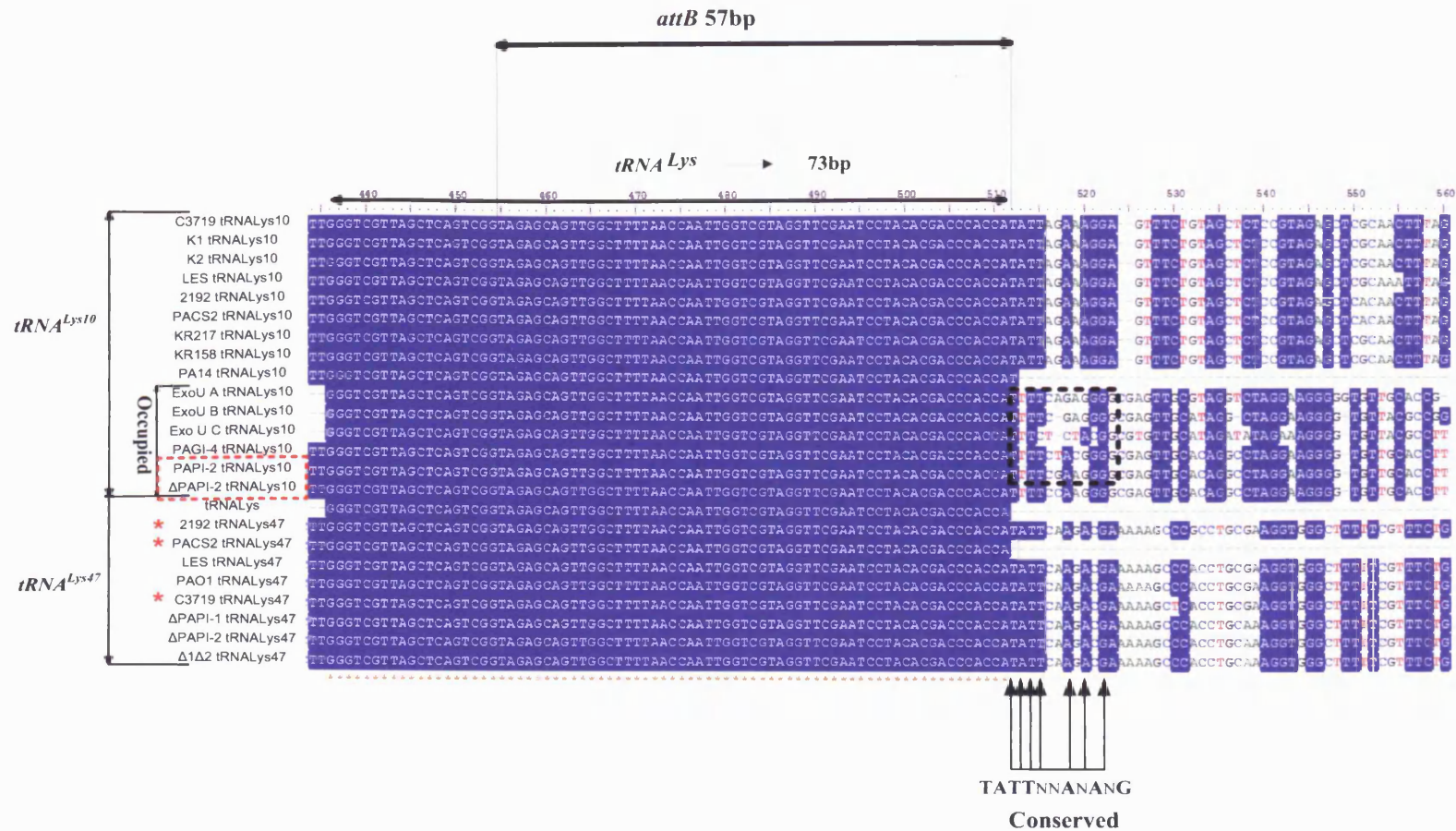
Figure 6.8: Showing ClustalX aligment of the attB site within *tRNA^Lys* and downstream sequence.
The red box marks the PAPI-2 (PA14 WT tRNA_Lys10) and the same location in ΔPAPI-2 mutant (PA14ΔPAPI-2). The arrows denote seven conserved bases downstream of the *attB* in empty sites in both *tRNA^Lys10* and *tRNA^Lys47*. The black hatched box marks the five 'non mobile' genomic islands with SNPs in the seven downstream conserved bases. The red stars denote site occupied by a mobile pKLC102 island.

173

6.4 Deletion of PAPI-2 encoded *xerC* integrase

The *xerC* integrase carried on the PAPI-2 island shares 96% a.a. identity with the corresponding *xerC* on the PAPI-1 island (Qiu et al., 2006). As with the rest of the genes on the PAPI-2 island this gene was deleted in the PA14ΔPAPI-2 strain. This integrase was reported to be non-functional based on the fact that when the homologous PAPI-1 *xerC* was deleted this caused PAPI-1 to become non mobile, suggesting that the presence of the PAPI-2 *xerC* did not complement the loss of the PAPI-1 integrase (Qiu et al., 2006). However, it was hypothesised that this integrase could be expressed, and was somehow inhibiting the integration of PAPI-1 at the $tRNA^{Lys10}$ site; by competitive binding to $tRNA^{Lys10}$ *attB*. This competitive binding of the PAPI-2 XerC to the *attB* site could take place with XerC as part of the intrasome (a DNA-protein-complex that forms between an *attP* site and the integrase before binding to the *attB*), or by direct binding of XerC as a single protein to the *attB* site. Thus preventing the functional PAPI-1 xerC integrase mediating the recombination of PAPI-1 in to the $tRNA^{Lys10}$site.

6.4.1 Construction of *PA14Δ*xerC mutant.

The construction of PA14ΔxerC is described in Appendix F.

6.5 Construction of a second PA14ΔPAPI-2 mutant

To investigate if the 'island hopping' phenomenon was due to a random event in strain PA14ΔPAPI-2 or if it was reproducible, a second PA14ΔPAPI-2 mutant was constructed. The mutant was constructed from KR 565 (PA14ΔPAPI-2:Gm^R:Amp^R) an independent single crossover from the original conjugation for the construction of PA14ΔPAPI-2 stored at -80°C. PA14ΔPAPI-2:GmR:AmpR was streaked heavily onto LA + 5% sucrose and grown overnight at 37°C the next day colonies were picked and patched onto LA + 30μg Gentamicin 30μg/ml and LA+ Carbenicillin 200μg/ml and

incubated overnight. Gm^R Cb^S were taken forward as putative double crossovers. Strains PA14ΔPAPI-2:Gm^R was stored at in 30% glycerol BHI at -20 and -80°C as strain KR713. The Gentamicin resistance cassette was then deleted as described previously using pFLP2. The strain was confirmed as PA14ΔPAPI-2.2 by patch plating and PCR as described before in the construction of the original mutant. The mutant strain PA14ΔPAPI-2.2 was stored as in 30% glycerol BHI at -20 and -80°C as strain KR717.

6.6 Quantitative-PCR (qPCR) investigations of island hopping

6.6.1 Overview

The first stages of the investigation used normal PCR to investigate the site specific integration of PAPI-1 showed that PAPI-1 had moved from integrating in $tRNA^{Lys47}$ to $tRNA^{Lys10}$. This finding needed to be confirmed using a quantitative approach. So PCR primers were designed to have produce an amplicon ~220 bp in size. The primers designed and their target regions are shown in Table 6.1. The primers designed could measure the copies of PAPI-1 integrated in $tRNA^{Lys10}$, copies of PAPI-1 integrated in $tRNA^{Lys47}$, Total PAPI-1 copies, Total PA genome copies (Normalisation control), Circular PAPI-1 copies, Empty $tRNA^{Lys10}$ copies, and Empty $tRNA^{Lys47}$ copies.

6.6.2 qPCR experimental conditions

For each sample, the test strain was grown in a 5 ml LB broth at 37°C and 200 rpm shaking for 12 hours in a minimum of biological replicate. The total DNA was then extracted and quantified. A working stock for each sample was then made up to be ~5 ng/μl. qPCRs were carried out as described in the materials and methods. Preliminary runs were carried out to optimise primer concentrations and annealing temperature.

Initial runs were also run on agarose gels to determine that a specific product was obtained. This was confirmed in the actual test runs by melt curve analysis.

Table 6.1: qPCR primers

Target to measure	Primer Reverse	Primer Reverse	Amplicon size	Source of Reference
PAPI-1 integrated in $tRNA^{Lys10}$	tRNA-LYS10-RT-F	PAPI-1-RT-F	215	This work
PAPI-1 integrated in $tRNA^{Lys47}$	tRNA-LYS47-RT-F	PAPI-1-RT-F	218	This work
Total PAPI-1 copies	Total-PAPI-1F	Total-PAPI-1-R	232	This work
Total PA genomes copies (*gyrB*) (Normalisation control)	gyrPA-398	gyrPA-620	222	(Qin *et al.*, 2003)
Circular PAPI-1 copies	PAPI-1-Circ-Soj	PAPI-1-RT-F	219	This work
Empty $tRNA^{Lys10}$	tRNA-LYS10-RT-F	PAPI-1-RT-F	217	This work
Empty $tRNA^{Lys47}$	tRNA-LYS47-RT-F	PAPI-1-RT-F	224	This work

Cycle thresholds (Ct) were assigned by the Rotor gene 6000 software, or manually when appropriate. Sample Ct values were only taken from a minimum of duplicate values, though most were triplicate, except when one value was removed due to being an obvious outlier. Values for both test sample and standards were only accepted with a repeat Ct standard deviation of < 0.05. Copy numbers were based on a standard curve generated from a quantified PCR fragment containing the target amplicon. All test copy numbers were normalised based on their total number of *P. aeruginosa* genomes in the input DNA (measured by the *gyrB* gene) to 1×10^6 genome equivalents to allow for comparisons across strains. During the optimisation process it was found that the primers for 'Empty $tRNA^{Lys47}$' always produced non-specific products, so were excluded from the data presented here, also in some strains the same was found for $tRNA^{Lys10}$ empty site. The strains investigated are shown in Table 6.2.

The different strains investigated allowed the testing of the hypotheses' raised (Section 6.1.9). The original (PA14ΔPAPI-2) the second PAPI-2 mutant (PA14ΔPAPI-2) was compared to investigate if 'island hopping' finding was a reproducible phenomenon. The strain PA14ΔxerC was investigated see if the PAPI-2 encoded *xerC* was playing a role. Finally, PA14ΔPro21 was investigated to see if deletion of another island at another locus would affect the recombination of PAPI-1 by altering PA14 genome structure. The results of the qPCRs are shown in Figure 6.9.

Table 6.2: Strains tested in qPCR

Lab number	Strain	Mutation	Other
KR125	PA14	None	Wildtype
KR572	PA14ΔPAPI-2	Deletion of PAPI-2	Original ΔPAPI-2
KR666	PA14ΔXerC	Deletion of PAPI-2 *xerC*	
KR717	PA14ΔPAPI-2.2	Deletion of PAPI-2	Repeat of ΔPAPI-2
KR1034	PA14ΔPro21	Deletion of *tRNA^{Pro21}* island	

6.6.3 qPCR results

6.6.4 PAPI-1 integration in PA14

The qPCR results for PA14 revealed similar findings as the standard PCR, that the majority of PAPI-1 copies are found integrated in $tRNA^{Lys47}$ (5.17 x 10^5 copies) compared to $tRNA^{Lys10}$ (6.18 x 10^1 copies). Thus confirming the earlier non-quantitative findings; that PAPI-1 has a preference for integration at $tRNA^{Lys47}$ over $tRNA^{Lys10}$ in PA14. The total copy number of PAPI-1 was 7.79 x 10^5. If we take into count the standard deviation present in the assay, then this probably represents most cells having ~ 1 copy. The circular copy number was found to be 1.49 x 10^4 which represents 0.02 % of the total PAPI-1 copies. A previous study using a semi-quantitative approach

estimated the copy number to be ~2% of PA14 genomes which in this assay would account for a similar figure of 2 x 10^4 (Klockgether *et al.*, 2007b). The copy number of the empty $tRNA^{Lys10}$ site was 1.06 x 10^6 which fits the finding that this site had only 6.18 x 10^1 copies of PAPI-1 integrated.

6.6.5 Effect of deletion of the PAPI-2 *xerC* (PA14ΔxerC)

The deletion of the PAPI-2 *xerC* did not seem to have any drastic effect on the recombination. Most importantly, the copy of number of PAPI-1 integrating into $tRNA^{Lys10}$ did not increase like seen in PA14ΔPAPI-2 background, PA14 had 6.18 x 10^1 copies compared to 1.28 x 10^2 in PA14ΔxerC. This increase is within the standard deviation of this assay, but could represent a modest increase in occupation. All the other values suggest that in PA14ΔxerC the integration and copy number of PAPI-1 is unchanged, therefore ruling out *xerC* as playing any major role in the 'island hopping' phenomena.

6.6.6 Effect of the deletion of $tRNA^{Pro21}$ island (PA14ΔPro21)

The deletion of the $tRNA^{Pro21}$ island did not seem to have any effect on the Total copy number or the integration of PAPI-1 in *tRNALys47*, with all the copy numbers for these values being in the same range as PA14. One change to be noted is the reduction in the copy number of the circular form of PAPI-1 from 1.49 x 10^4 in PA14 to 8.26 x 10^2 in PA14ΔPro21; almost a two log decrease in copy number. This suggests a decrease in the circular form of PAPI-1. The copy number of PAPI-1 in $tRNA^{Lys10}$ seems also to be reduced from 6.18 x 10^1 to 2.15 x 10^0 suggesting a reduction in the occupancy of this site. If this is the case and the occupancy of the $tRNA^{Lys10}$ is being reduced.

	Total PAPI-1*	Circular PAPI-1	PAPI-1 Lys47	PAPI-1 in Lys10	Empty Lys10
PA14 WT	7.79E+05	1.49E+04	5.17E+05	6.18E+01	1.07E+06
PA14dPAPI-2.1	8.39E+05	8.76E+03	6.07E+01	7.06E+05	3.33E+03
PA14dXerC	1.17E+06	2.65E+04	9.18E+05	1.28E+02	1.61E+06
PA14dPAPI-2.2	1.34E+06	1.60E+04	4.83E+05	4.74E+05	3.28E+03
PA14ΔPro21	9.39E+05	8.26E+02	1.09E+06	2.15E+00	1.68E+06
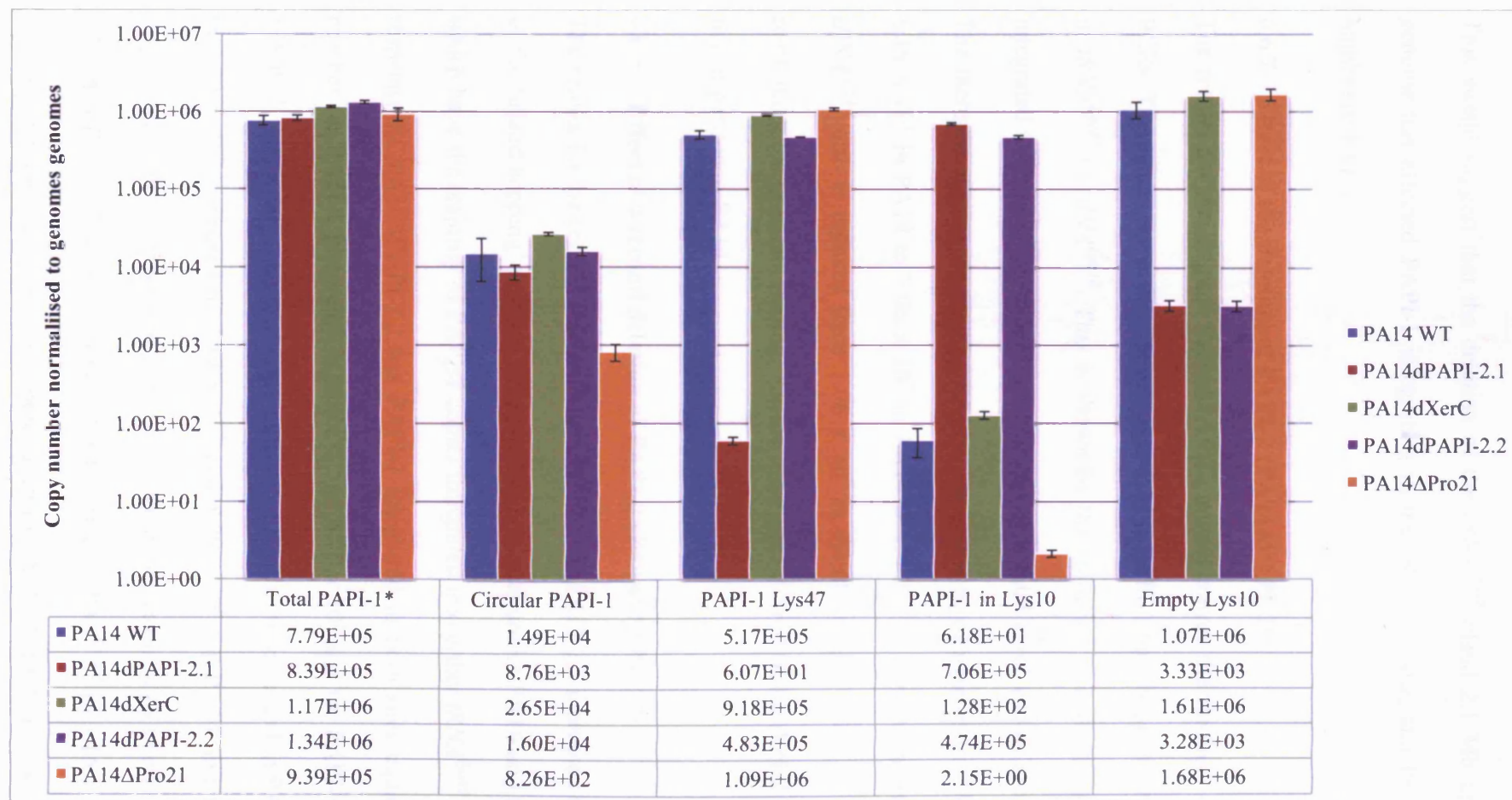
Figure 6.9: Graph showing the relative copy number of PAPI-1.
Normalised to 1 x 10^6 genomes integrated in sites $tRNA^{Lys10}$, $tRNA^{Lys47}$ Total and Circular copy numbers of PAPI-1 in strain PA14, PA14ΔPAPI-2, PA14ΔxerC, PA14ΔPAPI-2.2 and PA14ΔPro21.

179

This would suggest that the deletion of the $tRNA^{Pro21}$island 2.1 Mb upstream in the genome has affected PAPI-1 integrating in the $tRNA^{Lys10}$ site, and the circular copy number of PAPI-1.

6.6.7 Effect of the deletion of PAPI-2 (PA14ΔPAPI-2)

The results for the original PA14ΔPAPI-2 mutant mirror the findings of the original PCRs. The results show that compared to PA14; PAPI-1 has 'hopped' from integrating in $tRNA^{Lys47}$ to $tRNA^{Lys10}$. This is shown by the reduction in copy number of PAPI-1 integrated in $tRNA^{Lys47}$from 5.17 x 10^5 in PA14 to 6.07 x 10^1 copies in PA14ΔPAPI-2. The increase of copy number of PAPI-1 integrated in integrated in $tRNA^{Lys10}$ is from 6.18 x 10^1 in PA14 to 7.06 x 10^5 in PA14ΔPAPI-2. The copy number of the empty $tRNA^{Lys10}$ also is reduced from 1.06 x 10^6 in PA14 to 3.33 x 10^3 in PA14ΔPAPI-2 reinforcing the previous finding. All the other values for PA14ΔPAPI-2 are unchanged in comparison to PA14.

6.6.8 Effect of a second deletion of PAPI-2 (PA14ΔPAPI-2.2)

The results for the second deletion mutant of PA14ΔPAPI-2.2 increased the complexity of the 'island hopping' problem. The results show that unlike PA14 and PA14ΔPAPI-2 which have the majority of PAPI-1 copies integrated into either $tRNA^{lys47}$ or $tRNALys10$ respectively, PA14ΔPAPI-2.2 has PAPI-1 integrated in both sites equally. The copy number for PAPI-1 integrated in $tRNA^{Lys10}$ is 4.77 x 10^5 and for PAPI-1 integrated in $tRNA^{Lys47}$ 4.77 x 10^5. The total copy number of PAPI-1 is increased in PA14ΔPAPI-2.2 to 1.39 x 10^6 compared to 7.39 x 10^5 and 8.39 x 10^6 for PA14 and PA14ΔPAPI-2 respectively. This suggests that there is an overall increase in copy number of PAPI-1 in PA14ΔPAPI-2.2. The copy number for the empty $tRNA^{Lys10}$ is 3.16 x 10^3, which is virtually the same as 3.33 x 10^3 copies seen in PA14ΔPAPI-2. This suggests that the $tRNA^{Lys10}$ site is found occupied by PAPI-1 in the majority of the population of

PA14ΔPAPI-2.2. This along with the increased total copy number suggests that most strains in the population have both $tRNA^{Lys}$ sites with an integrated copy of PAPI-1. Therefore PA14ΔPAPI-2.2 most likely has a copy number of two for PAPI-1, compared to one in all the other strains measured. It is likely that the copy numbers for PAPI-1 integrated into $tRNA^{Lys10}$ and $tRNA^{Lys47}$ and Total PAPI-1 are just lower end of the standard deviation. This finding can be completely confirmed with a qPCR for the empty $tRNA^{Lys47}$.

6.7 PAPI-1 site specific recombination in other strain backgrounds

To investigate how PAPI-1 integrated in other host backgrounds PAPI-1 was transferred to other host strains.

6.7.1 Construction of dual Gm-FRT- sacB cassette

A Gm-FRT-sacB cassette was constructed to 'tag' the PAPI-1 island both with a resistance cassette and sacB cassette. Once the PAPI-1 island was tagged both parts of the cassette could be used, firstly the gentamicin cassette could be used to select for strains that had gained the PAPI-1 island in conjugation from one strain to another. Secondly both the Gentamicin cassette and the sacB cassette could be use could be used for island probing experiments as detailed in Section 7.

To construct the dual cassette, the FRT flanked gentamicin cassette as used before from pPS856 was amplified by PCR along with the sacB from pEX18Ap using primers Gm-F / R and SacB-R / SacB-F-Gm respectively. The two fragments have overlapping homologies to each other included in the Gm-R and SacB-F-Gm, which were then used to join the two fragments together in a SOE-PCR reaction, the structure of the cassette is shown in Figure 6.10 A.

6.7.2 Construction of pEX-Isprob suicide vector

6.7.2.1 *SOE fragment*

The next stage was to join the Gm-FRT-*sacB* cassette to the up and down stream flanking regions. The region to be targeted was PA14 genome coordinate 5288187, this location as can be seen in Figure 6.10 E, is located between the ends of two divergently orientated genes, as to not cause any polar effects. For the upstream homology primers PAPI-1IP-US-F-GWL / PAPI-1IP-US-R-Gm were used to amplify a 564 bp region, and for the downstream homology primers PAPI-1IP-DS-SacB / PAPI-1IP-DS-R-GWR were used to amplify a 586 bp region. The homologous sequence had overlaps to the Gm-FRT-*sacB* cassette and to the gateway system. The two flanking homologies and the Gm-FRT-*sacB* were then joined together as a single 4007 bp fragment by a SOE PCR, as shown in Figure 6.10 B. The Isprob SOE fragment was then transferred into pDONR221 via the BP clonase reaction using the Gateway site specific recombination system (Invitrogen, UK) to create pDONR221-Isprob as previously described. The correct construct was confirmed by restriction digestion with *Xba*I (data not shown). The next stage was to transfer the Isprob fragment to the suicide vector from pDONR221-Isprob to pEX18ApGW, this was carried out using a LR clonase reaction as described previously. The resultant vector pEX-Isprob (Figure 6.10 C), was confirmed by restriction digests with *Xba*I (Figure 6.10 D), and then stored in 30% glycerol BHI at -20 and -80°C as strain KR906.

6.7.3 Construction of strain PA14-Isprob.

To transfer the suicide vector pEX-Isprob to *P. aeruginosa* strain PA14 (KR125) firstly the pEX-Isprob, was transferred to *E.coli* SM10 γ-pir to enable conjugative transfer. This strain was then conjugated with strain PA14 as described before and selected on VBMM + 30 μg/ml gentamicin.
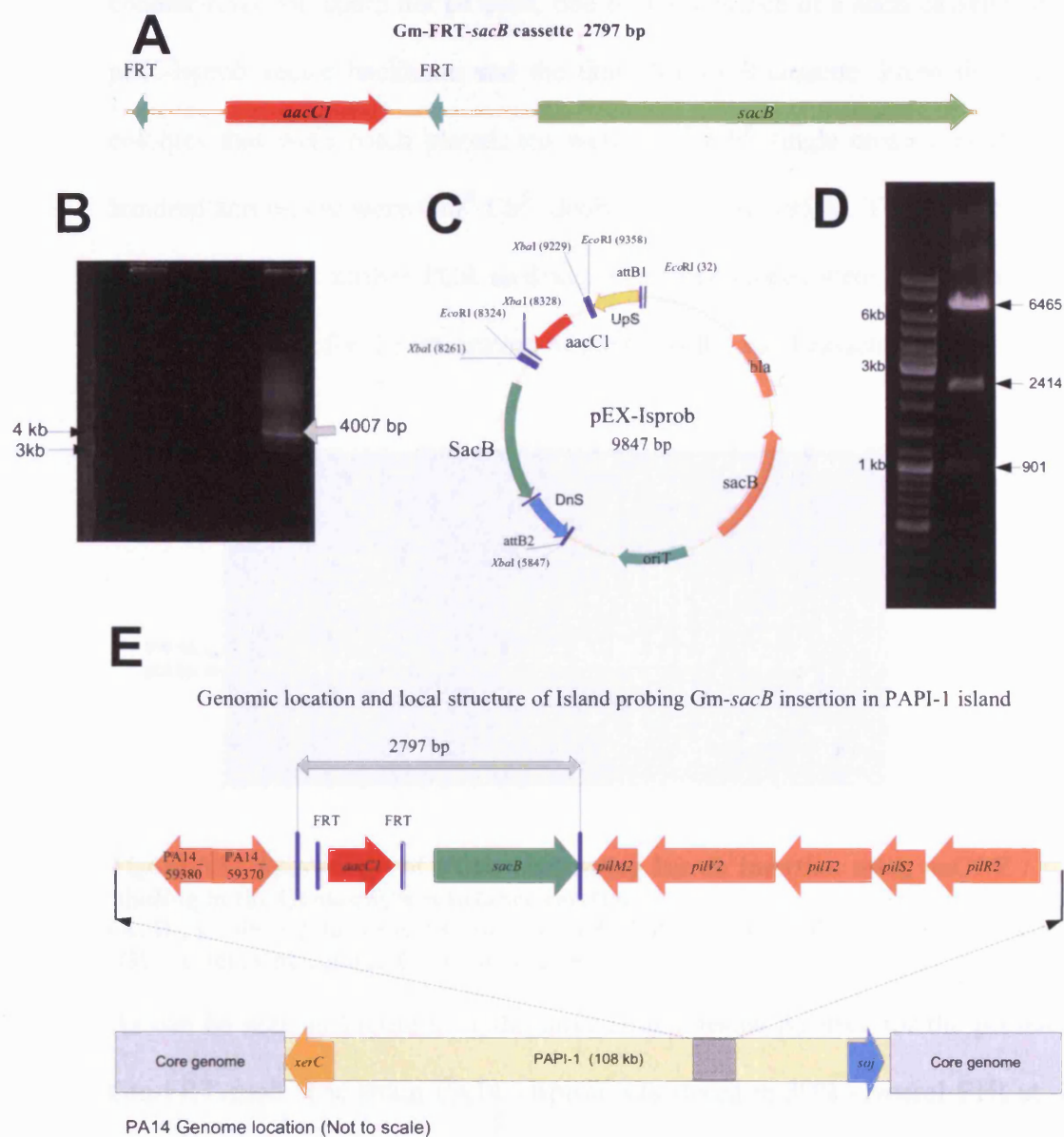
Figure 6.10: Island probing construction.
(A) Structure of Gm-FRT-*sacB* cassette. (B) Agarose gel electrophoresis showing 4007 bp SOE PCR fragment for Island probing. (C) pEX-Isprob suicide vector for allelic exchange containing the SOE product. (D) *Xba*I digest of pEX-Isprob showing predicted fragments 6465, 2414, 901, and 67 bp (67 bp not shown) (E) Genomic location within PAPI-1 and local structure of insertion of Gm-FRT-*sacB* cassette inserted into PAPI-1 island.

After colonies appeared, two hundred colonies were picked and patched onto VBMM + Gm 30 μg/ml and LA + 200 μg/ml to differentiate between single (Gm^R Cb^R) and double (Gm^R Cb^S) crossover strains. This had to be done on a large scale as sucrose

183

counter-selection could not be used, due to the presence of a *sacB* cassette on both the pEX-Isprob vector backbone and the Gm-FRT-*sacB* cassette. From the two hundred colonies that were patch plated, ten were $Gm^R Cb^R$ single crossovers (5%) and one hundred and ninety were $Gm^R Cb^S$ double crossovers (95%). Three double crossovers were selected for further PCR analysis. The three clones were tested using a primers aaC1-F / R to test for the integration of the Gm-FRT-*sacB* cassette into the genome.
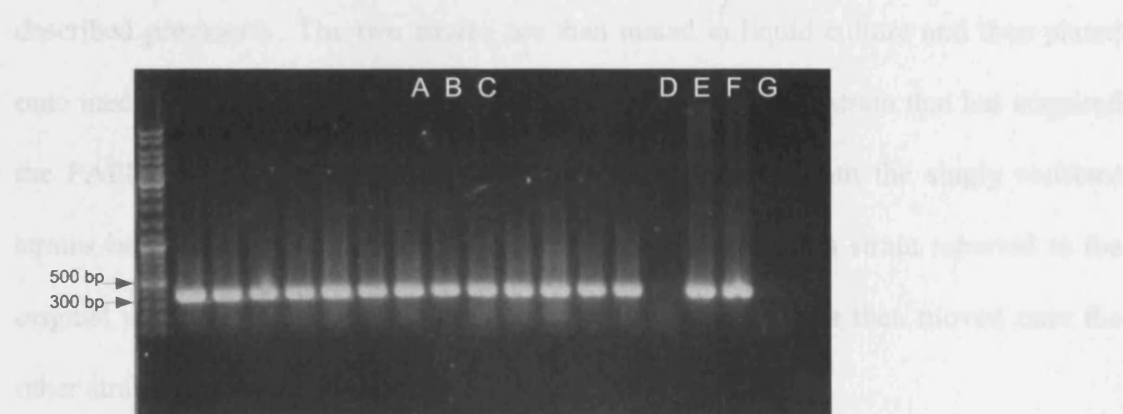
Figure 6.11 Agarose gel of PCRs confirming Isprob insertion using aaC1-F / R primers binding to the Gentamicin resistance casette.
(A, B , C) three putative test strains, (D) PA14 WT –ve control, (E , F) positive controls, and (G) –ve template control. Generuler marker.

As can be seen in Figure 6.11 the three strains tested positive for the presence of the Gm-FRT-*sacB*. The strain PA14 –Isprob was stored in 30% glycerol BHI at -20 and -80°C as strain KR848.

6.7.4 Strain to strain transfer of PAPI-1

6.7.4.1 *Overview*

To investigate the site specific recombination and stability of the PAPI-1 Island in different genome host backgrounds it was necessary to transfer PAPI-1 from its original host strain into four other genomic backgrounds (PAO1 (KR124), PAO1ΔLys10island (KR716), LES (KR129), C3719 (KR479). It had been previously reported that PAPI-1 can be transferred from one strain to another via conjugation at varying levels of

184

efficiency $(3.1 \times 10^{-7}$ to 5.4×10^{-4}) (Qiu et al., 2006). To transfer the island, the techniques used were based on those described by Qiu et al the basic overview of this technique is shown in Figure 6.12 (Qiu et al., 2006). In essence the technique was as follows; the recipient strain for the island to transfer into is tagged with an antibiotic cassette in a stable genomic location, in this case a tetracycline resistance cassette. The PAPI-1 island in the donor strain is tagged with a gentamicin resistance cassette as described previously. The two strains are then mated in liquid culture and then plated onto media containing both antibiotics to select for the recipient strain that has acquired the PAPI-1 island, and thus is resistant to both antibiotics, both the singly resistant strains being killed. To begin with the technique was used in a strain reported in the original report (PAO1) once the technique was optimised it was then moved onto the other strains (Qiu et al., 2006).

PAO1 with genome
tagged with Tetracycline
cassette inserted in Tn7
transposon

PA14 with PAPI-1 island tagged
with Gm-FRT-*sacB* cassette

Conjugation

PAPI-1 transferred via
conjugation

Type IV Pilus

Select on Tetracycline and Gentamicin
containing media

PAO1 + PAPI-1

PAO1 with genome tagged with Tet cassette and with
PAPI-1 island tagged with Gm-FRT-*sacB* cassette
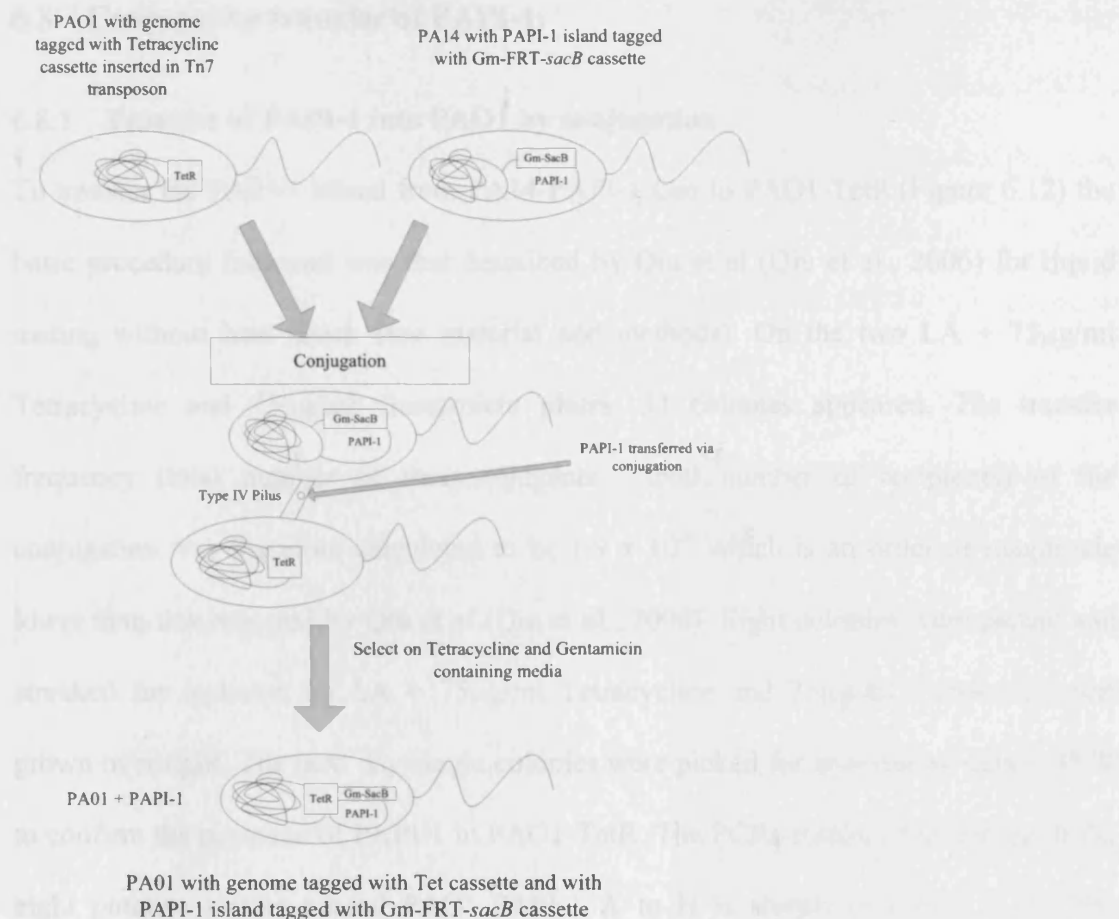
Figure 6.12: Showing overview of PAPI-1 transfer method example strain PAO1

6.7.5   Construction of Tetracycline resistant Tn7 vector (pUC18T-mini-Tn7T-Tet-F)

The construction of the tetracycline resistant suicide vector pUC18T-mini-Tn7T-Tet-F
is described in Appendix H.

6.7.6   Transposition of Tn7-Tet^R into PAO1, PAO1ΔLys10, LESB58 and C3719

The insertion of the Tn7-Tet^R transposon into PAO1, PAO1ΔLys10, LESB58 and
C3719 is described in Appendix I.

186

6.8 Conjugative transfer of PAPI-1.

6.8.1 Transfer of PAPI-1 into PAO1 by conjugation

To transfer the PAPI-1 island from PA14-PAPI-1-Gm to PAO1-TetR (Figure 6.12) the basic procedure followed was that described by Qiu et al (Qiu et al., 2006) for liquid mating without heat shock (see material and methods). On the two LA + 75μg/ml Tetracycline and 75μg/ml Gentamicin plates, 33 colonies appeared. The transfer frequency (total number of transconjugants / total number of recipients) of the conjugation was therefore calculated to be 1.9 x 10^{-6} which is an order of magnitude lower than that reported by Qiu et al (Qiu et al., 2006). Eight colonies were picked and streaked for isolation on LA + 75μg/ml Tetracycline and 75μg/ml Gentamicin and grown overnight. The next day single colonies were picked for analysis by colony PCR to confirm the presence of PAPI-1 in PAO1-TetR. The PCRs results of screening of the eight putative strains named PAO1-PAPI-1 A to H is shown in Figure 6.13. Five different sets of PCRs were carried out to confirm the correct genotype of the PAO1: PAPI-1 strain.

The first set of PCRs (Figure 6.13 A) were using the tRIP primers for tmRNA, which should test positive for PAO1 derivatives (recipient) and negative for PA14 derivatives (donor) as can be seen the highlighted strain (PAO1-PAPI-1-D) was positive confirming it as a PAO1 derivative. The second set (Figure 6.13 B) was for the presence of the tetracycline cassette inserted in strain PAO1-TetR again the highlight strain (PAO1-PAPI-1-D) tested positive confirming it as PAO1-TetR. The next two sets were to confirm the presence of the PAPI-1 island, the first (Figure 6.13 C) set of primers is the aaC1-F /R primers which amplify the Gentamicin cassette inserted in PAPI-1, and the second set (Figure 6.13 D) amplify a PAPI-1 unique region. As can be seen the highlighted strain (PAO1-PAPI-D) tested positive for both, indicating the presence of

187

PAPI-1. The final PCRs (Figure 6.13 D) is for the presence of the *exoU* gene which is only present in the PA14 but not the PAO1 genome; the highlighted strain (PAO1-PAPI-1 D) was negative, confirming the strain was not PA14. In conclusion the PCR results showed that the highlighted strain; PAO1-PAPI-1 D is a PAO1-TetR strain carrying the PAPI-1 island. This strain was then named PAO1-PAPI-1 and stored in 30% glycerol BHI at -20 and -80°C as strain KR 948.
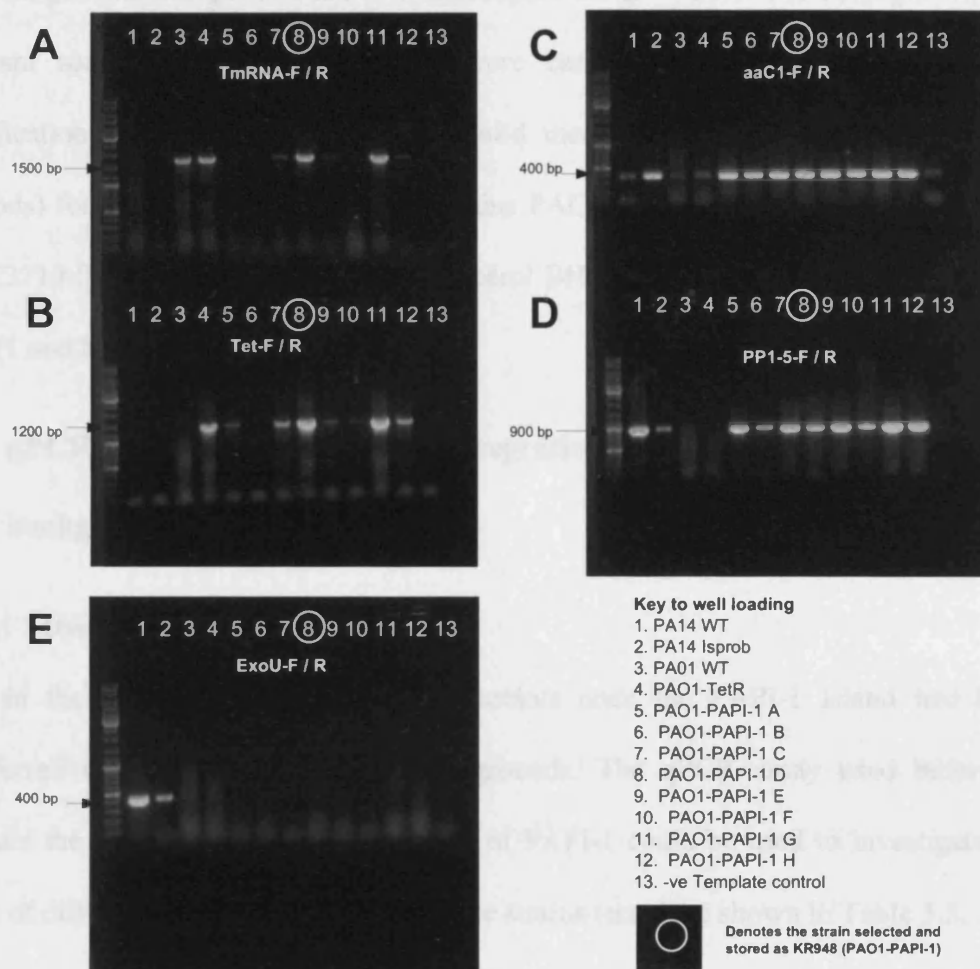
Figure 6.13: Results of genotype screening of PAO1:PAPI-1.
(A) PCR results of tRIP PCR of tmRNA (B) PCR result testing for presence of Tetracycline cassette. (C) PCR results for presence of Gentamicin resistance cassette. (D) PCR results for presence of PAPI-1 (E) PCR results for presences of exoU gene.

6.8.2 Conjugation to create PAO1ΔLys10 -PAPI-1, LESB58-PAPI-1 and C3719:PAPI-1.

To be able to investigate the effect of the deletion of a second independent genomic island at the $tRNA^{Lys10}$ locus in a different genomic background on the integration of PAPI-1, the transfer of the PAPI-1 island was carried out in the PAO1ΔLys10 strain (KR716). Also conjugated was the sequenced strain LESB58 which as well as being a different genome background has two unoccupied $tRNA^{Lys}$ sites. The conjugations and subscant screening of transconjugants were carried out as for PAO1 with the modification of using plate mating on solid media (as described in material and methods) for LESB58 and C3719. The strains PAO1ΔLys10:PAPI-1, LESB58:PAPI-1 and C3719:PAPI-1 were stored in 30% glycerol BHI at -20 and -80°C as strain KR950, KR971 and KR1032 respectably.

6.9 qPCR analysis of PAPI-1 integration in different host genome backgrounds

6.9.1.1 *Overview*

Like in the previously PA14 isogenic mutants once the PAPI-1 island had been transferred into four different host backgrounds. The qPCR assay used before to measure the integration and copy numbers of PAPI-1 could be used to investigate the effect of different genomic backgrounds. The strains tested are shown in Table 3.3.

Table 6.3: Occupancy of tRNA sites in various genome backgrounds.

Strain	$tRNA^{Lys10}$	$tRNA^{Lys47}$
PAO1	Occupied by Island	Empty
PAO1ΔLys10	Empty (island deleted)	Empty
LESB58	Empty	Empty
C3719	Empty	Occupied by C3719-PAI (according to genome seq.)

6.10 Results of qPCR.

6.10.1 PAPI-1 integration in PAO1 (PAO1-PAPI-1)

The qPCR results for PAO1 are shown in Figure 6.14. PAO1 like PA14 has an island occupying the $tRNA^{Lys10}$, this strain was interesting in terms of what the effect of another island integrated in the $tRNA^{Lys10}$ site would have on PAPI-1 integration in a distinct genomic background. Fascinatingly just like PA14 in PAO1, PAPI-1 is found integrated in $tRNALys47$ with a copy number of 1.01 x 10^6 compared to 4.31 x 10^0 for PAPI-1 integrated into $tRNA^{Lys10}$. This suggests that like in PA14 that the PAO1 $tRNA^{Lys10}$ island prevents PAPI-1 integrating into $tRNA^{Lys10}$ in PAO1. The total copy number of PAPI-1 in PAO1 is 8.65 x 10^5 copies compared to 7.7 x 10^5 for PA14, suggesting the total copy number is similar to PA14. The copy number for the circular form is 2.11 x 10^3 which nearly one log is lower than 1.49 x 10^4 in PA14. The copy number of the empty site of $tRNA^{Lys10}$ was not measured in either of the PAO1 backgrounds due problems with non specific products.

6.10.2 Effect of the deletion of PAO1 tRNA^{Lys10} island. (PAO1ΔLys10-PAPI-1)

The qPCR results for PAO1ΔLys10 are shown in Figure 6.14. The results for PAO1ΔLys10 were similar to those of PA14ΔPAPI-2.2. PAPI-1 was found integrated into $tRNA^{Lys10}$ in 1.56 x 10^5 copies and 1.20 x 10^6 in $tRNA^{Lys47}$. Demonstrating, that like in the second PA14 background mutant (PA14ΔPAPI-2.2) the deletion of a $tRNA^{Lys10}$ island causes PAPI-1 to start integrating into $tRNA^{Lys10}$ as well as in $tRNA^{Lys47}$. This seems to confirm that the presence of one genomic island at a locus prevents another integrating there. The ~ one log discrepancy between the copy number of PAPI-1 integrating in $tRNA^{Lys10}$ and $tRNA^{Lys47}$ is interesting, this seems to suggest that PAPI-1 still seems to prefer integrating into $tRNA^{Lys47}$. However the increased total copy number of 8.65 x 10^5 in PAO1 to 2.24 x 10^6 in PAO1ΔLys10 would seem to suggest

again like in PA14ΔPAPI-2.2 that the copy number of PAPI-1 has increased from one to two copy of PAPI-1 in the majority of cells. Suggesting that both sites are equally occupied by PAPI-1, further repeat assays are required to confirm this is the case. The circular copy number for PAPI-1 is 5.56 x 10^3 in PAO1ΔLys10 compared to 2.11 x 10^3 in PAO1, suggesting the deletion of the $tRNA^{Lys10}$ Island did not affect the copy number of PAPI-1.

6.10.3 PAPI-1 integration in LESB58

The qPCR results for LESB58 are shown in Figure 6.14. Strain LESB58 was of particular interest because it has both $tRNA^{Lys}$ sites unoccupied. Therefore this strain was an opportunity to see if PAPI-1 has a preference for either $tRNA^{Lys}$ site in the absence of genomic island at the $tRNA^{Lys10}$ site. The qPCR results are shown in Figure 6.14. The results of the qPCR showed that PAPI-1 seems to integrate into both sites with $tRNA^{Lys47}$ having 1.22 x 10^6 copies of PAPI-1 integrated and $tRNA^{Lys10}$ having 6.47 x 10^5 copies. Suggesting again like PAO1ΔLys10 that slightly $tRNA^{Lys47}$ is the favoured site for integration by PAPI-1. However, again the total copy number reflects equal integration, with the total PAPI-1 copy being 1.86 x 10^6 suggesting ~ two copies per cell. This is further reinforced by a copy number of 5.3 x 10^3 for the empty $tRNA^{Lys10}$ which reflects that this site is always occupied by PAPI-1. These results suggest that in LESB58, PAPI-1 occupies both sites equally, and that the copy number measurements for PAPI-1 integrated in $tRNA^{Lys10}$ maybe consistently underestimating copy number. The copy number for the circular PAPI-1 is 2. 4 x 10^4 this is similar to that seen PA14 background strains.

	Total PAPI-1*	Circular PAPI-1	PAPI-1 Lys47	PAPI-1 in Lys10	Empty Lys10	Total PAPI-1 in C3719
■ PA14	7.79E+05	1.49E+04	5.17E+05	6.18E+01	1.07E+06	
■ LES-PAPI-1	1.86E+06	2.40E+04	1.22E+06	6.47E+05	5.30E+03	
■ C3719-PAPI-1	1.45E+06	3.78E+02	2.54E+02	3.84E+05	3.73E+03	7.83E+05
■ PAO1-PAPI-1	8.65E+05	2.11E+03	1.01E+06	4.31E+00		
■ PAO1dLys10-PAPI-1	2.24E+06	5.56E+03	1.20E+06	1.56E+05		
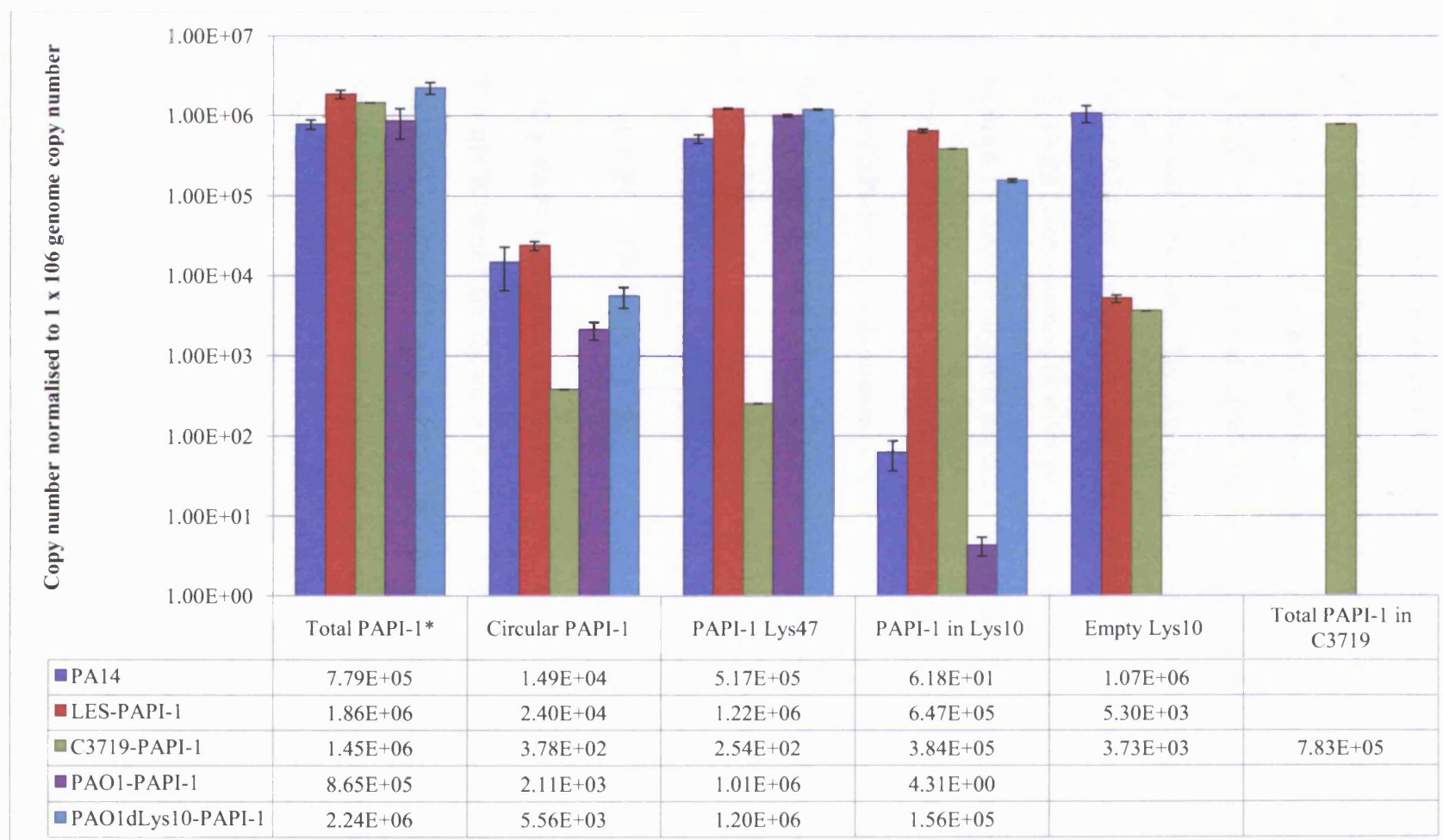
Figure 6.14: Graph showing the relative copy number of PAPI-1.
Normalised to 1 x 10^6 genomes integrated in sites $tRNA^{Lys10}$, $tRNA^{Lys47}$,Total and Circular copy numbers of PAPI-1 in strain PA14 WT, LES, C3719, PAO1, PAO1ΔLys10. *Total PAPI-1 measures both PAPI-1 and the C3719-PAI, so an additional column shows the Total PAPI-1/ C3719-PAI – C3719-PAI which gives the Total PAPI-1 in C3719.

192

6.10.4 PAPI-1 in C3719: One strain, two islands

As was mentioned previously C3719 already carries an 87 kb pKLC102-family island

called C3719-PAI. The whole genome sequence of this island shows it to be integrated

into $tRNA^{Lys47}$, C3719-PAI has been shown to excise from the genome and form a

circular form (Mathee et al., 2008). However if C3719-PAI integrates into the $tRNA^{Lys10}$

site as well is unknown. The data for the copy numbers of C3719-PAPI-1 are shown in

Figure 6.14 for comparison with other strains. The data regarding the PAPI-1 and

C3719-PAI copy numbers in wildtype C3719 and C3719-PAPI-1 are shown together in

Figure 6.15. Additionally, it is important to note that due to the high level of homology

between PAPI-1 and C3719-PAI the primers used for Total PAPI-1 copy number

(TotalPAPI-1-F /R) will measure both the copy number of PAPI-1 and C3719-PAI. So a

new set were designed (TotalC3719PAI-F / R) that only measure the total copy number

of C3719-PAI. To calculate the 'Total PAPI-1 in C3719-PAPI-1' the copy number of

Total C3719-PAI (TotalC3719PAI-F / R) was subtracted from the copy number from

Total PAPI-1 (TotalPAPI-1-F /R).

6.10.5 PAPI-1 integration in C3719

The qPCR results are shown in Figure 6.14. The results show that PAPI-1 is found

integrated in $tRNA^{Lys10}$ with 3.85 x 10^5 copies compared to 3.73 x 10^3 in $tRNA^{Lys47}$.

Suggesting PAPI-1 preferentially integrates into $tRNA^{Lys10}$ in this genome or is unable to

access $tRNA^{Lys47}$. The total copy number of PAPI-1 (calculated by Total PAPI-1 – Total

C3719-PAI) is 7.83 x 10^5 which is what would be expect for a single site integration

like in PA14 or PAO1. The circular copy number of PAPI-1 is 3.78 x 10^2 which is

almost two logs lower than in PA14 and LESB58, and almost one log lower than PAO1

suggesting something in C3719 is preventing the formation of the circular form of

PAPI-1 in the same numbers as other strains. The copy number of the empty $tRNA^{Lys10}$

site also reflects that PAPI-1 is found integrated in this site as the copy number is 3.73 x 10^3 suggesting this site is found occupied in the majority of cells within the population.

6.10.6 C3719-PAI integration in C3719 and C3719-PAPI-1

The integration and total copy number of C3719-PAI was measured in both the wildtype C3719 and in C3719-PAPI-1. The results are compared in Figure 6.15. This allows for the measurement of the effect of the acquisition of PAPI-1 in C3719 on C3719-PAI. In wild type C3719, C3719-PAI is found integrated in the $tRNA^{Lys47}$ site in 8.40×10^5 compared to 5.83×10^3 in $tRNA^{Lys10}$. This suggests even though the C3719 $tRNA^{Lys10}$ is not occupied by another island, that the C3719-PAI preferentially integrates into the $tRNA^{Lys47}$. The total copy number of the C3719-PAI is 6.68×10^5 which reflects a single integration in $tRNA^{Lys47}$. The copy number of C3719-PAI was unaltered by the acquisition of PAPI-1 in C3719-PAPI-1 with a total copy number of 7.61×10^5 suggesting the acquisition of PAPI-1 did not affect the copy number of C3719-PAI. Nor did the integration of PAPI-1 seem to have any effect on the site specific integration of C3719-PAI. In strain C3719-PAPI-1 it is found integrated in similar copy numbers as C3719 in both $tRNA^{Lys47}$ 9.68×10^5 and 7.46×10^3 in $tRNA^{Lys10}$. This reflects the finding that PAPI-1 was found predominantly integrated in the $tRNA^{Lys10}$ site in C3719-PAPI-1. This suggests that the C3719-PAI has some level of site specificity to $tRNA^{Lys47}$ that was not affected by the acquisition of PAPI-1. Furthermore despite both PAPI-1 and C3719-PAI being found integrated in both $tRNA^{Lys10}$ and $tRNA^{Lys47}$, in the population of C3719-PAPI-1 for some reason the predominate integration of C3719-PAI in $tRNA^{Lys47}$ and PAPI-1 in $tRNA^{Lys10}$ remain stable. The copy number of circular PAPI-1 forms in C3719 was 3.78×10^2 which is two logs lower than seen in its wildtype strain PA14.

	Total PAPI-1*	Circular PAPI-1	PAPI-1 Lys47	PAPI-1 in Lys10	Empty Lys10	Total C3719-PAI	C3719-PAI in Lys10	C3719-PAI in Lys47	Total PAPI-1 in C3719
■C3719 - PAPI-1	1.45E+06	3.78E+02	2.54E+02	3.84E+05	3.73E+03	6.68E+05	5.85E+03	8.40E+05	7.83E+05
■C3719 WT						7.61E+05	7.46E+03	9.68E+05	
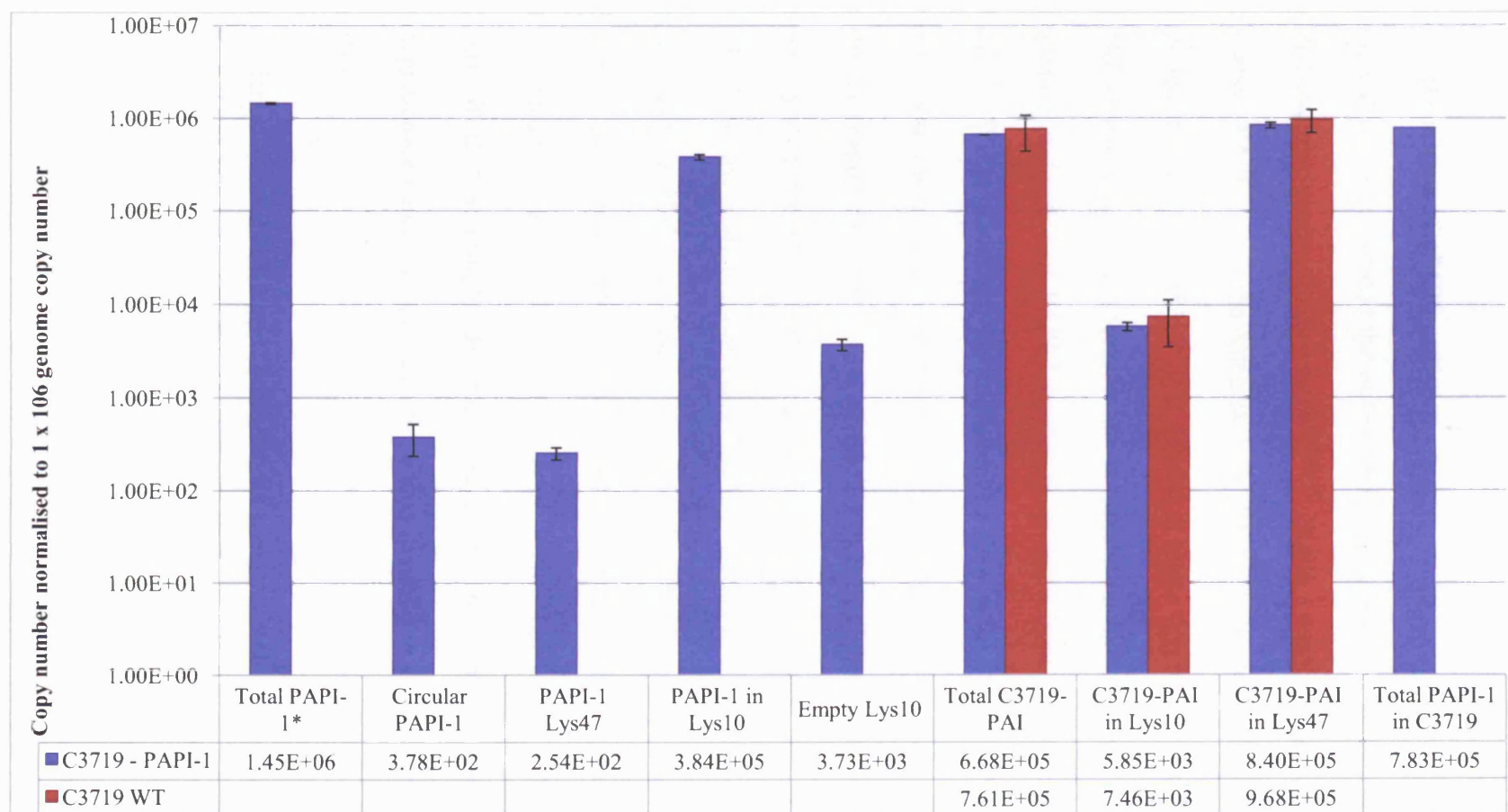
Figure 6.15: Graph showing the relative copy number of PAPI-1 and C3719-PAI-1.
Normalised to 1 x 10^6 genomes integrated in sites tRNA^{Lys47} and $tRNA^{Lys47}$, Total and Circular copy (not for C3719 PAI) numbers of PAPI-1 and C3719-PAI in strain C3719, and C3719 –PAPI-1. *Total PAPI-1 measures both PAPI-1 and C3719-PAI, so the additional column shows the Total PAPI-1 in C3719 calculated from Total PAPI-1 -Total C3719-PAI.

6.11 Discussion

6.11.1 Discussion of qPCR

The qPCR assays confirmed the earlier finding that in PA14 the majority of copies of PAPI-1 integrate preferentially into $tRNA^{Lys47}$. But in a small number of cells within the population PAPI-1 is found integrated in $tRNA^{Lys10}$. Interestingly when the PAPI-2 island located next to the $tRNA^{Lys10}$ is deleted, it seems that two different configurations in PAPI-1 integration can occur. In one configuration like seen in PA14ΔPAPI-2, the integration preference of PAPI-1 is seemly reversed from preference for $tRNA^{Lys47}$ to $tRNA^{Lys10}$. While in another like configuration seen in PA14ΔPAPI-2.2 the integration preference seems to be abolished with PAPI-1 integrating into both sites equally, and seemly increasing the copy number of PAPI-1 to two. Therefore in total there are three seemingly dynamic integration configurations of PAPI-1 that can exist. However, which of the two configurations caused by the deletion of PAPI-2 is the most likely to occur is not yet clear and further what underlies the difference between the two. A number of previous reports of genomic islands integrating into multiple tRNA sites exist (Sentchilo et al., 2009, Buchrieser *et al.*, 1998, Hare *et al.*, 1999, Doublet *et al.*, 2008a). If this seemingly dynamic integration into one site and excision and reintegration into another exists in other genomic island in a similar manner remains to be seen.

The deletion of the PAPI-2 *xerC* gene did not seem to cause any major change in PAPI-1 integration thus ruling out the hypothesis that the *xerC* was involved in some kind of competition or cross talk with the PAPI-1 encoded integrase. There did seem to be a slight increase in the occupancy of PAPI-1 in $tRNA^{Lys10}$ compared to PA14, but this increase was modest compared to that seen when the whole island was deleted.

Again the deletion of the $tRNA^{Pro21}$ island didn't make any major difference to the integration of PAPI-1, except for seemly marginally reducing the integration of PAPI-1 into $tRNA^{Lys10}$. One major difference observed was the near two log decrease in the circular copy number of PAPI-1. How the deletion of the $tRNA^{Pro21}$ island caused a change in the circular form of PAPI-1 is an interesting question. The $tRNA^{Pro21}$ island does not seem to share any genes with PAPI-1. It does encode a large ATP-dependent Helicase (PA14_28810) which could have some cross talk effect on the formation of the circular form of PAPI-1, but this seems highly unlikely. How the deletion of the $tRNA^{Pro21}$ island effects the formation of circular copies of PAPI-1 remains to be seen.

The deletion of PAPI-2 did have one common feature in both independently derived PAPI-2-minus mutants, $tRNA^{Lys10}$ was now occupied at moderate to high levels in both strains where as in PA14, PAPI-1 rarely was found integrated at this site. This suggested that the presence of the $tRNA^{Lys10}$-locked in PAPI-2 in PA14 somehow prevented or markedly inhibited the integration of PAPI-1 into this same site. The presence of PAGI-4 in a Clone C strain prevented pKLC102 integrating into $tRNA^{Lys10}$ (Klockgether et al., 2004). Therefore as in the case of PAPI-2 here it seems that somehow the integration of one island at one site blocks another integrating. As the deletion of xerC didn't seem to make a drastic effect like the deletion of the whole island, it can be assumed that it the 'island hopping' effect is cause by the whole deletion of the island and not the loss of the xerC gene. How the deletion of the whole island caused this change remained to be determined.

The result from LESB58 seems to show that both $tRNA^{Lys}$ sites can be occupied by PAPI-1 equally in the absence of another genomic island being integrated. Indicating that PAPI-1 probably does not have attB sequence based preference for either site. However this may not be true for all pKLC102 family islands, as the result from C3719

197

for C3719-PAI seemingly compounds this, as the C3719-PAI island has a preference for the $tRNA^{Lys47}$ while being able to integrate into $tRNA^{Lys10}$ site in a strain without another genomic island. The fact that PAPI-1 could integrate into $tRNA^{Lys10}$ suggests that there is nothing to prevent integration there. A further experiment should be carried out in a strain lacking C3719-PAI to see in the absence of competition where PAPI-1 will integrate. This will shed light on if C3719-PAI has a site specific preference and can somehow prevent PAPI-1 integrating in $tRNA^{Lys10}$, or if this site is somehow preferential for integration of C3719-PAI. This was the first work to show that two pKLC102 like islands can exist without seemly effecting each other's copy number or integration dynamics. If this remains true under more 'selective' or stressful conditions remains to be seen.

A fascinating finding from the transfer of PAPI-1 into other strain backgrounds was the difference between PAO1 and PAO1ΔLys10. The result for PAO1 shows that like in PA14 the presence of a genomic island integrated into $tRNA^{Lys10}$ seems to prevent PAPI-1 integrating into $tRNA^{Lys10}$. As when the PAO1 $tRNA^{Lys10}$ genomic island was deleted PAPI-1 started to integrate equally into this site. This finding mirrors that of PA14ΔPAPI-2.2 suggesting that this is most likely confirmation of island integration in the absence of a $tRNA^{Lys10}$ integrated island. It then follows that the movement of integration of the majority of copies of PAPI-1 from $tRNA^{Lys47}$ to $tRNA^{Lys10}$ to PA14ΔPAPI-2 is a unique event. The reason why the $tRNA^{Lys47}$ site occupation was reduced in PA14ΔPAPI-2 remains unknown, further investigations to elucidate this are described in Section 8 and 9.

The reason that PAPI-2 and the PAO1 $tRNA^{Lys10}$ genomic island prevent the integration of PAPI-1 into $tRNA^{Lys10}$ is not clear. A comparison of PAPI-2 and the PAO1 $tRNA^{Lys10}$ islands is shown in Figure 6.16 and shows that PAPI-2 and PAO1 $tRNA^{Lys10}$ genomic

island share a number of homologous genes. A particularly large region of homology is PA0978 to PA0981 at the beginning of the island. Whether loss of these gene products affects PAPI-1 integration, remains to be seen. However, what is even more striking when viewing this diagram is the region of low G/C content between genes PA0978 to PA0981 in PAO1 and their homologs in PAPI-2. The two genomic islands have an average G/C content of 53 % across all four genes compared to the 66% PAO1 average. This is shown clearly as a marked drop in the G/C content in Figure 6.16 as highlighted by the double-ended yellow arrow.

Histone-like nucleoid-structuring (H-NS) proteins are known to have a preference for binding regions that are highly AT-rich compared to the rest of genome (Castang *et al.*, 2008). Further, DNA curvature has been demonstrated in a number of studies to increase H-NS binding (Navarre *et al.*, 2007).Comparative models of the local DNA structure for *tRNA*^{Lys10} and *tRNA*^{Lys47} were constructed for PA14 (Figure 6.17). The structural map clearly shows that PAPI-2 is a region of A/T rich DNA with a high intrinsic DNA curvature compared to the region around *tRNA*^{Lys47} and therefore is likely to be a preferential H-NS binding site. The effect of the deletion of PAPI-2 at this site can be seen in Figure 6.18. The deletion of PAPI-2 removes the large region of A/T rich

Figure 6.16: Artemis comparison tool comparison (ACT) of PAPI-2 and PAO1 tRNA^{Lys10} genomic island.
Red regions highlight homologous sequence. Yellow arrows highlights homologous low G/C content region present in both islands

DNA with a high intrinsic DNA curvature from the proximity of $tRNA^{Lys10}$ and therefore would theoretically abolish the H-NS binding. Experimental evidence in PAO1 shows that all the genes on the PAO1 $tRNA^{Lys10}$ genomic island and six genes upstream (PA0978 to PA0994) are bound by MvaT and MvaU the *P. aeruginosa* H-NS-like proteins (Castang et al., 2008). Two of the genes PA0984 and PA0985 were also demonstrated to be up-regulated in an *mvaT* mutant (Castang et al., 2008). This seems to confirm that the whole region is bound by MvaT and MvaU. Conversely, none of the region around the $tRNA^{Lys47}$ in PAO1 (conserved in PA14) is part of the MvaT and MvaU regulon. This finding would suggest that in PAO1 the region around the $tRNA^{Lys10}$ is bound by MvaT and MvaU, H-NS family proteins. This binding could by modulation of DNA topology (DNA bridging, compacting, looping and constraint of supercoils) prevent the integration of PAPI-1 into the $tRNA^{Lys10}$ *attB* site (Lucchini *et al.*, 2006). If this region of low G/C content is the cause of the H-NS binding in PAO1, then the presence of the same region and the overall high intrinsic curvature of PAPI-2 in PA14 would suggest the same is occurring there. If H-NS binding is causing the 'island hopping' then this fascinating finding demonstrating that the integration of one horizontally acquired region of DNA can prevent the integration of another, adding a new level of complexity to horizontal gene transfer. The construction of *mvaT* mutants is underway to investigate this is the case.

Local structure comparison of PA14 WT *tRNA*^Lys10^ and *tRNA*^Lys47^

tRNA^Lys10^ Local Region

tRNA^Lys47^ Local Region

High Intrinsic DNA curvature (associated with H-NS binding, domain boundaries, and supercoiling)

A/T rich region (associated with increased H-NS binding)

High propeller twist (rigid DNA)
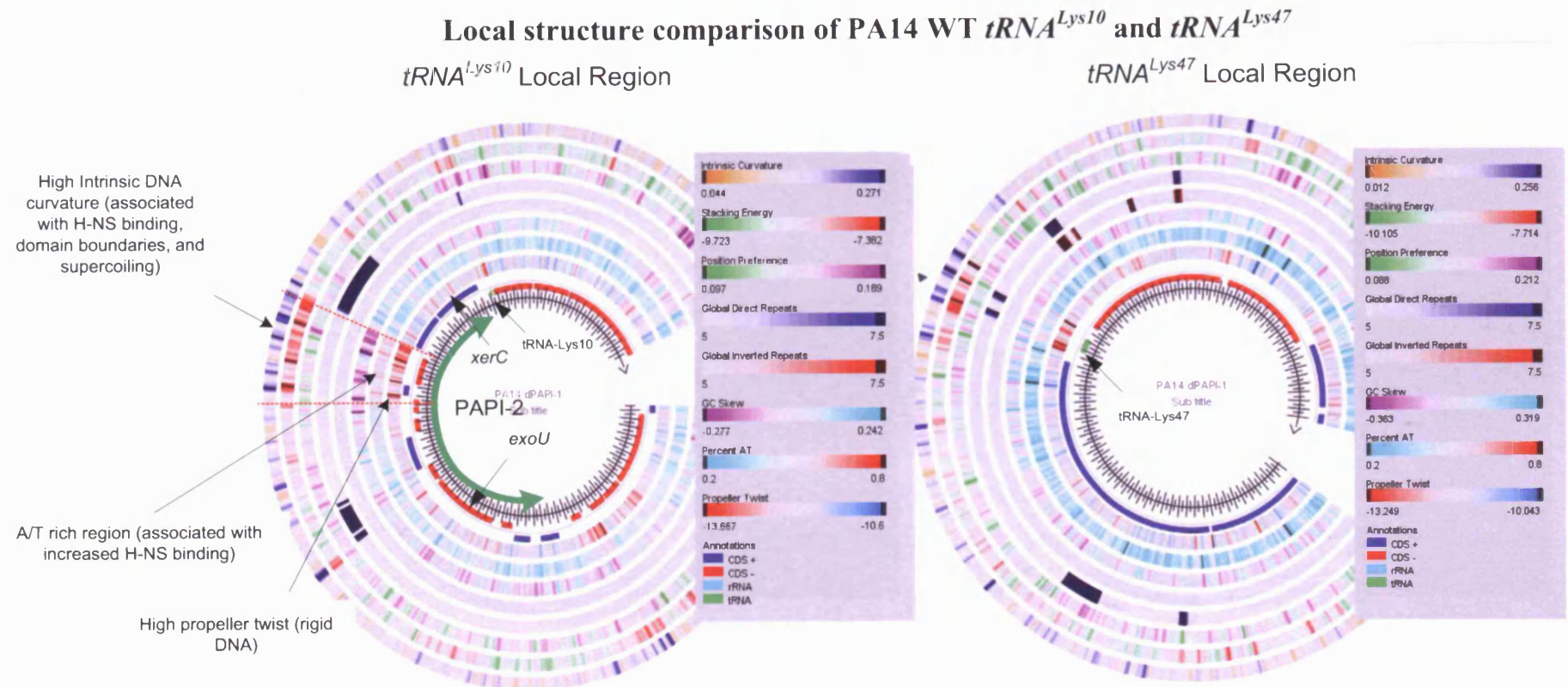
Figure 6.17: Comparisons of the local DNA structure of *tRNA*^Lys10^ and *tRNA*^Lys47^ in strain PA14.
Images generated using GeneWiz browser 0.91 server to create a custom genome structural atlas (**http://www.cbs.dtu.dk/services/gwBrowser/**) (Pedersen *et al.*, 2000)
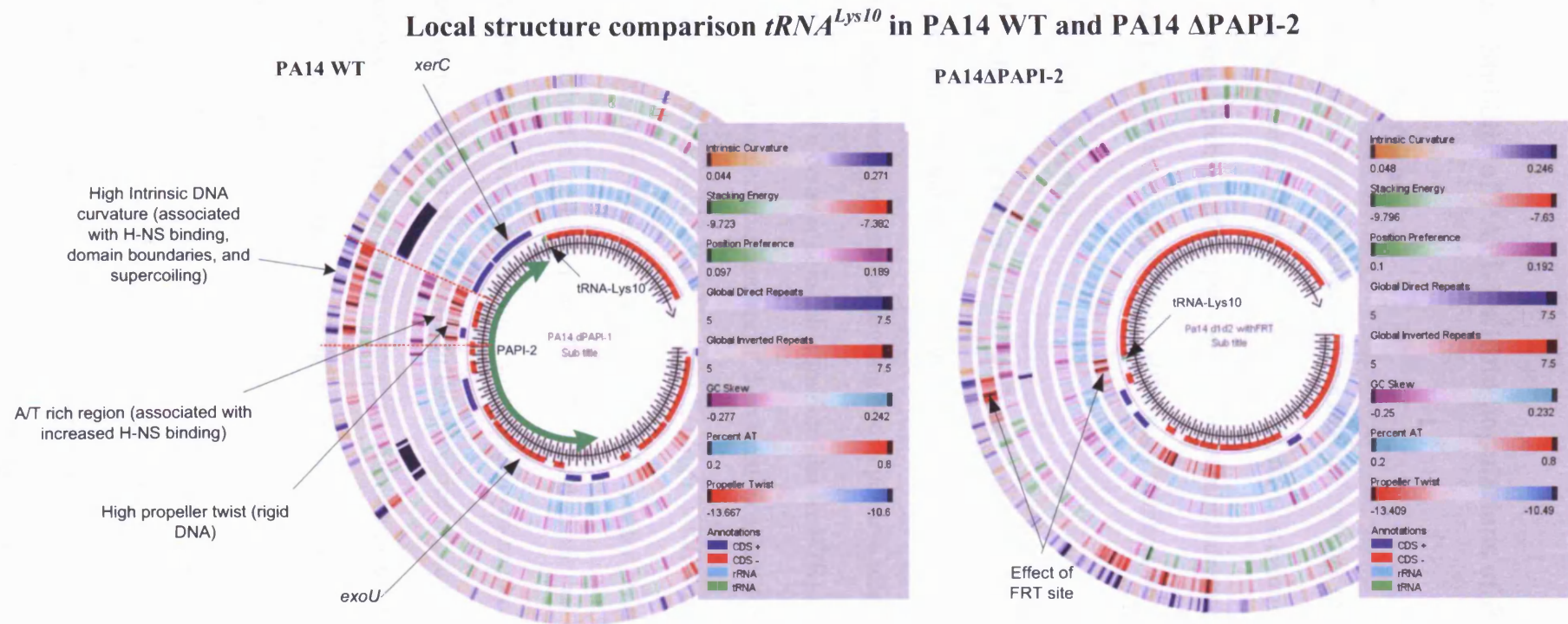
Figure 6.18: Comparisons of the local DNA structure of *tRNA^Lys10* in strain PA14 and PA14ΔPAPI-2.
Images generated using GeneWiz browser 0.91 server to create a custom genome structural atlas (**http://www.cbs.dtu.dk/services/gwBrowser/**) (Pedersen *et al.*, 2000)

7 Stability of PAPI-1 within populations of *P. aeruginosa*

7.1.1 Overview

This chapter describes investigations into the stability of PAPI-1 in a range of different host backgrounds. The stability of the island was determined using a technique known as 'island probing'. Comparisons of the stability are made with the previously data on integration site specificity and PAPI-1 copy numbers in different genomic backgrounds.

7.2 Introduction

A technique known as 'island probing' was developed (Rajakumar *et al.*, 1997) to determine the stability of genomic islands within a particular bacterial strain. This technique works by first introducing both a positive selectable gene such as an antibiotic cassette and a counter-selectable marker like *tetAR*(B) or *sacB* into the genomic island. The counter-selectable marker is then used to select for derivative bacterial cells that have lost the tagged island by using the appropriate counter-selection medium. Having both the selectable and counters selectable marker on the island makes it possible to detect bacterial cells carrying the island and those that have lost it. In this work the PAPI-1 island was tagged with a dual gentamicin-*sacB* cassette encoding a levansucrase which is lethal for the bacteria in the presence of sucrose. The strain was then serially diluted onto separate plates containing either antibiotic or sucrose. The colonies that grow on the sucrose containing media should have lost the genomic island. The numbers of colonies appearing on sucrose-containing medium is then compared with number of colonies that grew on the antibiotic-supplemented medium (in this case gentamicin) to determine the numbers of cells without and with the island, respectively. The 'deletion rate' can then be approximated by the ratio of the number of cells that have lost the island (Scr^s) to the number of cells that have retained the island (antibiotic

resistant) as the proportion of island-free cells is extremely low. This proportion-based deletion rate estimate can be used as a measure of the stability of the island, as islands that are less stable will be absent from a higher of the bacterial population than islands that are stably integrated. The technique has been extensively used to study the stability of *E. coli* and *Shigella flexneri* and *Yersinia pseudotuberculosis* pathogenicity islands (Hochhut *et al.*, 2006, Middendorf *et al.*, 2004, Rajakumar et al., 1997, Biliana *et al.*, 2004). This is the first time this technique has been used to study any of the islands in *P. aeruginosa*. In previous work the deletion rate of the PAPI-1 island was estimated using semi-quantitative PCR in which the spontaneous excision rate was estimated at 3 x 10^{-3} of PAPI-1 from the *tRNA^{Lys47}* site (Klockgether *et al.*, 2007b). However this study was published before the discovery that PAPI-1 can integrate into both *tRNA^{Lys}* sites (Qiu et al., 2006), as the study only measured the number of empty *tRNA^{Lys47}* sites, rather than an estimation of the total number of PAPI-1 free chromosomes (both *tRNA^{Lys10}* and *tRNA^{Lys47}*). In this work the use of the island probing approach aimed to investigate the relative stability of PAPI-1 by measuring the deletion rate of PAPI-1 from a population following sucrose counter-selection. This technique was used to investigate the difference in stability of PAPI-1; in various host strain backgrounds, and in isogenic mutants of these strains.

The strain PA14-Isprob was used in the conjugation experiments (Chapter 5) to transfer the PAPI-1 island from PA14 into PAO1, PAO1ΔLys10 island, LES, and C3719. In these strains the PAPI-1 island had a dual gentamicin-*sacB* cassette inserted in a intergenic region. This then allows for an examination at any one time point the number of cells that have lost the island.

In this study the results of the island probing can then be analysed and compared with the data from the qPCR assays. This will allow for the study of the stability of the

PAPI-1 island in a range of different host strain backgrounds, and relating this back to the qPCR data regarding the occupancy of $tRNA^{Lys}$ genes and PAPI-1 copy number.

The strains tested were the strains PA14-Isprob, PAO1-PAPI-1, LES-PAPI-1 and C3719-PAPI-1, which are essentially wild-type strains carrying a tagged PAPI-1 island. Additionally two mutant strains PAO1ΔLys10:PAPI-1 which has the $tRNA^{Lys10}$ island deleted from the genome, and PA14Δsoj with the PAPI-1 encoded soj insertionally inactivated. As was demonstrated by qPCR; PAPI-1 is integrated in either one $tRNA^{Lys}$ site (PA14:Isprob, PAO1:PAPI-1, and C3719:PAPI-1) or two sites (LES:PAPI-1, and PAO1Δlys10:PAPI-1). This is the first time the stability of a single genomic island has been measured in different host backgrounds and the effect of the number of integration sites (and therefore chromosomal copy number) has been investigated. Also Qiu and co-workers reported that the deletion of the soj destabilised the PAPI-1, resulting in loss of PAPI-1 from the population of PA14 over time (Qiu et al., 2006). Using the island probing method it should be possible to quantify the effect of deletion of soj on the stability of PAPI-1.

7.3 Island probing experiments

The island probing experiments were carried out by growing the various test strains overnight at 37°C and 200 rpm shaking for 17 hours in 5 ml LB broths without antibiotics. Then inoculating then into fresh 5 ml LB broths and growing for 8 hours at 37°C at 200 rpm with CFU/ml taken on LA, LA+ Gentamicin / Carbenicillin, and LA + 5% (w/v) sucrose at time zero (T0) and after eight hours growth (T8). The three media allow for quantification of the total number of bacteria (LA), the total number carrying the PAPI-1 (LA + Gentamicin / Carbenicillin (the island is tagged with the resistance cassette), and the total number lacking the PAPI-1 island (LA+ 5% (w/v) sucrose (the island is tagged with sacB). The natural loss of the island from the population was then

studied, by measuring the difference between the proportion of the population that has the island under antibiotic selection (assuming this is 100% of the population), to the number after 8 hours growth that had lost the island. The stability of the island is measured by calculating the so called 'deletion rate' which is calculated by dividing the CFU/ml of LA+ 5% (w/v) sucrose (the total number without an island) by the CFU/ml LA + Gentamicin / Carbenicillin (the total with PAPI-1). The deletion rate as described above, measures the proportion of the population that has lost the PAPI-1 island.

7.3.1 Effect of the deletion of *soj* on the deletion rate of PAPI-1

The results for the island probing are shown in Figure 7.1. The deletion rate for PAPI-1 in it s original host strain PA14:Isprob was found to be 4.98×10^{-4}. This is the highest spontaneous deletion rate of any genomic island described so far. As expected the PA14Δ*soj* has an increased deletion rate of 6.93×10^{-3} compared to the wild type, although as was noted in the construction of this strain a truncated form of Soj may still be expressed and have some residual functionality.

7.3.2 PAPI-1 copy number and deletion rate are correlated

Strain PA14-Isprob, PAO1-PAPI-1 and C3719-PAPI-1 all have one chromosomal insertion of PAPI-1 as determined by qPCR. As can be seen in Figure 7.1 all the strains with a single integration have similar deletion rates of 4.98×10^{-4}, 8.87×10^{-4}, and 6.34×10^{-4} for strains PA14:Isprob, PAO1:PAPI-1 and C3719:PAPI-1 respectively. The three rates are not statistically significant from ($p < 0.05$), suggesting these values do not represent real differences in deletion rate from each other. This is in contrast to strains LES:PAPI-1 and PAO1ΔLys10:PAPI-1 that have two integrations of PAPI-1 and have deletion rates about four logs lower of 7.78×10^{-8} and 1.1×10^{-7} respectively.
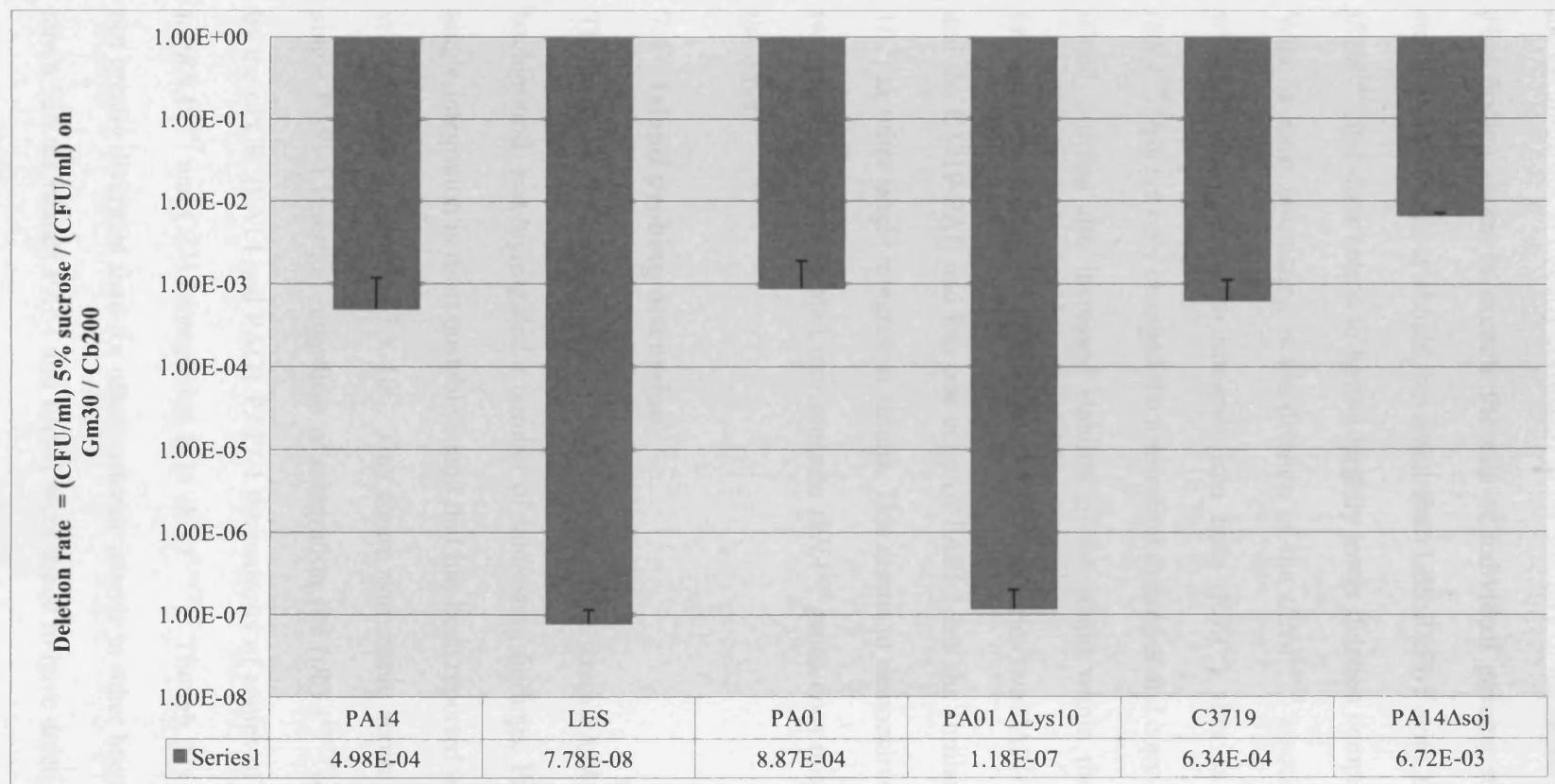
Figure 7.1: Deletion rate of PAPI-1 in various strain backgrounds after 8 hours growth in antibiotic free media.
Strains shown are: PA14 = PA14:Isprob, LES = LES:PAPI-1, PAO1 = PAO1:PAPI-1, PAO1ΔLys10 = PAO1ΔLys10:PAPI-1, C3719 = C3719:PAPI-1, PA14Δ*soj* = PA14Δ*soj*. Deletion rate == (CFU/ml) 5% sucrose / (CFU/ml) on Gm30 / Cb200.

This result shows that in two independent strains that number of PAPI-1 integrations in the chromosome is directly correlated to the stability of the island within the population. This finding seems to exclude the role of individual genome structures affecting the stability. Although it should be noted that LES:PAPI-1 with two 'wildtype' empty $tRNA^{Lys}$ sites does seems to have a slightly lower deletion compared to PAO1ΔLys10. What is most fascinating is the deletion of the $tRNA^{Lys10}$ associated island in PAO1, which caused PAPI-1 to integrate into both $tRNA^{Lys}$ sites as opposed to just the $tRNA^{Lys47}$ has not only changed the integration dynamics and copy number of the PAPI-1 island, but has also increased stability of the island within the population. Also of interest is the finding for C3719:PAPI-1 which carries two PAPI-1 like islands (PAPI-1 and the C3719-PAI) and has one copy of PAPI-1 has the similar deletion rate (6.34 x 10^{-4}) as other single integration strains. This seems to demonstrate that the presence of two islands both integrated into separate $tRNA^{Lys}$ genes does not affect the stability of the other.

7.4 Island probing discussion

The study of the stability of the PAPI-1 in its native strain PA14 and in different strain backgrounds has highlighted a number of interesting findings. Firstly, the PAPI-1 in a single integration is most unstable island that has been reported in any bacterial species with a deletion rate of ~5 x 10^{-4}. This figure was stable across all the strains with a single PAPI-1 insertion regardless of integration site ($tRNA^{Lys10}$ or $tRNA^{Lys47}$) identified by the qPCR. (PA14 and PAO1 PAPI-1 the majority of copies of PAPI-1 are integrated in $tRNA^{Lys47}$ and C3719 integration is in $tRNA^{Lys10}$). Though this higher deletion rate is not greatly divergent than for other genomic islands in other bacterial species. In *E.coli* strain 536 the islands PAI-I and PAI-II were found to have deletion rates of 1.36 x 10^{-5} and 3.0 x 10^{-5} respectively (Hochhut et al., 2006). While the high pathogenicity island

(HPI) of *Y. pseudotuberculosis* was found to have a similar deletion rate of 6 x 10^{-5} (Biliana et al., 2004). As was the Shigella resistance locus (SRL) and *she* pathogenicity islands in *S. flexneri* with deletion rates of 10^{-5} and 10^{-5} to 10^{-6} respectively (Rajakumar et al., 1997, Sakellaris *et al.*, 2004, Luck *et al.*, 2004). Suggesting that deletion rates between 10^{-4} to 10^{-6} are the normal range.

In strains with two copies of PAPI-1 the deletion rate is increased by a huge four logs. Suggesting having two integrated copies of PAPI-1 exponentially increases the stability of PAPI-1 within a population. This is particularly interesting in relation to the 'island hopping' in PAO1 and PAO1ΔLys10. The deletion of the PAO1 $tRNA^{Lys10}$ genomic island causing the increase in PAPI-1 copy number from one to two and this in turn dramatically increases the stability of PAPI-1. Demonstrating that the presence of one island in the genome can affect the stability of another in the population, this finding could have significant implications in the evolution of genomes. This is first report that the number of insertions (copy number) of a genomic islands directly correlates with the stability of an island within a population.

The ICE element SXT in *Vibrio cholerae* has a deletion rate reported to be at ~ 1 x10^{-7}. This low deletion rate was reported to be maintained by the presence of a toxin-antitoxin system that activates on excision of SXT from the genome (Wozniak and Waldor, 2009). Suggesting that factors encoded on genomic islands enable some genomic islands to minimise the high deletion rates in cells where they are unstable. The finding that stability of PAPI-1 is even greater than this in a strain with multiple copy insertions, may shed light on why a number of reported genomic islands target multiple copy tRNA as insertion sites so to increase their stability in a population (Sentchilo *et al.*, 2009, Buchrieser *et al.*, 1998).

The reduction in the stability of PAPI-1 island in the PA14Δsoj mutant of ~ 1 log

suggests this deletion did have an effect on the stability of PAPI-1. But the partial

deletion of *soj* did not seem to result in a large reduction in stability; further studies are

required to see if PAPI-1 is lost from the population over longer periods of time as

previously reported (Qiu et al., 2006).

8 Use of an artificial, newly introduced Third chromosomal *attB* site to investigate site specific integration of PAPI-1.

8.1 Chapter overview

The previous finding that deletion of PAPI-2 island caused PAPI-1 to seemingly 'hop' from one lysine tRNA site to the other as indicated by the marked shift in preference for integrating into the $tRNA^{Lys10}$ gene rather than $tRNA^{Lys47}$ native-preferred integration site raised a number of intriguing questions. This chapter aimed to investigate if the genomic location of the of the *attB* site ($tRNA^{Lys}$) of PAPI-1 effects site specific recombination and integration.

This was investigated by cloning various *attB* fragments (Figure 8.1 A and C) into the Tn7 site-specific mini-transposon system (Choi and Schweizer, 2006b) and then using the Tn7 to insert the *attB* fragments in the genome at a location independent from the wildtype $tRNA^{Lys10}$ and $tRNA^{Lys47}$. Tn7 inserts at a transcriptionally silent location downstream of the *glmS* gene distantly (> 1 Mb) located with respect to the two $tRNA^{Lys}$ genes (Figure 8.1 B). The integration of PAPI-1 was then measured using the previously described qPCR approach (Chapter 6 and Figure 8.1 A). The same approach was used to investigate if the 86 bp FLP recombinase target site (FRT) left by artificially facilitated deletion of PAPI-2 and the orientation of the *attB* site affect PAPI-1 integration.

A

1.'Empty site'

Various attB sites tested

Tn7QPCR-L ~230bp attB regions Tn7QPCR-R

Not to scale

glmS Tn7-att L TetR tRNA attB PCR Amplicon Tn7-att R

2.'PAPI-1 integrated'

Tn7QPCR-L tRNA PAPI-1-RT-F

glmS Tn7-att L TetR Tn7 Primer attB PCR Amplicon PAPI-1

qPCR quantification of the two possible forms:

B Third Site genomic location

'Third site' artificial attB
6516367..6518202 Ori

5359396..5359468
attB – tRNA^{Lys47}

PA14
6.54 Mb

attP

PAPI-1

Extrachromosomal
DNA

4591106..4591178
attB – tRNA^{Lys10} PAPI-2

Not to scale

C Construction of strains

pTNS2

PCR amplification Cloned into Cut out with EcoRI and ligated into Plate mated with transposase expressing plasmid

attB pGEM-T Easy pUC18T-Tn7-Tet P. aeruginosa PA14

Figure 8.1: 'Third' attB site overview.
(A) Diagram showing two overview of the qPCR technique to detect the unoccupied and occupied Tn7 integrated *att*B site with PAPI-1 integrated or the site empty. (B) Relative genomic locations of PA14 of the *tRNA^{Lys}* genes and the Third *att*B site. (C) Construction of strains.

8.2 Construction of Third site strains

8.3 Cloning of the *attB* fragments into pUC18T-mini-Tn7T-Tet-F

Two different fragments were cloned into pUC18T-mini-Tn7T-Tet-F. Firstly, $tRNA^{Lys10}$-*attB*: a 264 bp fragment containing 91 bp of the upstream flanking DNA, the 76 bp *tRNA*, and 97 bp of the flanking downstream DNA of the $tRNA^{Lys10}$ gene. Secondly, $tRNA^{Lys10}$-*attB*:FRT: a 371 bp fragment with the same 91 bp upstream, the 76 bp *tRNA*, and 204 bp downstream including the 86 bp FRT scar. The two fragments $tRNA^{Lys10}$-*attB* and $tRNA^{Lys10}$-*attB*:FRT were amplified by using primers attB-Lys10U / attB-WTLys10-D and attB-Lys10U / attB-d2Lys10FRT-D respectively using KOD Hotstart Polymerase.

The PCR fragments were then A-tailed and then ligated into pGEM-T-Easy (Promega, UK). Plasmid DNA was extracted and digested with *EcoR*I and run on an agarose gel electrophoresis. The correct size *EcoR*I fragments for containing the $tRNA^{Lys10}$-*attB* / FRT were excised from the gel and cleaned up (Figure 8.2 A). The fragments were ligated overnight into dephosphorylated *EcoR*I digested pUC18T-mini-Tn7T-Tet-F. Plasmids were then digested with *EcoR*I to confirm the correct size insert (Figure 8.2 B). Once suitable clones were identified, the orientation of insertion of the *attB* contain fragments was ascertained by using colony PCR. To detect insertions that would be in the same orientation as both $tRNA^{Lys}$ genes in the PA14 genome which are on the negative (-ve) strand) primers bla-R / attB- Lys10U were used. To detect constructs on the in the opposite orientation and thus would be on the positive (+ve) strand primers Tet-F / attBLys10U was used. Colonies were screened and plasmids in orientations +ve and –ve for the $tRNA^{Lys10}$-*attB* named pUC18T-Tn7T-TetF-attBWT-ve and pUC18T-Tn7T-TetF-attBWT+ve respectively were stored in 30% glycerol BHI at -20 and -80°C

as strain KR 965 and KR1220 respectively. A single plasmid with a -ve orientation for

$tRNA^{Lys10}$-$attB$:FRT called pUC18T-Tn7T-TetF-attBFRT-ve was stored in 30% glycerol

BHI at -20 and -80°C as strain KR 966.

8.4   Conjugation of *attB* containing Tn*7* vectors

Vectors pUC18T-Tn7T-TetF- $tRNA^{Lys10}$-$attB$-ve / $attB$+ve / FRT-ve were conjugated

into *P. aeruginosa* PA14 (KR125) in a triparental conjugation with pTNS2 helper

plasmid (strain KR740). The pTNS2 helper plasmid expresses components of the

TnsABCD site-specific transposition pathway to enable insertion of the Tn*7* transposon.

After overnight conjugation the conjugation mixture was spread onto VBMM plates +

75 μg/ml tetracycline. After overnight incubation at 37°C, colonies appeared and two

colonies from each putative strain PA14$tRNA^{Lys10}$+ve, PA14$tRNA^{Lys10}$-ve and

PA14$tRNA^{Lys10}$FRT-ve were streaked for isolation on VBMM + 75 μg/ml tetracycline

and incubated at 37°C.
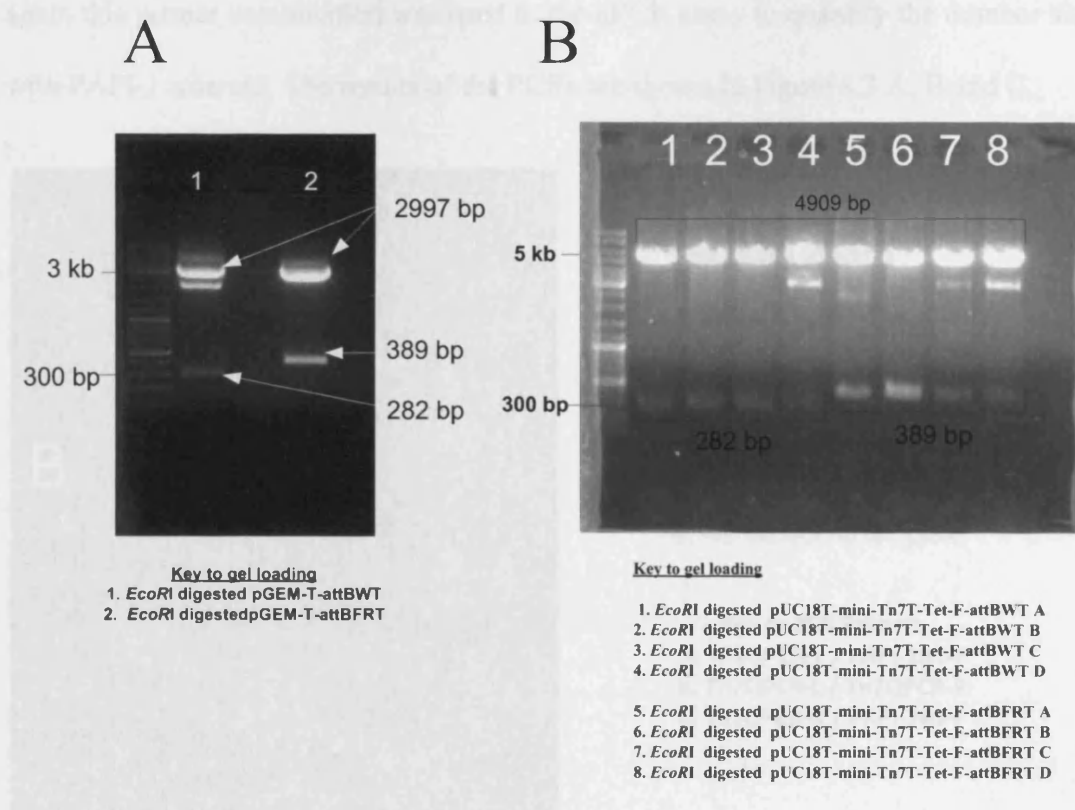
Figure 8.2: Construction of Third site Tn7 vectors.
(A) Agarose gel electrophoresis of pGEM-T-Easy third site containing constructs digested with *EcoR*I. (B) Agarose gel electrophoresis of pUC18T-Tn7T-TetF- *tRNA^{Lys10}-attB* / FRT *EcoR*I digested vectors.

8.5 Detection of Tn7 integration and insertion of PAPI-1 in third attB site.

To confirm the insertion of the Tn7 transposons and that PAPI-1 was able to integrate into the third site, colonies from each of the three newly constructed 'third site' strains: PA14*tRNA^{Lys10}+ve* , PA14*tRNA^{Lys10}-ve* and PA14*tRNA^{Lys10}FRT-ve* were tested by colony PCR (Figure 8.3). The first set used is Tn7QPCR-L and Tn7QPCR-R (Figure 8.3 B) which amplify across the inserted *attB* region, and was used in the qPCR assay to quantify the number of unoccupied sites. The second primer set is Tn7QPCR-L or R (dependent of the orientation of the inserted *attB* site) with PAPI-1RT-F (Figure 8.3 A and C) which detects the presence of the PAPI-1 island integrated into the Third site,

again this primer combination was used in the qPCR assay to quantify the number sites

with PAPI-1 inserted. The results of the PCRs are shown in Figure 8.3 A, B and C.

Key to gel loading

1. PA14-3rd tRNALys10-ve A
2. PA14-3rd tRNALys10-ve B
3. PA14-3rd tRNALys10FRT-ve A
4. PA14-3rd tRNALys10FRT-ve B
5. PA14-3rd tRNALys10+ve A
6. PA14-3rd tRNALys10+ve B
7. PA14
8. -ve control no template

Key to PCR Primers
A. Tn7QPCR-L / PAPI-1RT-F
B. Tn7QPCR-L / Tn7QPCR-R
C. Tn7QPCR-R / PAPI-1RT-F
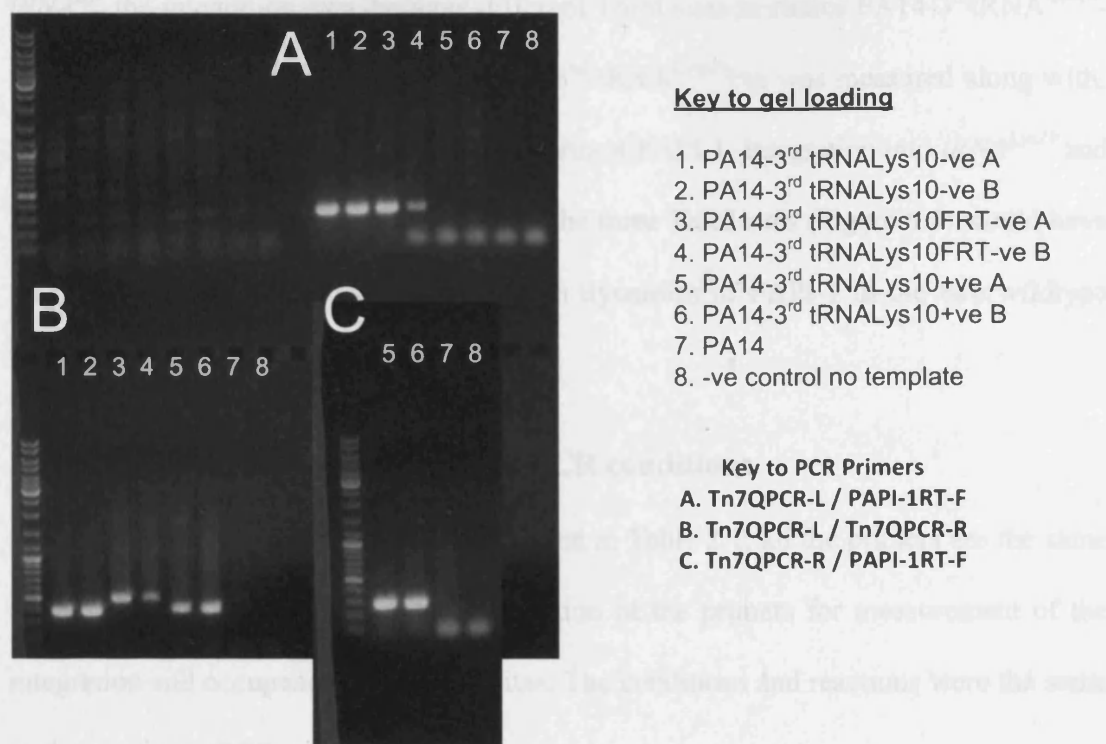
Figure 8.3: PCR confimation of Insertion of third sites into PA14.
Agarose gel electrophoresis of PCRs: (A) Detecting the insertion of PAPI-1 in the Third sites in the –ve orientation only (5 + 6 negative due to being in +ve orientation) (264 bp). (B) Amplifying across the 'empty' third sites (371 bp). (C) Detecting the insertion of PAPI-1 in the third sites in the +ve orientation (264 bp). For further information regarding the location of the primers see Figure 8.1 A.

The results showed for all the strains tested that the various Tn*7* transposons had

inserted into the genome (Figure 8.3 B), and that PAPI-1 was integrating into all three

third sites (Figure 8.3 A and C). This confirmed that PAPI-1 was able to integrate into

an artificially introduced *attB* site in the PA14 genome. The three strains PA14-

3rdtRNA^{Lys10}-ve, PA14-3rd-tRNA^{Lys10}FRT-ve, and PA14-3rd-tRNA^{Lys10}+ve were stored

in 30% glycerol BHI at -20 and -80°C as strain KR962, KR963, and KR964

respectively.

217

8.6 Overview of qPCR for Third site

Like in the previous qPCR assays to measure the integration of PAPI-1 in the two $tRNA^{Lys}$, the integration into the three different Third sites in strains PA14-3rdtRNA^{Lys10}-ve, PA14-3rd-tRNA^{Lys10}FRT-ve, and PA14-3rd-tRNA^{Lys10}+ve was measured along with; the total copy number of PAPI-1, circular form of PAPI-1, integration into $tRNA^{Lys10}$ and $tRNA^{Lys47}$. To investigate what the effect of the three Third sites (Figure 8.4) would have on the overall copy number and integration dynamics of PAPI-1 in the two wildtype $tRNA^{Lys}$ genes in PA14.

8.7 qPCR – DNA preparation and PCR conditions

The primers used in the qPCR assay are listed in Table 2.1; all the primers are the same as the original set for qPCR with the addition of the primers for measurement of the integration and occupancy of the third sites. The conditions and reactions were the same as the previous qPCR experiments.

Table 8.1: qPCR primers used for Third site investigations

Target	Forward primer name	Reverse primer	Reference
Total copy number of PAPI-1	Total-PAPI-1-F	Total-PAPI-1-Rt	This work
Circular form of PAPI-1	PAPI-1-Circ-Soj	PAPI-1-RT-F	This work
Total genome copy number (for normalisation)	gyrPA-398	gyrPA-620	(Qin *et al.*, 2003)
PAPI-1 in $tRNA^{Lys10}$	tRNA-LYS10-RT-F	PAPI-1-RT-F	This work
PAPI-1 in $tRNA^{Lys47}$	tRNA-LYS47-RT-F	PAPI-1-RT-F	This work
Empty $tRNA^{Lys10}$	tRNA-LYS47-RT-F	Empty10-RT	This work
Empty Third site	Tn7QPCR-F	Tn7QPCR-R	This work
PAPI-1 in Third site (-ve orientation)	Tn7QPCR-F	PAPI-1-RT-F	This work
PAPI-1 in Third site (+ve orientation)	Tn7QPCR-R	PAPI-1-RT-F	This work

8.8 qPCR results for Third site strains

The results from the qPCR are shown in Figure 8.5, which is made up of six sets of histogram bars that represent normalised (to a genome copy number of 1.0×10^6) copy number measurements of the following entities: total PAPI-1, circular PAPI-1, PAPI-1 integrated in $tRNA^{Lys47}$ (PAPI-1 in Lys47), PAPI-1 integrated in $tRNA^{Lys10}$ (PAPI-1 in Lys10), unoccupied $tRNA^{Lys10}$ (Empty Lys10), and PAPI-1 integrated in the third site (PAPI-1 in 3rd site). However, as the Third $attB$ site was created by cloning the regions from $tRNA^{Lys10}$, the PAPI-1 in $tRNA^{Lys10}$ data measured the integration into the $tRNA^{Lys10}$ and/or the Third $attB$ site. The same applied to the $tRNA^{Lys10}$ empty site data that assayed levels of unoccupied $tRNA^{Lys10}$ and/or the empty Third site. Therefore although the data for integration of PAPI-1 in $tRNA^{Lys10}$ was presented for comparison only, the data relating to the third site was analysed further.
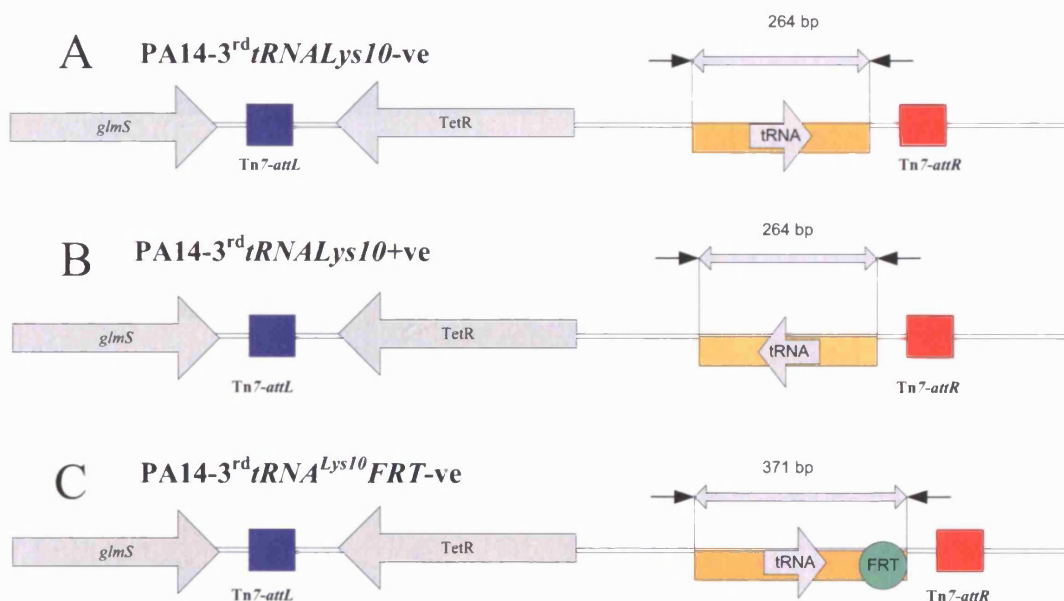
Figure 8.4: Genetic maps of Third site strains Tn7 insertions.
Showing locations, size of inserts, orientation of $tRNA^{Lys10}$ in strains: (A) PA14-3^{rd}tRNA^{Lys10}-ve. (B) PA14-3^{rd}tRNA^{Lys10}+ve (C) PA14-3^{rd}tRNA^{Lys10}FRT-ve.

	Total PAPI-1	Circular PAPI-1	PAPI-1 in Lys47	PAPI-1 in Lys10	Empty Lys10	PAPI-1 in 3rd site
PA14 WT	7.79E+05	1.49E+04	5.17E+05	6.18E+01	1.07E+06	
3rd Lys10 -	1.73E+06	1.09E+06	4.48E+03	1.36E+06	5.39E+04	8.14E+05
3rd Lys10 - FRT	9.79E+05	1.97E+03	6.86E+02	6.05E+05	1.84E+06	8.27E+05
3rd Lys10 +	9.28E+05	3.32E+03	3.73E+02	1.17E+06	6.73E+03	9.76E+05
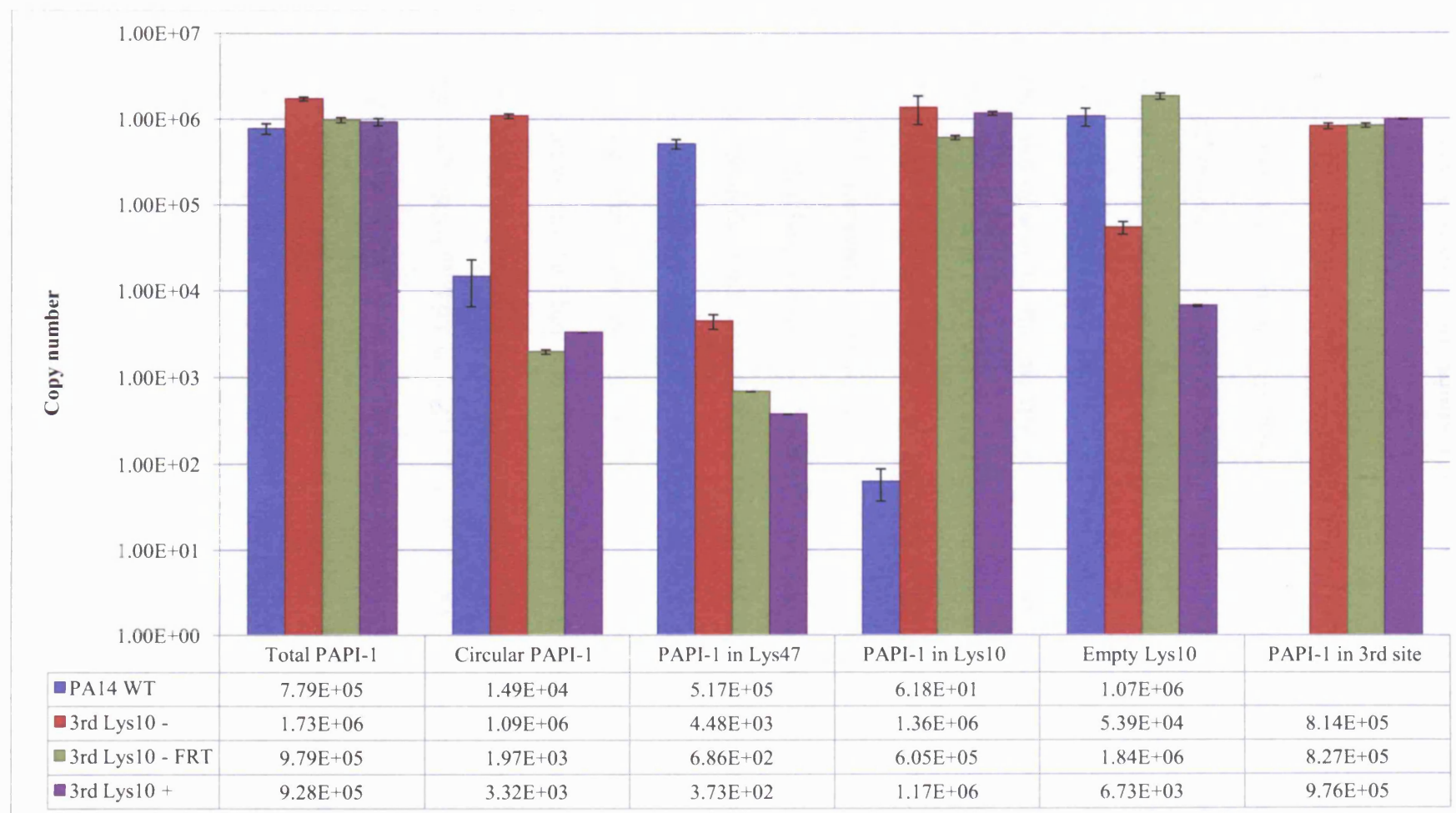
Figure 8.5: Graph showing the relative copy number of PAPI-1 as determined by qPCR.
Normalised to 1×10^6 genomes. PAPI-1 integrated in sites $tRNA^{Lys10}$, $tRNA^{Lys47}$ and Third site, Total and Circular copy numbers of PAPI-1 in strain PA14, PA14-3rdtRNA^{Lys10}-ve, PA14-3rd tRNA^{Lys10}FRT-ve, and PA14-3rd tRNA^{Lys10}+ve.

220

8.9 qPCR results for stains PA14-3rd-tRNA^{Lys10}FRT-ve and PA14-3rd-tRNA^{Lys10}+ve

Strains PA14-3rd-tRNA^{Lys10}+ve and PA14-3rd-tRNA^{Lys10}FRT-ve show similar results. In both strains the insertion of the third site seems to have caused similar effects on the integration and copy number of PAPI-1. Both strains showed similar total PAPI-1 copy numbers as the wild type PA14; with copy numbers of 7.79 x 10^5, 9.79 x 10^5 and 9.28 x 10^5 for PA14, PA14-3rd- tRNA^{Lys10}FRT-ve and PA14-3rd-tRNA^{Lys10}+ve respectively. They also showed that the majority of copies of PAPI-1 changed from integrating in the $tRNA^{Lys47}$ site as in PA14 WT to the Third site. PA14-3rd- tRNA^{Lys10}FRT-ve, and PA14-3rd-tRNA^{Lys10}+ve had 4.48 x 10^3 and 6.86 x 10^2 copies of PAPI-1 integrated in $tRNA^{Lys47}$ respectively compared to 5.17 x 10^5 copies for PA14. Both PA14-3rd-tRNA^{Lys10}FRT-ve and PA14-3rd-tRNA^{Lys10}+ve had similar copy numbers of PAPI-1 integrated in the third site with 8.27 x 10^5 and 9.76 x 10^5 copies respectively. The copy numbers of PAPI-1 integrated in the Third site in all three strains are virtually identical suggesting that neither the orientation nor the presence of the FRT site affected PAPI-1 integration into the Third site. The copy number of PAPI-1 integrated into $tRNA^{Lys10}$ (measuring integration in both PAPI-1 in $tRNA^{Lys10}$ and the Third site) is 6.05 x 10^5 for PA14-3rd- tRNA^{Lys10}FRT-ve and 1.17 x 10^6 for PA14-3rd-tRNA^{Lys10}+ve. Both similar copy values to PAPI-1 in the Thirds site suggesting there is only minimal integration into $tRNA^{Lys10}$ and that the predominate integration site of PAPI-1 is in the Third site. The copy numbers for empty $tRNA^{Lys10}$ were perplexing with copy numbers of 5.93 x 10^4 and 6.73 x 10^3 for PA14-3rd- tRNA^{Lys10}FRT-ve and PA14-3rd-tRNA^{Lys10}+ve. The primers for empty $tRNA^{Lys10}$ measure copies of two independent empty sites, in both the $tRNA^{Lys10}$ site and the Third site. As PAPI-1 was found integrated into the Third site and not in $tRNA^{Lys10}$ it should then follow that the $tRNA^{Lys10}$ site is empty. Therefore as one

of the two sites is empty it would be expected that the copy number would be more in the order of 5 x 10^5 to 1 x 10^6 copies. But the lower copy numbers of the empty $tRNA^{Lys10}$ of 10^3 and 10^4 copies do not reflect this. Therefore further investigation will be required to identify the reason behind this.

8.10 PA14-3rd-$tRNA^{Lys10}$-ve

PA14-3rd-tRNA^{Lys10}-ve contains a 264 bp fragment from the PA14 $tRNA^{Lys10}$ in the same orientation of that of the two PA14 $tRNA^{lys}$ genes. The total copy number of PAPI-1 in this strain is 1.73 x 10^6 which represents ~ 1.73 copies of PAPI-1 per genome. Compared to 0.77, 0.97 and 0.92 for PA14, PA14-3rd- tRNA^{Lys10}FRT-ve and PA14-3rd-tRNA^{Lys10}+ve respectively. This would seem to be an increase in copy number of ~1. Integration of PAPI-1 in the $tRNA^{Lys47}$ site is 5.17 x 10^5 for PA14 compared to 6.86 x 10^2 for PA14-3rd-tRNA^{Lys10}–ve. This suggested that the introduction of a Third site, like the other two strains with a Third site, had caused PAPI-1 to exhibit preferential integration into the third $attB$ site rather than its native $tRNA^{Lys47}$ locus. Integration of PAPI-1 into the third site is 8.14 x 10^5 copies which is similar to the values seen in PA14-3rd- tRNA^{Lys10}FRT-ve and PA14-3rd-tRNA^{Lys10}+ve. This finding suggests that the differences between the three third sites made little or no difference in the integration of PAPI-1. The copy number of PAPI-1 in $tRNA^{Lys10}$ which was 1.36 x 10^6 copies, which although being 5.46 x 10^5 copies higher than the Third site, this is within the standard deviation of this strain. Again like in the two other thirds site strains $tRNA^{Lys10}$ it is not significantly high enough to show up in the total PAPI-1, or as a major discrepancy in copy number between the Third site and PAPI-1 in $tRNA^{Lys10}$ values. However like for the other two third site strains without further experimentation this is not certain, further PCR primers will need to be designed to answer this.

The most interesting result for PA14-3rd-tRNA^{Lys10}-ve is that for the circular form of PAPI-1. This is 1.09 x 10^6 compared to 1.49 x 10^4, 1.97 x 10^3 and 3.32 x 10^3 for PA14, PA14-3rd-tRNA^{Lys10}FRT-ve and PA14-3rd-tRNA^{Lys10}+ve respectively. This result fits with the increase in the total PAPI-1 copy number seen; an increase of ~1 copy per genome from the other strains. It seems that PA14-3rd-tRNA^{Lys10}-ve has one copy integrated in the Third site and one additionally as in the the circular form, giving the total PAPI-1 copy number of ~ 2.

8.11 Third site qPCR discussion and analysis

The results of the use of the Third site answer some of the questions posed at the outset. Firstly it seems that the orientation of the tRNA and the presence or absence of the FRT recombination site seemed to make no difference in the integration of PAPI-1. Suggesting the presence of the FRT site in PA14ΔPAPI-2, PA14ΔPAPI-2.2 and PAO1ΔtRNA^{Lys10} island played no role in the island hopping. A most interesting finding was that the Third site in all three constructs seemed to be the preferred integration site for PAPI-1 in the genome; above the two natural integration sites (*tRNA*^{Lys10} and *tRNA*^{Lys47}) suggesting chromosomal location of the *attB* site contributes to the integration of PAPI-1. This result fits in with the earlier findings that the deletion of the islands (PAPI-2 and PAO1 *tRNA*^{Lys10} island) made the *tRNA*^{Lys10} a more suitable insertion site for PAPI-1. However, further studies integrating the same the Third site into different regions of the genome are needed to confirm the findings here. As previously studies have found that for a related element; the ICE*clc* element of *Pseudomonas knackmussii* sp. strain B13 the chromosomal location of the *attB* site did not make any difference to the integration (Sentchilo *et al.*, 2009).

One result of particular interest was the almost two log increase in the copy number of the circular form in strain PA14-3rd-tRNA^{Lys10}–ve. This strain had a copy

223

number of 1.09×10^6 compared to 1.49×10^4 in PA14. In actual fact the copy number of the circular form varied in a number of strains with the lowest copy number being in C3719-PAPI-1 of 3.78×10^2 and other strains having varying copy numbers in the order of 10^4 to 10^2 (Table 8.2). It is hard to see how the incorporation of the Third site in just one orientation and not the other could have altered the number of copies of circular PAPI-1 so drastically, as the integration has not physically manipulated the PAPI-1 island or factors encoded on it.

Table 8.2: Circular copy numbers of all strains tested by qPCR

Strain	Circular copy number
PA14 WT	1.49×10^4
PA14ΔPAPI-2	8.76×10^3
PA14ΔXerC	2.65×10^4
PA14ΔPAPI-2.2	1.60×10^4
PA14-3rd-tRNA^{Lys10}-attB -ve	1.09×10^6
PA14-3rd-tRNA^{Lys10}-attB FRT-ve	1.97×10^3
PA14-3rd-tRNA^{Lys10}-attB +ve	3.32×10^3
LES-PAPI-1	2.40×10^4
C3719 - PAPI-1	3.78×10^2
PA14ΔPro21	8.26×10^2
PA01-PAPI-1	2.11×10^3
PA01ΔLys10-PAPI-1	5.56×10^3

Furthermore the significant variation seen in copy number of PAPI-1 between host strains and in some of the mutants adds to the complexity. In the case of the island mutants (PA14ΔPAPI-2 and PA14ΔPro21) it would be very coincidental that two different islands both encode factors that regulate the excision and formation of circular copies of PAPI-1. Therefore it is more likely that the problem actually lies with what is being measured by the PCR for the circular copies. As can be seen in Figure 8.6; there are three theoretical forms of PAPI-1 that could produce a positive PCR product for the circular PAPI-1. There is no data available regarding if the different multiple forms of

PAPI-1 do exist *in vivo* and which (if any), is the dominate form. The first form; which is a singular circle is shown in Figure 8.6 A, is how PAPI-1 and related islands are thought to exist as a extrachromosomal form after excision from in the genome (Wurdemann and Tummler, 2007, Mathee et al., 2008, Qiu et al., 2006). However, direct evidence other than PCR amplification across the *attP* site of this specific form has not been carried out. The insertion of tandem islands as shown in Figure 8.6 C; have been described for a number of other genomic islands (Pavlovic et al., 2004, Doublet et al., 2008a, Hochhut *et al.*, 2001, Ravatn *et al.*, 1998). However, again this has not been specifically demonstrated for PAPI-1. The final form shown in Figure 8.6 B is an entirely theoretical form that could be formed by one of two mechanisms. Firstly, the *attP* site of a circular island could act as an *attB* site for second resulting in a site-specific extra-chromosomal recombination event. Secondly, this hypothetical structure could form if a tandem island excised from the genome as an intact tandem island and formed a duplex circle. Therefore, it is entirely possible that the circular form of PAPI-1 was present in only very low copy numbers and that the PCR for the circular form, as is shown in the Figure 8.6 C, maybe in fact be detecting tandem insertions instead. Further work is required to establish if tandem PAPI-1 islands form *in vivo* and to confirm which of the three forms exist in individual cells and the population as a whole. The relative ratios of each of the existent additional PAPI-1 forms will also have to be determined. Finally, issues relating to potential interactions between the multiple co-existent PAPI-1 forms and the impact of all these factors on PAPI-1 replication and transfer dynamics will need to be investigated to gain a better insight into the life style and life cycle of PAPI-1 both from the perspective of a single bacterium and wider *P. aeruginosa* clonal and non-clonal populations.
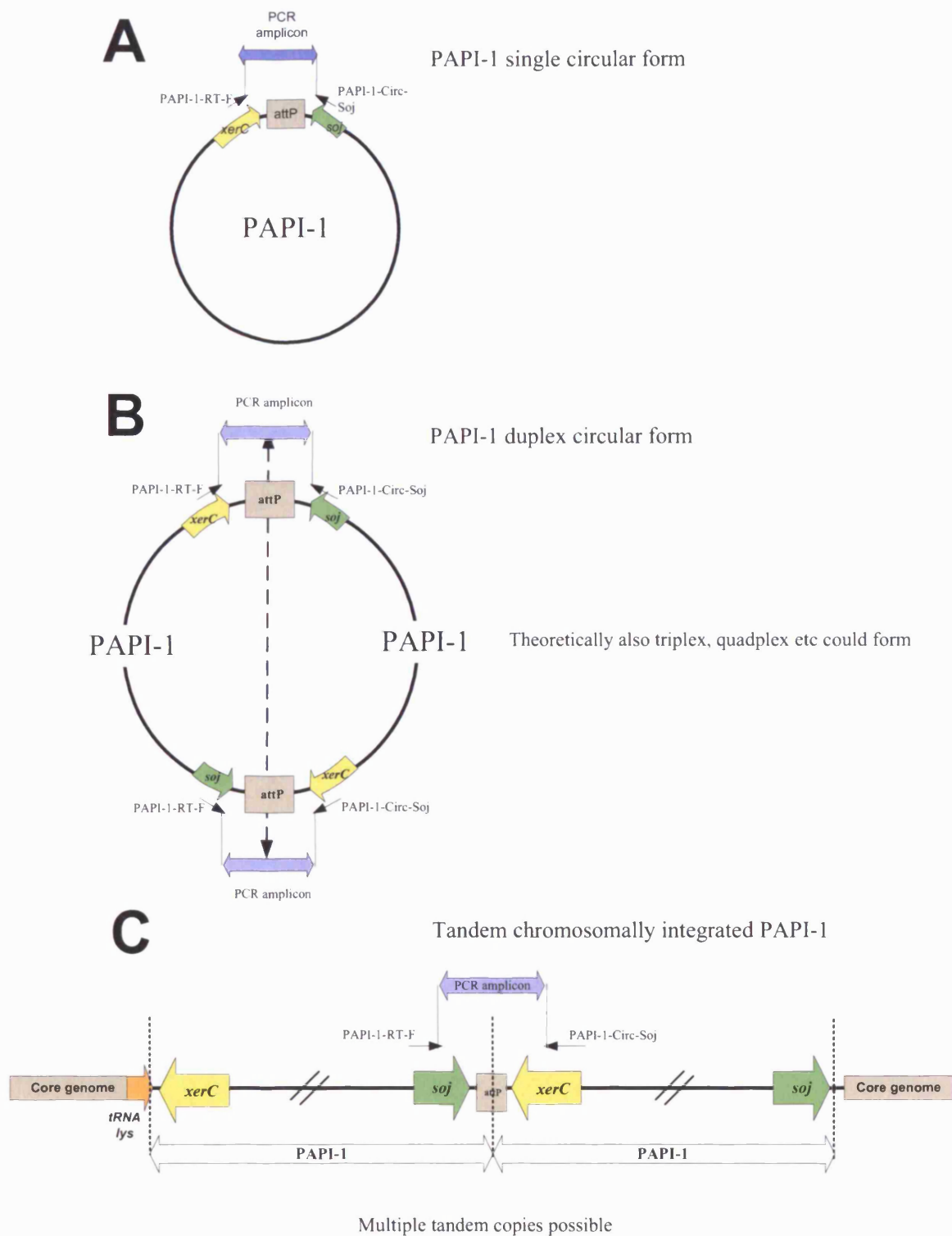
Figure 8.6: The possible PAPI-1 configurations that will produce a positive 'circular form' PCR product.
(A) Single circular form (B) Duplex circular form (C) Tandem chromosomally integrated.

Of the three forms described above, it is most likely that the variation seen in circular copy number is actually due to increased / decreased formation of tandem islands. It is conceivable that the variation in circular copy numbers seen across the different strains is due to the suitability of the different *attB* regions for the integrations of tandem islands. Due to the different host genome structures (PAO1 / LESB58 etc) and different global and local genome structures created by the deletions made.

Finally, the use of a chromosomally integrated third site and qPCR assay was validated as a method to measure recombination in the genome. It is a very simple and highly sensitive method to measure the site specific recombination of genomic islands. Other studies have made use of plasmid-based recombination reporter systems (Wilde et al., 2008), and a very recent publication used a Tn*5* system linked with a green fluorescent protein (GFP) reporter to detect the integration of the genomic island (Sentchilo et al., 2009). These systems like the one described here are a powerful set of tools to investigate the site-specific recombination of the genomic islands and related mobile genetic elements.

9 Genome dynamics : Genome inversions in *Pseudomonas aeruginosa*

9.1 Pulse field gel electrophoresis (PFGE) analysis to determine site of PAPI-1 integration and detect potential genome inversion events.

9.2 Overview

The qPCR results demonstrated that the majority of copies of PAPI-1 lay within the $tRNA^{Lys10}$ rather than $tRNA^{Lys47}$ sites in PA14ΔPAPI-2. Surprisingly, in the second independently derived PAPI-2-minus mutant (PA14ΔPAPI-2.2) PAPI-1 was found to be integrated equally frequently in both $tRNA^{Lys47}$ and $tRNA^{Lys10}$. The fact that the two strains differed led to the hypothesis that a genomic inversion in one of the strains may have altered the structure of its genome relative to that of its genetically engineered 'clone'. It was hypothesised that this change in genome structure accounted for the differential PAPI-1-integration profiles of the two strains.

9.3 Introduction

Large chromosomal inversions (LCI) have been reported in a number of bacterial species, the best studied are in *Salmonella*, and *E. coli*. In both species a range of inversions mediated by recombination between inversely orientated rRNA (*rrn*) operons (Charlebois, 1999) have been shown to occur. In most cases these inversions are between *rrn* operons that are symmetrical in respect to the origin of replication. These inversions are thought not to greatly affect growth rates, and may select for higher gene expression due to changes in orientation of genes with respect to the direction of chromosomal replication (Charlebois, 1999, Rocha, 2008, Rocha and Danchin, 2003). Some genomic inversions in *rrn* operons in *E.coli* that have resulted in unbalanced replichores have been reported to be deleterious to growth rates (Charlebois, 1999). It seems that in a number of bacterial genomes there is a tendency towards a physical

balance between the origin of replication (*ori*) and termination region (*ter*) loci of the chromosome (Song *et al.*, 2003). Physical balance in relation to genomes means that the two replichores are of equal size, if they are not then the genome is said to be unbalanced in respect to the *ori* and *ter*. However, a number of sequenced genomes have been reported to be unbalanced (Deng *et al.*, 2003). Additionally in *E. coli* inversions that effect genome macrodomains have been reported to be deleterious (Esnault *et al.*, 2007). The rate at which inversion mediated rearrangements occur in genomes is largely unknown with estimates ranging from 10^{-7} to 10^{-5} for large scale deletions in *Salmonella* (Helm *et al.*, 2003, Charlebois, 1999) to 10^{-9} - 10^{-8} for inversions mediated by small (12 -23 bp) repeats in *E. coli* (Charlebois, 1999). In *Yesinia pestis* the causative agent of plague, large genomic inversion have been reported to be found in the same DNA samples, with one form predominating, over others, suggesting that *Y. pestis* genomes are in a constant state of flux as a result of inversions (Parkhill *et al.*, 2001).

In *P. aeruginosa* a number of studies on genomic inversion have been published, in particular focusing on the evolution of *P. aeruginosa* genomes in the CF lung and within clonal groups of CF-adapted clones such as 'Clone C' (Kresse *et al.*, 2003, Romling *et al.*, 1997). Most inversions in *P. aeruginosa* occur between *rrn* operons or between copies of the insertion element IS*6100* (Kresse et al., 2003, Romling et al., 1997). In a number of sequenced *P. aeruginosa* genomes a range of inversions between the *rrn* operons have been noted, however the frequency of such events has yet to be determined (Stover *et al.*, 2000, Lee *et al.*, 2006b, Mathee *et al.*, 2008).

To predict how the PFGE profiles of PA14 and the various isogenic mutants strains would look, Vector NTI (Invitrogen, UK) software was used to create *in silico* predictions for PFGE-resolved *P. aeruginosa* PA14 DNA double digests with *Pac*I and

I-*ceu*I and *Spe*I digested alone. The PA14 genome is fully sequenced so it was possible to create *in silico* versions of genomes belonging to the various PA14 insertion and/or deletion mutants and/or hypothetical derivatives under study. This allowed for *in silico* generation and comparison of PFGE banding patterns for selected 'genomic snap-shot' 'strains' such as the previously discussed PA14ΔPAPI-2 with the PAPI-1 island integrated only in *tRNA^{Ly10}* and PA14ΔPAPI-2.2 with the PAPI-1 island integrated in both *tRNA^{Lys10}* and *tRNA^{Lys47}*. In reality none of the strains possessed a single state of PAPI-1 as the island had been shown to exhibit dynamic mobility in each and every derivative examined in the previous qPCR analysis (Chapter 6). These predictions were then compared to the experimental PFGE images to determine if these matched *in silco* predictions and qPCR results. It was expected that if any genomic inversions were present that these could then be detected based on banding variation compared to the predicted PFGE patterns.

9.4 Pulse field gel electrophoresis

1. *S. cerevisiae* marker
2. PAO1
3. PA14
4. PA14ΔPAPI-1
5. PA14ΔPAPI-2 with PAPI-1 in *tRNALys10*
6. PA14ΔPAPI-2 with PAPI-1 in *tRNALys47*
7. PA14ΔPAPI-2 with PAPI-1 in *tRNALys10* and *tRNALys47*
8. PA14Δ1Δ2
9. PA14ΔPro21
10. PA14Δ1Δ2ΔPro21
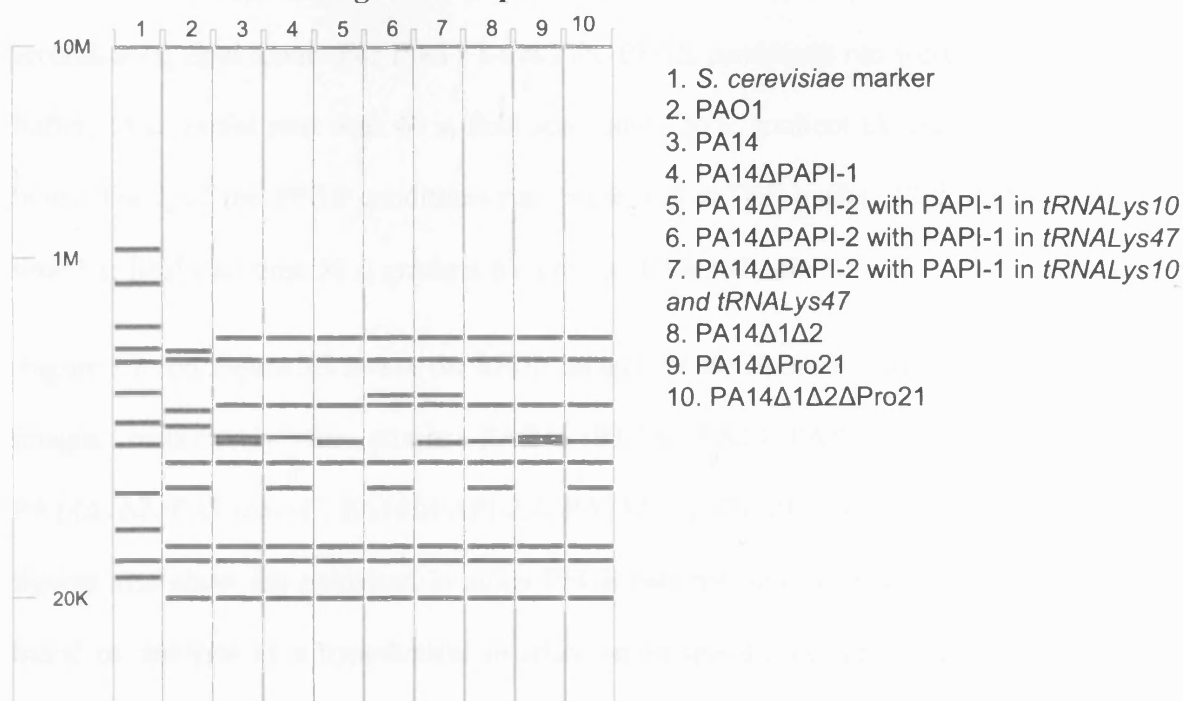
Figure 9.1: Predicted PFGE banding pattern for *Pac*I / I-*Ceu*I digested DNA.
1.2% agarose gel run with TBE buffer, 6 Volts/cm, and pulse time of 120 seconds, run for 35 hours.

9.4.1 PFGE results

As can be seen in Figure 9.1, the *in silico* predictions of the PFGE banding patterns for *Pac*I / I-*Ceu*I digested DNA produced by the Vector NTI software gives a basic outline of the predicted banding pattern that would be expected to be observed following experimental PFGE analysis. This could then be used to compare to the real PFGE to confirm the qPCR identified dominant PAPI-1 integration sites in each of the strains examined. The data could also potentially be analysed and compared to this to see if detectable genomic inversions had occurred.

9.5 *Pac*I / I-*Ceu*I and *Spe*I

The preparation of high molecular weight DNA plugs, restriction digestion and conditions used for PFGE gel are outlined in the Materials and Methods. Two different

231

digestions were performed; the first was a double digest using *Pac*I / I-*Ceu*I and the second using *Spe*I alone. For *Pac*I / I-*Ceu*I the PFGE conditions run were: 0.5 x TBE buffer, 14°C, initial start time 60 s; final start time 120 s; gradient 6V/cm; run time 30 hours. For *Spe*I the PFGE conditions run were: 0.5 x TBE buffer, 12°C, initial start time 1 s; final start time 50 s; gradient 6V/cm; run time 30 hours.

Figure 9.2 and Figure 9.3 shows the PFGE images for the *Pac*I / I-*Ceu*I and *Spe*I PFGE images respectively for strains PAO1, PA14, PA14ΔPAPI-1, PA14ΔPAPI-2, PA14Δ1Δ2, PA14Δ*xerC*, PA14ΔPAPI-2.2, PA14Δ1Δ2ΔPro21, and PA14ΔPro21. The figures also show the predicted *in silico* PFGE patterns generated using Vector NTI, based on analysis of a hypothetical *in silico* strain-specific genome informed by the strain construction process and the qPCR results that revealed the favoured PAPI-1 integration site. Virtual genomes of PAO1, PA14ΔPAPI-1 and PA14Δ1Δ2ΔPro21 which had not been analysed by the qPCR assay as these lacked PAPI-1 were generated solely on the basis of predicted structures based on the defined deletions introduced.

9.5.1 PAPI-1 is inserted in tRNA^{Lys10} *in* PA14ΔPAPI-2 and PA14Δ2.9kbPAPI-2

The results for PA14ΔPAPI-2 matched that of the *in silico* PFGE banding pattern (Figure 9.2 B and Figure 9.3 B) for PAPI-1 being inserted predominantly in the *tRNA^{Lys10}* site. This result mirrored that gained by the qPCR assay and confirmed that PAPI-1 was inserted predominantly in the *tRNA^{Lys10}* site in this strain, thus validating the accuracy of the qPCR to provide a representative view of the site PAPI-1 integration within the clonal population that arises from the strain.

9.5.2 PAPI-1 is present in two copies in PA14ΔPAPI-2.2 inserted in both tRNA^{Lys}

As can be seen in Figure 9.2, the *Pac*I / I-*Ceu*I PFGE for PA14ΔPAPI-2.2 matches the *in silico* prediction for PA14ΔPAPI-2.2 having PAPI-1 inserted into both *tRNA^{Lys}* sites,

thus having a PAPI-1 copy number of two. This finding matched the qPCR result and validated the conclusion that this strain has two chromosomally-integrated copies of PAPI-1.

9.5.3 All other strains match predicted PFGE patterns and show no genomic inversions

All the other strains matched their predicted PFGE patterns, confirming the selected defined regions had been deleted as planned and that no other large-scale secondary genomic inversions, deletions or duplications had occurred. This was particularly relevant for strain PA14Δ1Δ2ΔPro21, which has two inversely orientated FRT scars within its genome as these sites have been reported to cause large scale genomic inversions (Barekzi et al., 2000).

9.5.4 PA14ΔPAPI-2 and PA14Δ1Δ2 show no detectable genomic inversions or deletions

Both strains PA14ΔPAPI-2.1 and PA14Δ1Δ2 have the same parent PA14 strain, with PA14Δ1Δ2 being isogenic to PA14ΔPAPI-2.1. No obvious chromosomal inversion or deletion could be seen in the experimental *Pac*I / I-*Ceu*I (Figure 9.2 A) profiles compared to the *in silico* predicted PFGE banding patterns (Figure 9.2 B). Similarly, examination of the *Spe*I PFGE profiles failed to reveal evidence of any large scale inversions or deletions (Figure 9.3). However, the smaller *Spe*I bands did not resolve adequately, potentially obscuring events involving parts of the genome represented by these bands.

A. PFGE image

1. *S. cerevisiae* marker (in kb)
2. PAO1
3. PA14
4. PA14ΔPAPI-1
5. PA14ΔPAPI-2
6. PA14Δ1Δ2
7. PA14ΔxerC
8. N/A
9. PA14ΔPAPI-2.2
10. PA14Δ1Δ2ΔPro21
11. PA14ΔPro21
12. *S. cerevisiae* marker (in kb)

B. *in silico* predictions of strains

1. S. cerevisiae marker (in kb) (Note: not the same scale as experimental marker)
2. PAO1
3. PA14 (PAPI-1 in tRNALys47)
4. PA14ΔPAPI-1
5. PA14ΔPAPI-2 (PAPI-1 in tRNALys10)
6. PA14Δ1Δ2
7. PA14ΔxerC (PAPI-1 in tRNALys47)
8. N/A
9. PA14ΔPAPI-2 (PAPI-1 in tRNALys10 and 47)
10. PA14Δ1Δ2ΔPro21
11. PA14ΔPro21 (PAPI-1 in tRNALys47)
12. S. cerevisiae marker (in kb) (Note: not the same scale as experimental marker)

Figure 9.2: PFGE of PacI / I-CeuI digest *P. aeruginosa* strains and isogenic mutants.
A. PFGE image B. *in silico* predictions of strains.
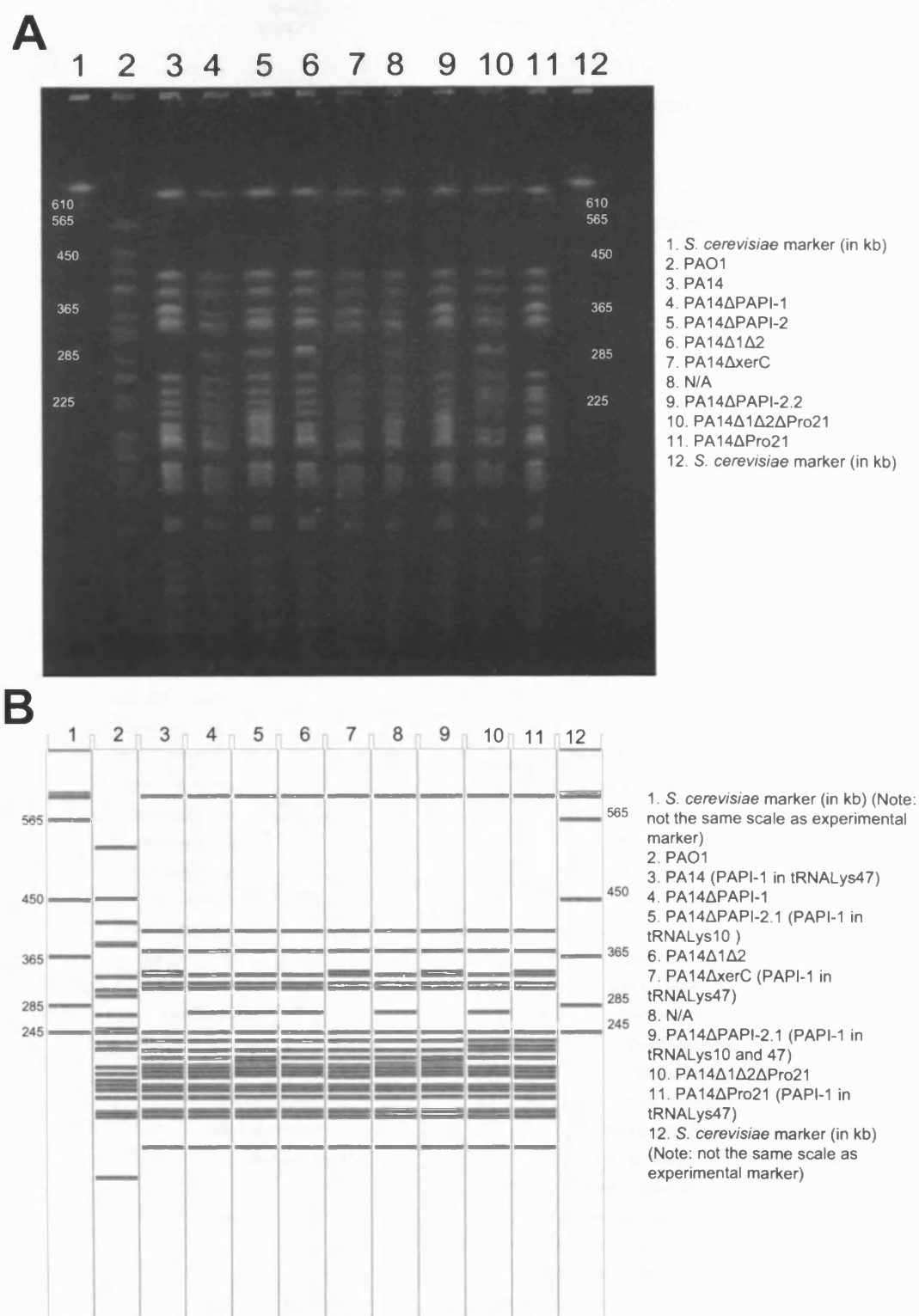
Figure 9.3: *SpeI* PFGE of P. aeruginosa strain PA14 and isogenic mutants
A. PFGE image B. *in silico* predictions of strains.
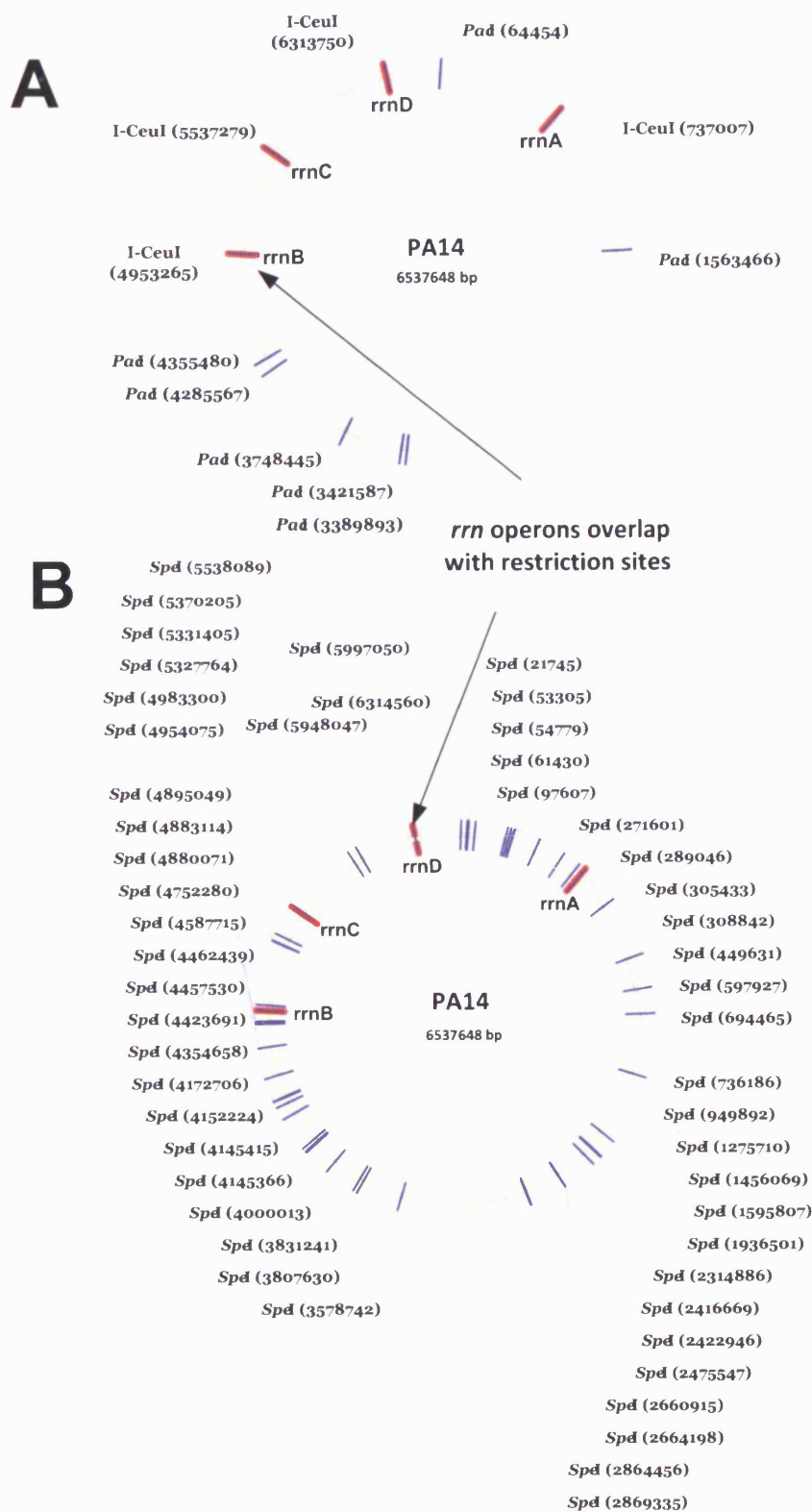
Figure 9.4: Restriction maps of the PA14 genome based on the enzymes used for PFGE analysis.

A. PA14 digested with *I-ceuI*-I and *Pac*I. *rrn* operons highlighted in red. B. PA14 digested with *Spe*I. *rrn* operons highlighted in red.

However the PFGE analysis of *Pac*I / I-*ceu*I- and *Spe*I-digested DNA is not sufficient to detect all genomic inversions. As two of the *rrn* operons in PA14 are located almost perfectly symmetrically on either side of the origin of replication (Lee *et al.*, 2006b) (Figure 9.4 A and B), inversions involving these sites would not be readily detected by PFGE.. This is due to the genomic location of the *rrn* operons coinciding with both I-*ceu*I and *Spe*I restriction sites (Figure 9.4 A and B). Hence, not all *rrn*-related inversions would be detectable with the conditions and enzymes used

9.6   PCR detection of genomic inversions

9.6.1   Overview

To detect if inversions had occurred between the *rrn* operons in strain PA14ΔPAPI-2.1 and PA14ΔPAPI-2.2 a PCR based approach was used. In the paper that originally described the PA14 genome sequence the following PCR primers were designed to identify inversions between two ribosomal RNA operons (*rrn)* operons (*rrnA* and *rrnB*) (): 807.LL_rev + 2-5'_2 and 837.LL + 803.RR.rev (Lee *et al.*, 2006b).

Used in the combination 807.LL_rev + 2-5'_2 and 837.LL + 803.RR.rev, these primers would detect the 'PA14 genome orientation' (A), while 807.LL_rev + 803.RR.rev and 837.LL + 2-5'_2 would identify the 'PAO1 genome orientation' (Stover et al., 2000) (B). The four primers were then used to identify if the PA14-derived strains PA14ΔPAPI-2.1 and PA14ΔPAPI-2.2 had undergone a genomic inversion similar like that of PAO1.
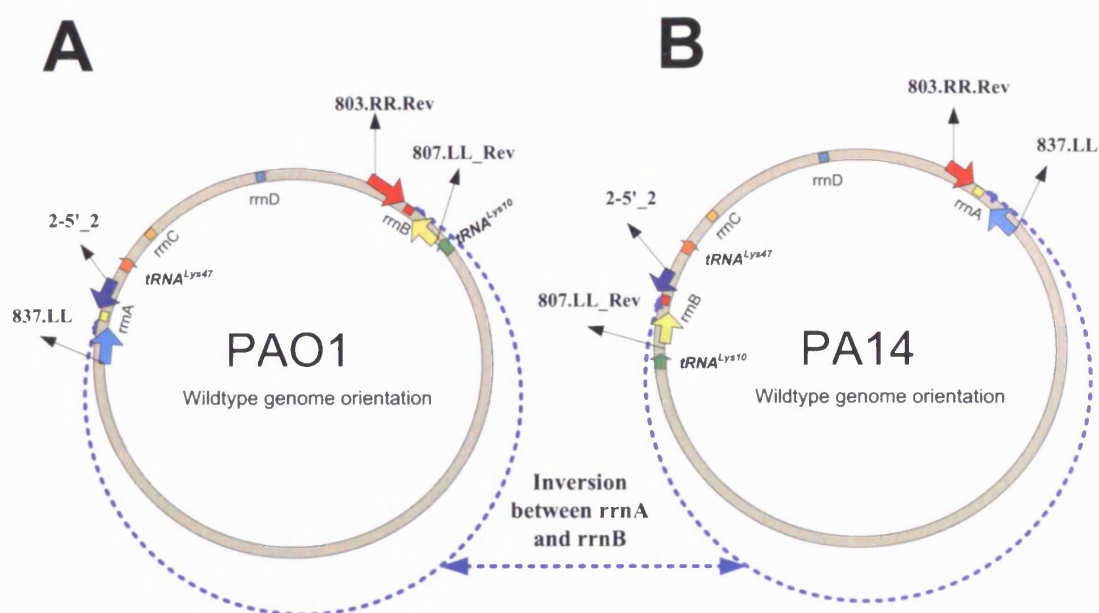
Figure 9.5: Genome orientations of PAO1 and PA14 and locations of *rrn* operons.
(A) Genome orientation of PAO1, locations of *rrn* operons and PCR primers for inversion detection. (B) Genome orientation of PA14, locations of *rrn* operons and PCR primers for inversion detection.

9.7   Results of *rrn* operon-specific PCR assays

9.7.1   Both genome orientations exist in *P. aeruginosa* populations

The first round of PCR was carried out on un-quantified genomic DNA from PAO1, PA14 and PA14ΔPAPI-2 grown under the same conditions. It was expected to be observed for each strain a single *rrn* operon orientation, as had been previously reported (Lee *et al.*, 2006b). For example, PAO1 would be positive for one type of orientation (A) and PA14 another (B). However as is shown in Figure 9.6 A this was not the case. For PAO1, PA14 and PA14ΔPAPI-2 bands were amplified for all four sets of PCRs suggesting that both orientations of genome were present within the population (Figure 9.6 A, i and ii).

238

A

i

Un-quantified Genomic DNA

PA14 Orientation   PAO1 Orientation

807.LL_Rev + 2-5'_2
837.LL + 803.RR.Rev
837.LL + 2-5'_2
807.LL_Rev + 803.RR.Rev

1 2 3 4   1 2 3 4   1 2 3 4   1 2 3 4

ii

Gel Run further

1 2 3 4   1 2 3 4   1 2 3 4   1 2 3 4

Key to gel loading
1. PA14
2. PAO1
3. PA14ΔPAPI-2
4. -ve

B

10ng Genomic DNA

PA14 Orientation   PAO1 Orientation

807.LL_Rev + 2-5'_2
837.LL + 803.RR.Rev
837.LL + 2-5'_2
807.LL_Rev + 803.RR.Rev

A B C D   A B C D   A B C D   A B C D

Key to gel loading
A. PAO1
B. PA14
C. PA14ΔPAPI-2
D. -ve

Figure 9.6: PCR assays for detection of *rrn* operon inversions.
(A) i. Using un-quantified genomic DNA as template ii. The same gel run further. (B) Using 10ng of Genomic DNA as template.

This experiment was repeated again but this time instead of uncontrolled inputs of template, a controlled amount of template DNA (10 ng) was used so the results would be comparable across strains. The results using 10 ng of template DNA (Figure 9.6 B) confirmed previous observation with the uncontrolled template input, that in PA14 and PA14ΔPAPI-2 (PAO1 failed in all PCRs for an unknown reason) both the PAO1 and the PA14 orientations exist in the population (PAO1 and PA14 orientations shown in). From the relative brightness of the PCR amplicons produced it seemed that the 'PA14 orientation' was more prevalent in PA14 and PA14ΔPAPI-2 (primer combinations: 807.LL_rev + 2-5'_2 and 837.LL + 803.RR.rev) than the 'PAO1 orientation' (primer combinations: 807.LL_rev + 803.RR.rev and 837.LL + 2-5'_2) (Figure 9.6 B). Furthermore, it seemed that there was also a difference in the prevalence between the two set of PCRs to detect 'PAO1 orientation' with the orientation detected by 837.LL + 2-5'_2 being more prevalent than 807.LL_rev + 803.RR.rev (Figure 9.6 B). These findings suggested that *rrn* operon inversions were continually taking place in within the populations of PA14 and PA14ΔPAPI-2 and that certain orientations were dominant.

9.8 PA14ΔPAPI-2.2 has an altered genome structure

To further confirm these findings and to apply the PCRs to PAO1, PA14, PA14ΔPAPI-2 and PA14ΔPAPI-2.2 the PCR assays were repeated with a modification. To try to identify the relative ratio of the various genome orientations in the populations a semi-quantitative approach was used. Single PCRs were made up again using 10 ng of template for each reaction and split into two separate PCR tubes. One of these tubes was removed after 22 cycles and the other left until 35 cycles. This then allowed comparison of the amount of each of the product produced at an earlier cycle number. As strains with more copies would be detectable earlier while strains with low copies would either

240

have produced very low or no PCR product at this point and would only be detectable at

later cycles.
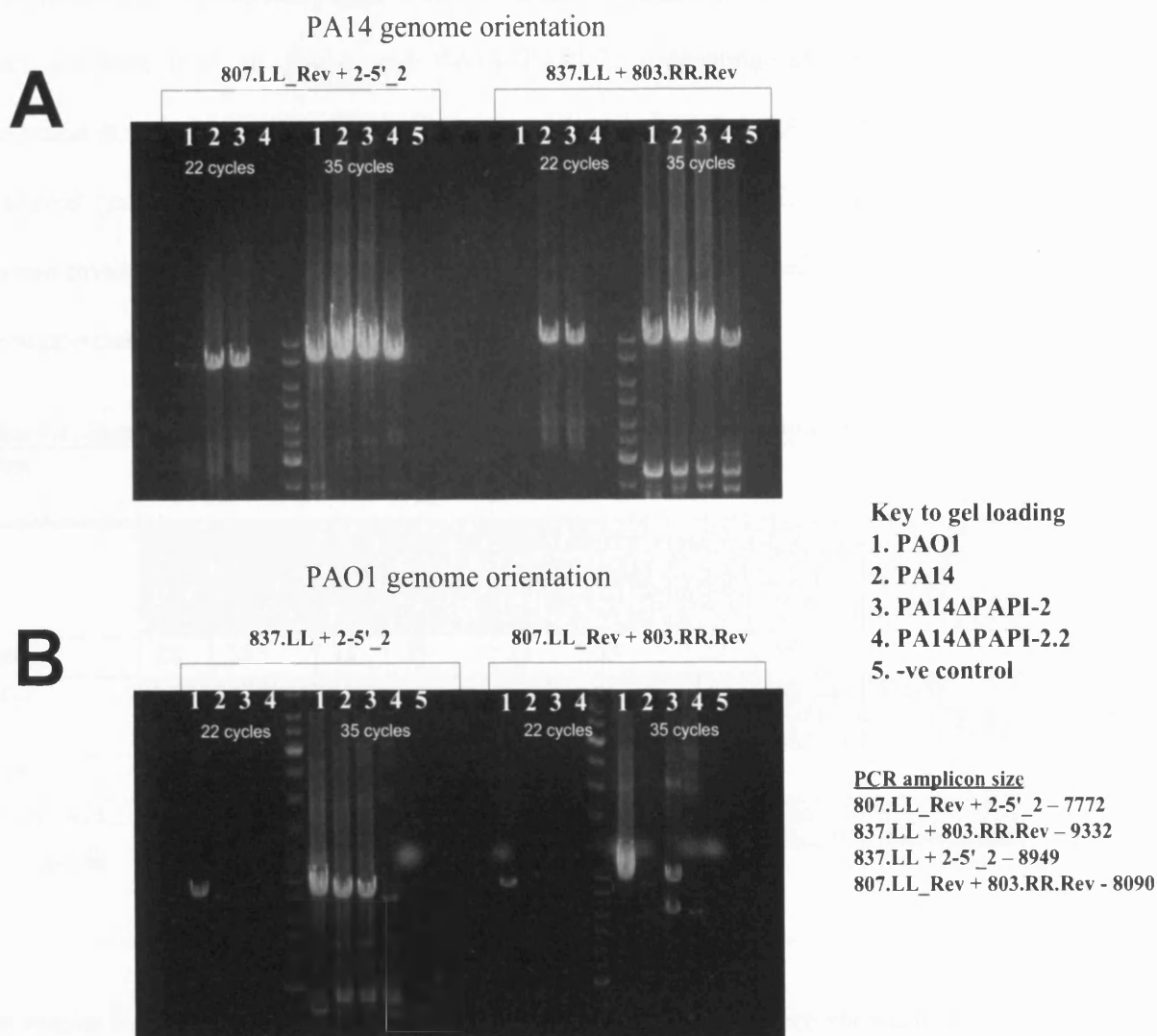
Figure 9.7: PCRs for detection of *rrn* operon inversions.
PCRs amplified for 22 cycles and 35 cycles are shown as semi-quantitative measure of the relative abundance of each orientation in a sample. A. PCRs to detect PA14 genome orientations B. PCRs to detect PAO1 genome orientation.

Figure 9.7 A shows the results for 'PA14 genome orientation' this data is summarised in

Table 9.1. It seems that PA14 and PA14ΔPAPI-2 share the same genome structure with

both sets of primers producing bright bands at 22 cycles suggesting this is the

predominant orientation in these two genomes. While PA14ΔPAPI-2.2 and PAO1 did

241

not produce bands with either primer set until 35 cycles (except for a very faint band at cycle 22 for PAO1 with 807.LL_rev + 2-5'_2). This suggested that in both PAO1 and PA14ΔPAPI-2.2 populations, cells with the 'PA14 orientation' do exist but in much lower numbers than in PA14 and PA14ΔPAPI-2, suggesting an alternative *rrn* orientation is dominant. This finding therefore demonstrated that PA14ΔPAPI-2.2 had an altered genome structure compared to PA14 and PA14ΔPAPI-2, suggesting that a genome inversion has occurred in this strain between an as yet undefined combination of *rrn* operons.

Table 9.1: Summary of the PCRs results of the *rrn*A and *rrn*B orientation PCRs

Strain	PA14 orientation		PAO1 orientation		Dominate orientation
	807.LL_rev + 2-5'_2	837.LL + 803.RR.rev	807.LL_rev + 803.RR.rev	837.LL + 2-5'_2	
Cycles	22 | 35	22 | 35	22 | 35	22 | 35	
PAO1	+ | +++	+ | +++	++ | ++++	++ | ++++	PAO1
PA14	++ | ++++	++ | ++++	+ | +++	/ | +	PA14
PA14ΔPAPI-2	++ | ++++	++ | ++++	+ | +++	/ | ++	PA14
PA14ΔPAPI-2.2	/ | +++	/ | ++	/ | +	/ | +	Unknown

The results for the PCRs to detect the 'PAO1 genome orientation' are shown in Figure 9.7 B and summarised in Table 9.1. The results show that as expected that in PAO1 that this was the dominant genomic orientation producing bright bands at 22 cycles for both primer sets 807.LL_rev + 803.RR.rev and 837.LL + 2-5'_2. Interestingly, strains PA14, PA14ΔPAPI-2 and PA14ΔPAPI-2.2 all produced different amounts of products with the two primer sets. This data is overviewed in Table 9.1, which shows the varying intensities of the PCR amplicons produced. This result suggested that all three strains possessed varying extents of the alternative PAO1-like genome structure in populations

derived from these strains. In particular this demonstrated that strain PA14ΔPAPI-2.2 has a divergent genome structure population from PAO1, PA14 and PA14ΔPAPI-2 in terms of the *rrn* operons (Table 9.1). This finding shows that even within the non-dominate genome orientation there seems to be variation between strains, suggesting that there is variation in genomic structure even of the rare orientations.

9.9 $tRNA^{Lys}$ mediated genome inversions

A previously mentioned it had been reported that inversions have been seen between strains at the $tRNA^{Lys}$. However in the PA14 genome $tRNA^{Lys}$ are orientated in the same direction and so are direct repeats, so it should not be possible for a genome inversion to occur. But if a genome inversion between two of the *rrn* operons occur as shown in Figure 9.8 A, then the two $tRNA^{Lys}$ genes are inverted repeats and are therefore capable of inversions as shown in Figure 9.8 B. To test if this was the case PCRs were carried out using the tRIP primers for $tRNA^{Lys10}$ and $tRNA^{Lys47}$ located in the flanks up and downstream of the $tRNA^{Lys}$ genes. Normally the primers pairs; tRNA_Lys10-U / D and tRNA_Lys47-U / D will amplify the across the tRNA gene at the respective locations (Figure 9.8 B i).

However if a genomic inversion had occurred then it should be possible to use the following non-cognate primers as paired sets and still obtain amplicons: tRNA_Lys10-U + tRNA_Lys47-D and tRNA_Lys47-U + tRNA_Lys10-D (Figure 9.8 B ii) . This was carried out and the results are shown in Figure 9.9. The PCRs were carried out using tRNA_Lys10-U + tRNA_Lys47-D in both PA14 and PA14ΔPAPI-2 at two concentrations as before.
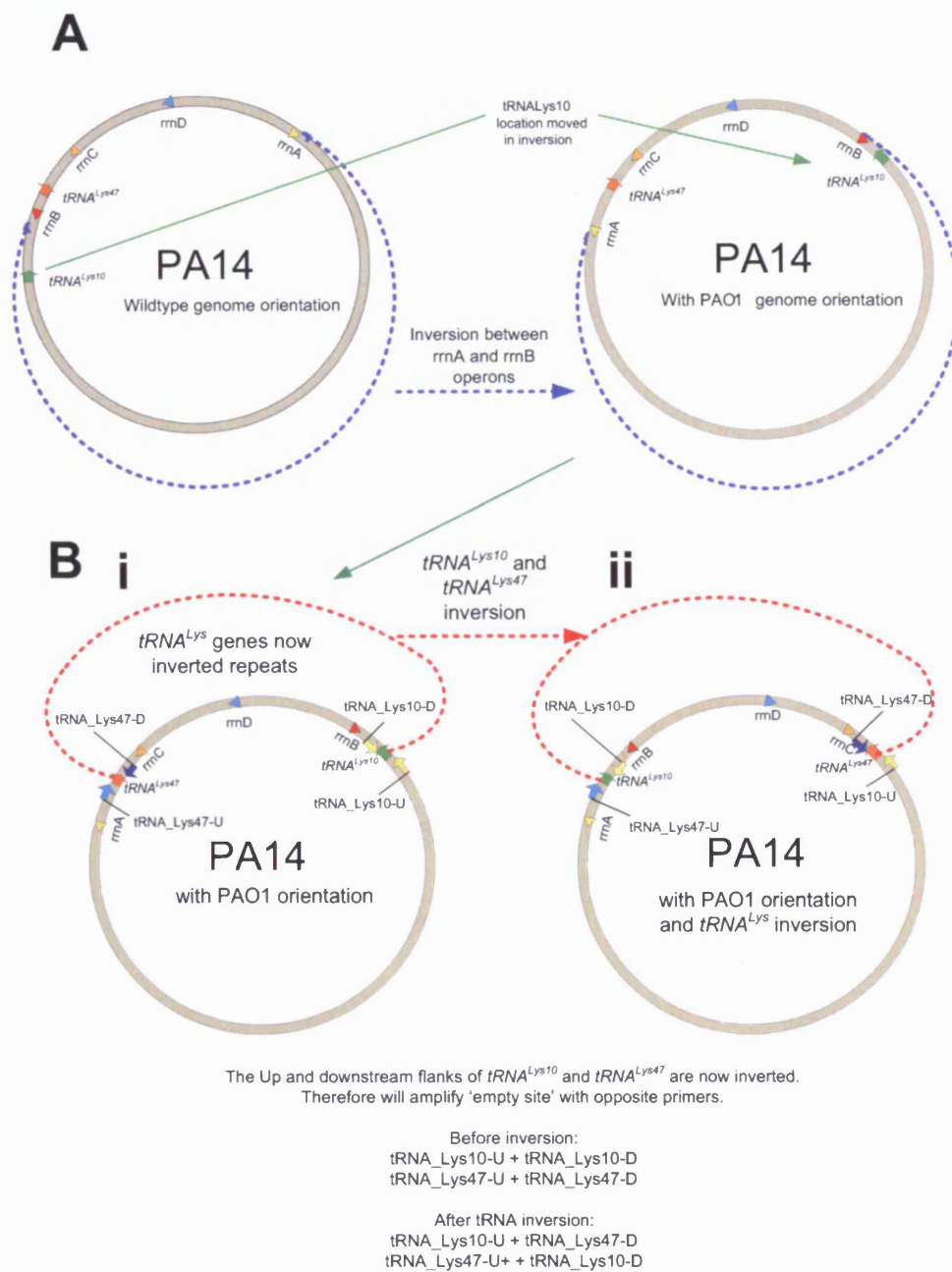
Figure 9.8: *tRNA^Lys* inversions in PA14.
A. *rrnA* and *rrnB* operon inversions change orientation of the tRNA^Lys genes from direct to inverted repeats. **B.** Theoretical *tRNA^Lys* mediated genome inversions.

The product size predicted from the relative distances of the two primers from the $tRNA^{Lys}$ is 798bp. As can be seen in Figure 9.9 in both PA14 and PA14ΔPAPI-2 at both the high and low (10 ng) concentrations of DNA a ~800 bp band is produced. This result suggests that the $tRNA^{Lys10}$ upstream and the $tRNA^{Lys47}$ downstream flanks are found aligned together (Figure 9.7) in the population. This results suggests that like rrn-related inversions, $tRNA^{Lys}$ associated inversions were also manifested by cells within the population.

Key to gel loading

1. PA14: High concentration template
2. PA14ΔPAPI-2: High concentration template
3. PA14: 10 ng template
4. PA14ΔPAPI-2: 10ng template
5. -ve control

PCR reactions

Primers: tRNA_Lys10U + tRNA_Lys47D
Expected PCR product: 798 bp
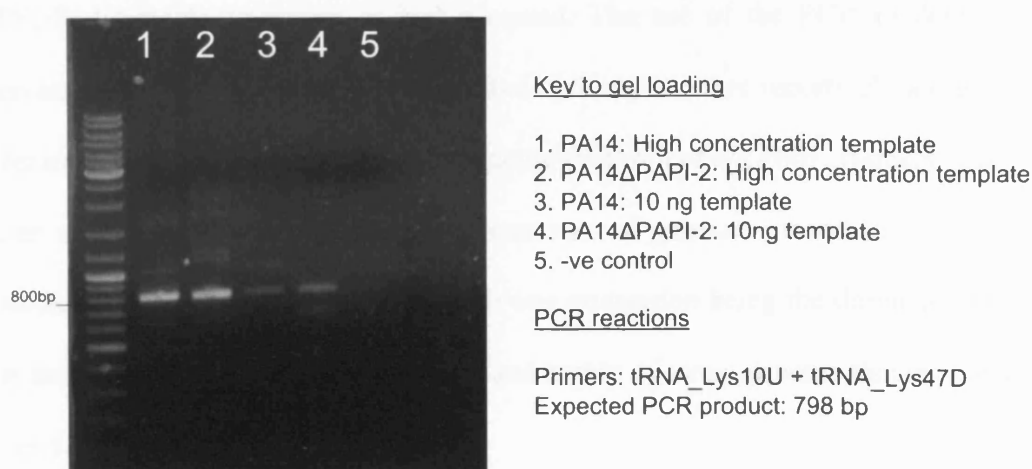
Figure 9.9: PCR amplification detection of the inversion of $tRNA^{Lys}$ flanking regions.

9.10   Discussion

The use of the combination of *in silico* generation of virtual genomes representative of a range of strains, *in silico* PFGE and experimental PFGE was found to be a very useful strategy in analysing and predicting genome structure and confirming large scale deletions. The results obtained via these *in silico–in vitro* PFGE experiments have confirmed the original data obtained by qPCR analysis that demonstrated that in PA14ΔPAPI-2.1 the PAPI-1 island had appeared to re-locate or hop into $tRNA^{Lys10}$ from its original $tRNA^{Lys47}$ site. In the second independently constructed PAPI-2-minus mutant, strain PA14ΔPAPI-2.2, PFGE yet again confirmed the qPCR finding that PAPI-

1 was integrated into both $tRNA^{Lys}$ sites at an equal frequency. No large chromosomal inversions or deletions were detected by PFGE in either PA14ΔPAPI-2.1 or PA14ΔPAPI-2.2 to suggest a possible basis for the distinct PAPI-1 integration site patterns. However due to the limits of the enzyme cut sites (Figure 9.4 A and B) and resolution of the gels, genomic inversions in rrn operons that had not affected the PacI / I-CeuI or SpeI band patterns could not be ruled out.

Further studies into genomic inversions were therefore required to investigate if a non-PFGE detectable inversion or had occurred. The use of the PCR to detect the rrn inversions was enlightening, it seems that contrary to other reports P. aeruginosa like Yersina pestis has a highly dynamic genome (Parkhill et al., 2001, Barekzi et al., 2000, Lee et al., 2006b). With multiple orientations of genome present in the population mediated by rrn operon inversions with one orientation being the dominate orientation in the population. This suggests a fluid and highly dynamic genome that is able to adapt rapidly.

The PCR assays aimed at detecting inversions associated with rrnA and rrnB demonstrated that PA14ΔPAPI-2.2 had undergone genomic inversion that had aligned the rrnA and rrnB operons distinctly compared to the arrangement of these operons in PA14 and PA14ΔPAPI-2, meaning that the flanking regions of rrnA and rrnB were no longer aligned in either orientation (PAO1 and PA14). This suggests that an inversion mediated between rrn A and B has occurred with rrn C and D changing the genomic structure. This finding could be a factor in the distinct PAPI-1 integration site patterns of the two mutants that were engineered to be identical. This rrn mediated inversion must be in a manner that has unaffected the general location of the PacI / I-CeuI and SpeI restriction sites as no major genomic inversions were detected by PFGE. A further investigation using primers for the other rrn operons is required to define which of the

rrn operons (*rrn* A, B, C and D) the inversion has occurred. Also of interest was the variation in the relative presence of the 'PAO1 orientation' products between PA14, PA14ΔPAPI-2 and PA14ΔPAPI-2.2 which suggests there is variation in the presence of the rarer orientations between these strains. This again like the inversion in PA14ΔPAPI-2.2 requires more detailed investigations to determine the frequency and abundance of these alternative genome orientations.

The increased copy number of PAPI-1 in PA14ΔPAPI-2.2 suggests that perhaps the inversion occurred to balance the replicore as a result of an imbalance secondary to two copies of the large PAPI-1 having integrated into the genome. This kind of genome balancing in response to horizontal transfer of large genomic islands has been reported to occur in *Salmonella* Typhi in the response to integration of *Salmonella* pathogenicity island 7 (SPI7) (Liu *et al.*, 2006). Equally, it could be that PAPI-1 entered a cell with a prior genome inversion and this allowed the duplicate PAPI-1 insertions to occur.

The detection of the *tRNA^{Lys}* inversions was another interesting finding that requires more follow up work. This is very preliminary data and if it is biologically relevant is yet to be seen. None of the sequenced genomes of *P. aeruginosa* seem to have a *tRNA^{Lys}* inversion. This would be the first reported case of tRNA inversion in prokaryotes; tRNA inversions are thought to occur in yeast (Gordon *et al.*, 2009) and have been reported in both wasps (Dowton *et al.*, 2002) and in chloroplast genomes in plants (Haberle *et al.*, 2008).

In conclusion this finding suggests that bacteria like *P. aeruginosa* have highly dynamic genomes that allow for genome 'flexibility' in response to loss and gain of large horizontally acquired elements. This flexibility may act as a buffer to cushion potential detrimental effects on replichore balance and/or gene expression patterns caused by the

247

acquisition of elements that offer positive fitness benefits. In other bacterial species, such as *Salmonella*, *rrn* operon inversions could not be detected using a similar PCR assay (Helm et al., 2003) suggesting that the high frequency of genomic inversions observed in *P. aeruginosa* and previously in *Y. pestis* (Parkhill et al., 2001) may not occur in all bacterial species and maybe an adaptation to a specific lifestyle.

.

10 Final Conclusion

10.1 Genomic diversity and tRNA sites

This study set out to investigate the diversity of *P. aeruginosa* genomes and the role played by tRNA sites in mediating diversity. Using the tRNAcc program a total of 15 tRNA sites and tmRNA were identified as potential 'hotspots' for the integration of genomic islands, leading to a significant increase in the number of tRNA sites that had been identified to be targeted by mobile elements in *P. aeruginosa*. Eight tRNA sites and one tmRNA sites (nine in total) in 38 clinical isolates were investigated for patterns of island occupation. Despite the moderate number of strains analysed and the limited number of tRNA and tmRNA sites interrogated, there were twenty three different genotypes and surprisingly 42% of strains were found to have a unique pattern of occupation found in no other test strain. Furthermore, a number of tRNA sites seemed to be much more commonly occupied than others including $tRNA^{Pro21}$, $tRNA^{Gly23}$ and *tmRNA*. Why these sites are more commonly targeted remains to be investigated. It may be partly that these sites are occupied by islands which would be better classed as the 'outer core' genome comprising conserved, clone-specific islands, while tRNA sites that are less commonly occupied may harbour islands that truly belong to the recently acquired accessory genome of *P. aeruginosa*. In conclusion this study further cemented the role of tRNA sites as major 'hotspots' for the integration of horizontally acquired DNA in *P. aeruginosa*.

10.2 The contribution of genomic islands in *P. aeruginosa* to fitness and virulence

This study also sought to demonstrate the role of genomic islands in the virulence and fitness of *P. aeruginosa* by examining mutants harbouring deletions of four different

islands integrated into three different tRNA sites alongside their cognate wild-type parent strains. This 'whole island' deletion approach with treated genomic islands as '*en bloc*' entities was hypothesised to potentially reveal traits that would remain hidden were a single gene knock out approach to be taken. Data generated through this study has clearly demonstrated that deletion of large genomic islands is a suitable method for initial mapping of genes coding for virulence factors on large regions of horizontally acquired DNA. Given the level of diversity seen in *P. aeruginosa* this would be a powerful tool to carry out further investigations of other genomic islands present in this bacterium.

The role of genomic islands in the virulence of *P. aeruginosa* was demonstrated in strain PA14 by the deletion of PAPI-1, PAPI-2, and/or the *tRNA*^{Pro21} island. Loss of each island independently resulted in varying degrees of attenuation relative to PA14. Furthermore, loss of more than one island appeared to result in synergistic attenuation. In particular, the double PAPI-1 and PAPI-2 mutant (PA14Δ1Δ2), that had lost both recognized pathogenicity islands, exhibited a near complete attenuation (10% vs 100% mortality) during the first 48 h period post intra-nasal infection relative to PA14 in acute murine pneumonia model (Carter, 2009). These data demonstrate the complex relationships not only between the core genome and individual islands but also potentially between different, co-resident horizontally acquired DNA elements, and confirm the truly multilateral nature of the bacterial 'genomic dialogue'. The discovery that the *tRNA*^{Pro21} island is involved in virulence is a novel finding as this genomic island has not been previously reported to play a role in virulence. This work clearly demonstrated the combinatorial nature of virulence in *P. aeruginosa* which almost certainly required multiple, web-like interactions between core genome- and accessory genome-encoded virulence factors.

10.3 PAPI-1 'island hopping' and genome dynamics

This work investigated the dynamic nature of the integration and excision of PAPI-1. The PAPI-1 island was investigated in a range of distinct strain backgrounds and and a set of isogenic mutants derived from PA14. The results showed that the integration of PAPI-1 was a truly dynamic process. In some strains the majority of copies of PAPI-1 integrated into both $tRNA^{Lys}$ equally, while in others the island was almost exclusively integrated into only one $tRNA^{Lys}$. This integration in one site only was seemingly caused by the presence another genomic island being inserted into the other $tRNA^{Lys}$ site. As deletion of the island inserted at this $tRNA^{Lys}$ allowed integration of the PAPI-1 into the other site. In one such deletion strain PA14ΔPAPI-2 the majority of copies of PAPI-1 were found to be integrated in $tRNA^{Lys10}$. While in a second, independently derived PAPI-2-minus mutant (PA14ΔPAPI-2.2) and in PAO1ΔLys10 the deletion the $tRNA^{Lys10}$ islands caused PAPI-1 to integrate into both $tRNA^{Lys10}$ sites. The reason that the presence of a second genomic island integrated at the $tRNA^{Lys10}$ prevented integration of PAPI-1 is unknown. The use of a novel 'Third $attB$ site' approach showed that the presence of the FRT scar integrated as part of the island deletion process or the orientation of the newly introduced third $attB$ site does not appear to affect the integration preferences of PAPI-1. This work validated the use of a 'Third site' as a powerful tool for the study of the site-specific recombination dynamics of genomic islands such as PAPI-1.

Bioinformatics analysis showed the presence of A/T rich regions with high DNA curvature that are predominant targets for H-NS binding within the PA14 and PAO1 $tRNA^{Lys10}$ islands. Linked with the report that the PAO1 $tRNA^{Lys10}$ island is bound by MvaT / MvaU, *P. aeruginosa* H-NS-like proteins, the identification of similar A/T rich regions with high DNA curvature on both islands supports the hypothesis that PAPI-2

may also be bound by MvaT / MvaU, potentially preventing or hindering integration of PAPI-1 into the $tRNA^{Lys10}$ site. Further work is underway to address this idea.

Further investigations were carried out to investigate the distinct PAPI-1 integration site patterns of the two mutants that were engineered to be identical. The strains were investigated using PFGE and PCR approaches to identify potential *rrn* operon-mediated inversions. No obvious inversions could be detected by PFGE. However, the very much more sensitive PCR-based approach yielded firm evidence of multiple genomic structures and *rrn* operon-associated inversions affecting a minority of bacterial cells within the clonal population arising from of a single strain of *P. aeruginosa*. As expected these data confirmed that the previously reported genome orientations for PAO1 and PA14 (Lee *et al.*, 2006b, Mathee *et al.*, 2008) were conceptually correct but that rather than representing an absolute genomic configuration these sequences represented the major dominant orientation within a population that also contained other minor genomic variants. This is first time that such a high frequency of genomic inversions has been identified in *P. aeruginosa*. This work also demonstrated that strain PA14ΔPAPI-2.2 has undergone an as yet undefined *rrn* operon-linked inversion that appeared to have not affected PFGE restriction profiles examined. This suggests that the multiple integration of PAPI-1 in the two $tRNA^{Lys}$ sites in this strain compared to single integration in both PA14 and PA14ΔPAPI-2 is either the response to, or the cause of an *rrn* operon inversion. If this is the case it suggests that the genome dynamics in response to the integration and loss of mobile elements is a highly dynamic process that is continually shaping bacterial genome structure in *P. aeruginosa* and potentially many other bacterial species as well.

The stability of PAPI-1 in the population was investigated using an island probing strategy (Rajakumar *et al.*, 1997). These experiments revealed the deletion rate of PAPI-

1 to be ~ 5 x 10^{-4} making PAPI-1 the most unstable genomic island reported so far. This rate was found to be similar in different host strain backgrounds suggesting that the islands stability is uniform across host strains and independent of the host genome's makeup. In addition, a study aimed at examining the possible association between PAPI-1 integration sites, number of islands integrated per cell and the stability of PAPI-1 within the population was performed. This analysis demonstrated a potential correlation between the stability of PAPI-1 within a population of cells and the number of integrated copies per genome. This finding therefore suggests that the overall genome structure of *P. aeruginosa* dictates the stability of PAPI-1 in the population directly by allowing or preventing multiple integrations of PAPI-1. Further work is required to identify the mechanisms underpinning this process.

To conclude this work has demonstrated that diverse tRNA associated genomic islands are key to the fitness and virulence of *P. aeruginosa*. Further it seems that the presence of islands and their chosen sites of integration within the *P. aeruginosa* population is a very much more dynamic process than previously thought and that this lively shuffling process may be playing a major part in the shaping of the genome structure, gene expression patterns, phenotype and even longer term evolutionary outcomes. Importantly, the question of whether this level of genomic dynamism is unique to *P. aeruginosa* or if it is a feature of other bacterial pathogens remains to be seen.

11 Appendix A

All media were purchased from Sigma unless otherwise stated in parentheses.
1 M CaCl$_2$
147 g CaCl$_2$·2H$_2$O
H$_2$O to 1 litre

EDTA (ethylenediaminetetraacetic acid), 0.5 M (pH 8.0)
186.1 g disodium EDTA dihydrate in 700 ml H$_2$O.
pH to 8.0 with 10 M NaOH (~50 ml).
H$_2$O to 1 litre and filter sterilize.

Gram-positive lysis buffer
6mM Tris-HCl,
100mM EDTA Na$_2$,
M NaCl,
0.5% (w/v) Brij 58,
0.2% (w/v) sodium deoxycholate,
0.5% lauroyl sarcosine,
pH7.5 Store at RT°.

Gram-negative lysis buffer
1% (w/v) lauroyl sarcosine,
500mM EDTA Na$_2$ pH 9.5.
Filter sterilise and store at RT°.

6 x loading dye
11 mM EDTA
3.3 mM Tris-HCL
2.5% (w/v) Ficoll 400
0.0017 % SDS
0.15 % Orange G
pH 8.0

Luria Bertani agar (LA)
5 g Bacto-tryptone (Difco)
2.5g Bacto-yeast extract (Difco)
5 g NaCl
7.5 g Bacto-agar (Difco)
Up to 500 ml in ddH2O
Autoclaved at 121 °C at 15 psi for 15 min

Luria Bertani broth (LB)
5 g Bacto-tryptone
2.5g Bacto-yeast extract
5 g NaCl
Up to 500 ml in ddH2O
Autoclaved at 121 °C at 15 psi for 15 m

5× M9 minimal salts

30 g Na_2HPO_4
15 g KH_2PO_4
5 g NH_4Cl
2.5 g NaCl
15 mg $CaCl_2$ (optional)
Adjust volume to 1 litre with H_2O
Filter sterilise
Before use, dilute 1:5 with water, and sterilize by autoclaving. Cool to <50°C and add:
1 ml 1 M $MgSO_4$ and 10 ml 20% glucose (or other carbon source), filter sterilize.
Store indefinitely at room temperature

5x M63 Stock solution

10g $(NH_4)_2SO_4$
68g KH_2PO_4
2.5mg $FeSO_4$
Made up to 1 litre with distilled water
Adjust to pH 7.0 with KOH
Autoclave

1x M63 (0.2% glucose, 1 mM $MgSO_4$, 0.5% casamino acids (CAA)

Make and autoclave:
50ml 20% (w/v) glucose solution
50ml 20% (w/v) casamino acids (CAA)
When the 5x M63 has cooled to room temperature add 1ml of sterile 1M $MgSO_4$.7H20.
To make 100ml M63 with glucose (0.2%), MgSO4 (1 mM), and casamino acids (CAA, 0.5%) add
to a sterile Durant bottle:
- 1ml 20% (w/v) glucose solution
- 2.5ml 20% (w/v) casamino acids (CAA)
- 20ml 5x M63 1mM M $MgSO_4$
- 76.5ml Sterile distilled H_2O

1 M $MgSO_4$

24.6 g $MgSO_4 \cdot 7H_2O$
H_2O to 100 ml

5 M NaCl

292 g NaCl
H2O to 1 litre

0.9% NaCl (saline)

9 g NaCl (154 mM final; 0.9% w/v)
H2O to 1 litre
Filter sterilise

10 M NaOH

Dissolve 400 g NaOH in 450 ml H2O
Add H2O to 1 litre

PBS (phosphate-buffered saline)

10× stock solution, 1 litre:
80 g NaCl

2 g KCl
11.5 g $Na_2HPO_4 \cdot 7H_2O$
2 g KH_2PO_4

Working solution, pH 7.3:
137 mM NaCl
2.7 mM KCl
4.3 mM Na_2 HPO_4 .$7H_2O$
1.4 mM KH_2PO_4

20% (w/v) SDS
20 g sodium dodecyl sulfate (SDS) in H2O in a total volume of 100 ml with stirring. Heat to dissolve, filter sterilise.

SE buffer
75mM NaCl,
25mM EDTA Na_2 (from 10x stock).
Filter sterilise and store at 4°C.

SOC
4 g Bacto-tryptone
1 g Bacto-yeast extract
0.1 g NaCl
Made up to 200 ml in ddH2O
Autoclaved at 121 °C at 15 psi for 15 min
After autoclaving add to 10 ml of medium:
50 µl of filter sterilised 2 M $MgCl_2$
200 µl of filter sterilised 1 M glucose

TAE (Tris/acetate/EDTA) electrophoresis buffer
50× stock solution:
242 g Tris base
57.1 ml glacial acetic acid
37.2 g $Na_2EDTA \cdot 2H_2O$
H2O to 1 liter

TBE (Tris/borate/EDTA) electrophoresis buffer
10× stock solution, 1 liter:
108 g Tris base (890 mM)
55 g boric acid (890 mM)
40 ml 0.5 M EDTA, pH 8.0 (see recipe; 20 mM)

TE buffer
10 mM Tris-HCl
1 mM EDTA
Made from sterile 1 M stock of Tris-HCl (pH 7.5) and 500 mM stock of EDTA (pH 8.0)

1 M Tris·Cl (pH 7.4 and pH8.0)

121 g Tris base in 800 ml H_2O

Adjust to desired pH with 1 M HCl

Adjust volume to 1 litre with H_2O

~70 ml HCl is needed to achieve a pH 7.4 solution and ~42 ml for a solution that is pH 8.0.

VBMM stock solution

500 ml of 10 x VBMM stock solution:

30 g l- 1 of trisodium citrate,

20 g l- 1 of citric acid,

100 g l- 1 of K_2HPO_4 ,

35 g l- 1 of $NaNH_4PO_4$ 4H2O,

pH 7;

Autoclave and store at room temperature (20–25 °C).

VBMM plates: 1 litre of media for VBMM plates

15 g of bacto-agar in 900 ml of H_2O

Add 100 ml of autoclaved 10x VBMM stock solution.

Cool to ~50 °C before adding 1 ml of 1 M $MgSO_4$ and 0.1 ml of 1 M $CaCl_2$ (the $CaCl_2$ and $MgSO_4$ stock solutions are sterilized by autoclaving).

12 Appendix B: PFGE Restriction fragments for *Pac*I / I-*ceu*I digested PAO1, PA14, and isogenic mutants generated by Vector NTI.

PA01

1750358: PA01 genome: PacI(2244309) - PacI(3994667)

795152: PA01 genome: PacI(3994667) - I-CeuI(4789819)

775484: PA01 genome: I-CeuI(5265347) - I-CeuI(6040831)

659923: PA01 genome: PacI(66094) - I-CeuI(726017)

623015: PA01 genome: I-CeuI(726017) - PacI(1349032)

537199: PA01 genome: PacI(1349032) - PacI(1886231)

475528: PA01 genome: I-CeuI(4789819) - I-CeuI(5265347)

326383: PA01 genome: PacI(1886231) - PacI(2212614)

289667: PA01 genome: I-CeuI(6040831) - PacI(66094)

31695: PA01 genome: PacI(2212614) - PacI(2244309)

PA14

1826427: PA14 genome: PacI(1563466) - PacI(3389893)

826459: PA14 genome: I-CeuI(737007) - PacI(1563466)

776471: PA14 genome: I-CeuI(5537279) - I-CeuI(6313750)

672553: PA14 genome: PacI(64454) - I-CeuI(737007)

597785: PA14 genome: PacI(4355480) - I-CeuI(4953265)

584014: PA14 genome: I-CeuI(4953265) - I-CeuI(5537279)

537122: PA14 genome: PacI(3748445) - PacI(4285567)

326858: PA14 genome: PacI(3421587) - PacI(3748445)

288352: PA14 genome: I-CeuI(6313750) - PacI(64454)

69913: PA14 genome: PacI(4285567) - PacI(4355480)

31694: PA14 genome: PacI(3389893) - PacI(3421587)

PA14ΔPAPI-1

1826427: PA14 dPAPI-1 genome: PacI(1563466) - PacI(3389893)

826459: PA14 dPAPI-1 genome: I-CeuI(737007) - PacI(1563466)

776471: PA14 dPAPI-1 genome: I-CeuI(5429323) - I-CeuI(6205794)

672553: PA14 dPAPI-1 genome: PacI(64454) - I-CeuI(737007)

597785: PA14 dPAPI-1 genome: PacI(4355480) - I-CeuI(4953265)

537122: PA14 dPAPI-1 genome: PacI(3748445) - PacI(4285567)

476058: PA14 dPAPI-1 genome: I-CeuI(4953265) - I-CeuI(5429323)

326858: PA14 dPAPI-1 genome: PacI(3421587) - PacI(3748445)

288352: PA14 dPAPI-1 genome: I-CeuI(6205794) - PacI(64454)

69913: PA14 dPAPI-1 genome: PacI(4285567) - PacI(4355480)

31694: PA14 dPAPI-1 genome: PacI(3389893) - PacI(3421587)

<u>PA14 ΔPAPI-2 - PAPI-1 in Lys10 only</u>

1826427: PA14 dPAPI-2 with PAPI-I in lys10 only genome: PacI(1563466) - PacI(3389893)

826459: PA14 dPAPI-2 with PAPI-I in lys10 only genome: I-CeuI(737007) - PacI(1563466)

776471: PA14 dPAPI-2 with PAPI-I in lys10 only genome: I-CeuI(5526864) - I-CeuI(6303335)

695355: PA14 dPAPI-2 with PAPI-I in lys10 only genome: PacI(4355480) - I-CeuI(5050835)

672553: PA14 dPAPI-2 with PAPI-I in lys10 only genome: PacI(64454) - I-CeuI(737007)

537122: PA14 dPAPI-2 with PAPI-I in lys10 only genome: PacI(3748445) - PacI(4285567)

476029: PA14 dPAPI-2 with PAPI-I in lys10 only genome: I-CeuI(5050835) - I-CeuI(5526864)

326858: PA14 dPAPI-2 with PAPI-I in lys10 only genome: PacI(3421587) - PacI(3748445)

288352: PA14 dPAPI-2 with PAPI-I in lys10 only genome: I-CeuI(6303335) - PacI(64454)

69913: PA14 dPAPI-2 with PAPI-I in lys10 only genome: PacI(4285567) - PacI(4355480)

31694: PA14 dPAPI-2 with PAPI-I in lys10 only genome: PacI(3389893) - PacI(3421587)

<u>PA14 ΔPAPI-1 - PAPI-1 in Lys47 only</u>

1826427: PA14 dPAPI-2 genome: PacI(1563466) - PacI(3389893)

826459: PA14 dPAPI-2 genome: I-CeuI(737007) - PacI(1563466)

776471: PA14 dPAPI-2 genome: I-CeuI(5526904) - I-CeuI(6303375)

672553: PA14 dPAPI-2 genome: PacI(64454) - I-CeuI(737007)

587410: PA14 dPAPI-2 genome: PacI(4355480) - I-CeuI(4942890)

584014: PA14 dPAPI-2 genome: I-CeuI(4942890) - I-CeuI(5526904)

537122: PA14 dPAPI-2 genome: PacI(3748445) - PacI(4285567)

326858: PA14 dPAPI-2 genome: PacI(3421587) - PacI(3748445)

288352: PA14 dPAPI-2 genome: I-CeuI(6303375) - PacI(64454)

69913: PA14 dPAPI-2 genome: PacI(4285567) - PacI(4355480)

31694: PA14 dPAPI-2 genome: PacI(3389893) - PacI(3421587)

<u>PA14 ΔPAPI-2 PAPI-1 in both Lys10 and Lys47</u>

1826427: PA14 dPAPI-2 10 and 47 with PAPI-I in lys10 and ly47: PacI(1563466) - PacI(3389893)

826459: PA14 dPAPI-2 10 and 47 with PAPI-I in lys10 and ly47: I-CeuI(737007) - PacI(1563466)

776471: PA14 dPAPI-2 10 and 47 with PAPI-I in lys10 and ly47: I-CeuI(5634897) - I-CeuI(6411368)

695355: PA14 dPAPI-2 10 and 47 with PAPI-I in lys10 and ly47: PacI(4355480) - I-CeuI(5050835)

672553: PA14 dPAPI-2 10 and 47 with PAPI-I in lys10 and ly47: PacI(64454) - I-CeuI(737007)

584062: PA14 dPAPI-2 10 and 47 with PAPI-I in lys10 and ly47: I-CeuI(5050835) - I-CeuI(5634897)

537122: PA14 dPAPI-2 10 and 47 with PAPI-I in lys10 and ly47: PacI(3748445) - PacI(4285567)

326858: PA14 dPAPI-2 10 and 47 with PAPI-I in lys10 and ly47: PacI(3421587) - PacI(3748445)

288352: PA14 dPAPI-2 10 and 47 with PAPI-I in lys10 and ly47: I-CeuI(6411368) - PacI(64454)

69913: PA14 dPAPI-2 10 and 47 with PAPI-I in lys10 and ly47: PacI(4285567) - PacI(4355480)

31694: PA14 dPAPI-2 10 and 47 with PAPI-I in lys10 and ly47: PacI(3389893) - PacI(3421587)

1826427: PA14 dPAPI-1 dPAPI-2 genome: PacI(1563466) - PacI(3389893)

826459: PA14 dPAPI-1 dPAPI-2 genome: I-CeuI(737007) - PacI(1563466)

776471: PA14 dPAPI-1 dPAPI-2 genome: I-CeuI(5418830) - I-CeuI(6195301)

672553: PA14 dPAPI-1 dPAPI-2 genome: PacI(64454) - I-CeuI(737007)

587322: PA14 dPAPI-1 dPAPI-2 genome: PacI(4355480) - I-CeuI(4942802)

537122: PA14 dPAPI-1 dPAPI-2 genome: PacI(3748445) - PacI(4285567)

476028: PA14 dPAPI-1 dPAPI-2 genome: I-CeuI(4942802) - I-CeuI(5418830)

326858: PA14 dPAPI-1 dPAPI-2 genome: PacI(3421587) - PacI(3748445)

288352: PA14 dPAPI-1 dPAPI-2 genome: I-CeuI(6195301) - PacI(64454)

69913: PA14 dPAPI-1 dPAPI-2 genome: PacI(4285567) - PacI(4355480)

31694: PA14 dPAPI-1 dPAPI-2 genome: PacI(3389893) - PacI(3421587)

PA14ΔPro21

1808412: PA14 genome dpro21: PacI(1563466) - PacI(3371878)

826459: PA14 genome dpro21: I-CeuI(737007) - PacI(1563466)

776471: PA14 genome dpro21: I-CeuI(5519264) - I-CeuI(6295735)

672553: PA14 genome dpro21: PacI(64454) - I-CeuI(737007)

597785: PA14 genome dpro21: PacI(4337465) - I-CeuI(4935250)

584014: PA14 genome dpro21: I-CeuI(4935250) - I-CeuI(5519264)

537122: PA14 genome dpro21: PacI(3730430) - PacI(4267552)

326858: PA14 genome dpro21: PacI(3403572) - PacI(3730430)

288352: PA14 genome dpro21: I-CeuI(6295735) - PacI(64454)

69913: PA14 genome dpro21: PacI(4267552) - PacI(4337465)

31694: PA14 genome dpro21: PacI(3371878) - PacI(3403572)

PA14 Δ1Δ2 Δpro21

1808394: PA14 dPAPI-1 dPAPI-2 dpro21: PacI(1563466) - PacI(3371860)

826459: PA14 dPAPI-1 dPAPI-2 dpro21: I-CeuI(737007) - PacI(1563466)

776471: PA14 dPAPI-1 dPAPI-2 dpro21: I-CeuI(5400797) - I-CeuI(6177268)

672553: PA14 dPAPI-1 dPAPI-2 dpro21: PacI(64454) - I-CeuI(737007)

587322: PA14 dPAPI-1 dPAPI-2 dpro21: PacI(4337447) - I-CeuI(4924769)

537122: PA14 dPAPI-1 dPAPI-2 dpro21: PacI(3730412) - PacI(4267534)

476028: PA14 dPAPI-1 dPAPI-2 dpro21: I-CeuI(4924769) - I-CeuI(5400797)

326858: PA14 dPAPI-1 dPAPI-2 dpro21: PacI(3403554) - PacI(3730412)

288352: PA14 dPAPI-1 dPAPI-2 dpro21: I-CeuI(6177268) - PacI(64454)

69913: PA14 dPAPI-1 dPAPI-2 dpro21: PacI(4267534) - PacI(4337447)

31694: PA14 dPAPI-1 dPAPI-2 dpro21: PacI(3371860) - PacI(3403554)

<u>PA14Δ2.9kbPAPI-2 (PAPI-1 with Lys10)</u>

1826427: PA14 genome d2.9kb with FRT with PAPI-1 in Lys10: PacI(1563466) - PacI(3389893)

826459: PA14 genome d2.9kb with FRT with PAPI-1 in Lys10: I-CeuI(737007) - PacI(1563466)

776471: PA14 genome d2.9kb with FRT with PAPI-1 in Lys10: I-CeuI(5534432) - I-CeuI(6310903)

702909: PA14 genome d2.9kb with FRT with PAPI-1 in Lys10: PacI(4355480) - I-CeuI(5058389)

672553: PA14 genome d2.9kb with FRT with PAPI-1 in Lys10: PacI(64454) - I-CeuI(737007)

537122: PA14 genome d2.9kb with FRT with PAPI-1 in Lys10: PacI(3748445) - PacI(4285567)

476043: PA14 genome d2.9kb with FRT with PAPI-1 in Lys10: I-CeuI(5058389) - I-CeuI(5534432)

326858: PA14 genome d2.9kb with FRT with PAPI-1 in Lys10: PacI(3421587) - PacI(3748445)

288352: PA14 genome d2.9kb with FRT with PAPI-1 in Lys10: I-CeuI(6310903) - PacI(64454)

69913: PA14 genome d2.9kb with FRT with PAPI-1 in Lys10: PacI(4285567) - PacI(4355480)

31694: PA14 genome d2.9kb with FRT with PAPI-1 in Lys10: PacI(3389893) - PacI(3421587)

13 Appendix C: tRNAcc output

Figure 1: Output from tRNAcc DNAnalyser for tRNAcc analysis of two genomes (PAO1 and PA14). tRNA

Loci with a manually assessed putative GI highlighted in **Bold**. Total number of sites identified = 7.

PAO1 # of GIs = 8			Number of manually selected GI = 2				
Hotspot delta*1000(SD)	Orient.	Start	End	Size	CDS	GC%	
5_tRNA-Gly	**-**	**785275**	**797720**	**12.45**	**0**	**56.37**	**93.59**
19_tRNA-Gly	-	2922579	2923221	0.64	0	60.96	N/D
21_tRNA-Pro	**-**	**3087538**	**3099305**	**11.77**	**0**	**56.81**	**33.91**
23_tRNA-Gly	-	3171554	3173598	2.04	0	66.36	26.92
24_tRNA-Gly	-	3171554	3173758	2.21	0	65.62	31.82
39_tRNA-Leu	+	4281752	4282138	0.39	0	60.98	N/D
49_tRNA-Asn	-	5086926	5087096	0.17	0	54.97	N/D
57_tRNA-Sec	-	5386924	5387765	0.84	0	69.24	N/D

PA14 # of GIs = 13			Number of manually selected GI = 7				
Hotspot delta*1000(SD)	Orient.	Start	End	Size	CDS	GC%	
1_tRNA-Arg	**-**	**290262**	**312957**	**22.70**	**0**	**58.53**	**36.07**
5_tRNA-Gly	**+**	**4860217**	**48951263**	**4.91**	**0**	**61.46**	**36.53**
19_tRNA-Gly	+	2658714	2661136	2.42	0	55.30	79.08
21_tRNA-Pro	**+**	**2474665**	**2492548**	**17.88**	**0**	**55.76**	**49.33**
23_tRNA-Gly	**+**	**2395783**	**2402711**	**6.93**	**0**	**65.94**	**26.77**
24_tRNA-Gly	+	2395623	2402711	7.09	0	65.74	31.04
38_tRNA-Arg	**+**	**1760612**	**1767953**	**7.34**	**0**	**56.59**	**100.38**
39_tRNA-Leu	-	1243654	1244739	1.09	0	56.72	92.64
47_tRNA-Lys	**-**	**5251440**	**5359392**	**107.95**	**0**	**59.74**	**33.27**
48_tRNA-Pro	-	5251440	5359478	108.04	0	59.73	33.36
49_tRNA-Asn	-	5251440	5359564	108.13	0	59.73	33.37
57_tRNA-Sec	-	5657286	5658406	1.12	0	59.23	35.43
64_tmRNA	**+**	**4750084**	**4755867**	**5.78**	**0**	**47.29**	**86.05**

Table 1: tRNA loci, number of strains with GI (Frequency) and strains with GIs identified using tRNAcc analyses of two genomes.

Number	Site	Frequency	Strains
1	tRNA_Arg1	2	PAO1 / PA14
2	tRNA_Gly5	2	PAO1 / PA14
3	tRNA_Pro21	2	PAO1 / PA14
4	tRNA_Gly23	2	PAO1 / PA14
5	tRNA_Arg38	1	PA14
6	tRNA_Lys47	1	PA14
7	tmRNA	1	PAO1 / PA14

Figure 2: Output from tRNAcc DNAnalyser for tRNAcc analysis of six genomes (PAO1 PA14, 2192, C3719, LES, and PACS2). tRNA Loci with a manually assessed putative GI highlighted in **Bold**. Total number of sites identified = 16.

PAO1 # of GIs = 21   **Number of manually selected GI = 5**

Hotspot	Orient. delta*1000(SD)	Start	End	Size	CDS	GC%	
1_tRNA-Arg	-	**288337**	**298815**	**10.48**	**0**	**62.19**	**60.21**
2_tRNA-Met	-	630149	630433	0.29	0	58.95	N/D
5_tRNA-Gly	-	**785077**	**797720**	**12.64**	**0**	**56.45**	**94.31**
6_tRNA-Ser	+	991351	991706	0.36	0	52.53	N/D
7_tRNA-Arg	+	991545	991706	0.16	0	57.41	N/D
10_tRNA-Lys	+	**1060432**	**1069727**	**9.30**	**0**	**53.63**	**89.68**
12_tRNA-Arg	+	1947397	1947663	0.27	0	57.68	N/D
13_tRNA-His	+	1947524	1947663	0.14	0	60.00	N/D
19_tRNA-Gly	-	2921215	2923221	2.01	0	62.68	42.24
21_tRNA-Pro	-	**3087535**	**3099305**	**11.77**	**0**	**56.80**	**33.80**
23_tRNA-Gly	-	3171531	3173598	2.07	0	66.49	29.50
24_tRNA-Gly	-	3171531	3173758	2.23	0	65.75	32.49
25_tRNA-Glu	-	3171531	3173836	2.31	0	65.52	35.01
38_tRNA-Arg	-	3778156	3778653	0.50	0	64.06	N/D
39_tRNA-Leu	+	4281752	4282139	0.39	0	60.82	N/D
47_tRNA-Lys	-	5086316	5086924	0.61	0	63.88	N/D
48_tRNA-Pro	-	5086316	5087010	0.70	0	62.16	N/D
49_tRNA-Asn	-	5086316	5087096	0.78	0	61.84	N/D
56_tRNA-Leu	-	5332103	5332253	0.15	0	56.29	N/D
57_tRNA-Sec	-	5386924	5387765	0.84	0	69.24	N/D
64_tmRNA	-	**895823**	**901519**	**5.70**	**0**	**57.17**	**79.11**

PA14 # of GIs = 20   **Number of manually selected GI = 9**

Hotspot	Orient.	Start	End	Size	CDS	GC%	delta*1000(SD)
1_tRNA-Arg	-	**278152**	**312957**	**34.81**	**0**	**59.56**	**32.39**
5_tRNA-Gly	+	**4860217**	**4895324**	**35.11**	**0**	**61.45**	**35.53**
6_tRNA-Ser	-	4659888	4660240	0.35	0	52.12	N/D
7_tRNA-Arg	-	4659888	4660046	0.16	0	55.97	N/D
10_tRNA-Lys	-	**4580199**	**4591102 1**	**0.90**	**0**	**56.46**	**49.98**
12_tRNA-Arg	-	3687016	3687279	0.26	0	57.58	N/D
13_tRNA-His	-	3687016	3687152	0.14	0	59.85	N/D
19_tRNA-Gly	+	**2658714**	**2662500**	**3.79**	**0**	**58.54**	**64.69**
21_tRNA-Pro	+	**2474665**	**2492551 1**	**7.89**	**0**	**55.76**	**49.24**
23_tRNA-Gly	+	**2395783**	**2402729**	**6.95**	**0**	**65.94**	**26.36**
24_tRNA-Gly	+	2395623	2402729	7.11	0	65.74	30.42
25_tRNA-Glu	+	2395545	2402729	7.19	0	65.66	32.53
38_tRNA-Arg	+	**1760612**	**1768453**	**7.84**	**0**	**57.01**	**95.25**
39_tRNA-Leu	-	1243653	1244739	1.09	0	56.67	93.21
47_tRNA-Lys	-	**5250828**	**5359392**	**108.57**	**0**	**59.77**	**33.10**
48_tRNA-Pro	-	5250828	5359478	108.65	0	59.76	33.19
49_tRNA-Asn	-	5250828	5359564	108.74	0	59.76	33.20
56_tRNA-Leu	-	5604033	5604183	0.15	0	56.29	N/D
57_tRNA-Sec	-	5657286	5658407	1.12	0	59.27	34.93
64_tmRNA	+	**4750084**	**4761554**	**11.47**	**0**	**52.27**	**81.92**

2192 # of GIs = 23   **Number of manually selected GI = 9**

Hotspot	Orient.	Start	End	Size	CDS	GC%	delta*1000(SD)	
1_tRNA-Arg	-	**4659214**	**4669699**	**10.49**	**0**	**61.92**	**44.39**	
2_tRNA-Met	-	**5000083**	**5010681**	**10.60**	**0**	**53.99**	**43.18**	
5_tRNA-Gly	-	**6509823**	**6553724**	**43.90**	**0**	**64.82**	**75.90**	
6_tRNA-Ser	+	6787760	6788121	0.36	0	50.55	N/D	
7_tRNA-Arg	+	6787954	6788121	0.17	0	52.98	N/D	
10_tRNA-Lys	+	6856872	6857217	0.35	0	56.65	N/D	
12_tRNA-Arg	+	828541	892697	64.16	0	63.96	70.91	
13_tRNA-His	+	828668	892697	64.03	0	63.98	70.84	
14_tRNA-Leu	+	**828807**	**892697**	**63.89**	**0**	**63.99**	**70.93**	
19_tRNA-Gly	-	1940508	1942516	2.01	0	62.82	43.31	
21_tRNA-Pro	-	**2105524**	**2168883**	**63.36**	**0**	**57.21**	**40.03**	
23_tRNA-Gly	-	**2242471**	**2466969**	**224.50**	**0**	**64.08**	**42.27**	
24_tRNA-Gly	-	2242471	2467129	224.66	0	64.08	42.07	
25_tRNA-Glu	-	2242471	2467207	224.74	0	64.08	41.98	
38_tRNA-Arg	-	3112562	3113059	0.50	0	63.05	N/D	
39_tRNA-Leu	+	3632120	3632507	0.39	0	60.57	N/D	
47_tRNA-Lys	+	**6067254**	**6152981**	**85.73**	**0**	**60.25**	**43.91**	
48_tRNA-Pro	+	6067168	6152981	85.81	0	60.24	43.96	
49_tRNA-Asn	+	6067082	6152981	85.90	0	60.24	44.01	
56_tRNA-Leu	+	5811106	5811260	0.16	0	54.19	N/D	
57_tRNA-Sec	+	5757053	5757897	0.84	0	69.35	N/D	
61_tRNA-Thr	-	**5328207**	**5335135**	**6.93**	**0**	**50.21**	**75.60**	
64_tmRNA	-	**6651839**	**6697491**	**45.65**	**0**	**59.88**	**28.58**	

C3719   # of GIs = 22   **Number of manually selected GI = 6**

Hotspot	Orient.	Start	End	Size	CDS	GC%	delta*1000(SD)	
1_tRNA-Arg	+	**3985696**	**3996183**	**10.49**	**0**	**61.96**	**44.53**	
2_tRNA-Met	+	3655204	3655491	0.29	0	58.68	N/D	
5_tRNA-Gly	-	5898833	5899081	0.25	0	61.85	N/D	
6_tRNA-Ser	+	6091413	6091768	0.36	0	52.53	N/D	
7_tRNA-Arg	+	6091607	6091768	0.16	0	57.41	N/D	
10_tRNA-Lys	+	6160552	6160897	0.35	0	56.94	N/D	
11_tRNA-Ser	+	**6188108**	**6201364**	**13.26**	**0**	**55.38**	**72.69**	
12_tRNA-Arg	+	825657	825923	0.27	0	57.68	N/D	
13_tRNA-His	+	825784	825923	0.14	0	60.00	N/D	
19_tRNA-Gly	-	1713750	1715757	2.01	0	62.60	44.39	
21_tRNA-Pro	-	**1881445**	**1897770**	**16.33**	**0**	**57.33**	**47.33**	
23_tRNA-Gly	-	**1972347**	**1979286**	**6.94**	**0**	**65.99**	**33.34**	
24_tRNA-Gly	-	1972347	1979286	6.94	0	65.99	33.34	
25_tRNA-Glu	-	1972347	1979364	7.02	0	65.92	33.56	
38_tRNA-Arg	-	2586230	2586727	0.50	0	63.86	N/D	
39_tRNA-Leu	+	3067605	3068695	1.09	0	56.46	96.21	
47_tRNA-Lys	+	**5460419**	**5542151**	**81.73**	**0**	**60.94**	**42.84**	
48_tRNA-Pro	+	5460333	5542151	81.82	0	60.93	42.87	
49_tRNA-Asn	+	5460247	5542151	81.91	0	60.92	42.90	
56_tRNA-Leu	+	5218308	5218462	0.16	0	54.19	N/D	
57_tRNA-Sec	+	5164180	5165024	0.84	0	69.23	N/D	
64_tmRNA	-	**5997299**	**6001555**	**4.26**	**0**	**57.27**	**71.00**	

LES # of GIs = 22 **Number of manually selected GI = 6**

Hotspot	Orient.	Start	End	Size	CDS	GC%	delta*1000(SD)
1_tRNA-Arg	-	**281281**	**291765**	**10.48**	**0**	**62.01**	**51.14**
2_tRNA-Met	-	621278	621562	0.29	0	58.95	N/D
5_tRNA-Gly	+	5070253	5070490	0.24	0	60.08	N/D
6_tRNA-Ser	-	4846686	4847038	0.35	0	52.12	N/D
7_tRNA-Arg	-	4846686	4846844	0.16	0	56.60	N/D
10_tRNA-Lys	-	4777616	4777958	0.34	0	56.27	N/D
12_tRNA-Arg	-	3920422	3920685	0.26	0	57.58	N/D
13_tRNA-His	-	3920422	3920558	0.14	0	59.85	N/D
19_tRNA-Gly	+	**2796710**	**29098221**	**13.11**	**0**	**64.39**	**38.96**
20_tRNA-Ser	+	**2690385**	**27405705**	**0.19**	**0**	**59.17**	**29.38**
21_tRNA-Pro	+	**2504343**	**2549289**	**44.95**	**0**	**56.93**	**52.96**
23_tRNA-Gly	+	**2421548**	**2428489**	**6.94**	**0**	**65.93**	**29.06**
24_tRNA-Gly	+	2421388	2428489	7.10	0	65.73	32.00
25_tRNA-Glu	+	2421310	2428489	7.18	0	65.65	34.10
38_tRNA-Arg	+	**1814342**	**1824687**	**10.35**	**0**	**56.00**	**78.47**
39_tRNA-Leu	-	1247841	1248928	1.09	0	56.53	93.83
47_tRNA-Lys	-	5421444	5422052	0.61	0	64.20	N/D
48_tRNA-Pro	-	5421444	5422138	0.70	0	62.45	N/D
49_tRNA-Asn	-	5421444	5422224	0.78	0	62.10	N/D
56_tRNA-Leu	-	5665930	5666080	0.15	0	56.29	N/D
57_tRNA-Sec	-	5719424	5720265	0.84	0	69.24	N/D
64_tmRNA	+	**4966312**	**4972140**	**5.83**	**0**	**57.01**	**76.76**

PACS2 # of GIs = 22 **Number of manually selected GI = 11**

Hotspot	Orient.	Start	End	Size	CDS	GC%	delta*1000(SD)
2_tRNA-Met	-	**616572**	**620877**	**4.31**	**0**	**55.02**	**70.36**
5_tRNA-Gly	-	**1359799**	**1367375**	**7.58**	**0**	**52.91**	**55.00**
6_tRNA-Ser	+	1568533	1568888	0.36	0	52.53	N/D
7_tRNA-Arg	+	1568727	1568888	0.16	0	57.41	N/D
10_tRNA-Lys	+	1637615	1637960	0.35	0	56.65	N/D
12_tRNA-Arg	+	2507714	2507980	0.27	0	57.30	N/D
13_tRNA-His	+	2507841	2507980	0.14	0	59.29	N/D
19_tRNA-Gly	-	**3492032**	**3584023**	**91.99**	**0**	**62.83**	**29.41**
21_tRNA-Pro	-	**3750145**	**3796331**	**46.19**	**0**	**56.97**	**50.65**
23_tRNA-Gly	-	**3869940**	**3876885**	**6.95**	**0**	**66.02**	**28.23**
24_tRNA-Gly	-	3869940	3877045	7.11	0	65.80	32.11
25_tRNA-Glu	-	3869940	3877123	7.18	0	65.73	34.21
38_tRNA-Arg	-	**4476498**	**4485239**	**8.74**	**0**	**55.61**	**100.94**
39_tRNA-Leu	+	**4971265**	**4975651**	**4.39**	**0**	**50.44**	**92.81**
47_tRNA-Lys	+	**896324**	**100339210**	**7.07**	**0**	**60.41**	**38.49**
48_tRNA-Pro	+	896238	100339210	7.16	0	60.40	38.58
49_tRNA-Asn	+	896152	100339210	7.24	0	60.40	38.62
56_tRNA-Leu	-	5542391	5542541	0.15	0	56.29	N/D
57_tRNA-Sec	-	5595898	5596739	0.84	0	69.36	N/D
60_tRNA-Phe	+	**6007379**	**6017428**	**10.05**	**0**	**53.29**	**73.34**
61_tRNA-Thr	+	**6028840**	**6037971**	**9.13**	**0**	**51.38**	**76.51**
64_tmRNA	-	**1465475**	**14786871**	**3.21**	**0**	**54.60**	**65.97**

Table 2: tRNA loci, number of strains with GI (Frequency) and strains with GIs identified using tRNAcc analyses of six genomes.

Number	Site	Frequency	Strains
1	tRNA_Arg1	5	PAO1 / PA14 / 2192 / C3719/ LES
2	tRNA_Met2	2	2192 / PACS2
3	tRNA_Gly5	4	PAO1 / PA14 / 2192 / PACS2
4	tRNA_Lys10	2	PAO1 / PA14
5	tRNA_Ser11	1	C3719
6	tRNA_Leu14	1	2192
7	tRNA_Gly19	3	PA14 / LES / PACS2
8	tRNA_Ser20	1	LES
9	tRNA_Pro21	6	PAO1 / PA14 / 2192 / C3719 / LES / PACS2
10	tRNA_Gly23	5	PA14 / 2192 / C3719 / LES / PACS2
11	tRNA_Arg38	3	PA14 / LES / PACS2
12	tRNA_Leu39	1	PACS2
13	tRNA_Lys47	4	PA14 / 2192 / C3719 / PACS2
14	tRNA_Phe60	1	PACS2
15	tRNA_Thr61	2	2192 / PACS2
16	tmRNA	5	PAO1 / PA14 / 2192 / C3719 / LES / PACS2

14 Appendix D: PAO1 tRNA loci names

Table 14.1: tRNAcc output for PAO1 tRNA gene loci and names used

Start	Finish	Orientation	tRNA gene name
298816	298892	-	1_tRNA-Arg
630434	630510	-	2_tRNA-Met
4792055	4792131	-	3_tRNA-Ile
4791951	4792026	-	4_tRNA-Ala
797721	797794	-	5_tRNA-Gly
991260	991350	+	6_tRNA-Ser
991468	991544	+	7_tRNA-Arg
991656	991732	+	8_tRNA-Arg
1007727	1007803	-	9_tRNA-Met
1060356	1060431	+	10_tRNA-Lys
1096867	1096956	+	11_tRNA-Ser
1947320	1947396	+	12_tRNA-Arg
1947448	1947523	+	13_tRNA-His
1947578	1947662	+	14_tRNA-Leu
1947729	1947804	+	15_tRNA-His
1959083	1959159	+	16_tRNA-Asp
2905965	2906051	-	17_tRNA-Leu
2918603	2918676	-	18_tRNA-Cys
2923222	2923297	-	19_tRNA-Gly
2947583	2947672	-	20_tRNA-Ser
3099306	3099382	-	21_tRNA-Pro
3133449	3133525	-	22_tRNA-Val
3173599	3173674	-	23_tRNA-Gly
3173759	3173834	-	24_tRNA-Gly
3173837	3173912	-	25_tRNA-Glu
3206408	3206497	+	26_tRNA-Ser
3395190	3395266	+	27_tRNA-Pro
3475457	3475533	-	28_tRNA-Asp
3475648	3475724	-	29_tRNA-Asp
3475741	3475816	-	30_tRNA-Val
3514723	3514798	-	31_tRNA-Glu
3514845	3514920	-	32_tRNA-Ala
3515014	3515089	-	33_tRNA-Glu
3515138	3515213	-	34_tRNA-Ala
3524012	3524087	+	35_tRNA-Asn
3650722	3650798	-	36_tRNA-Asp
3650815	3650890	-	37_tRNA-Val
3778654	3778730	-	38_tRNA-Arg
4281665	4281751	+	39_tRNA-Leu
4784184	4784259	-	40_tRNA-Trp
4785593	4785668	-	41_tRNA-Thr
4785688	4785761	-	42_tRNA-Gly
4785788	4785872	-	43_tRNA-Tyr

4791951	4792026	-	44_tRNA-Ala
4792055	4792131	-	45_tRNA-Ile
5068932	5069007	-	46_tRNA-Thr
5086925	5087000	-	47_tRNA-Lys
5087011	5087087	-	48_tRNA-Pro
5087097	5087172	-	49_tRNA-Asn
5131082	5131155	+	50_tRNA-Arg
5238277	5238351	+	51_tRNA-Gln
5242026	5242102	+	52_tRNA-Met
5267479	5267554	-	53_tRNA-Ala
5267583	5267659	-	54_tRNA-Ile
5332087	5332163	-	55_tRNA-Met
5332254	5332339	-	56_tRNA-Leu
5387766	5387857	-	57_tRNA-Sec
5541614	5541700	+	58_tRNA-Leu
5541830	5541916	+	59_tRNA-Leu
5798560	5798635	+	60_tRNA-Phe
5809970	5810045	+	61_tRNA-Thr
6042963	6043038	-	62_tRNA-Ala
6043067	6043143	-	63_tRNA-Ile
901520	901872	-	64_tmRNA

15 Appendix E: Construction of PA14Δ*xerC*

The similar technique to the deletion of the PAPI-2 island was used, 924 bp upstream and 916 bp downstream flanking sequences were PCR amplified using primers XerC-UF-F-Gm/ XerC-UF-R-GWR and XerC-DF-F-GWL / XerC-DF-R-Gm respectively. DetThe primers like before contained overlapping sequences to the 1053 bp FRT- flanked Gentamicin resistance cassette derived from pPS856. The three fragments were joined together in the SOE-PCR (Figure 15.1 A and B) and gel purified. The purified SOE product was incubated with 150 ng of pDONR221 vector and BP clonase (Invitrogen, UK) according to manufactures instructions (see Materials and methods) overnight at 25^0C. The reaction was then transformed into *E.coli* Oneshot Omnimax T1-R (Invitrogen, UK), and plated on to LA agar with Kanamycin 50μg/ml, and Gentamicin 10μg/ml. After overnight growth at 37^0C single colonies were picked and grown in 5 ml LB broths with Gentamicin 10μg/ml and grown overnight at 37^0C and plasmid DNA extracted. The extracted plasmid DNA was digested with *Xba*I (Roche, UK) the construct pDONR221-*xerC* gave the predicted restriction banding pattern (data not shown).

Gateway entry vector Plasmid DNA for pDONR221-xerC was dried down by vacuum centrifugation and washed in 1 ml of 70% ethanol and centrifuged at 13,000rpm for 10mins twice, then vacuum dried and eluted in a TE buffer (pH8.0) and quantified by gel electrophoresis. For the LR recombination reaction equimolar concentrations of the entry vector pDONR221-xerC and the destination vector pEX18ApGW were incubated with LR clonase (Invitrogen, UK) according to manufactures instructions (see Materials and methods) overnight at 25^0C. The reactions were then transformed into *E.coli* Oneshot Omnimax T1-R (Invitrogen, UK), and plated on to LA agar supplemented with Ampicillin 100μg/ml, and Gentamicin 10μg/ml, and incubated overnight at 37^0C. 20 single colonies were then picked and patched onto LA + Ampicillin (Amp) 100μg/ml, LA+ Gentamicin (Gm) 10μg/ml, and LA + Kanamycin (Km) 50μg/ml. The patch plating was to detect which of the clones had lost the entry vector as they would be Km[R] if the entry vector was also being harboured by the strain along with the correct pEX18ApGW clones, or a cointegrate of both plasmids had formed (Choi and Schweizer, 2005). Colonies that were Km[R] Amp[R] Gm[R] and therefore harboured both pDONR221-xerC and pEX-xerC were

grown overnight in 5ml LB broths + Gm 10μg/ml at 37⁰C and 200rpm. Plasmid DNA was extracted and digested with *Pst*I and *Hinc*II, to check the correct fragment were present in the vectors. All clones gave the correct predicted restriction pattern for pEX-xerC (Figure 15.1) as shown in Figure 15.1 D. The new vector pEX-xerC was transformed into E.coli SM10λ-pir and stored in 30% glycerol BHI at -20 / -80°C as strain KR656.
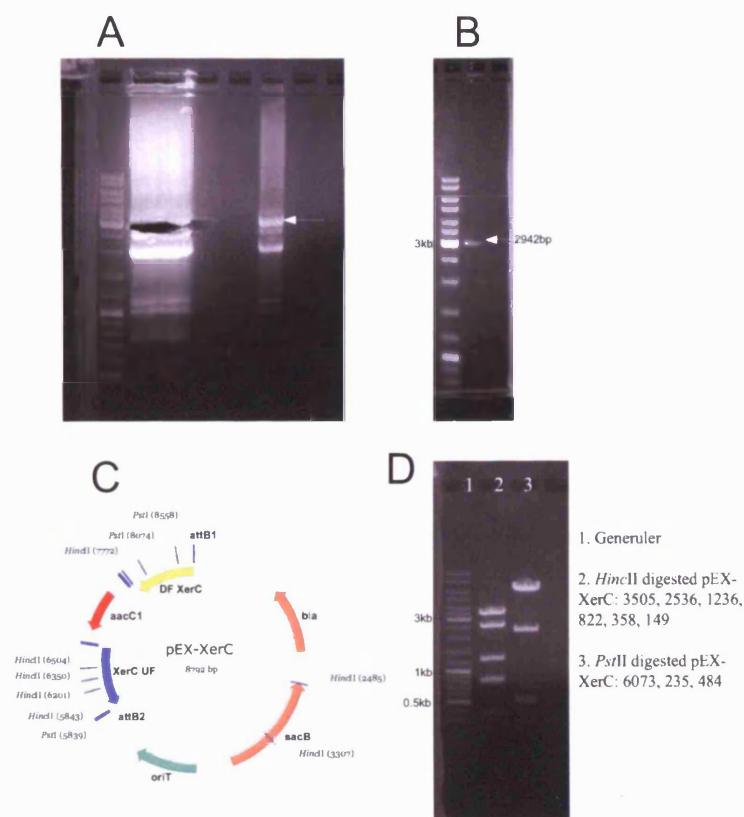
Figure 15.1: Construction of pEX-XerC.
(A): Agarose gel electrophoresis of splicing overlap extension (SOE) PCR of fragment for deletion of PAPI-2 *xerC*. (B) Agarose gel electrophoresis of gel extracted and purified SOE fragment. (C) Plasmid map of pEX-XerC. (D) Agarose gel electrophoresis of restriction digestions of pEX-XerC.

The strain KR656, was plate mated overnight with strain PA14 (KR125) and plated onto 2 x VBMM plates supplemented with Gentamicin 30μg/ml, to select for merodiploids. After overnight growth at 37°C ~600 colonies appeared, 54 colonies were picked and patched onto VBMM + Gentamicin 30μg/ml and VBMM + Carbenicillin 200μg/ml to differentiate

between single and double crossovers. After overnight growth at 37°C, 39 (73%) were Gm^R Cb^S single crossovers and 14 (27%) were Gm^R Cb^R double crossovers. A single putative double crossover was streaked for islolation on a VBMM + Gentamicin 30μg/ml and tested by PCR for the presence of the Gentamicin resistance cassette using primers (aacC1-F / R), and the beta-lactamase cassette (bla-F / R) present on the backbone of pEX-xerC. The strain tested positive for the presence of the Gentamicin cassette and negative for the beta-lactamse cassette, confirming it was a double crossover. The strain PA14Δ$xerC$-Gm was stored in 30% glycerol BHI at -20 / -80°C as strain KR661.

15.1 Deletion of FRT flanked Gentamicin resistance cassette

Electrocompetent cells of PA14Δ$xerC$ were made (see materials and methods) and the FLP expressing plasmid pFLP2 (Choi and Schweizer, 2005) introduced by electroporation. The electroporation was serially diluted in LB broth and plated from 10^{-4} to 10^{-1} on VBMM + 200μg/ml Carbenicillin, plates were grown overnight at 37^{0}C. Twenty single colonies were picked and patched onto LA + 200μg/ml Carbenicillin and LA + 30μg/ml Gentamicin to identify clones with the gentmicin resistance cassette deleted. All twenty were Gm^S and Cb^R, one strain was heavily streaked onto a LA + 5% sucrose plate and grown overnight at 37^{0}C. Single colonies from the LA+5% sucrose plate were patched onto LA and LA + 200μg/ml Carbenicllin to detect loss of the pFLP2 plasmid which encodes for Carbenicillin resistance. A Cb^S patch was selected and streaked to isolation on a LA plate and further tested by PCR to confirm deletion of the $xerC$ gene (Figure 15.2 A (y) B, C, and D) and Gentamicin resistance cassette (Figure 15.2A (x)). The PCRs showed the deletion of the Gentamicin cassette, and the deletion of the $xerC$ and the removal of the Gentamicin resistance cassette (Figure 15.2 B, C, and D). Once the strain thPA14Δ$xerC$ had been confirmed, the strain was stored in 30% glycerol BHI at -20 and -80°C and given the strain number KR666.
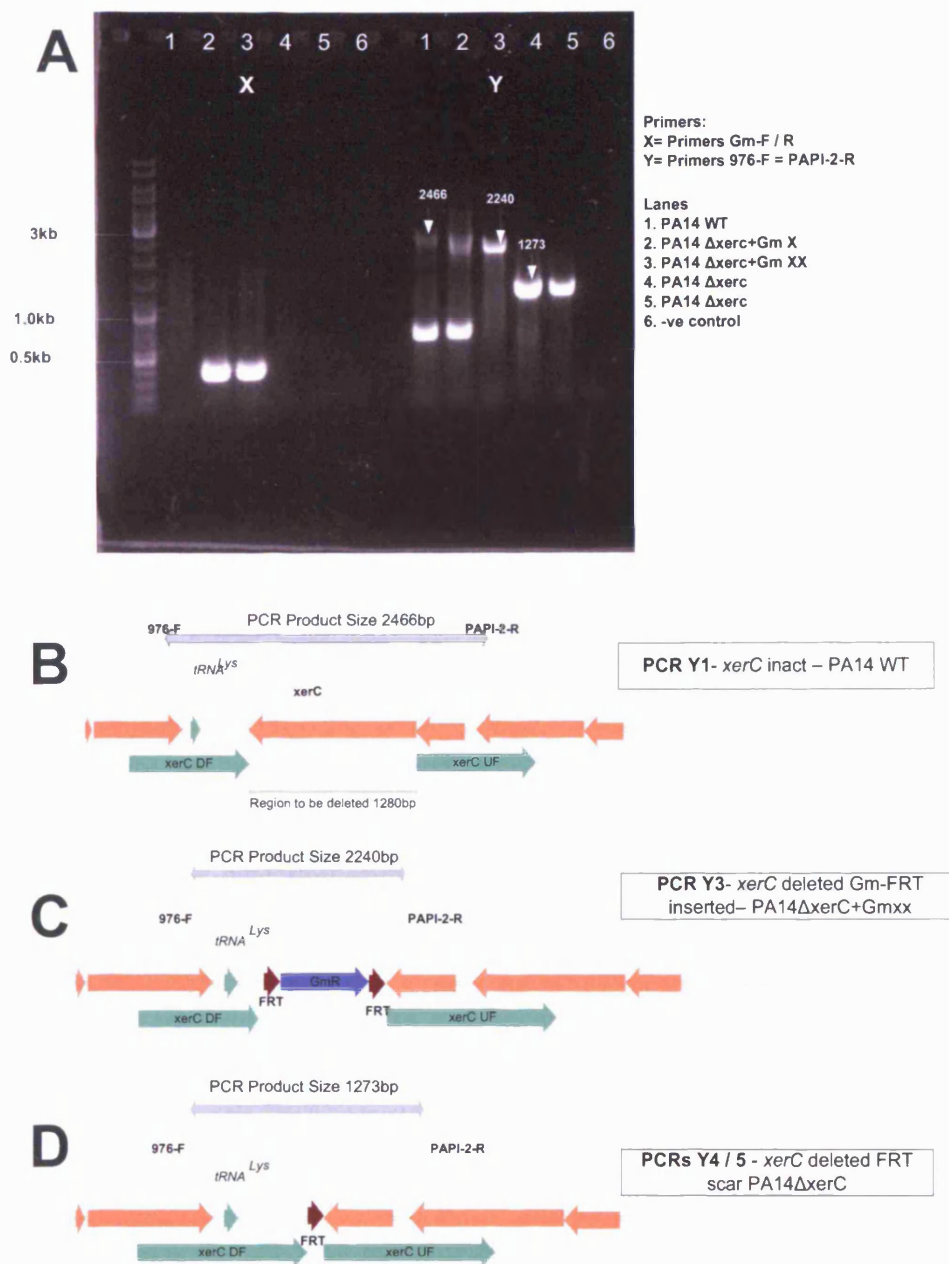
Figure 15.2: Confirmation of deletion of *xerC*
(A)Agarose gel electrophoresis showing results of PCRs for confirmation of the deletion of *xerC* (x) PCRs results for presence of Gentamicin cassette (y) PCRs results using 976-F / PAPI-2-R. (B) Diagram showing wildtype *xerC* region in PA14 WT and locations of PCR primers (976-F / PAPI-2-R) and PCR product size. (C) Diagram showing deleted *xerC* region with GmR-FRT cassette in PA14Δxerc+Gmxx and locations of PCR primers (976-F / PAPI-2-R) and PCR product size. (D) Diagram showing deleted *xerC* region with FRT scar in PA14Δxerc and locations of PCR primers (976-F / PAPI-2-R) and PCR product size.

16 Appendix G: Construction of PA14ΔPro21 and PA14Δ1Δ2 ΔPro21

Plasmid pEXΔPro21 was a kind gift from Dr Barbara Rieck. Its construction was the same as previously described for pEXΔPAPI-2. It contains the conserved up and downstream sequences of the *tRNA^Pro21* identified by tRNAcc. The primers used to construct the plasmid are shown in Table 16.1.

Table 16.1: Primers used for construction of pEXΔPro21 suicide vector

Primer name	Sequence 5' to 3'
Pro21UfGWL	TACAAAAAAGCAGGCTCAGAACATCGTCACGTC
Pro21UrGm	TCAGAGCGCTTTTGAAGCTAATTCGTCGGGACGGAGTGATTCG
Pro21DfGM	AGGAACTTCAAGATCCCCAATTCGCACCAGAGGGTTTCGATGT
Pro21DrGWR	TACAAGAAAGCTGGGTCTCCAGGAAAACGCCAG

Plasmid pEXΔPro21 was conjugated into strains PA14 and PA14Δ1Δ2 as previously described; transconjugants were selected in VBMM + 30µg/ml Gentamicin. After 24 hours growth at 37oC, colonies were picked and patched onto LA + 30µg/ml Gentamicin and LA + 500µg/ml Carbencillin. Colonies that were putative double crossovers (GmR CbS) were confirmed by PCR detection of the Gentamicin cassette (Gm-F / R) and the absence of the bla cassette carried on the pEXΔPro21 backbone (Bla-F / R) (data not shown). Two strains that were confirmed to be double crossovers were prepared for electroporation as described before, and electroporated with pFLP2 to delete the Gentamicin cassette. The electroporations were plated onto LA + 200µg/ml Carbenicillin and incubated at 37oC. Colonies were picked and patched on to LA + 30µg/ml Gentamicin and LA + 500µg/ml Carbenicillin to detect strains that had lost the Gentamicin resistance cassette. A Gm^S Cb^R colony for each mutant was streaked heavily onto LA + 5% sucrose. After incubation overnight at 37°C colonies were picked and patched onto LA+ 5% and LA + 200µg/ml Carbenicillin; to identify strains that were Carbenicillin sensitive and therefore had lost pFLP2. Two strains of each mutant (PA14ΔPro21 and PA14Δ1Δ2ΔPro21) that were sensitive to Carbenicillin were streaked to isolation and tested by colony PCR for the occupancy of the *tRNA^Pro21* locus and the presence of the Gentamicin resistance cassette. The results are shown in Figure 16.1. The results confirmed the deletion of the *tRNA^Pro21* island and the removal of the Gentamicin resistance cassette. PCRs using the tRIP primers

for $tRNA^{Pro21}$ (tRNA-Pro21-U /D2) confirmed the island had been deleted (PCRs 10 - 14:Figure 16.1) (when the island is present the distance is too great to be amplified) and that the Gentamicin cassette was removed, due to the reduction in the size of the band amplified compared (PCRs 10 -14:Figure 16.1) to original double crossover strain (PCR 15: FigureFigure 16.1). The deletion of the Gentamicin cassette was further confirmed by the negative PCRs using primers which detect the Gentamicin cassette (Gm-F /R) (PCR 1-2:Figure 16.1). The confirmed mutant strains were PA14ΔPro21 and PA1Δ1Δ2ΔPro21 were stored on 30% glycerol BHI at -20 and -80°C as strain KR1034 and KR1036 respectively.

PCR number	Template	Primers	Predicted result	Result
1	PA14ΔPro21 A	Gm-F / R	-ve	-ve
2	PA14ΔPro21 B	Gm-F / R	-ve	-ve
3	PA14Δ1Δ2ΔPro21 A	Gm-F / R	-ve	-ve
4	PA14Δ1Δ2ΔPro21 B	Gm-F / R	-ve	-ve
5	PA14ΔPro21X	Gm-F / R	+ve	+ve
6	PA14Δ1Δ2ΔPro21X	Gm-F / R	+ve	+ve
7	PA14	Gm-F / R	-ve	-ve
8	PA14Δ1Δ2	Gm-F / R	-ve	-ve
9	-ve	Gm-F / R	-ve	-ve
10	PA14ΔPro21 A	tRNAPro21U /D2	+ve 1084bp	+ve
11	PA14ΔPro21 B	tRNAPro21U /D2	+ve 1084bp	+ve
12	PA14Δ1Δ2ΔPro21 A	tRNAPro21U /D2	+ve 1084bp	+ve
13	PA14Δ1Δ2ΔPro21 B	tRNAPro21U /D2	+ve 1084bp	+ve
14	PA14ΔPro21X	tRNAPro21U /D2	+ve 2051bp	-ve
15	PA14Δ1Δ2ΔPro21X	tRNAPro21U /D2	+ve 2051bp	+ve
16	PA14	tRNAPro21U /D2	-ve	-ve
17	PA14Δ1Δ2	tRNAPro21U /D2	-ve	-ve
18	-ve	tRNAPro21U /D2	-ve	-ve

Figure 16.1: Agarose gel electrophoresis of PCR confirmation of deletion of $tRNA^{Pro21}$ island in strains PA14 and PA14Δ1Δ2 backgrounds.

17 Appendix H: Construction of Tn7-Tet^R

To make the recipient strains antibiotic resistance, the use of a newly described Tn7 vector system which allows for site specific integration stably into the *P. aeruginosa* genome 25 bp downstream of the highly conserved glucosamine-6-phosphate synthetase (*glms*) (Choi and Schweizer, 2006b). The choice of the resistance cassette to use to make the PAO1 resistant and in particular the other strains antibiotic resistant required the construction of a new a Tn7 vector, as the vectors available were either Gentamicin resistant, which was already used to tag the PAPI-1 island, or Kanamycin resistant, which most of the strain used were found to have a high level of intrinsic resistance (data not shown). Tetracycline was chosen due to the fact that is not used clinically to treat *P. aeruginosa* infections, and therefore it seems strains show greater sensitivity.

The first stage in the construction of the Tn7 vector was to amplify by PCR the tetracycline resistance cassette from the plasmid pUCP26 (West et al., 1994) using the primers Tet-F / R and KOD hotstart polymerase to amplify a blunt ended 1394bp fragment, this was then run on an agarose gel and the correct size band extracted and cleaned up. Plasmid DNA was extracted from strain KR742, the pUC18T-mini-Tn7-T (Choi and Schweizer, 2006a) After digestion the was run on an agarose gel and correct size band extracted and cleaned up. The blunt ended 1394bp Tet fragment and the *EcoR*V (Promega, UK) and cut pUC18*T*-mini-Tn7-T and were then ligated overnight and transformed into *E.coli* DH5α, and plated onto LA + Tetracycline 10 μg/ml. After overnight growth a 37°C, four colonies were picked and grown overnight in 5ml LB + 10μg/ml Tetracycline at 37°C and 200 rpm shaking. Plasmid DNA was extracted and digested with *Cla*I (Promega, UK) to determine the orientation of the Tetracycline cassette (Figure: 1.17.1).

Figure: 1.17.1 shows the *Cla*I digests confirming the originations of the Tetracycline cassette within the pUC18T-mini-Tn7T; the 'forward' orientation of pUC18T-mini-Tn7T-Tet^R-F was selected to be used downstream as the Tetracycline cassette is in the same orientation as other antibiotic cassettes used previously in the Tn7 system without any problems of expression of the resistance cassettes (Choi and Schweizer, 2006b) (Figure: 1.17.1). The vector was additionally transformed into *E. coli* Sm10 γ-pir to allow the vector to be transferred by conjugation. Both strains *E. coli* DH5α and *E. coli* Sm10 γ-pir

harbouring pUC18T-mini-Tn7-Tet^R-F in were stored in 30% glycerol BHI at -20 and -80°C as strain KR905 and KR903 respectively.
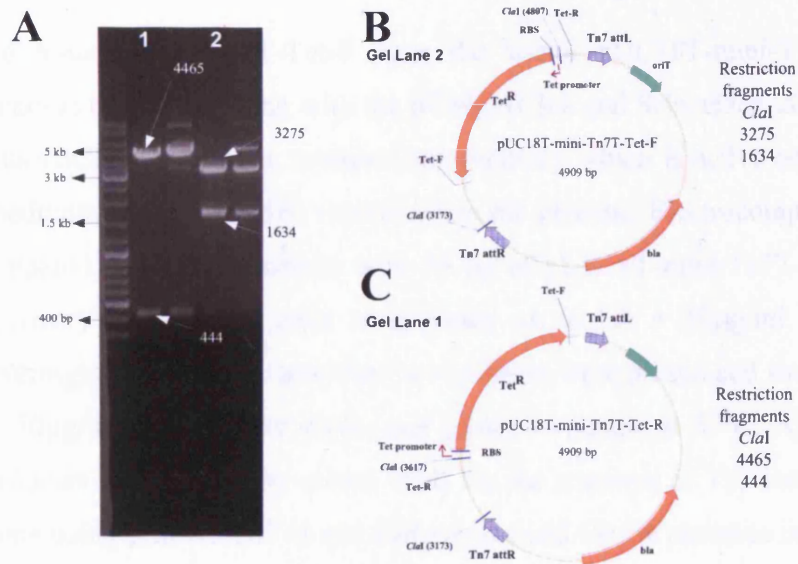
Figure: 1.17.1: Confirmation of pUC18T-mini-Tn7T-Tet-F / R.
(A) Agarose gel electrophoresis of ClaI digested pUC18T-mini-Tn7T-Tet-F in lane 2 and pUC18T-mini-Tn7T-Tet-r in lane 1 (B) plasmid map and predicted restriction fragments for pUC18T-mini-Tn7T-Tet-F (C) plasmid map and predicted restriction fragments for pUC18T-mini-Tn7T-Tet-R

18 Appendix I: Transposition of Tn7-Tet^R into PAO1 and other genomes

18.1 PAO1

To transfer the Tn7T-Tet-F from the vector pUC18T-mini-Tn7T-Tet-F to the PAO1 genome the vector along with the pTNS2 (Choi and Schweizer, 2006a) which expresses the TnsABCD site-specific transposition pathway which is active on the Tn7 transposon and meditates the site specific insertion into the genome. Electrocompetent cells of PAO1 were prepared and electroporated with 50 ng of pUC18T-mini-Tn7T-Tet-F and pTNS2. After recovery for 2 h the cells were plated on to LA + 50μg/ml Tetracycline, and grown overnight at 37°C. The next day two colonies were picked and streaked for isolation on LA + 50μg/ml Tetracycline plates and grown overnight at 37°C. After overnight growth the colonies were screen by colony PCR for the presence of Tn7 integrated adjacent the *glmS* gene using primers Tn7-R and Glms-down and for the presence of the Tetracycline cassette using primers Tet-F / R. The results of the PCRs are shown in Figure 18.1, which shows both clones screen were PCR positive for the insertion of Tn7-Tet-F (Figure 18.1 A) and the tetracycline resistance cassette (Figure 18.1 B). The two confirmed PAO1-TetR was stored in 30% glycerol BHI at -20 and -80°C as strain KR 910.
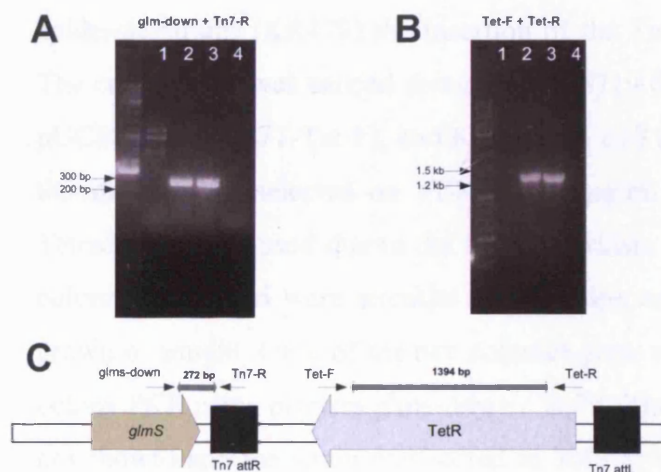
Figure 18.1: Confirmation of Tn7-Tet-F insertion into PAO1.
(A) Agarose gel of glm-down + Tn7-R; 1. PAO1 WT 2. PAO1-Tn7-Tet-F-1 3. PAO1-Tn7-Tet-F-2. 4. –ve no template control. (B) Agarose gel of Tet-F + Tet-R; 1. PAO1 WT 2. PAO1-Tn7-Tet-F-1

3. PAO1-Tn7-Tet-F-2. 4. –ve no template control. (C) Digram of *glmS* genomic location showing the location of the inserted Tn7-Tet-F and location of PCR primers and PCR amplicon size.

18.2 LES and PAO1ΔLys10island

Once the technique was used in the relatively simple PAO1, the Tn7 system was then used in the PAO1 derivative PAO1ΔLys10 (KR716), and the clinically derived LESB58 (Winstanley et al., 2009) (KR130). The process was repeated as for PAO1 WT, both strains were grown overnight and prepared as electrocompetent cells, they were then electroporated with ~50 ng of pUC18T-mini-Tn7T-Tet-F and pTNS2, and plated onto LA + Tetracycline 50μg/ml and incubated at 37°C until colonies appeared. Single colonies were visible after 12 hours for PAO1ΔLys10, but not until 24 hours for LESB58, which would be expected as LESB58 produces smaller slow growing colonies. Single colonies were picked and streak for isolation tested by colony PCR for the presence of the Tetracycline cassette using primers Tet-F / R (data not shown). Colonies for both PAO1ΔLys10 and LESB58 that tested positive were stored in 30% glycerol BHI at -20 and -80°C as strains KR 946 and KR947 for PAO1ΔLys10-TetR and, LESB58-TetR respectively.

18.3 C3719

Differently from the other strains that used electroporation for C3719 (Manchester epidemic strain) (KR479) the insertion of the Tn7-Tet-F was by tri-parental conjugation. The conjugation was carried using strain C3719 (KR479), KR 905 (*E. coli* SM10 (λ-pir) - pUC18T-mini-Tn7T-Tet-F), and KR 740 (*E. coli* DH5α (λ-pir) - pTNS2. After conjugation the strains were selected on VBMM + 75μg/ml Tetracycline, a higher concentration of Tetracycline was used due to the higher intrinsic resistance of C3719. After 18 hours two colonies grew and were streaked for isolation on VBMM + 75μg/ml Tetracycline, and grown overnight. Once of the two colonies grew well and was selected for further study by colony PCR using primers glms-down / Tn7R. The PCR showed the correct size band (data not shown) and the strain was stored in 30% glycerol BHI at -20 and -80°C as strain KR 970.

19 Appendix J: *P. aeruginosa* and *E. coli* strains

Table 19.1: : Wild-type *Pseudomonas aeruginosa* strains

Strain No	Species	Alternative Designation	Clinical Source	Reference or Source
KR 115	*P. aeruginosa*	MG958448P/PL51429	Bloodstream infection (BSI) isolate	Leicester royal infirmary
KR 124	*P. aeruginosa*	PAO1	Wound isolate	(Stover *et al.*, 2000)
KR 125	*P. aeruginosa*	PA14	Burn isolate	(Lee *et al.*, 2006b)
KR 126	*P. aeruginosa*	MID9245	CF	(Smart *et al.*, 2006)
KR 127	*P. aeruginosa*	Clone C	CF	Dr Craig Winstanley
KR 128	*P. aeruginosa*	LES400	CF	(Salunkhe *et al.*, 2005)
KR 129	*P. aeruginosa*	LES431	CF	(Salunkhe *et al.*, 2005)
KR 130	*P. aeruginosa*	LESB58	CF	(Salunkhe *et al.*, 2005)
KR 131	*P. aeruginosa*	K1	Keratitis isolate	Dr Craig Winstanley
KR 132	*P. aeruginosa*	K2	Keratitis isolate	Dr Craig Winstanley
KR 133	*P. aeruginosa*	K6	Keratitis isolate	Dr Craig Winstanley
KR 134	*P. aeruginosa*	K30	Keratitis isolate	Dr Craig Winstanley
KR 154	*P. aeruginosa*	51397	BSI isolate	Leicester royal infirmary
KR 155	*P. aeruginosa*	51331	BSI isolate	Leicester royal infirmary
KR 156	*P. aeruginosa*	51315	BSI isolate	Leicester royal infirmary
KR 158	*P. aeruginosa*	51355	BSI isolate	Leicester royal infirmary
KR 159	*P. aeruginosa*	51400	BSI isolate	Leicester royal infirmary
KR 160	*P. aeruginosa*	51481	BSI Isolate	Leicester royal infirmary
KR 222	*P. aeruginosa*	7133912	Sputum - ITU renal patient	Leicester royal infirmary
KR 223	*P. aeruginosa*	713444W	Sputum - bronchiectasis	Leicester royal infirmary
KR 224	*P. aeruginosa*	713382N	Sputum - ITU bilateral pneumonia	Leicester royal infirmary
KR 225	*P. aeruginosa*	7135807	Sputum - ITU	Leicester royal infirmary
KR 226	*P. aeruginosa*	713581	Endo-Trac Aspirate ITU	Leicester royal infirmary
KR 227	*P. aeruginosa*	G180162C	Ear swab discharging ear	Leicester royal infirmary
KR 228	*P. aeruginosa*	MG713392	ITU - sputum	Leicester royal infirmary
KR 229	*P. aeruginosa*	M713446A	Sputum - bronchiectasis	Leicester royal infirmary
KR 230	*P. aeruginosa*	713446A	Sputum - bronchiectasis	Leicester royal infirmary
KR 231	*P. aeruginosa*	713434A	ITU - Sputum -Renal patient	Leicester royal infirmary
KR 232	*P. aeruginosa*	MG180219M	Wound swab	Leicester royal infirmary

KR 233	*P. aeruginosa*	MG180219M	Wound swab	Leicester royal infirmary
KR 234	*P. aeruginosa*	MG1801589C	Otis media	Leicester royal infirmary
KR 235	*P. aeruginosa*	MG180139C	Wound Swab	Leicester royal infirmary
KR 479	*P. aeruginosa*	C3719	CF	(Lewis *et al.*, 2005)
KR 732	*P. aeruginosa*	PA2192	CF	(Mathee *et al.*, 2008)

Table 1.19.2: *E.coli* strains and plasmids

Strain Catalogue No	Species	Parent Strain	Plasmids	Antibiotic Selection	Relevant features	Reference
KR 136	*Escherichia coli*	DH5α	pPS856	Ampicillin 100µg/ml	Source of Gentamicin resistance cassette, Gm^R, Amp^R	(Hoang *et al.*, 1998)
KR 137	*Escherichia coli*	DH5α	pFLP2	Ampicillin 100µg/ml	FLP recombinase expressing plasmid, *sacB*, Amp^R	(Choi and Schweizer, 2005)
KR 138	*Escherichia coli*	HPS1	pEX18Ap	Ampicillin 100µg/ml	*P. aeruginosa* suicide vector, *sacB*, Amp^R	(Hoang et al., 1998)
KR 139	*Escherichia coli*	DB3.1	pEX18GW	Ampicillin 100µg/ml	Gateway compatible destination vectors*P. aeruginosa* suicide vector, *sacB*, Amp^R	(Choi and Schweizer, 2005)
KR 140	*Escherichia coli*	DH5αF'	pUCP20	Ampicillin 100µg/ml	*E.coli – P. aeruginosa* shuttle vector, Amp^R	(West *et al.*, 1994)
KR 141	*Escherichia coli*	DH5α	pUCP24	Gentamicin 10µg/ml	*E.coli – P. aeruginosa* shuttle vector, Gm^R	(West *et al.*, 1994)
KR 142	*Escherichia coli*	HPS1	pUCP26	Tetracycline 10µg/ml	*E.coli – P. aeruginosa* shuttle vector, Tc^R	(West et al., 1994)
KR 307	*Escherichia coli*	One shot T1r	pDONR221-ΔPAPI2	Gentamicin 10µg/ml Kanamycin 50µg/ml	Plasmid pDONR221 with a ~2KB derived from up and downstream regions of PAPI-2 island from PA14 and FRT flanked Gentamicin cassette from pP856, Gm^R, Km^R	This work
KR 328	*Escherichia coli*	One shot T1r	pEXΔPAPI2	Gentamicin 10µg/ml Amp 100µg/ml	Plasmid pEX18ApGW with a ~2KB derived from up and downstream regions of PAPI-2 island from PA14 and FRT flanked Gentamicin	This work

					cassette from pP856, Gm^R, Amp^R, sacB	
KR 481	*Escherichia coli*	Top10	pCR4115Soj	Ampicillin 50µg/ml	498bp PCR fragment from strain KR115 from the *soj* gene in pCR4-Topo. Km^R	This work
KR 501	*Escherichia coli*	Top10	pCR4125Soj	Ampicillin 50µg/ml	498bp PCR fragment from strain KR125 from the *soj* gene in pCR4-Topo. Km^R	This work
KR 502	*Escherichia coli*	Top10	pCR4127Soj	Ampicillin 50µg/ml	498bp PCR fragment from strain KR127 from the *soj* gene in pCR4-Topo. Km^R	This work
KR 503	*Escherichia coli*	Top10	pCR4158Soj	Ampicillin 50µg/ml	498bp PCR fragment from strain KR158 the *soj* gene in pCR4-Topo. Km^R	This work
KR 537	*Escherichia coli*	DH5α	pEX115SOJ	Ampicillin 50µg/ml	pEX18Ap suicide vector with 498bp region of *soj* gene from KR115. Amp^R, sacB	This work
KR 538	*Escherichia coli*	DH5α	pEX125SOJ	Ampicillin 50µg/ml	pEX18Ap suicide vector with 498bp region of *soj* gene from KR125. Amp^R, sacB	This work
KR 539	*Escherichia coli*	DH5α	pEX127SOJ	Ampicillin 50µg/ml	pEX18Ap suicide vector with 498bp region of *soj* gene from KR127. Amp^R, sacB	This work
KR 540	*Escherichia coli*	DH5α	pEX158SOJ	Ampicillin 50µg/ml	pEX18Ap suicide vector with 498bp region of *soj* gene from KR158. Amp^R, sacB	This work
KR 553	*Escherichia coli*	SM10 (λ pir)	pEXΔPAPI2	Gentamicin 10µg/ml	Plasmid pEX18ApGW with a ~2KB derived from up and downstream regions of PAPI-2 island from PA14 and FRT flanked Gentamicin cassette from pP856, Gm^R, Amp^R, sacB	This work
KR 554	*Escherichia coli*	SM10 (λ pir)	pEXΔ2.9kbPAPI-2	Gentamicin 10µg/ml	Plasmid pEX18ApGW with ~1.6KB derived from upstream and centre of PAPI-2 island from PA14 and FRT	This work

281

					flanked Gentamicin cassette from pP856, Gm^R, Amp^R, sacB	
KR 555	*Escherichia coli*	SM10 (λ pir)	pEX115Soj	Ampicillin 50μg/ml	pEX18Ap suicide vector with 498bp region of *soj* gene from KR115. Amp^R, sacB	This work
KR 556	*Escherichia coli*	SM10 (λ pir)	pEX125Soj	Ampicillin 50μg/ml	pEX18Ap suicide vector with 498bp region of *soj* gene from KR125. Amp^R, sacB	This work
KR 557	*Escherichia coli*	SM10 (λ pir)	pEX127Soj	Ampicillin 50μg/ml	pEX18Ap suicide vector with 498bp region of *soj* gene from KR127. Amp^R, sacB	This work
KR 558	*Escherichia coli*	SM10 (λ pir)	pEX158Soj	Ampicillin 50μg/ml	pEX18Ap suicide vector with 498bp region of *soj* gene from KR158. Amp^R, sacB	This work
KR 654	*Escherichia coli*	One shot T1r	pDONR221Δ Xerc	Kanamycin 50μg/ml, Gentamicin 10μg/ml	pDONR221 with SOE PCR fragment of UF + DF of PAPI-1 *xerC* derived from Pseudomonas aeruginosa PA14 (KR125) with Gm-FRT cassette in the centre. Gm^R, Km^R	This work
KR 655	*Escherichia coli*	One shot T1r	pEXΔXerC	Ampicillin 100μg/ml	pEX18ApGW with SOE PCR fragment of UF + DF of PAPI-1 *xerC* derived from Pseudomonas aeruginosa PA14 (KR125) with Gm-FRT cassette in the centre. Gm^R, Amp^R	This work
KR 656	*Escherichia coli*	SM10 (λ pir)	pEXΔXerC	Ampicillin 100μg/ml	pEX18ApGW with SOE PCR fragment of UF + DF of PAPI-1 *xerC* derived from Pseudomonas aeruginosa PA14 (KR125) with Gm-FRT cassette in the centre. Gm^R, Amp^R	This work
KR 740	*Escherichia coli*	DH5α (λ pir)	pTNS2	Ampicillin 100μg/ml	Transposition helper plasmid, Amp^R	(Choi and Schweizer, 2006b)
KR 741	*Escherichia coli*	HPS1	pUC18-mini-Tn7T	Ampicillin 100μg/ml	mini-Tn7 base vector with transcriptional terminators and MCS; for cloning of suitable selection markers or other	(Choi and Schweizer, 2006b)

					functional and selectable elements, Amp^R	
KR 742	*Escherichia coli*	HPS1	pUC18T-mini-Tn7T	Ampicillin 100µg/ml	Mobilizable base vector with MCS; for cloning of suitable selection markers or other functional and selectable elements, Amp^R	(Choi and Schweizer, 2006b)
KR 743	*Escherichia coli*	CC118 (λ pir)	pUC18R6KT-mini-Tn7T	Ampicillin 100µg/ml	Mobilizable mini-Tn7 base vector with MCS; for cloning of suitable selection markers or other functional and selectable elements, Amp^R	(Choi and Schweizer, 2006b)
KR 744	*Escherichia coli*	DH5α (λ pir)	pUC18R6K-mini-Tn7T-Gm	Ampicillin 100µg/ml Gentamicin 15µg/ml	Gentamicin resistant mini-Tn7; for gene insertion in Gms bacteria, Amp^R, Gm^R	(Choi and Schweizer, 2006b)
KR 746	*Escherichia coli*	HPS1	pUC18T-mini-Tn7T-Gm	Ampicillin 100µg/ml Gentamicin 15µg/ml	Gentamicin resistant mini-Tn7T; mobilizable; for gene insertion in Gms bacteria. Amp^R, Gm^R	(Choi and Schweizer, 2006b)
KR 858	*Escherichia coli*	DH5α	pDONR221-Isprob	Gentamicin 10µg/ml Kanamycin 50µg/ml	Gentamicin resistance cassette from pPS856 joined together with the sacB cassette from pEX18Ap in PCR with up and downstream flanking DNA from PAPI-1 of PA14 in pDONR221. Km^R, Amp^R	This work
KR 903	*Escherichia coli*	DH5α	pUC18T-mini-Tn7T-Tet-F	Tetracycline 10µg/ml Ampicillin 100µg/ml	pUC18T-mini-Tn7T with 1394 bp Tetracycline cassette from pUCP26 cloned into EcoRV site same orientation as Gm cassettes in Gm^R version, Amp^R, Tc^R	This work
KR 904	*Escherichia coli*	DH5α	pUC18T-mini-Tn7T-Tet-R	Tetracycline 10µg/ml Ampicillin 100µg/ml	pUC18T-mini-Tn7T with 1394 bp Tetracycline cassette from pUCP26 cloned into EcoRV site in opposite orientation as Gm cassettes in Gm^R version. Amp^R, Tc^R	This work
KR 905	*Escherichia coli*	Sm10 (λ pir)	pUC18T-mini-Tn7T-	Tetracycline 10µg/ml Ampicillin 100µg/ml	pUC18T-mini-Tn7T with 1394 bp Tetracycline cassette from pUCP26	This work

283

			Tet-F		cloned into EcoRV site in same orientation as Gm cassettes in Gm^R version. Amp^R, Tc^R	
KR 906	*Escherichia coli*	One shot	pEXIsprob	Gentamicin 10µg/ml Ampicillin 100µg/ml	Gentamicin resistance cassette from pPS856 joined together with the sacB cassette from pEX18Ap in PCR with up and downstream flanking DNA from PAPI-1 of PA14 in pEX18ApGW. Gm^R, Amp^R	This work
KR 909	*Escherichia coli*	DH5α	pGEM-Tet	Tetracycline 10µg/ml Ampicillin 100µg/ml	pGEM-T Easy with 1394 bp Tetracycline cassette from pUCP26 cloned . Amp^R Tet^R	This work
KR 965	*Escherichia coli*	DH5α	pUC18T-Tn7T-TetF-attBWT-ve	Tetracycline 10µg/ml Ampicillin 100µg/ml	pUC18-T-Tn7-T-Tet-F plasmid with 230bp Lys10 attB fragment in -ve orientation from *P. aeruginosa* PA14. Amp^R Tet^R	This work
KR 966	*Escherichia coli*	DH5α	pUC18T-Tn7T-TetF-attBFRT-ve	Tetracycline 10µg/ml Ampicillin 100µg/ml	pUC18-T-Tn7-T-Tet-F plasmid with 230bp Lys10 attB fragment in -ve orientation plus a 86bp FRT scar from *P. aeruginosa* PA14. Amp^R Tet^R	This work
KR1115	*Escherichia coli*	SM10 (λ pir)	pEXΔpro21	Gentamicin 30 µg/ml	Up and downstream conserved flanking regions from *tRNA^{Pro21}* around a Gentamicin cassette from pPS856. Amp^R, Gm^R	Gift from Dr Barbara Rieck
KR1220	*Escherichia coli*	DH5α	pUC18T-Tn7-T-Tet-F-attB+ve	Tetracycline 10µg/ml	pUC18-T-Tn7-T-Tet-F plasmid with 230bp Lys10 attB fragement in +ve orientation from P.aeruginosa PA14. Amp^R Tet^R	This work
KR1309	*Escherichia coli*	HB101	pRK2013	Kanamycin 50µg/ml	E. coli HB101 carrying the helper plasmid pRK2013, Km^R	(Figurski and Helinski, 1979)

284

Table 19.3: *P. aeruginosa* mutant strains

Strain Catalogue No	Species	Strain name	Parent Strain	Antibiotic Selection	Relevant features
KR 564	*P. aeruginosa*	PA14:pEXΔ2.9kbPAPI-2:Gm^R:Cb^R	PA14 (KR125)	Gentamicin 30µg/ml and Carbencillin 200µg/ml	Single crossover of pEXΔ2.9kbPAPI-2 in PA14, Cb^R, Gm^R
KR 565	*P. aeruginosa*	PA14:pEXΔPAPI-2X:Gm^R:Cb^R	PA14 (KR125)	Gentamicin 30µg/ml and Carbencillin 200µg/ml	Single crossover of pEXΔPAPI-2 in PA14, Cb^R, Gm^R
KR 567	*P. aeruginosa*	PA14:pEX125soj:Cb^R	PA14 (KR125)	Carbencillin 200µg/ml	Single crossover of pEX125soj in PA14, Cb^R
KR 572	*P. aeruginosa*	PA14ΔPAPI-1	KR125 (PA14)	None	PA14 (KR125) with the 108 Kb PAPI-1 island deleted from the genome via sucrose selection.
KR 573	*P. aeruginosa*	PA14ΔPAPI-2	KR125 (PA14)	None	PA14 (KR125) with PAPI-2 genomic island deleted
KR 601	*P. aeruginosa*	PAO1ΔLys10:Gm^R	KR124 (PAO1)	Gentamicin 30µg/ml	Strain PAO1 (KR124) with *tRNA^{Lys10}* associated genomic island deleted leaving marked deletion with Gentamicin flanked FRT cassette. Gm^R
KR 607	*P. aeruginosa*	PA14 ΔPAPI-2 :pEX125Soj	KR573	Carbenicillin 200µg/ml	Single crossover of pEX125soj in PA14ΔPAPI-2, Cb^R
KR 608	*P. aeruginosa*	PA14 ΔPAPI-1 ΔPAPI-2 (PAΔ1Δ2)	KR607	None	Strain PA14 (KR125) with pathogenicity islands PAPI-1 and PAPI-2 deleted.
KR 660	*P. aeruginosa*	PA14:pEXΔxerC:Gm^R:Cb^R	KR125 (PA14)	Gentamicin 30µg/ml and Carbenicillin 200µg/ml	Strain PA14 with a single crossover insertion of pEXΔxerc. Gm^R, Cb^R
KR 661	*P. aeruginosa*	PA14ΔXerC:Gm^R	KR660	Gentamicin 30µg/ml	Strain PA14 (KR125) with PAPI-2 XerC integrase deleted replace by Gentamicin FRT flanked cassette. Gm^R
KR 666	*P. aeruginosa*	PA14dXerC	KR661	None	Strain PA14 (KR125) with PAPI-2 XerC integrase deleted
KR 713	*P. aeruginosa*	PA14ΔPAPI-2:Gm^R	KR565	Gentamicin 30µg/ml	PA14 (KR125) with PAPI-2 genomic island deleted with Gentamicin cassette. Gm^R -

					Version 2
KR 716	*P. aeruginosa*	PA01ΔLys10	KR601	none	Strain PAO1 (KR124) with *tRNA*[Lys10] associated genomic island deleted
KR 717	*P. aeruginosa*	PA14ΔPAPI-2.2	KR713	none	PA14 with PAPI-2 genomic island deleted. Repeated construction same as strain KR573
KR 848	*P. aeruginosa*	PA14:Isprob:Gm^R	PA14 (KR125)	Gentamicin 30μg/ml	Strain PA14 (KR125) with PAPI-1 island tagged with Gm-sacB casette
KR 850	*P. aeruginosa*	PA14:pEXIsprob:Gm^R:Cb^R	PA14 (KR125)	Gentamicin 30μg/ml Carbenicillin 200μg/ml	Strain PA14 with PAPI-1 island tagged with pEXIsprob inserted in a single crossover into PAPI-1 island. Gm^R, Cb^R
KR 910	*P. aeruginosa*	PA01:Tet^R	PA01 (KR124)	Tetracycline 50μg/ml	Strain PA01 with Tn7T with Tetracycline cassette inserted by transposition downstream of glms gene, Tc^R
KR 911	*P. aeruginosa*	PA01: PAPI-1	KR910	Gentamicin 30μg/ml Tetracycline 50μg/ml	Strain PAO1:Tet^R with PAPI-1 tagged with Gentamicin:*sacB* cassette. Tc^R, Gm^R.
KR 946	*P. aeruginosa*	PAO1ΔLys10 :Tet^R	PA01 (KR124)	Tetracycline 50 μg/ml	Strain with PAO1ΔLys10 (KR716) with Tn7T with Tetracycline cassette inserted by transposition downstream of glms gene, Tc^R
KR 947	*P. aeruginosa*	LESB58:Tet^R	LES B58 (KR130)	Tetracycline 50 μg/ml	Strain LESB58 (KR130) with Tn7T with Tetracycline cassette inserted by transposition downstream of glms gene. Tc^R
KR 950	*P. aeruginosa*	PAO1ΔLys10:PAPI-1	KR716	Tetracycline 50 μg/ml + Gentamicin 30μg/ml	PAO1ΔLys10 (KR716) strain carrying with PAPI-1 tagged with Gentamicin:*sacB* cassette. Tc^R, Gm^R.
KR 958	*P. aeruginosa*	PA14ΔPro21:pEXΔPro21:Gm^R:Cb^R	KR125 (PA14)	Gentamicin 30μg/ml Carbenicillin 200μg/ml	Strain PA14 (KR125) with a Single crossover insertion of pEXdpro21. Gm^R, Amp^R
KR 959	*P. aeruginosa*	PA14 ΔPro21:Gm^R	KR125 (PA14)	Gentamicin 30μg/ml Carbenicillin	Strain PA14 (KR125) with the *tRNA*[Pro21] associated island deleted by replacement with Gentamicin FRT cassette. Gm^R.

286

				200µg/ml	
KR 960	*P. aeruginosa*	PA14Δ1Δ2:pEXΔPro21:Gm^R:Cb^R	KR608	Gentamicin 30µg/ml Carbenicillin 200µg/ml	Strain PA14Δ1Δ2 (KR608) with a Single crossover insertion of pEXΔPro21. Gm^R, Amp^R
KR 961	*P. aeruginosa*	PA14 Δ1Δ2ΔPro21:Gm^R	KR608	Gentamicin 30µg/ml	Strain PA14Δ1Δ2 (KR608) with the t*RNA^{Pro21}* associated island deleted by replacement with Gentamicin FRT cassette. Gm^R.
KR 962	*P. aeruginosa*	PA14-3rd- tRNA^{Lys10}-attB-ve	KR125 (PA14)	Tetracycline 50µg/ml	Tn7-Tet-F-attBWT-ve inserted into glmS site via transposition containing a 289bp attB fragment from *tRNA^{Lys10} attB* site from PA14 (KR125) in -ve orientation. Tc^R
KR 963	*P. aeruginosa*	PA14-3rd- tRNA^{Lys10}-attB:FRT-ve	KR125 (PA14)	Tetracycline 50µg/ml	Tn7-Tet-F-attBWT-ve inserted into glmS site via transposition containing an *attB* fragment from *tRNA^{Lys10} attB* site from PA14ΔPAPI-2 (KR573) in +ve orientation. Tc^R
KR 964	*P. aeruginosa*	PA14-3rd- tRNA^{Lys10}-attB+ve	KR125 (PA14)	Tetracycline 50µg/ml	Tn7-Tet-F-attBWT-ve inserted into glmS site via tranposition containing a 289bp attB fragment from *tRNA^{Lys10} attB* site from PA14 (KR125) in +ve orientation. Tc^R
KR 970	*P. aeruginosa*	C3719:Tet^R	KR479 (C3719)	Tetracycline 50µg/ml	Strain C3719 (KR479) with Tn7T with Tetracycline cassette inserted by transposition downstream of glms gene, Tc^R
KR 971	*P. aeruginosa*	LES:PAPI-1	KR947	Tetracycline 50µg/ml Gentamicin 30µg/ml	Strain LESB58:Tet^R with PAPI-1 tagged with Gentamicin:*sacB* cassette. Tc^R, Gm^R.
KR1032	*P. aeruginosa*	C3719:PAPI-1	KR970	Tetracycline 50µg/ml Gentamicin 30µg/ml	Strain C3719:Tet^R with PAPI-1 tagged with Gentamicin:*sacB* cassette. Tc^R, Gm^R.
KR1034	*P. aeruginosa*	PA14ΔPro21	KR959		Strain PA14 (KR125) with t*RNA^{Pro21}* island deleted.
KR1036	*P. aeruginosa*	PA14 Δ1Δ2ΔPro21	KR961		Strain PA14Δ1Δ2 (KR608) with t*RNA^{Pro21}* island deleted.

287

20 Appendix K: Primers

Table 20.1: PCR primers for construction of mutants

Primer name	Sequence	Source / Reference
PAPI2UFFW-Gm	AGGAACTTCAAGATCCCCAATTCGACGTCAATGCGGGCCTAATGTTCG	s work
PAPI2UFRS-GWR	TACAAGAAAGCTGGGTGCTGCCCCCTGCGCTGTCACT	This work
PAPI2DFFW-GWL	TACAAAAAAGCAGGCTGCAGACCGTCCAGGCAATGTT	This work
PAPIDFRS-Gm	TCAGAGCGCTTTTGAAGCTAATTCGGCAAGGGGAAGGAGCGATACTG	This work
PAPI2intFW-GWL	TACAAAAAAGCAGGCTCAGTGCTGCCCAATCTCATCC	This work
PAPIintRS-Gm	TCAGAGCGCTTTTGAAGCTAATTCGATATCGCTTTCTCCCGCTCCAATC	This work
XerC-DF-F-GWL	TACAAAAAAGCAGGCTTATACCGGTGACTTACGTGCCC	This work
XerC-DF-R-Gm	TCAGAGCGCTTTTGAAGCTAATTCGAGCGATACCGATACTGAGGGGC	This work
XerC-UF-F-Gm	AGGAACTTCAAGATCCCCAATTCGTCCACACCTCCTTCGGCATC	This work
XerC-UF-R-GWR	TACAAGAAAGCTGGGTTCACCTACGTCTGGGCGCAA	This work
PAPI-1IP-DS-SacB	AAACGCAAAAGAAAATGCCGGATGACCGTCAGTAGCCAGC	This work
PAPI-1IP-DS-R-GWR	TACAAGAAAGCTGGGTCGTTACCTGCGTGAACTAGC	This work
PAPI-1IP-US-F-GWL	TACAAAAAAGCAGGCTAAGTGTCAAGGTCAAGCAGGA	This work
PAPI-1IP-US-R-Gm	TCAGAGCGCTTTTGAAGCTAATTCGAGTAGCGCCCTGGTGATGC	This work
Gm-F	CGAATTAGCTTCAAAAGCGCTCTGA	(Choi and Schweizer, 2005)
Gm-R	CGAATTGGGGATCTTGAAGTTCCT	(Choi and Schweizer, 2005)
GW-attb1	GGGGACAAGTTTGTACAAAAAAGCAGGCT	(Choi and Schweizer, 2005)
Gw-attb2	GGGGACCACTTTGTACAAGAAAGCTGGGT	(Choi and Schweizer, 2005)
SacB-R	CGGCATTTTCTTTTGCGTTT	This work
SacB-R-Gm	AGGAACTTCAAGATCCCCAATTCGTCTTTAGGCCCGTAGTCTGC	This work
bla-F	CAGTGCTGCAATGATACCGCG	This work
bla-R	CCCGAAGAACGTTTTCCAATG	This work
ExoU-F	GGGAATACTTTCCGGGAAGTT	(Allewelt *et al.*, 2000)
ExoU-R	CGATCTCGCTGCTAATGTGTT	(Allewelt *et al.*, 2000)
Tet-F	TGGAGTGGTGAATCCGTTAGCG	This work
Tet-R	CGGTATCAGCTCACTCAAAGGCG	This work
Bact-8F	AGAGTTTGATCCTGGCTCAG	(Eckburg *et al.*, 2005)
Bact-1391R	GACGGGCGGTGTGTRCA	(Eckburg *et al.*, 2005)
PAPI-1-1F	GGTTGAGGCCCTGATTTTGTAAGT	This work
PAPI-1-1R	GAACGATTGCCTGACCTATTTGAA	This work
PAPI-1-2 F	CTTCGGGCATGGGAAGGCCCTTACAT	This work
PAPI-1-2 R	TAGCCGCACAAGCCATTAATATAAAC	This work
PAPI-1-3 F	CGCGGTGCCCCTCGGCGATTATTGC	This work
PAPI-1-3 R	CAATGGCGGGCTCTCCTACCTAGTTTC	This work
PAPI-1-4 F	CCTTGAGTCGTGGCGACCTGCTAGTT	This work
PAPI-1-4 R	CCCGGCAAAGCCTATGGAGATAACAC	This work
PAPI-1-5 F	GCCAACTGGGCCAGCTCCCTATTA	This work
PAPI-1-5 R	ATGTGGCCGACCCCCTTCCCTATA	This work

Table 20.2: tRIP PCR primers

Primer name	Sequence	Source / Reference
PR1UtRNAGly23	AATGGCGATTAGGAGGGC	This work
PR1DtRNAGly23	CGCGAAACCCTTTATACTGC	This work
PR1UtRNAPro21	AGGCTGTTTGATGTGTATCACG	This work
PR1DtRNAPro21_2	GACATCGAAACCCTCTGGTG	This work
PR1DtRNAPro21	AGAAGTGGCGTTGAAGGAGATTG	This work
PR1UtmRNA	GGCCATCCTTTTACTGGTTCTC	This work
PR1DtmRNA	TACCCTGGTAGTGAGTGTCTAGCTC	This work
PR1UtRNALys47	ATCGGGGTATAGCGCAGTC	This work
PR1DtRNALys47	GCCACTACAACCTGTGAATCG	This work
PR1UtRNAArg1	CGAAATCACGAACGTACGC	This work
PR1DtRNAArg1	AGTCTGATTGTCCAAACGTTCAC	This work
PR1UtRNAGly5	ACTGACGCTCACGTTGTGAC	This work
PR1DtRNAGly5	GTCGGTAGAACCTGTAATCATCG	This work
PR1UtRNAArg38	GACCACCATGTCTTCGAGAATC	This work
PR1DtRNAArg38	CTGTACGTATGCGTTAGGTTCG	This work
PR1UtRNALys10	AAGGTATACCGGTGACTTACGTG	This work
PR1DtRNALys10	ACTGAAAACGAGAAAGAATGCG	This work
PR1UtRNASer11	GTTCTTCGTACAAGCTGGTATCAT	This work
PR1DtRNASer11	TACTTCGAGATATTGAAACAGGCG	This work

Table 20.3: qPCR primers

Primer name	Sequence	Source / Reference
gyrPA-398	CCTGACCATCCGTCGCCACAAC	(Qin *et al.*, 2003)
gyrPA-620	CGCAGCAGGATGCCGACGCC	(Qin *et al.*, 2003)
Total-PAPI-1-F	GAGGGCTCGAACTACAGACG	This work
Total-PAPI-1-R	TGCAACATGCAGAAAAGGAG	This work
tRNA-LYS47-RT-F	GTATAGCGCAGTCCGGTAGC	This work
tRNA-LYS10-RT-F	GACCCGACGCCATATTTCT	This work
PAPI-1-RT-F	GCTAGACAAGAACCGGCGTA	This work
PAPI-1-Circ-Soj	ACTCGTTGTAACGGGAGTGG	This work
Empty47-R	TCGGAAAGTAATGGCACAGA	This work
Lys10Empsite	GCTGGACAAGTAAAAGGTGCA	This work
GyrBOuter-F	TCGAGGTGGTGGATAACTCC	This work
GyrBOuter-R	TACTCTTCCATGGCCTGGTC	This work
TotalPAPI-1outer-F	CGGCAACTTGGATCCAGTCC	This work
TotalPAPI-1outer-R	GGCACGCTGAAACAACAGACA	This work
C3719 Total - F	TCCCGGAAAATCTTCATCAG	This work
C3719 Total - R	AGAGCTTCGCGAATGGATAA	This work
C3719Island forward	CTGGACAAGTAAAAGGTGCAAC	This work

Table 20.4: Third site primers

Primer name	Sequence	Source / Reference
attB-Lys10U	CTGGTATTTCCGACCCGACGC	This work
attB-d2Lys10FRT-D	AGTATCGCTCCTTCCCCTTGC	This work
attB-WTLys10-D	GACGTCAATGCGGGCCTAAT	This work
attB-Lys47U	CAATCGGGGTATAGCGCAGTC	This work
attB-Lys47d	AGCGGCCCCTCCTCCTTCCCA	This work
attB-Lys10D-C3719	TCGGTCGATTCTGGCCAGTT	This work
Tn7QPCR-R	TGCAAGGCCTTCGCGAGGTAC	This work
Tn7QPCR-F2	TGATACCGATCATGCATGAGCTC	This work
PTn7R	CACAGCATAACTGGACTGATTTC	(Choi and Schweizer, 2006b)
PTn7L	ATTAGCTTACGACGCTACACCC	(Choi and Schweizer, 2006b)
PglmS-down	GCACATCGGCGACGTGCTCTC	(Choi and Schweizer, 2006b)
PglmS-up	CTGTGCGACTGCTGGAGCTGA	(Choi and Schweizer, 2006b)

21 References

ABD, H., WRETLIND, B., SAEED, A., IDSUND, E., HULTENBY, K. & SANDSTROM, G. (2008) Pseudomonas aeruginosa Utilises Its Type III Secretion System to Kill the Free-Living Amoeba Acanthamoeba castellanii. *J Eukaryot Microbiol,* 55, 235-43.

ABE, H., MIYAHARA, A., OSHIMA, T., TASHIRO, K., OGURA, Y., KUHARA, S., OGASAWARA, N., HAYASHI, T. & TOBE, T. (2008) Global regulation by horizontally transferred regulators establishes the pathogenicity of Escherichia coli. *DNA Res,* 15, 25-38.

ALLEN, L., DOCKRELL, D. H., PATTERY, T., LEE, D. G., CORNELIS, P., HELLEWELL, P. G. & WHYTE, M. K. B. (2005) Pyocyanin Production by Pseudomonas aeruginosa Induces Neutrophil Apoptosis and Impairs Neutrophil-Mediated Host Defenses In Vivo. *J Immunol,* 174, 3643-3649.

ALLEWELT, M., COLEMAN, F. T., GROUT, M., PRIEBE, G. P. & PIER, G. B. (2000) Acquisition of expression of the Pseudomonas aeruginosa ExoU cytotoxin leads to increased bacterial virulence in a murine model of acute pneumonia and systemic spread. *Infect Immun,* 68, 3998-4004.

ANGUS, A. A., LEE, A. A., AUGUSTIN, D. K., LEE, E. J., EVANS, D. J. & FLEISZIG, S. M. J. (2008) Pseudomonas aeruginosa Induces Membrane Blebs in Epithelial Cells, Which Are Utilized as a Niche for Intracellular Replication and Motility. *Infect. Immun.,* 76, 1992-2001.

ANTONOPOULOU, A., RAFTOGIANNIS, M., GIAMARELLOS-BOURBOULIS, E. J., KOUTOUKAS, P., SABRACOS, L., MOUKTAROUDI, M., ADAMIS, T., TZEPI, I., GIAMARELLOU, H. & DOUZINAS, E. E. (2007) Early apoptosis of blood monocytes is a determinant of survival in experimental sepsis by multi-drug-resistant Pseudomonas aeruginosa. *Clin Exp Immunol,* 149, 103-8.

ARORA, S. K., NEELY, A. N., BLAIR, B., LORY, S. & RAMPHAL, R. (2005) Role of motility and flagellin glycosylation in the pathogenesis of Pseudomonas aeruginosa burn wound infections. *Infect Immun,* 73, 4395-8.

ARORA, S. K., WOLFGANG, M. C., LORY, S. & RAMPHAL, R. (2004) Sequence polymorphism in the glycosylation island and flagellins of Pseudomonas aeruginosa. *J Bacteriol,* 186, 2115-22.

ASHARE, A., MONICK, M. M., NYMON, A. B., MORRISON, J. M., NOBLE, M., POWERS, L. S., YAROVINSKY, T. O., YAHR, T. L. & HUNNINGHAKE, G. W. (2007) Pseudomonas aeruginosa delays Kupffer cell death via stabilization of the X-chromosome-linked inhibitor of apoptosis protein. *J Immunol,* 179, 505-13.

ASIKYAN, M. L., KUS, J. V. & BURROWS, L. L. (2008) Novel proteins that modulate type IV pilus retraction dynamics in Pseudomonas aeruginosa. *J Bacteriol,* 190, 7022-34.

AUGUSTIN, D. K., SONG, Y., BAEK, M. S., SAWA, Y., SINGH, G., TAYLOR, B., RUBIO-MILLS, A., FLANAGAN, J. L., WIENER-KRONISH, J. P. & LYNCH, S. V. (2007) Presence or absence of lipopolysaccharide O antigens affects type III secretion by Pseudomonas aeruginosa. *J Bacteriol,* 189, 2203-9.

BABIC, A., LINDNER, A. B., VULIC, M., STEWART, E. J. & RADMAN, M. (2008) Direct Visualization of Horizontal Gene Transfer. *Science,* 319, 1533-1536.

BAREKZI, N., BEINLICH, K., HOANG, T. T., PHAM, X. Q., KARKHOFF-SCHWEIZER, R. & SCHWEIZER, H. P. (2000) High-frequency flp

recombinase-mediated inversions of the oriC-containing region of the Pseudomonas aeruginosa genome. *J Bacteriol,* 182, 7070-4.

BARKER, A. P., VASIL, A. I., FILLOUX, A., BALL, G., WILDERMAN, P. J. & VASIL, M. L. (2004) A novel extracellular phospholipase C of Pseudomonas aeruginosa is required for phospholipid chemotaxis. *Mol Microbiol,* 53, 1089-98.

BATTLE, S. E., MEYER, F., RELLO, J., KUNG, V. L. & HAUSER, A. R. (2008) The Hybrid Pathogenicity Island PAGI-5 Contributes to the Highly Virulent Phenotype of a Pseudomonas aeruginosa Isolate in Mammals. *J. Bacteriol.,* JB.00785-08.

BATTLE, S. E., RELLO, J. & HAUSER, A. R. (2009) Genomic islands of Pseudomonas aeruginosa. *FEMS Microbiol Lett,* 290, 70-8.

BIANCHI, S. M., PRINCE, L. R., MCPHILLIPS, K., ALLEN, L., MARRIOTT, H. M., TAYLOR, G. W., HELLEWELL, P. G., SABROE, I., DOCKRELL, D. H., HENSON, P. W. & WHYTE, M. K. B. (2008) Impairment of Apoptotic Cell Engulfment by Pyocyanin, a Toxic Metabolite of Pseudomonas aeruginosa. *Am. J. Respir. Crit. Care Med.,* 177, 35-43.

BILIANA, L., SANDRINE, B., JEAN-MARC, G., ULRICH, D., JÖRG, H. & ELISABETH, C. (2004) Excision of the high-pathogenicity island of <i>Yersinia pseudotuberculosis</i> requires the combined actions of its cognate integrase and Hef, a new recombination directionality factor. *Molecular Microbiology,* 52, 1337-1348.

BIN THANI, A. S. (2007) Genomic diversity of ten Escherichia coli strains associated with bloodstream infections. *Department of Infection, immunity and inflammation* University of Leicester.

BIRNBOIM, H. C. & DOLY, J. (1979) A rapid alkaline extraction procedure for screening recombinant plasmid DNA. *Nucleic Acids Res,* 7, 1513-23.

BJARNSHOLT, T. & GIVSKOV, M. (2007) The role of quorum sensing in the pathogenicity of the cunning aggressor Pseudomonas aeruginosa. *Anal Bioanal Chem,* 387, 409-14.

BJARNSHOLT, T., JENSEN, P. O., BURMOLLE, M., HENTZER, M., HAAGENSEN, J. A. J., HOUGEN, H. P., CALUM, H., MADSEN, K. G., MOSER, C., MOLIN, S., HOIBY, N. & GIVSKOV, M. (2005a) Pseudomonas aeruginosa tolerance to tobramycin, hydrogen peroxide and polymorphonuclear leukocytes is quorum-sensing dependent. *Microbiology,* 151, 373-383.

BJARNSHOLT, T., JENSEN, P. O., RASMUSSEN, T. B., CHRISTOPHERSEN, L., CALUM, H., HENTZER, M., HOUGEN, H. P., RYGAARD, J., MOSER, C., EBERL, L., HOIBY, N., GIVSKOV, M., HARJAI, K., KUMAR, R., SINGH, S., WU, H., ANDERSEN, J. B., RIEDEL, K., BAGGE, N., KUMAR, N., SCHEMBRI, M. A., SONG, Z., KRISTOFFERSEN, P., MANEFIELD, M., COSTERTON, J. W., MOLIN, S., STEINBERG, P. & KJELLEBERG, S. (2005b) Garlic blocks quorum sensing and promotes rapid clearing of pulmonary Pseudomonas aeruginosa infections

Garlic blocks quorum sensing and attenuates the virulence of Pseudomonas aeruginosa

Attenuation of Pseudomonas aeruginosa virulence by quorum sensing inhibitors. *Microbiology,* 151, 3873-80.

BOECHAT, A. L. & BALDINI, R. L. (2007) Expression of genes in the Pathogenicity island PAPI-1 of Pseudomonas aeruginosa PA14 and their role in virulence in the Dictyostelium discoiduem model. *XXXVI Annual Meeting of the Brazilian*

BOONTHAM, P., ROBINS, A., CHANDRAN, P., PRITCHARD, D., CAMARA, M., WILLIAMS, P., CHUTHAPISITH, S., MCKECHNIE, A., ROWLANDS, B. J. & EREMIN, O. (2008) Significant immunomodulatory effects of Pseudomonas aeruginosa quorum-sensing signal molecules: possible link in human sepsis. *Clin Sci (Lond)*, 115, 343-51.

BOUZA, E., SAN JUAN, R., MUNOZ, P., VOSS, A. & KLUYTMANS, J. (2001) A European perspective on nosocomial urinary tract infections II. Report on incidence, clinical characteristics and outcome (ESGNI-004 study). European Study Group on Nosocomial Infection. *Clin Microbiol Infect*, 7, 532-42.

BOYD, E. F., ALMAGRO-MORENO, S. & PARENT, M. A. (2009) Genomic islands are dynamic, ancient integrative elements in bacterial evolution. *Trends Microbiol*, 17, 47-53.

BROWN, S. P., WEST, S. A., DIGGLE, S. P. & GRIFFIN, A. S. (2009) Social evolution in micro-organisms and a Trojan horse approach to medical intervention strategies. *Philos Trans R Soc Lond B Biol Sci*, 364, 3157-68.

BRZUSZKIEWICZ, E., BRÃ¼GGEMANN, H., LIESEGANG, H., EMMERTH, M., Ã–LSCHLÃ¤GER, T., NAGY, G. B., ALBERMANN, K., WAGNER, C., BUCHRIESER, C., EMÅ'DY, L., GOTTSCHALK, G., HACKER, J. R. & DOBRINDT, U. (2006) How to become a uropathogen: Comparative genomic analysis of extraintestinal pathogenic Escherichia coli strains. *Proceedings of the National Academy of Sciences*, 103, 12879-12884.

BUCHRIESER, C., BROSCH, R., BACH, S., GUIYOULE, A. & CARNIEL, E. (1998) The high-pathogenicity island of Yersinia pseudotuberculosis can be inserted into any of the three chromosomal asn tRNA genes. *Mol Microbiol*, 30, 965-78.

CABALLERO, A., THIBODEAUX, B., MARQUART, M., TRAIDEJ, M. & O'CALLAGHAN, R. (2004) Pseudomonas keratitis: protease IV gene conservation, distribution, and production relative to virulence and other Pseudomonas proteases. *Invest Ophthalmol Vis Sci*, 45, 522-30.

CARTER, M. E. K. (2009). University of Leicester.

CASTANG, S., MCMANUS, H. R., TURNER, K. H. & DOVE, S. L. (2008) H-NS family members function coordinately in an opportunistic pathogen. *Proc Natl Acad Sci U S A*, 105, 18947-52.

CHARLEBOIS, R. L. (1999) *Organization of the prokaryotic genome* Washington, D.C., ASM Press.

CHEN, J. & NOVICK, R. P. (2009) Phage-mediated intergeneric transfer of toxin genes. *Science*, 323, 139-41.

CHHABRA, S. R., HARTY, C., HOOI, D. S., DAYKIN, M., WILLIAMS, P., TELFORD, G., PRITCHARD, D. I. & BYCROFT, B. W. (2003) Synthetic analogues of the bacterial signal (quorum sensing) molecule N-(3-oxododecanoyl)-L-homoserine lactone as immune modulators. *J Med Chem*, 46, 97-104.

CHOI, K.-H. & SCHWEIZER, H. P. (2006a) mini-Tn7 insertion in bacteria with single attTn7 sites: example Pseudomonas aeruginosa. *Nat. Protocols*, 1, 153-161.

CHOI, K. H., KUMAR, A. & SCHWEIZER, H. P. (2005) A 10-min method for preparation of highly electrocompetent Pseudomonas aeruginosa cells:

Application for DNA fragment transfer between chromosomes and plasmid transformation. *J Microbiol Methods*.

CHOI, K. H. & SCHWEIZER, H. P. (2005) An improved method for rapid generation of unmarked Pseudomonas aeruginosa deletion mutants. *BMC Microbiol*, 5, 30.

CHOI, K. H. & SCHWEIZER, H. P. (2006b) mini-Tn7 insertion in bacteria with single attTn7 sites: example Pseudomonas aeruginosa. *Nat Protoc*, 1, 153-61.

CHOLLEY, P., THOUVEREZ, M., FLORET, N., BERTRAND, X. & TALON, D. (2008) The role of water fittings in intensive care rooms as reservoirs for the colonization of patients with Pseudomonas aeruginosa. *Intensive Care Med*.

COBURN, P. S., BAGHDAYAN, A. S., DOLAN, G. T. & SHANKAR, N. (2008) An AraC-type transcriptional regulator encoded on the Enterococcus faecalis pathogenicity island contributes to pathogenesis and intracellular macrophage survival. *Infect Immun*, 76, 5668-76.

COMOLLI, J. C., HAUSER, A. R., WAITE, L., WHITCHURCH, C. B., MATTICK, J. S. & ENGEL, J. N. (1999) Pseudomonas aeruginosa gene products PilT and PilU are required for cytotoxicity in vitro and virulence in a mouse model of acute pneumonia. *Infect Immun*, 67, 3625-30.

CORNELIS, G. R. (2006) The type III secretion injectisome. *Nat Rev Microbiol*, 4, 811-25.

CORNELIS, P. (Ed.) (2008) *Pseudomonas: Genomics and Molecular biology*, Caister Academic Press.

COWELL, B. A., TWINING, S. S., HOBDEN, J. A., KWONG, M. S. F. & FLEISZIG, S. M. J. (2003) Mutation of lasA and lasB reduces Pseudomonas aeruginosa invasion of epithelial cells. *Microbiology*, 149, 2291-2299.

DARLING, A. C. E., MAU, B., BLATTNER, F. R. & PERNA, N. T. (2004) Mauve: Multiple Alignment of Conserved Genomic Sequence With Rearrangements. *Genome Research*, 14, 1394-1403.

DAVIES, D. G., PARSEK, M. R., PEARSON, J. P., IGLEWSKI, B. H., COSTERTON, J. W. & GREENBERG, E. P. (1998) The involvement of cell-to-cell signals in the development of a bacterial biofilm. *Science*, 280, 295-8.

DENG, Q., ZHANG, Y. & BARBIERI, J. T. (2007) Intracellular Trafficking of Pseudomonas ExoS, a Type III Cytotoxin. *Traffic*, 8, 1331-1345.

DENG, W., LIOU, S.-R., PLUNKETT III, G., MAYHEW, G. F., ROSE, D. J., BURLAND, V., KODOYIANNI, V., SCHWARTZ, D. C. & BLATTNER, F. R. (2003) Comparative Genomics of Salmonellaenterica Serovar Typhi Strains Ty2 and CT18. *J. Bacteriol.*, 185, 2330-2337.

DIGGLE, S. P., CORNELIS, P., WILLIAMS, P. & CÁMARA, M. (2006) 4-Quinolone signalling in Pseudomonas aeruginosa: Old molecules, new perspectives. *International Journal of Medical Microbiology*, 296, 83-91.

DIGGLE, S. P., CRUSZ, S. A. & CAMARA, M. (2007a) Quorum sensing. *Curr Biol*, 17, R907-10.

DIGGLE, S. P., GRIFFIN, A. S., CAMPBELL, G. S. & WEST, S. A. (2007b) Cooperation and conflict in quorum-sensing bacterial populations. *Nature*, 450, 411-4.

DIGGLE, S. P., WINZER, K., CHHABRA, S. R., WORRALL, K. E., CAMARA, M. & WILLIAMS, P. (2003) The Pseudomonas aeruginosa quinolone signal molecule overcomes the cell density-dependency of the quorum sensing hierarchy, regulates rhl-dependent genes at the onset of stationary phase and can be produced in the absence of LasR. *Mol Microbiol*, 50, 29-43.

DORING, G. & PIER, G. B. (2008) Vaccines and immunotherapy against Pseudomonas aeruginosa. *Vaccine,* 26, 1011-24.

DORMAN, C. J. (2007) H-NS, the genome sentinel. *Nat Rev Micro,* 5, 157-161.

DOUBLET, B., GOLDING, G. R., MULVEY, M. R. & CLOECKAERT, A. (2008a) Secondary chromosomal attachment site and tandem integration of the mobilizable Salmonella genomic island 1. *PLoS One,* 3, e2060.

DOUBLET, B., PRAUD, K., BERTRAND, S., COLLARD, J. M., WEILL, F. X. & CLOECKAERT, A. (2008b) Novel insertion sequence- and transposon-mediated genetic rearrangements in genomic island SGI1 of Salmonella enterica serovar Kentucky. *Antimicrob Agents Chemother,* 52, 3745-54.

DOUGLAS, M. W., MULHOLLAND, K., DENYER, V. & GOTTLIEB, T. (2001) Multi-drug resistant Pseudomonas aeruginosa outbreak in a burns unit--an infection control study. *Burns,* 27, 131-5.

DOWTON, M., BELSHAW, R., AUSTIN, A. D. & QUICKE, D. L. (2002) Simultaneous molecular and morphological analysis of braconid relationships (Insecta: Hymenoptera: Braconidae) indicates independent mt-tRNA gene inversions within a single wasp family. *J Mol Evol,* 54, 210-26.

DRENKARD, E. & AUSUBEL, F. M. (2002) Pseudomonas biofilm formation and antibiotic resistance are linked to phenotypic variation. *Nature,* 416, 740-743.

DRISCOLL, J. A., BRODY, S. L. & KOLLEF, M. H. (2007) The epidemiology, pathogenesis and treatment of Pseudomonas aeruginosa infections. *Drugs,* 67, 351-68.

DUBERN, J. F. & DIGGLE, S. P. (2008) Quorum sensing by 2-alkyl-4-quinolones in Pseudomonas aeruginosa and other bacterial species. *Mol Biosyst,* 4, 882-8.

ECKBURG, P. B., BIK, E. M., BERNSTEIN, C. N., PURDOM, E., DETHLEFSEN, L., SARGENT, M., GILL, S. R., NELSON, K. E. & RELMAN, D. A. (2005) Diversity of the Human Intestinal Microbial Flora. *Science,* 308, 1635-1638.

EL SOLH, A. A., AKINNUSI, M. E., WIENER-KRONISH, J. P., LYNCH, S. V., PINEDA, L. A. & SZARPA, K. (2008) Persistent Infection with Pseudomonas Aeruginosa in Ventilator Associated Pneumonia. *Am J Respir Crit Care Med.*

ENGEL, J. & BALACHANDRAN, P. (2009) Role of Pseudomonas aeruginosa type III effectors in disease. *Current Opinion in Microbiology,* 12, 61-66.

ENGEL, L. S., HILL, J. M., CABALLERO, A. R., GREEN, L. C. & OÂ€™CALLAGHAN, R. J. (1998) Protease IV, a Unique Extracellular Protease and Virulence Factor from Pseudomonas aeruginosa. *Journal of Biological Chemistry,* 273, 16792-16797.

ERNST, R. K., D'ARGENIO, D. A., ICHIKAWA, J. K., BANGERA, M. G., SELGRADE, S., BURNS, J. L., HIATT, P., MCCOY, K., BRITTNACHER, M., KAS, A., SPENCER, D. H., OLSON, M. V., RAMSEY, B. W., LORY, S. & MILLER, S. I. (2003) Genome mosaicism is conserved but not unique in Pseudomonas aeruginosa isolates from the airways of young children with cystic fibrosis. *Environ Microbiol,* 5, 1341-9.

ESNAULT, E., VALENS, M., ESPELI, O. & BOCCARD, F. (2007) Chromosome structuring limits genome plasticity in Escherichia coli. *PLoS Genet,* 3, e226.

FARINHA, M. A., CONWAY, B. D., GLASIER, L. M., ELLERT, N. W., IRVIN, R. T., SHERBURNE, R. & PARANCHYCH, W. (1994) Alteration of the pilin adhesin of Pseudomonas aeruginosa PAO results in normal pilus biogenesis but a loss of adherence to human pneumocyte cells and decreased virulence in mice. *Infect Immun,* 62, 4118-23.

FASS, E. & GROISMAN, E. A. Control of Salmonella pathogenicity island-2 gene expression. *Current Opinion in Microbiology,* In Press, Corrected Proof %U http://www.sciencedirect.com/science/article/B6VS2-4VRWHC8-1/2/85e34616c850d6c6d12ee6ff9a0f41e8.

FELTMAN, H., SCHULERT, G., KHAN, S., JAIN, M., PETERSON, L. & HAUSER, A. R. (2001) Prevalence of type III secretion genes in clinical and environmental isolates of Pseudomonas aeruginosa. *Microbiology,* 147, 2659-69.

FIGURSKI, D. H. & HELINSKI, D. R. (1979) Replication of an origin-containing derivative of plasmid RK2 dependent on a plasmid function provided in trans. *Proceedings of the National Academy of Sciences of the United States of America,* 76, 1648-1652.

FINNAN, S., MORRISSEY, J. P., O'GARA, F. & BOYD, E. F. (2004) Genome diversity of Pseudomonas aeruginosa isolates from cystic fibrosis patients and the hospital environment. *J Clin Microbiol,* 42, 5783-92.

FLEISCHMANN, R. D., ADAMS, M. D., WHITE, O., CLAYTON, R. A., KIRKNESS, E. F., KERLAVAGE, A. R., BULT, C. J., TOMB, J. F., DOUGHERTY, B. A., MERRICK, J. M. & ET AL. (1995) Whole-genome random sequencing and assembly of Haemophilus influenzae Rd. *Science,* 269, 496-512.

FONSECA, A. P., CORREIA, P., SOUSA, J. C. & TENREIRO, R. (2007) Association patterns of Pseudomonas aeruginosa clinical isolates as revealed by virulence traits, antibiotic resistance, serotype and genotype. *FEMS Immunol Med Microbiol,* 51, 505-16.

GADBERRY, M. D., MALCOMBER, S. T., DOUST, A. N. & KELLOGG, E. A. (2005) Primaclade--a flexible tool to find conserved PCR primers across multiple species. *Bioinformatics,* 21, 1263-4.

GAILLARD, M., PERNET, N., VOGNE, C., HAGENBUCHLE, O. & VAN DER MEER, J. R. (2008) Host and invader impact of transfer of the clc genomic island into Pseudomonas aeruginosa PAO1. *Proc Natl Acad Sci U S A,* 105, 7058-63.

GAL-MOR, O. & FINLAY, B. B. (2006) Pathogenicity islands: a molecular toolbox for bacterial virulence. *Cell Microbiol,* 8, 1707-19.

GANG, R. K., BANG, R. L., SANYAL, S. C., MOKADDAS, E. & LARI, A. R. (1999) Pseudomonas aeruginosa septicaemia in burns. *Burns,* 25, 611-6.

GERMON, P., ROCHE, D., MELO, S., MIGNON-GRASTEAU, S., DOBRINDT, U., HACKER, J., SCHOULER, C. & MOULIN-SCHOULEUR, M. (2007) tDNA locus polymorphism and ecto-chromosomal DNA insertion hot-spots are related to the phylogenetic group of Escherichia coli strains. *Microbiology,* 153, 826-837.

GIAMARELLOS-BOURBOULIS, E. J., ROUTSI, C., PLACHOURAS, D., MARKAKI, V., RAFTOGIANNIS, M., ZERVAKIS, D., KOUSSOULAS, V., ORFANOS, S., KOTANIDOU, A., ARMAGANIDIS, A., ROUSSOS, C. & GIAMARELLOU, H. (2006) Early apoptosis of blood monocytes in the septic host: is it a mechanism of protection in the event of septic shock? *Crit Care,* 10, R76.

GIAMARELLOU, H. & KANELLAKOPOULOU, K. (2008) Current therapies for pseudomonas aeruginosa. *Crit Care Clin,* 24, 261-78, viii.

GILTNER, C. L., VAN SCHAIK, E. J., AUDETTE, G. F., KAO, D., HODGES, R. S., HASSETT, D. J. & IRVIN, R. T. (2006) The Pseudomonas aeruginosa type IV

pilin receptor binding domain functions as an adhesin for both biotic and abiotic surfaces. *Mol Microbiol,* 59, 1083-96.

GORDON, J. L., BYRNE, K. P. & WOLFE, K. H. (2009) Additions, losses, and rearrangements on the evolutionary route from a reconstructed ancestor to the modern Saccharomyces cerevisiae genome. *PLoS Genet,* 5, e1000485.

GROISMAN, E. A. & OCHMAN, H. (1996) Pathogenicity islands: bacterial evolution in quantum leaps. *Cell,* 87, 791-4.

HABERLE, R. C., FOURCADE, H. M., BOORE, J. L. & JANSEN, R. K. (2008) Extensive rearrangements in the chloroplast genome of Trachelium caeruleum are associated with repeats and tRNA genes. *J Mol Evol,* 66, 350-61.

HACKER, J., BENDER, L., OTT, M., WINGENDER, J., LUND, B., MARRE, R. & GOEBEL, W. (1990) Deletions of chromosomal regions coding for fimbriae and hemolysins occur in vitro and in vivo in various extraintestinal Escherichia coli isolates. *Microb Pathog,* 8, 213-25.

HANEDA, T., ISHII, Y., DANBARA, H. & OKADA, N. (2009) Genome-wide identification of novel genomic islands that contribute to Salmonella virulence in mouse systemic infection. *FEMS Microbiol Lett.*

HARE, J. M., WAGNER, A. K. & MCDONOUGH, K. A. (1999) Independent acquisition and insertion into different chromosomal locations of the same pathogenicity island in Yersinia pestis and Yersinia pseudotuberculosis. *Mol Microbiol,* 31, 291-303.

HARRISON, E. M., CARTER, M. E. K., LUCK, S., OU, H.-Y., HE, X., DENG, Z., O'CALLAGHAN, C., KADIOGLU, A. & RAJAKUMAR, K. (2009) The pathogenicity islands PAPI-1 and PAPI-2 contribute en bloc individually and synergistically to virulence of Pseudomonas aeruginosa strain PA14 in murine models of acute pneumonia and bacteraemia. *Infect Immun.*

HAUSER, A. R. (2009) The type III secretion system of Pseudomonas aeruginosa: infection by injection. *Nat Rev Microbiol,* 7, 654-65.

HE, J., BALDINI, R. L., DEZIEL, E., SAUCIER, M., ZHANG, Q., LIBERATI, N. T., LEE, D., URBACH, J., GOODMAN, H. M. & RAHME, L. G. (2004) The broad host range pathogen Pseudomonas aeruginosa strain PA14 carries two pathogenicity islands harboring plant and animal virulence genes. *Proc Natl Acad Sci U S A,* 101, 2530-5.

HEAD, N. E. & YU, H. (2004) Cross-sectional analysis of clinical and environmental isolates of Pseudomonas aeruginosa: biofilm formation, virulence, and genome diversity. *Infect Immun,* 72, 133-44.

HELM, R. A., LEE, A. G., CHRISTMAN, H. D. & MALOY, S. (2003) Genomic rearrangements at rrn operons in Salmonella. *Genetics,* 165, 951-9.

HENDRICKSON, E. L., PLOTNIKOVA, J., MAHAJAN-MIKLOS, S., RAHME, L. G. & AUSUBEL, F. M. (2001) Differential Roles of the Pseudomonas aeruginosa PA14 rpoN Gene in Pathogenicity in Plants, Nematodes, Insects, and Mice. *J. Bacteriol.,* 183, 7126-7134.

HENSEL, M. (2004) Evolution of pathogenicity islands of Salmonella enterica. *Int J Med Microbiol,* 294, 95-102.

HENTZER, M., WU, H., ANDERSEN, J. B., RIEDEL, K., RASMUSSEN, T. B., BAGGE, N., KUMAR, N., SCHEMBRI, M. A., SONG, Z., KRISTOFFERSEN, P., MANEFIELD, M., COSTERTON, J. W., MOLIN, S., EBERL, L., STEINBERG, P., KJELLEBERG, S., HOIBY, N. & GIVSKOV, M. (2003) Attenuation of Pseudomonas aeruginosa virulence by quorum sensing inhibitors. *EMBO J,* 22, 3803-15.

HEYDORN, A., ERSBOLL, B., KATO, J., HENTZER, M., PARSEK, M. R., TOLKER-NIELSEN, T., GIVSKOV, M. & MOLIN, S. (2002) Statistical Analysis of Pseudomonas aeruginosa Biofilm Development: Impact of Mutations in Genes Involved in Twitching Motility, Cell-to-Cell Signaling, and Stationary-Phase Sigma Factor Expression. *Appl. Environ. Microbiol.,* 68, 2008-2017.

HINCHLIFFE, S. J., HOWARD, S. L., HUANG, Y. H., CLARKE, D. J. & WREN, B. W. (2008) The importance of the Rcs phosphorelay in the survival and pathogenesis of the enteropathogenic yersiniae. *Microbiology,* 154, 1117-1131.

HOANG, T. T., KARKHOFF-SCHWEIZER, R. R., KUTCHMA, A. J. & SCHWEIZER, H. P. (1998) A broad-host-range Flp-FRT recombination system for site-specific excision of chromosomally-located DNA sequences: application for isolation of unmarked Pseudomonas aeruginosa mutants. *Gene,* 212, 77-86.

HOCHHUT, B., BEABER, J. W., WOODGATE, R. & WALDOR, M. K. (2001) Formation of Chromosomal Tandem Arrays of the SXT Element and R391, Two Conjugative Chromosomally Integrating Elements That Share an Attachment Site. *J. Bacteriol.,* 183, 1124-1132.

HOCHHUT, B., WILDE, C., BALLING, G., MIDDENDORF, B., DOBRINDT, U., BRZUSZKIEWICZ, E., GOTTSCHALK, G., CARNIEL, E. & HACKER, J. (2006) Role of pathogenicity island-associated integrases in the genome plasticity of uropathogenic Escherichia coli strain 536. *Mol Microbiol,* 61, 584-95.

HOLLY, L. H. & JOSEPH, P. D. (2006) Natural transformation of *Neisseria gonorrhoeae*: from DNA donation to homologous recombination. *Molecular Microbiology,* 59, 376-385.

HPA (2009) Pseudomonas spp. and Stenotrophomonas maltophilia bacteraemia in England,

Wales, and Northern Ireland, 2004 to 2008. Health protection agency

HUANG, Y. H., FERRIERES, L. & CLARKE, D. J. (2006) The role of the Rcs phosphorelay in Enterobacteriaceae. *Research in microbiology,* 157, 206-212.

IMAMURA, Y., YANAGIHARA, K., TOMONO, K., OHNO, H., HIGASHIYAMA, Y., MIYAZAKI, Y., HIRAKATA, Y., MIZUTA, Y., KADOTA, J., TSUKAMOTO, K. & KOHNO, S. (2005) Role of Pseudomonas aeruginosa quorum-sensing systems in a mouse model of chronic respiratory infection. *Journal of medical microbiology,* 54, 515-518.

JAIN, S. & OHMAN, D. (2004) *Alginate Biosynthesis,* Springer.

JANDER, G., RAHME, L. G. & AUSUBEL, F. M. (2000) Positive correlation between virulence of Pseudomonas aeruginosa mutants in mice and insects. *J Bacteriol,* 182, 3843-5.

JONES, A. M., GOVAN, J. R., DOHERTY, C. J., DODD, M. E., ISALSKA, B. J., STANBRIDGE, T. N. & WEBB, A. K. (2001) Spread of a multiresistant strain of Pseudomonas aeruginosa in an adult cystic fibrosis clinic. *Lancet,* 358, 557-8.

JUHAS, M., CROOK, D. W., DIMOPOULOU, I. D., LUNTER, G., HARDING, R. M., FERGUSON, D. J. & HOOD, D. W. (2007a) Novel type IV secretion system involved in propagation of genomic islands. *J Bacteriol,* 189, 761-71.

JUHAS, M., CROOK, D. W. & HOOD, D. W. (2008) Type IV secretion systems: tools of bacterial horizontal gene transfer and virulence. *Cell Microbiol,* 10, 2377-86.

JUHAS, M., POWER, P. M., HARDING, R. M., FERGUSON, D. J., DIMOPOULOU, I. D., ELAMIN, A. R., MOHD-ZAIN, Z., HOOD, D. W., ADEGBOLA, R., ERWIN, A., SMITH, A., MUNSON, R. S., HARRISON, A., MANSFIELD, L.,

BENTLEY, S. & CROOK, D. W. (2007b) Sequence and functional analyses of Haemophilus spp. genomic islands. *Genome Biol,* 8, R237.

JUHAS, M., VAN DER MEER, J. R., GAILLARD, M., HARDING, R. M., HOOD, D. W. & CROOK, D. W. (2009) Genomic islands: tools of bacterial horizontal gene transfer and evolution. *FEMS Microbiol Rev,* 33, 376-93.

JYOT, J., SONAWANE, A., WU, W. & RAMPHAL, R. (2007) Genetic mechanisms involved in the repression of flagellar assembly by Pseudomonas aeruginosa in human mucus. *Mol Microbiol,* 63, 1026-38.

KIEWITZ, C., LARBIG, K., KLOCKGETHER, J., WEINEL, C. & TUMMLER, B. (2000) Monitoring genome evolution ex vivo: reversible chromosomal integration of a 106 kb plasmid at two tRNA(Lys) gene loci in sequential Pseudomonas aeruginosa airway isolates. *Microbiology,* 146 (Pt 10), 2365-73.

KINTZ, E. & GOLDBERG, J. B. (2008) Regulation of lipopolysaccharide O antigen expression in Pseudomonas aeruginosa. *Future Microbiol,* 3, 191-203.

KIPNIS, E., SAWA, T. & WIENER-KRONISH, J. (2006) Targeting mechanisms of Pseudomonas aeruginosa pathogenesis. *Med Mal Infect,* 36, 78-91.

KLAUSEN, M., HEYDORN, A., RAGAS, P., LAMBERTSEN, L., AAES-JORGENSEN, A., MOLIN, S. & TOLKER-NIELSEN, T. (2003) Biofilm formation by Pseudomonas aeruginosa wild type, flagella and type IV pili mutants. *Mol Microbiol,* 48, 1511-24.

KLOCKGETHER, J., REVA, O., LARBIG, K. & TUMMLER, B. (2004) Sequence analysis of the mobile genome island pKLC102 of Pseudomonas aeruginosa C. *J Bacteriol,* 186, 518-34.

KLOCKGETHER, J., REVA, O. & TUMMLER, B. (2006) Spread of genomic islands between and environmental strains. IN LOGAN, N. A., LAPPIN-SCOTT, H. M. & OYSTON, P. C. F. (Eds.) *Prokarotic diversity: mechanisms and significance* Cambridge University Press.

KLOCKGETHER, J., WURDEMANN, D., REVA, O., WIEHLMANN, L. & TUMMLER, B. (2007a) Diversity of the abundant pKLC102/PAGI-2 family of genomic islands in Pseudomonas aeruginosa. *Journal of Bacteriology,* 189, 2443-2459.

KLOCKGETHER, J., WURDEMANN, D., REVA, O., WIEHLMANN, L. & TUMMLER, B. (2007b) Diversity of the abundant pKLC102/PAGI-2 family of genomic islands in Pseudomonas aeruginosa. *J Bacteriol,* 189, 2443-59.

KNODLER, L. A. & BRETT FINLAY, B. (2001) Salmonella and apoptosis: to live or let die? *Microbes and Infection,* 3, 1321-1326.

KOMANO, T., UTSUMI, R. & KAWAMUKAI, M. (1991) Functional analysis of the fic gene involved in regulation of cell division. *Res Microbiol,* 142, 269-77.

KOTHAPALLI, S., NAIR, S., ALOKAM, S., PANG, T., KHAKHRIA, R., WOODWARD, D., JOHNSON, W., STOCKER, B. A., SANDERSON, K. E. & LIU, S. L. (2005) Diversity of genome structure in Salmonella enterica serovar Typhi populations. *J Bacteriol,* 187, 2638-50.

KRESSE, A. U., DINESH, S. D., LARBIG, K. & ROMLING, U. (2003) Impact of large chromosomal inversions on the adaptation and evolution of Pseudomonas aeruginosa chronically colonizing cystic fibrosis lungs. *Mol Microbiol,* 47, 145-58.

KUKAVICA-IBRULJ, I., BRAGONZI, A., PARONI, M., WINSTANLEY, C., SANSCHAGRIN, F., O'TOOLE, G. A. & LEVESQUE, R. C. (2008) In vivo growth of Pseudomonas aeruginosa strains PAO1 and PA14 and the

hypervirulent strain LESB58 in a rat model of chronic lung infection. *J Bacteriol*, 190, 2804-13.

KULASEKARA, B. R., KULASEKARA, H. D., WOLFGANG, M. C., STEVENS, L., FRANK, D. W. & LORY, S. (2006) Acquisition and evolution of the exoU locus in Pseudomonas aeruginosa. *J Bacteriol*, 188, 4037-50.

LANGILLE, M. G., HSIAO, W. W. & BRINKMAN, F. S. (2008) Evaluation of genomic island predictors using a comparative genomics approach. *BMC Bioinformatics*, 9, 329.

LARBIG, K. D., CHRISTMANN, A., JOHANN, A., KLOCKGETHER, J., HARTSCH, T., MERKL, R., WIEHLMANN, L., FRITZ, H. J. & TUMMLER, B. (2002) Gene islands integrated into tRNA(Gly) genes confer genome diversity on a Pseudomonas aeruginosa clone. *J Bacteriol*, 184, 6665-80.

LARKIN, M. A., BLACKSHIELDS, G., BROWN, N. P., CHENNA, R., MCGETTIGAN, P. A., MCWILLIAM, H., VALENTIN, F., WALLACE, I. M., WILM, A., LOPEZ, R., THOMPSON, J. D., GIBSON, T. J. & HIGGINS, D. G. (2007) Clustal W and Clustal X version 2.0. *Bioinformatics*, 23, 2947-8.

LATIFI, A., WINSON, M. K., FOGLINO, M., BYCROFT, B. W., STEWART, G. S., LAZDUNSKI, A. & WILLIAMS, P. (1995) Multiple homologues of LuxR and LuxI control expression of virulence determinants and secondary metabolites through quorum sensing in Pseudomonas aeruginosa PAO1. *Mol Microbiol*, 17, 333-43.

LAU, G. W., HASSETT, D. J., RAN, H. & KONG, F. (2004a) The role of pyocyanin in Pseudomonas aeruginosa infection. *Trends Mol Med*, 10, 599-606.

LAU, G. W., RAN, H., KONG, F., HASSETT, D. J. & MAVRODI, D. (2004b) Pseudomonas aeruginosa pyocyanin is critical for lung infection in mice. *Infection and immunity*, 72, 4275-4278.

LAU, G. W., RAN, H., KONG, F., HASSETT, D. J. & MAVRODI, D. (2004c) Pseudomonas aeruginosa pyocyanin is critical for lung infection in mice. *Infect Immun*, 72, 4275-8.

LEE, D. G., URBACH, J. M., WU, G., LIBERATI, N. T., FEINBAUM, R. L., MIYATA, S., DIGGINS, L. T., HE, J., SAUCIER, M., DEZIEL, E., FRIEDMAN, L., LI, L., GRILLS, G., MONTGOMERY, K., KUCHERLAPATI, R., RAHME, L. G. & AUSUBEL, F. M. (2006a) Genomic analysis reveals that Pseudomonas aeruginosa virulence is combinatorial. *Genome biology*, 7, R90.

LEE, D. G., URBACH, J. M., WU, G., LIBERATI, N. T., FEINBAUM, R. L., MIYATA, S., DIGGINS, L. T., HE, J., SAUCIER, M., DEZIEL, E., FRIEDMAN, L., LI, L., GRILLS, G., MONTGOMERY, K., KUCHERLAPATI, R., RAHME, L. G. & AUSUBEL, F. M. (2006b) Genomic analysis reveals that Pseudomonas aeruginosa virulence is combinatorial. *Genome Biol*, 7, R90.

LEHNHERR, H., MAGUIN, E., JAFRI, S. & YARMOLINSKY, M. B. (1993) Plasmid Addiction Genes of Bacteriophage P1: doc, which Causes Cell Death on Curing of Prophage, and phd, which Prevents Host Death when Prophage is Retained. *Journal of Molecular Biology*, 233, 414-428.

LEVY, H., KALISH, L. A., CANNON, C. L., GARCIA, K. C., GERARD, C., GOLDMANN, D., PIER, G. B., WEISS, S. T. & COLIN, A. A. (2008) Predictors of mucoid Pseudomonas colonization in cystic fibrosis patients. *Pediatr Pulmonol*, 43, 463-71.

LEWIS, D. A., JONES, A., PARKHILL, J., SPEERT, D. P., GOVAN, J. R., LIPUMA, J. J., LORY, S., WEBB, A. K. & MAHENTHIRALINGAM, E. (2005) Identification of DNA markers for a transmissible Pseudomonas aeruginosa cystic fibrosis strain. *Am J Respir Cell Mol Biol*, 33, 56-64.

LIANG, X., PHAM, X. Q., OLSON, M. V. & LORY, S. (2001) Identification of a genomic island present in the majority of pathogenic isolates of Pseudomonas aeruginosa. *J Bacteriol*, 183, 843-53.

LIU, G. R., LIU, W. Q., JOHNSTON, R. N., SANDERSON, K. E., LI, S. X. & LIU, S. L. (2006) Genome plasticity and ori-ter rebalancing in Salmonella typhi. *Mol Biol Evol*, 23, 365-71.

LONNEN, J. (2006) Characterising the mobile genome of Shigella. *Department of Infection, immunity, and inflammation*. University of Leicester.

LUCCHINI, S., ROWLEY, G., GOLDBERG, M. D., HURD, D., HARRISON, M. & HINTON, J. C. (2006) H-NS mediates the silencing of laterally acquired genes in bacteria. *PLoS Pathog*, 2, e81.

LUCK, S. N., TURNER, S. A., RAJAKUMAR, K., ADLER, B. & SAKELLARIS, H. (2004) Excision of the Shigella resistance locus pathogenicity island in Shigella flexneri is stimulated by a member of a new subgroup of recombination directionality factors. *J Bacteriol*, 186, 5551-4.

LYCZAK, J. B., CANNON, C. L. & PIER, G. B. (2000) Establishment of Pseudomonas aeruginosa infection: lessons from a versatile opportunist. *Microbes Infect*, 2, 1051-60.

MACKENZIE, F. M., STRUELENS, M. J., TOWNER, K. J. & GOULD, I. M. (2005) Report of the Consensus Conference on Antibiotic Resistance; Prevention and Control (ARPAC). *Clinical Microbiology & Infection*, 11, 938-954.

MAHAJAN-MIKLOS, S., RAHME, L. G. & AUSUBEL, F. M. (2000) Elucidating the molecular mechanisms of bacterial virulence using non-mammalian hosts. *Mol Microbiol*, 37, 981-8.

MAJDALANI, N. & GOTTESMAN, S. (2005) The Rcs phosphorelay: a complex signal transduction system. *Annu Rev Microbiol*, 59, 379-405.

MALLOY, J. L., VELDHUIZEN, R. A. W., THIBODEAUX, B. A., O'CALLAGHAN, R. J. & WRIGHT, J. R. (2005) Pseudomonas aeruginosa protease IV degrades surfactant proteins and inhibits surfactant host defense and biophysical functions. *Am J Physiol Lung Cell Mol Physiol*, 288, L409-418.

MARRIOTT, H. M., HELLEWELL, P. G., CROSS, S. S., INCE, P. G., WHYTE, M. K. & DOCKRELL, D. H. (2006) Decreased alveolar macrophage apoptosis is associated with increased pulmonary inflammation in a murine model of pneumococcal pneumonia. *J Immunol*, 177, 6480-8.

MATHEE, K., CIOFU, O., STERNBERG, C., LINDUM, P. W., CAMPBELL, J. I. A., JENSEN, P., JOHNSEN, A. H., GIVSKOV, M., OHMAN, D. E., SOREN, M., HOIBY, N. & KHARAZMI, A. (1999) Mucoid conversion of Pseudomonas aeruginos by hydrogen peroxide: a mechanism for virulence activation in the cystic fibrosis lung. *Microbiology*, 145, 1349-1357.

MATHEE, K., NARASIMHAN, G., VALDES, C., QIU, X., MATEWISH, J. M., KOEHRSEN, M., ROKAS, A., YANDAVA, C. N., ENGELS, R., ZENG, E., OLAVARIETTA, R., DOUD, M., SMITH, R. S., MONTGOMERY, P., WHITE, J. R., GODFREY, P. A., KODIRA, C., BIRREN, B., GALAGAN, J. E. & LORY, S. (2008) Dynamics of Pseudomonas aeruginosa genome evolution. *Proc Natl Acad Sci U S A*, 105, 3100-5.

MATXALEN, L., GOMIS-RÜTH, F. X., MIQUEL, C. & FERNANDO DE LA, C. (2002) Bacterial conjugation: a two-step mechanism for DNA transport. *Molecular Microbiology*, 45, 1-8.

MATZ, C., MORENO, A. M., ALHEDE, M., MANEFIELD, M., HAUSER, A. R., GIVSKOV, M. & KJELLEBERG, S. (2008) Pseudomonas aeruginosa uses type III secretion system to kill biofilm-associated amoebae. *ISME J.*

MCDANIEL, T. K. & KAPER, J. B. (1997) A cloned pathogenicity island from enteropathogenic Escherichia coli confers the attaching and effacing phenotype on E. coli K-12. *Mol Microbiol,* 23, 399-407.

MCMORRAN, B., TOWN, L., COSTELLOE, E., PALMER, J., ENGEL, J., HUME, D. & WAINWRIGHT, B. (2003) Effector ExoU from the type III secretion system is an important modulator of gene expression in lung epithelial cells in response to Pseudomonas aeruginosa infection. *Infect Immun,* 71, 6035-44.

MERLO, C. A., BOYLE, M. P., DIENER-WEST, M., MARSHALL, B. C., GOSS, C. H. & LECHTZIN, N. (2007) Incidence and risk factors for multiple antibiotic-resistant Pseudomonas aeruginosa in cystic fibrosis. *Chest,* 132, 562-8.

MIDDENDORF, B., HOCHHUT, B., LEIPOLD, K., DOBRINDT, U., BLUM-OEHLER, G. & HACKER, J. (2004) Instability of pathogenicity islands in uropathogenic Escherichia coli 536. *J Bacteriol,* 186, 3086-96.

MIKKELSEN, H., BALL, G., GIRAUD, C. & FILLOUX, A. (2009) Expression of Pseudomonas aeruginosa CupD fimbrial genes is antagonistically controlled by RcsB and the EAL-containing PvrR response regulators. *PLoS One,* 4, e6018.

MIKUNIYA, T., KATO, Y., IDA, T., MAEBASHI, K., MONDEN, K., KARIYAMA, R. & KUMON, H. (2007) Treatment of Pseudomonas aeruginosa biofilms with a combination of fluoroquinolones and fosfomycin in a rat urinary tract infection model. *J Infect Chemother,* 13, 285-90.

MIYATA, S., CASEY, M., FRANK, D. W., AUSUBEL, F. M. & DRENKARD, E. (2003) Use of the Galleria mellonella caterpillar as a model host to study the role of the type III secretion system in Pseudomonas aeruginosa pathogenesis. *Infect Immun,* 71, 2404-13.

MOHD-ZAIN, Z., TURNER, S. L., CERDENO-TARRAGA, A. M., LILLEY, A. K., INZANA, T. J., DUNCAN, A. J., HARDING, R. M., HOOD, D. W., PETO, T. E. & CROOK, D. W. (2004) Transferable Antibiotic Resistance Elements in Haemophilus influenzae Share a Common Evolutionary Origin with a Diverse Family of Syntenic Genomic Islands. *J. Bacteriol.,* 186, 8114-8122.

MULLANY, P. (2005) *The Dynamic Bacterial Genome.*

MUN, J. J., TAM, C., KOWBEL, D., HAWGOOD, S., BARNETT, M. J., EVANS, D. J. & FLEISZIG, S. M. (2009) Clearance of Pseudomonas aeruginosa from a healthy ocular surface involves surfactant protein D and is compromised by bacterial elastase in a murine null-infection model. *Infect Immun,* 77, 2392-8.

MURPHY, T. F., BRAUER, A. L., ESCHBERGER, K., LOBBINS, P., GROVE, L., CAI, X. & SETHI, S. (2008) Pseudomonas aeruginosa in chronic obstructive pulmonary disease. *Am J Respir Crit Care Med,* 177, 853-60.

NAVARRE, W. W., MCCLELLAND, M., LIBBY, S. J. & FANG, F. C. (2007) Silencing of xenogeneic DNA by H-NS-facilitation of lateral gene transfer in bacteria by a defense system that recognizes foreign DNA. *Genes Dev,* 21, 1456-71.

NEALSON, K. H., PLATT, T. & HASTINGS, J. W. (1970) Cellular control of the synthesis and activity of the bacterial luminescent system. *J Bacteriol,* 104, 313-22.

NICASTRO, G. G. & BALDINI, R. L. (2007) Functional characterization of Pseudomonas aeruginosa virulence-related genes located in a pathogenicity island. *XXXVI Annual Meeting of the Brazilian Society for Biochemistry and Molecular Biology (SBBq) and 10th IUBMB Conference.* Salvador da Bahia, Brazil, Sociedade Brasileira de Bioquimica e Biologia Molecular.

NOVICK, R. P. (2003) Mobile genetic elements and bacterial toxinoses: the superantigen-encoding pathogenicity islands of Staphylococcus aureus. *Plasmid,* 49, 93-105.

NOVICK, R. P., SCHLIEVERT, P. & RUZIN, A. (2001) Pathogenicity and resistance islands of staphylococci. *Microbes and Infection,* 3, 585-594.

O'TOOLE, G. A. & KOLTER, R. (1998a) Flagellar and twitching motility are necessary for Pseudomonas aeruginosa biofilm development. *Mol Microbiol,* 30, 295-304.

O'TOOLE, G. A. & KOLTER, R. (1998b) Initiation of biofilm formation in Pseudomonas fluorescens WCS365 proceeds via multiple, convergent signalling pathways: a genetic analysis. *Mol Microbiol,* 28, 449-61.

OCHMAN, H. & DAVALOS, L. M. (2006) The Nature and Dynamics of Bacterial Genomes. *Science,* 311, 1730-1733.

OCHSNER, U. A. & REISER, J. (1995) Autoinducer-mediated regulation of rhamnolipid biosurfactant synthesis in Pseudomonas aeruginosa. *Proc Natl Acad Sci U S A,* 92, 6424-8.

ORGEL, L. E. & CRICK, F. H. (1980) Selfish DNA: the ultimate parasite. *Nature,* 284, 604-7.

ORTIZ-MARTIN, I., MACHO, A. P., LAMBERSTEN, L., RAMOS, C. & BEUZON, C. R. (2006) Suicide vectors for antibiotic marker exchange and rapid generation of multiple knockout mutants by allelic exchange in Gram-negative bacteria. *J Microbiol Methods,* 67, 395-407.

OU, H.-Y., CHEN, L.-L., LONNEN, J., CHAUDHURI, R. R., THANI, A. B., SMITH, R., GARTON, N. J., HINTON, J., PALLEN, M., BARER, M. R. & RAJAKUMAR, K. (2006a) A novel strategy for the identification of genomic islands by comparative analysis of the contents and contexts of tRNA sites in closely related bacteria. *Nucl. Acids Res.,* 34, e3-.

OU, H. Y., CHEN, L. L., LONNEN, J., CHAUDHURI, R. R., THANI, A. B., SMITH, R., GARTON, N. J., HINTON, J., PALLEN, M., BARER, M. R. & RAJAKUMAR, K. (2006b) A novel strategy for the identification of genomic islands by comparative analysis of the contents and contexts of tRNA sites in closely related bacteria. *Nucleic Acids Res,* 34, e3.

OU, H. Y., CHEN, L. L., LONNEN, J., CHAUDHURI, R. R., THANI, A. B., SMITH, R., GARTON, N. J., HINTON, J., PALLEN, M., BARER, M. R. & RAJAKUMAR, K. (2006c) A novel strategy for the identification of genomic islands by comparative analysis of the contents and contexts of tRNA sites in closely related bacteria. *Nucleic acids research,* 34, e3.

OU, H. Y., HE, X., HARRISON, E. M., KULASEKARA, B. R., THANI, A. B., KADIOGLU, A., LORY, S., HINTON, J. C., BARER, M. R., DENG, Z. & RAJAKUMAR, K. (2007) MobilomeFINDER: web-based tools for in silico and experimental discovery of bacterial genomic islands. *Nucleic Acids Res.*

PALLEN, M. J. & WREN, B. W. (2007) Bacterial pathogenomics. *Nature,* 449, 835-42.

PARKHILL, J., WREN, B. W., THOMSON, N. R., TITBALL, R. W., HOLDEN, M. T. G., PRENTICE, M. B., SEBAIHIA, M., JAMES, K. D., CHURCHER, C., MUNGALL, K. L., BAKER, S., BASHAM, D., BENTLEY, S. D., BROOKS, K., CERDENO-TARRAGA, A. M., CHILLINGWORTH, T., CRONIN, A.,

DAVIES, R. M., DAVIS, P., DOUGAN, G., FELTWELL, T., HAMLIN, N., HOLROYD, S., JAGELS, K., KARLYSHEV, A. V., LEATHER, S., MOULE, S., OYSTON, P. C. F., QUAIL, M., RUTHERFORD, K., SIMMONDS, M., SKELTON, J., STEVENS, K., WHITEHEAD, S. & BARRELL, B. G. (2001) Genome sequence of Yersinia pestis, the causative agent of plague. *Nature*, 413, 523-527.

PAVLOVIC, G., BURRUS, V., GINTZ, B., DECARIS, B. & GUEDON, G. (2004) Evolution of genomic islands by deletion and tandem accretion by site-specific recombination: ICESt1-related elements from Streptococcus thermophilus. *Microbiology*, 150, 759-774.

PEARSON, J. P., FELDMAN, M., IGLEWSKI, B. H. & PRINCE, A. (2000) Pseudomonas aeruginosa cell-to-cell signaling is required for virulence in a model of acute pulmonary infection. *Infection and immunity*, 68, 4331-4334.

PEARSON, J. P., PESCI, E. C. & IGLEWSKI, B. H. (1997) Roles of Pseudomonas aeruginosa las and rhl quorum-sensing systems in control of elastase and rhamnolipid biosynthesis genes. *J Bacteriol*, 179, 5756-67.

PEDERSEN, A. G., JENSEN, L. J., BRUNAK, S. R., ST�RFELDT, H.-H. & USSERY, D. W. (2000) A DNA structural atlas for Escherichia coli. *Journal of Molecular Biology*, 299, 907-930 %U http: www.sciencedirect.com/science/article/B6WK7-45F51HT-FX 2 6249578b5f7841a5da1f4b53ddf42ab0.

PESSI, G. & HAAS, D. (2000) Transcriptional control of the hydrogen cyanide biosynthetic genes hcnABC by the anaerobic regulator ANR and the quorum-sensing regulators LasR and RhlR in Pseudomonas aeruginosa. *J Bacteriol*, 182, 6940-9.

PICHON, C. & FELDEN, B. (2005) Small RNA genes expressed from Staphylococcus aureus genomic and pathogenicity islands with specific expression among pathogenic strains. *Proceedings of the National Academy of Sciences of the United States of America*, 102, 14249-14254 %U http: www.pnas.org content 102 40 14249.abstract.

POPAT, R., CRUSZ, S. A. & DIGGLE, S. P. (2008) The social behaviours of bacterial pathogens. *Br Med Bull*, 87, 63-75.

POSFAI, G., PLUNKETT, G., 3RD, FEHER, T., FRISCH, D., KEIL, G. M., UMENHOFFER, K., KOLISNYCHENKO, V., STAHL, B., SHARMA, S. S., DE ARRUDA, M., BURLAND, V., HARCUM, S. W. & BLATTNER, F. R. (2006) Emergent properties of reduced-genome Escherichia coli. *Science*, 312, 1044-6.

PRIEBE, G. P., DEAN, C. R., ZAIDI, T., MELULENI, G. J., COLEMAN, F. T., COUTINHO, Y. S., NOTO, M. J., URBAN, T. A., PIER, G. B. & GOLDBERG, J. B. (2004) The galU Gene of Pseudomonas aeruginosa is required for corneal infection and efficient systemic spread following pneumonia but not for infection confined to the lung. *Infect Immun*, 72, 4224-32.

PULLINGER, G. D. & LAX, A. J. (1992) A Salmonella dublin virulence plasmid locus that affects bacterial growth under nutrient-limited conditions. *Mol Microbiol*, 6, 1631-43.

PUNDHIR, S., VIJAYVARGIYA, H. & KUMAR, A. (2008) PredictBias: a server for the identification of genomic and pathogenicity islands in prokaryotes. *In Silico Biol*, 8, 223-34.

QIN, X., EMERSON, J., STAPP, J., STAPP, L., ABE, P. & BURNS, J. L. (2003) Use of Real-Time PCR with Multiple Targets To Identify Pseudomonas aeruginosa

and Other Nonfermenting Gram-Negative Bacilli from Patients with Cystic Fibrosis. *J. Clin. Microbiol.*, 41, 4312-4317.

QIU, X., GURKAR, A. U. & LORY, S. (2006) Interstrain transfer of the large pathogenicity island (PAPI-1) of Pseudomonas aeruginosa. *Proc Natl Acad Sci U S A*, 103, 19830-5.

RAHME, L. G., AUSUBEL, F. M., CAO, H., DRENKARD, E., GOUMNEROV, B. C., LAU, G. W., MAHAJAN-MIKLOS, S., PLOTNIKOVA, J., TAN, M. W., TSONGALIS, J., WALENDZIEWICZ, C. L. & TOMPKINS, R. G. (2000) Plants and animals share functionally common bacterial virulence factors. *Proc Natl Acad Sci U S A*, 97, 8815-21.

RAHME, L. G., STEVENS, E. J., WOLFORT, S. F., SHAO, J., TOMPKINS, R. G. & AUSUBEL, F. M. (1995) Common virulence factors for bacterial pathogenicity in plants and animals. *Science*, 268, 1899-1902.

RAHME, L. G., TAN, M. W., LE, L., WONG, S. M., TOMPKINS, R. G., CALDERWOOD, S. B. & AUSUBEL, F. M. (1997) Use of model plant hosts to identify Pseudomonas aeruginosa virulence factors. *Proc Natl Acad Sci U S A*, 94, 13245-50.

RAJAKUMAR, K., SASAKAWA, C. & ADLER, B. (1997) Use of a novel approach, termed island probing, identifies the Shigella flexneri she pathogenicity island which encodes a homolog of the immunoglobulin A protease-like family of proteins. *Infect Immun*, 65, 4606-14.

RAJASHEKARA, G., COVERT, J., PETERSEN, E., ESKRA, L. & SPLITTER, G. (2008) Genomic island 2 of Brucella melitensis is a major virulence determinant: functional analyses of genomic islands. *J Bacteriol*, 190, 6243-52.

RASHID, M. H. & KORNBERG, A. (2000) Inorganic polyphosphate is needed for swimming, swarming, and twitching motilities of Pseudomonas aeruginosa. *Proc Natl Acad Sci U S A*, 97, 4885-90.

RAVATN, R., STUDER, S., SPRINGAEL, D., ZEHNDER, A. J. B. & VAN DER MEER, J. R. (1998) Chromosomal Integration, Tandem Amplification, and Deamplification in Pseudomonas putida F1 of a 105-Kilobase Genetic Element Containing the Chlorocatechol Degradative Genes from Pseudomonas sp. Strain B13. *J. Bacteriol.*, 180, 4360-4369.

RICE, S. A., TAN, C. H., MIKKELSEN, P. J., KUNG, V., WOO, J., TAY, M., HAUSER, A., MCDOUGALD, D., WEBB, J. S. & KJELLEBERG, S. (2008) The biofilm life cycle and virulence of Pseudomonas aeruginosa are dependent on a filamentous prophage. *ISME J*, 3, 271-282.

ROCCHETTA, H. L., BURROWS, L. L. & LAM, J. S. (1999) Genetics of O-antigen biosynthesis in Pseudomonas aeruginosa. *Microbiol Mol Biol Rev*, 63, 523-53.

ROCHA, E. P. (2008) The organization of the bacterial genome. *Annu Rev Genet*, 42, 211-33.

ROCHA, E. P. C. & DANCHIN, A. (2003) Gene essentiality determines chromosome organisation in bacteria. *Nucl. Acids Res.*, 31, 6570-6577.

ROMAN, G. G., NUNO, C., MANFRED, R., DANIELA, J., CAROLIN, W. & MICHAEL, H. (2008) Cooperation of *Salmonella* pathogenicity islands 1 and 4 is required to breach epithelial barriers. *Cellular Microbiology*, 10, 2364-2376.

ROMLING, U., SCHMIDT, K. D. & TUMMLER, B. (1997) Large genome rearrangements discovered by the detailed analysis of 21 Pseudomonas aeruginosa clone C isolates found in environment and disease habitats. *Journal of Molecular Biology*, 271, 386-404

ROY, C. R. & MUKHERJEE, S. (2009) Bacterial FIC Proteins AMP Up Infection. *Sci. Signal.*, 2, pe14-.

ROZEN S, S. H. (2000) *Primer3 on the WWW for general users and for biologist programmers*, Totowa, N.J., Humana.

RUMBAUGH, K. P., GRISWOLD, J. A. & HAMOOD, A. N. (2000) The role of quorum sensing in the in vivo virulence of Pseudomonas aeruginosa. *Microbes and Infection*, 2, 1721-1731.

RUMBAUGH, K. P., HAMOOD, A. N. & GRISWOLD, J. A. (1999) Analysis of Pseudomonas aeruginosa clinical isolates for possible variations within the virulence genes exotoxin A and exoenzyme S. *J Surg Res*, 82, 95-105.

RUST, L., PESCI, E. C. & IGLEWSKI, B. H. (1996) Analysis of the Pseudomonas aeruginosa elastase (lasB) regulatory region. *J. Bacteriol.*, 178, 1134-1140.

RYALL, B., DAVIES, J. C., WILSON, R., SHOEMARK, A. & WILLIAMS, H. D. (2008) Pseudomonas aeruginosa, Cyanide Accumulation and Lung Function in Cystic Fibrosis and Non-Cystic Fibrosis Bronchiectasis Patients. *Eur Respir J*.

SAKELLARIS, H., LUCK, S. N., AL-HASANI, K., RAJAKUMAR, K., TURNER, S. A. & ADLER, B. (2004) Regulated site-specific recombination of the she pathogenicity island of Shigella flexneri. *Mol Microbiol*, 52, 1329-36.

SALUNKHE, P., SMART, C. H., MORGAN, J. A., PANAGEA, S., WALSHAW, M. J., HART, C. A., GEFFERS, R., TUMMLER, B. & WINSTANLEY, C. (2005) A cystic fibrosis epidemic strain of Pseudomonas aeruginosa displays enhanced virulence and antimicrobial resistance. *J Bacteriol*, 187, 4908-20.

SAYEED, S., REAVES, L., RADNEDGE, L. & AUSTIN, S. (2000) The stability region of the large virulence plasmid of Shigella flexneri encodes an efficient postsegregational killing system. *J Bacteriol*, 182, 2416-21.

SCHIRM, M., ARORA, S. K., VERMA, A., VINOGRADOV, E., THIBAULT, P., RAMPHAL, R. & LOGAN, S. M. (2004) Structural and Genetic Characterization of Glycosylation of Type a Flagellin in Pseudomonas aeruginosa. *J. Bacteriol.*, 186, 2523-2531.

SCHUBERT, S. R., RAKIN, A. & HEESEMANN, J. R. (2004) The Yersinia high-pathogenicity island (HPI): evolutionary and functional aspects. *International Journal of Medical Microbiology*, 294, 83-94 %U http://www.sciencedirect.com/science/article/B7GW0-4D62BM5-6/2/fba35fda4bb9d5376becc4f44a76cc32.

SCHULER, G. D. (1997) Sequence mapping by electronic PCR. *Genome Res*, 7, 541-50.

SCHULERT, G. S., FELTMAN, H., RABIN, S. D., MARTIN, C. G., BATTLE, S. E., RELLO, J. & HAUSER, A. R. (2003) Secretion of the toxin ExoU is a marker for highly virulent Pseudomonas aeruginosa isolates obtained from patients with hospital-acquired pneumonia. *J Infect Dis*, 188, 1695-706.

SCHULTZ, M. J., RIJNEVELD, A. W., FLORQUIN, S., SPEELMAN, P., VAN DEVENTER, S. J. H. & VAN DER POLL, T. O. M. (2001) Impairment of host defence by exotoxin A in Pseudomonas aeruginosa pneumonia in mice. *J Med Microbiol*, 50, 822-827.

SCOTT, F. W. & PITT, T. L. (2004) Identification and characterization of transmissible Pseudomonas aeruginosa strains in cystic fibrosis patients in England and Wales. *J Med Microbiol*, 53, 609-15.

SENTCHILO, V., CZECHOWSKA, K., PRADERVAND, N., MINOIA, M., MIYAZAKI, R. & VAN DER MEER, J. R. (2009) Intracellular Excision and

Reintegration Dynamics of the ICEclc Genomic Island of Pseudomonas knackmussii sp. strain B13. *Mol Microbiol*, 8, 8.

SHAFIKHANI, S. H. & ENGEL, J. (2006) Pseudomonas aeruginosa type III-secreted toxin ExoT inhibits host-cell division by targeting cytokinesis at multiple steps. *Proceedings of the National Academy of Sciences*, 103, 15605-15610.

SHANKAR, N., BAGHDAYAN, A. S. & GILMORE, M. S. (2002) Modulation of virulence within a pathogenicity island in vancomycin-resistant Enterococcus faecalis. *Nature*, 417, 746-50.

SHAVER, C. M. & HAUSER, A. R. (2004) Relative contributions of Pseudomonas aeruginosa ExoU, ExoS, and ExoT to virulence in the lung. *Infect Immun*, 72, 6969-77.

SHEN, K., SAYEED, S., ANTALIS, P., GLADITZ, J., AHMED, A., DICE, B., JANTO, B., DOPICO, R., KEEFE, R., HAYES, J., JOHNSON, S., YU, S., EHRLICH, N., JOCZ, J., KROPP, L., WONG, R., WADOWSKY, R. M., SLIFKIN, M., PRESTON, R. A., ERDOS, G., POST, J. C., EHRLICH, G. D. & HU, F. Z. (2006) Extensive genomic plasticity in Pseudomonas aeruginosa revealed by identification and distribution studies of novel genes among clinical isolates. *Infect Immun*, 74, 5272-83.

SHIGEMURA, K., ARAKAWA, S., SAKAI, Y., KINOSHITA, S., TANAKA, K. & FUJISAWA, M. (2006) Complicated urinary tract infection caused by Pseudomonas aeruginosa in a single institution (1999-2003). *Int J Urol*, 13, 538-42.

SHIH, P. C. & HUANG, C. T. (2002) Effects of quorum-sensing deficiency on Pseudomonas aeruginosa biofilm formation and antibiotic resistance. *J Antimicrob Chemother*, 49, 309-14.

SIMON, R., PRIEFER, U. & PUHLER, A. (1983) A Broad Host Range Mobilization System for In Vivo Genetic Engineering: Transposon Mutagenesis in Gram Negative Bacteria. *Nat Biotech*, 1, 784-791.

SMART, C. H., SCOTT, F. W., WRIGHT, E. A., WALSHAW, M. J., HART, C. A., PITT, T. L. & WINSTANLEY, C. (2006) Development of a diagnosic test for the Midlands 1 cystic fibrosis epidemic strain of Pseuodmonas aeruginosa. *Journal of Medical Microbiology* 55, 1085-1091.

SMITH, L., ROSE, B., TINGPEJ, P., ZHU, H., CONIBEAR, T., MANOS, J., BYE, P., ELKINS, M., WILLCOX, M., BELL, S., WAINWRIGHT, C. & HARBOUR, C. (2006) Protease IV production in Pseudomonas aeruginosa from the lungs of adults with cystic fibrosis. *J Med Microbiol*, 55, 1641-1644.

SMITH, R. S., FEDYK, E. R., SPRINGER, T. A., MUKAIDA, N., IGLEWSKI, B. H. & PHIPPS, R. P. (2001) IL-8 production in human lung fibroblasts and epithelial cells activated by the Pseudomonas autoinducer N-3-oxododecanoyl homoserine lactone is transcriptionally regulated by NF-kappa B and activator protein-2. *J Immunol*, 167, 366-74.

SNYDER, L. & CHAMPNESS, W. (2007) *Molecular Genetics of Bacteria*, American Society for Microbiology.

SONG, J., WARE, A. & LIU, S. L. (2003) Wavelet to predict bacterial ori and ter: a tendency towards a physical balance. *BMC genomics*, 4, 17.

SPENCER, D. H., KAS, A., SMITH, E. E., RAYMOND, C. K., SIMS, E. H., HASTINGS, M., BURNS, J. L., KAUL, R. & OLSON, M. V. (2003) Whole-genome sequence variation among multiple isolates of Pseudomonas aeruginosa. *J Bacteriol*, 185, 1316-25.

STEPINSKA, M. & TRAFNY, E. A. (2008) Diverse type III secretion phenotypes among Pseudomonas aeruginosa strains upon infection of murine macrophage-like and endothelial cell lines. *Microbial Pathogenesis,* **44,** 448-458.

STOVER, C. K., PHAM, X. Q., ERWIN, A. L., MIZOGUCHI, S. D., WARRENER, P., HICKEY, M. J., BRINKMAN, F. S., HUFNAGLE, W. O., KOWALIK, D. J., LAGROU, M., GARBER, R. L., GOLTRY, L., TOLENTINO, E., WESTBROCK-WADMAN, S., YUAN, Y., BRODY, L. L., COULTER, S. N., FOLGER, K. R., KAS, A., LARBIG, K., LIM, R., SMITH, K., SPENCER, D., WONG, G. K., WU, Z., PAULSEN, I. T., REIZER, J., SAIER, M. H., HANCOCK, R. E., LORY, S. & OLSON, M. V. (2000) Complete genome sequence of Pseudomonas aeruginosa PA01, an opportunistic pathogen. *Nature,* **406,** 959-64.

SUZUKI, N., OKAYAMA, S., NONAKA, H., TSUGE, Y., INUI, M. & YUKAWA, H. (2005) Large-scale engineering of the Corynebacterium glutamicum genome. *Appl Environ Microbiol,* **71,** 3369-72.

TAN, M. W., RAHME, L. G., STERNBERG, J. A., TOMPKINS, R. G. & AUSUBEL, F. M. (1999) Pseudomonas aeruginosa killing of Caenorhabditis elegans used to identify P. aeruginosa virulence factors. *Proc Natl Acad Sci U S A,* **96,** 2408-13.

TANG, H., KAYS, M. & PRINCE, A. (1995) Role of Pseudomonas aeruginosa pili in acute pulmonary infection. *Infect Immun,* **63,** 1278-85.

TATEDA, K., ISHII, Y., HORIKAWA, M., MATSUMOTO, T., MIYAIRI, S., PECHERE, J. C., STANDIFORD, T. J., ISHIGURO, M. & YAMAGUCHI, K. (2003) The Pseudomonas aeruginosa autoinducer N-3-oxododecanoyl homoserine lactone accelerates apoptosis in macrophages and neutrophils. *Infect Immun,* **71,** 5785-93.

TERADA, L. S., JOHANSEN, K. A., NOWBAR, S., VASIL, A. I. & VASIL, M. L. (1999) Pseudomonas aeruginosa Hemolytic Phospholipase C Suppresses Neutrophil Respiratory Burst Activity. *Infect. Immun.,* **67,** 2371-2376.

TETTELIN, H., MASIGNANI, V., CIESLEWICZ, M. J., DONATI, C., MEDINI, D., WARD, N. L., ANGIUOLI, S. V., CRABTREE, J., JONES, A. L., DURKIN, A. S., DEBOY, R. T., DAVIDSEN, T. M., MORA, M., SCARSELLI, M., MARGARIT Y ROS, I., PETERSON, J. D., HAUSER, C. R., SUNDARAM, J. P., NELSON, W. C., MADUPU, R., BRINKAC, L. M., DODSON, R. J., ROSOVITZ, M. J., SULLIVAN, S. A., DAUGHERTY, S. C., HAFT, D. H., SELENGUT, J., GWINN, M. L., ZHOU, L., ZAFAR, N., KHOURI, H., RADUNE, D., DIMITROV, G., WATKINS, K., O'CONNOR, K. J., SMITH, S., UTTERBACK, T. R., WHITE, O., RUBENS, C. E., GRANDI, G., MADOFF, L. C., KASPER, D. L., TELFORD, J. L., WESSELS, M. R., RAPPUOLI, R. & FRASER, C. M. (2005) Genome analysis of multiple pathogenic isolates of Streptococcus agalactiae: implications for the microbial "pan-genome". *Proc Natl Acad Sci U S A,* **102,** 13950-5.

TETTELIN, H., RILEY, D., CATTUTO, C. & MEDINI, D. (2008) Comparative genomics: the bacterial pan-genome. *Current Opinion in Microbiology,* **11,** 472-477.

TOBE, T., ANDO, H., ISHIKAWA, H., ABE, H., TASHIRO, K., HAYASHI, T., KUHARA, S. & SUGIMOTO, N. (2005) Dual regulatory pathways integrating the RcsC-RcsD-RcsB signalling system control enterohaemorrhagic Escherichia coli pathogenicity. *Mol Microbiol,* **58,** 320-33.

TREGGIARI, M. M., ROSENFELD, M., RETSCH-BOGART, G., GIBSON, R. & RAMSEY, B. (2007) Approach to eradication of initial Pseudomonas aeruginosa infection in children with cystic fibrosis. *Pediatr Pulmonol,* 42, 751-6.

VAN DELDEN, C. (2007) Pseudomonas aeruginosa bloodstream infections: how should we treat them? *Int J Antimicrob Agents,* 30 Suppl 1, S71-5.

VASIL, M. L., CHAMBERLAIN, C. & GRANT, C. C. (1986) Molecular studies of Pseudomonas exotoxin A gene. *Infect Immun,* 52, 538-48.

VERMA, A., SCHIRM, M., ARORA, S. K., THIBAULT, P., LOGAN, S. M. & RAMPHAL, R. (2006) Glycosylation of b-Type flagellin of Pseudomonas aeruginosa: structural and genetic basis. *J Bacteriol,* 188, 4395-403.

VERNIKOS, G. S. & PARKHILL, J. (2008) Resolving the structural features of genomic islands: a machine learning approach. *Genome Res,* 18, 331-42.

VOGEL, H. J. & BONNER, D. M. (1956) Acetylornithinase of Escherichia coli: partial purification and some properties. *J Biol Chem,* 218, 97-106.

WAACK, S., KELLER, O., ASPER, R., BRODAG, T., DAMM, C., FRICKE, W. F., SUROVCIK, K., MEINICKE, P. & MERKL, R. (2006) Score-based prediction of genomic islands in prokaryotic genomes using hidden Markov models. *BMC Bioinformatics,* 7, 142.

WADE, D. S., CALFEE, M. W., ROCHA, E. R., LING, E. A., ENGSTROM, E., COLEMAN, J. P. & PESCI, E. C. (2005) Regulation of Pseudomonas quinolone signal synthesis in Pseudomonas aeruginosa. *J Bacteriol,* 187, 4372-80.

WAGNER, V. E., BUSHNELL, D., PASSADOR, L., BROOKS, A. I. & IGLEWSKI, B. H. (2003) Microarray Analysis of Pseudomonas aeruginosa Quorum-Sensing Regulons: Effects of Growth Phase and Environment. *J. Bacteriol.,* 185, 2080-2095.

WALKER, K. A. & MILLER, V. L. (2009) Synchronous gene expression of the Yersinia enterocolitica Ysa type III secretion system and its effectors. *J Bacteriol,* 191, 1816-26.

WAREHAM, D. W. & CURTIS, M. A. (2007) A genotypic and phenotypic comparison of type III secretion profiles of Pseudomonas aeruginosa cystic fibrosis and bacteremia isolates. *Int J Med Microbiol,* 297, 227-34.

WAREHAM, D. W., PAPAKONSTANTINOPOULOU, A. & CURTIS, M. A. (2005) The Pseudomonas aeruginosa PA14 type III secretion system is expressed but not essential to virulence in the Caenorhabditis elegans-P. aeruginosa pathogenicity model. *FEMS Microbiol Lett,* 242, 209-16.

WEISER, G. & KEREM, E. (2007) Early intervention in CF: how to monitor the effect. *Pediatr Pulmonol,* 42, 1002-7.

WEST, S. E., SCHWEIZER, H. P., DALL, C., SAMPLE, A. K. & RUNYEN-JANECKY, L. J. (1994) Construction of improved Escherichia-Pseudomonas shuttle vectors derived from pUC18/19 and sequence of the region required for their replication in Pseudomonas aeruginosa. *Gene,* 148, 81-6.

WIEHLMANN, L., WAGNER, G., CRAMER, N., SIEBERT, B., GUDOWIUS, P., MORALES, G., KOHLER, T., VAN DELDEN, C., WEINEL, C., SLICKERS, P. & TUMMLER, B. (2007) Population structure of Pseudomonas aeruginosa. *Proc Natl Acad Sci U S A,* 104, 8101-6.

WILDE, C., MAZEL, D., HOCHHUT, B., MIDDENDORF, B., LE ROUX, F., CARNIEL, E., DOBRINDT, U. & HACKER, J. (2008) Delineation of the recombination sites necessary for integration of pathogenicity islands II and III into the Escherichia coli 536 chromosome. *Mol Microbiol,* 68, 139-51.

WILLCOX, M. D. (2007) Pseudomonas aeruginosa infection and inflammation during contact lens wear: a review. *Optom Vis Sci,* 84, 273-8.

WILLIAMS, K. P. (2002) Integration sites for genetic elements in prokaryotic tRNA and tmRNA genes: sublocation preference of integrase subfamilies. *Nucleic Acids Res,* 30, 866-75.

WILSON, J. W. & NICKERSON, C. A. (2006) A new experimental approach for studying bacterial genomic island evolution identifies island genes with bacterial host-specific expression patterns. *BMC Evol Biol,* 6, 2.

WINSON, M. K., CAMARA, M., LATIFI, A., FOGLINO, M., CHHABRA, S. R., DAYKIN, M., BALLY, M., CHAPON, V., SALMOND, G. P., BYCROFT, B. W. & ET AL. (1995) Multiple N-acyl-L-homoserine lactone signal molecules regulate production of virulence determinants and secondary metabolites in Pseudomonas aeruginosa. *Proc Natl Acad Sci U S A,* 92, 9427-31.

WINSOR, G. L., VAN ROSSUM, T., LO, R., KHAIRA, B., WHITESIDE, M. D., HANCOCK, R. E. & BRINKMAN, F. S. (2009) Pseudomonas Genome Database: facilitating user-friendly, comprehensive comparisons of microbial genomes. *Nucleic Acids Res,* 37, D483-8.

WINSTANLEY, C. & FOTHERGILL, J. L. (2009) The role of quorum sensing in chronic cystic fibrosis Pseudomonas aeruginosa infections. *FEMS Microbiol Lett,* 290, 1-9.

WINSTANLEY, C., LANGILLE, M. G., FOTHERGILL, J. L., KUKAVICA-IBRULJ, I., PARADIS-BLEAU, C., SANSCHAGRIN, F., THOMSON, N. R., WINSOR, G. L., QUAIL, M. A., LENNARD, N., BIGNELL, A., CLARKE, L., SEEGER, K., SAUNDERS, D., HARRIS, D., PARKHILL, J., HANCOCK, R. E., BRINKMAN, F. S. & LEVESQUE, R. C. (2009) Newly introduced genomic prophage islands are critical determinants of in vivo competitiveness in the Liverpool Epidemic Strain of Pseudomonas aeruginosa. *Genome Res,* 19, 12-23.

WOLF, P. & ELSASSER-BEILE, U. (2009) Pseudomonas exotoxin A: from virulence factor to anti-cancer agent. *Int J Med Microbiol,* 299, 161-76.

WOLFGANG, M. C., KULASEKARA, B. R., LIANG, X., BOYD, D., WU, K., YANG, Q., MIYADA, C. G. & LORY, S. (2003) Conservation of genome content and virulence determinants among clinical and environmental isolates of Pseudomonas aeruginosa. *Proc Natl Acad Sci U S A,* 100, 8484-9.

WOODS, D. E., LAM, J. S., PARANCHYCH, W., SPEERT, D. P., CAMPBELL, M. & GODFREY, A. J. (1997) Correlation of Pseudomonas aeruginosa virulence factors from clinical and environmental isolates with pathogenicity in the neutropenic mouse. *Can J Microbiol,* 43, 541-51.

WORBY, C. A., MATTOO, S., KRUGER, R. P., CORBEIL, L. B., KOLLER, A., MENDEZ, J. C., ZEKARIAS, B., LAZAR, C. & DIXON, J. E. (2009) The Fic Domain: Regulation of Cell Signaling by Adenylylation. 34, 93-103.

WOZNIAK, R. A. & WALDOR, M. K. (2009) A toxin-antitoxin system promotes the maintenance of an integrative conjugative element. *PLoS Genet,* 5, e1000439.

WURDEMANN, D. & TUMMLER, B. (2007) In silico comparison of pKLC102-like genomic islands of Pseudomonas aeruginosa. *FEMS Microbiol Lett,* 275, 244-9.

YAHR, T. L. & WOLFGANG, M. C. (2006) Transcriptional regulation of the Pseudomonas aeruginosa type III secretion system. *Molecular Microbiology,* 62, 631-640.

YOON, S. H., HUR, C. G., KANG, H. Y., KIM, Y. H., OH, T. K. & KIM, J. F. (2005) A computational approach for identifying pathogenicity islands in prokaryotic genomes. *BMC Bioinformatics,* 6, 184.

ZAVASCKI, A. P., GOLDANI, L. Z., LI, J. & NATION, R. L. (2007) Polymyxin B for the treatment of multidrug-resistant pathogens: a critical review. *J Antimicrob Chemother*, 60, 1206-15.

ZHANG, J., LI, H., WANG, J., DONG, Z., MIAN, S. & YU, F. S. (2004) Role of EGFR transactivation in preventing apoptosis in Pseudomonas aeruginosa-infected human corneal epithelial cells. *Invest Ophthalmol Vis Sci*, 45, 2569-76.

ZHANG, Y., LI, X., CARPINTEIRO, A. & GULBINS, E. (2008) Acid Sphingomyelinase Amplifies Redox Signaling in Pseudomonas aeruginosa-Induced Macrophage Apoptosis. *J Immunol*, 181, 4247-4254.

ZOLFAGHAR, I., EVANS, D. J. & FLEISZIG, S. M. (2003) Twitching motility contributes to the role of pili in corneal infection caused by Pseudomonas aeruginosa. *Infect Immun*, 71, 5389-93.